UNIVERSITÀ DEGLI STUDI DI SALERNO
Dipartimento di Farmacia

PhD Program
in **Drug Discovery and Development**
XXXIV Cycle — Academic Year 2021/2022

PhD Thesis in

Design and synthesis of small molecules as ion channel modulators

Candidate   Supervisor

Vincenzo Vestuto   Prof. *Alessia Bertamino*

                                                          Co-Supervisor

                                           Prof. *Pietro Campiglia*

PhD Program Coordinator: Prof. *Gianluca Sbardella*

CHAPTER 2

Design, synthesis, and biological evaluation of neuronal K_{v7} channels activators

Abstract

My PhD research plan relates the exploration of the structural requirements for ionic channels modulation such as TRPM8 and K_{v7} receptors.

*About the first field, we prepared a series of tryptophan-based derivatives of our lead compound (**4**) with the purpose of increase the metabolic stability by decreasing its amino acid character, and to study new TRPM8/antagonist interactions leading to the potential discovery of SAR clues. Finally, all the synthetized compounds have been evaluated for their chemical stability and pharmacological activity by in vitro assays, and the most potent compounds identified were try out in several in vivo pain models. From these results, a promising scaffold (**31a**) for the treatment of chemotherapy-induced peripheral neuropathy is revealed.*

At the same time, I worked on the design, synthesis, purification, and characterization of a new small library of K_{v7} activators as retigabine analogues.

*In a first work, we designed some conformationally restricted analogues of retigabine with the aid of pharmacophore modelling and homology modelling. On these achievements and taking advantage of the recently published experimental structure of $K_{v7.2}$ in complex with retigabine, we performed molecular docking and molecular dynamics calculations to study the interactions of our more potent agonists (**23a** and **24a**) with $K_{v7.2}$. From these studies, we synthetized a new series of retigabine derivatives through a structure-based drug design approach. All the synthetized compounds have been evaluated in vitro for their pharmacological activity by electrophysiological patch-clamp experiments as well as for their metabolic and chemical UV stability. Hence, a very remarkable in vivo result has been obtained by the most active compound (**109**) of the last series on pentylenetetrazol-induced epilepsy model.*

CHAPTER 1

Design, synthesis, and biological evaluation of TRPM8 antagonists

1.1 The transient receptor potential (TRP) superfamily

Transient receptor potential (TRP) channels represent a wide group of cellular sensors involved in multifunctional signaling regulation allowing the cells to detect and respond to environmental and physiopathological stimuli. Actually, TRP channel activation is involved in temperature, taste, mechano-sensation, eyesight, sound, smell, and pain. Therefore, it is not surprising that these channels are implicated in several disorders, including hereditary channelopathies caused by defects in TRP genes encoding.[1,2]

The human genome encodes 27 TRP proteins, making them the second largest class of ion channels, overtaken only by K^+ channels. In addition, TRP channels are expressed from the genomes of a wide diversity of organisms, including animals, fungi, algae, and a lot more eukaryotes.[3]

Transient receptor potential channels are identified after the discovery of these photoreceptors in the fruit fly *Drosophila melanogaster*. A spontaneous mutation in the TRP gene led to blindness during prolonged intense light exposure so these mutants made it possible the discovery of the receptors.[4]

TRPs contain six putative transmembrane domains (TM1-6) and cytosolic N- and C-terminal tails, which assemble as homo- or hetero-tetramers to generate cation channels (**Figure 1**), although certain isoform in mitochondria and endoplasmic reticulum exhibit an unconventional structure with four transmembrane domains.[5]

TM5, TM6 and the connecting pore loop form the central cation-conducting pore, whereas TM1-TM4 and the cytoplasmic N- and C-terminal parts are thought to contain the regulatory domains that control channel gating.[6]
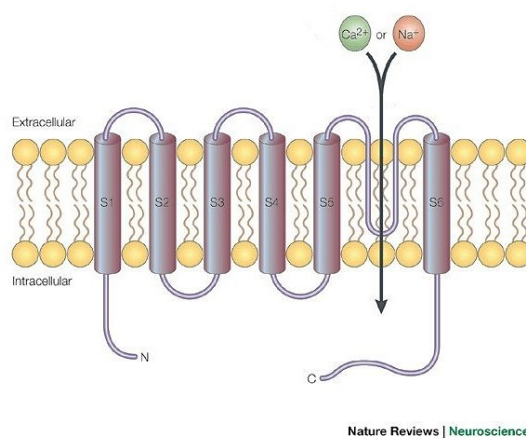
Figure 1. Architecture of TRP channels. (Adapted from Clapham *et al.*, 2001).

Though all TRPs are cation channels, the permeability for mono- and divalent cations varies widely between different isoforms.

The relevance of TRP receptors in cellular physiology is certainly due to their contribution on changes in $[Ca^{2+}]$, by providing calcium entry pathways besides the calcium release from cellular organelles.[7]

Based on amino acid homologies, the TRP channel are grouped in seven subfamilies: TRPM, TRPV, TRPC, TRPA, TRPP, TRPML, and TRPN (**Figure 2**).[3]
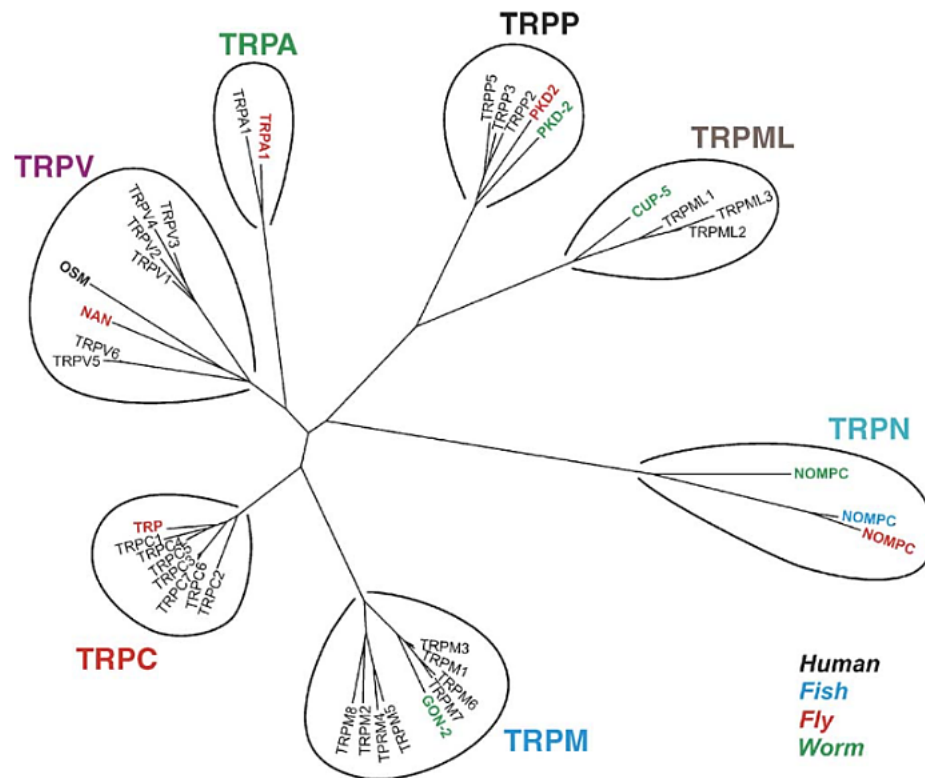
Figure 2. Phylogenetic tree of the TRP superfamily. (Adapted from Pedersen *et al*., 2005).

TRP subfamilies are so called based on the original name of the initially described member of each subfamily. The TRPM ('Melastatin') and TRPV ('Vanilloid') subfamilies including eight (TRPM1-8) and six (TRPV1-6) human members, respectively. The TRPC ('Canonical') subfamily presently comprises seven different (TRPC1-7) homologs of *Drosophila* TRP channels. TRPA ('Ankyrin') has only one mammalian member (TRPA1), a nociceptive channel characterized by the presence of about 14 ankyrin repeats. TRPMLs ('Mucolipin') and TRPPs ('Polycystin') are not adequately characterized but gain increasing interest because of their involvement in several human diseases. TRPNs ('no mechano potential C', or NOMPC) have

so far only been detected in *Caenorhabditis elegans*, *Drosophila*, and zebra fish. Finally, in yeast, the eighth TRP family was recently identified and named as TRPY.[8,9,10]

TRPs show very low primary sequence homology across various subfamilies. However, their varied tissue distribution suggests that the superfamily concern great part of organs of the human organism revealing different physiological functions as sensory apparatuses that detect and react to all possible thermal, chemical, and physiological stimuli. This stimulates drug discovery to target TRP channels given the broad spectrum of clinical indications, ranging from neurological disorders to pulmonary hypertension, diabetes, and cancer (**Figure 3**).[11,12]
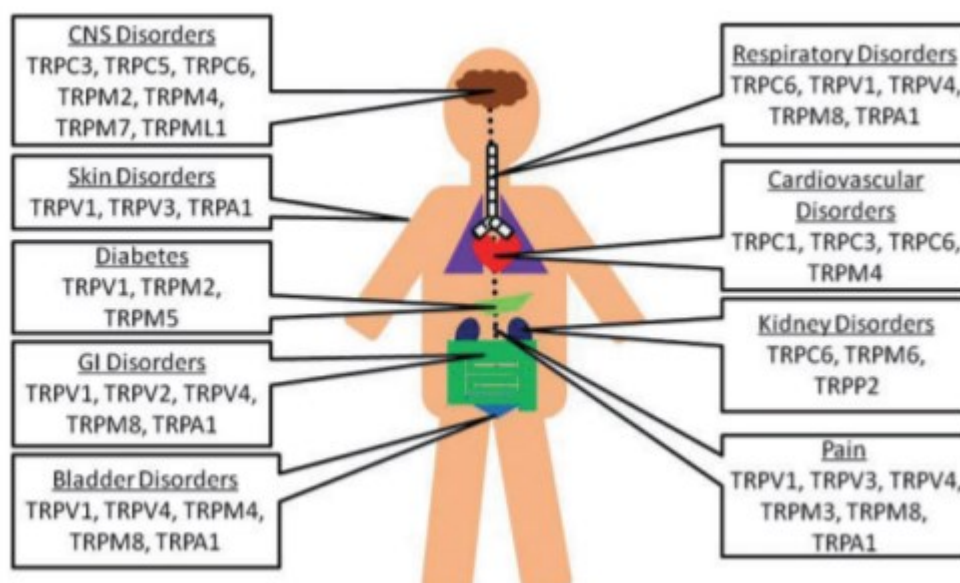
Figure 3. Simplified topographical distribution of TRP channels. (Adapted from Kaneko *et al*., 2013).

The heat activated TRPV1 was first identified by its responsiveness to capsaicin, a vanilloid derived, among a group of temperature sensitive TRPs (**Figure 4**), called thermoTRPs. TRPV1 also responded to noxious heat, with an activation threshold of approximately 42 °C.[13]

TRPM3, TRPV3, and TRPV4 (also known as VROAC or OTRPC4) are expressed in somatosensory neurons or in the case of TRPV3 peripheral targets of these nerves and their function is in nociception. They are characterized as heat or warm thermosensors.[14]

In contrast to these warmth- or heat-activated TRP channels, two other TRP channels TRPM8 and TRPA1 are activated by cold stimuli. TRPA1, initially termed ANKTM1 due to the presence of multiple N-terminal ankyrin repeats, was originally characterized as a noxious cold detector. TRPM8 is activated by cool temperatures starting in the innocuous range ($\leq$26 °C).[13]

All thermoTRPs, when expressed in native cells (HEK-293, CHO) have the property of

rendering the cells temperature sensitive. Each one has distinctive characteristics, highlighted by specific temperature thresholds of activation. Sensitization or desensitization to repeated thermal stimuli and the ability to be modulated by distinct signalling mechanisms further differentiate thermoTRPs.[15]
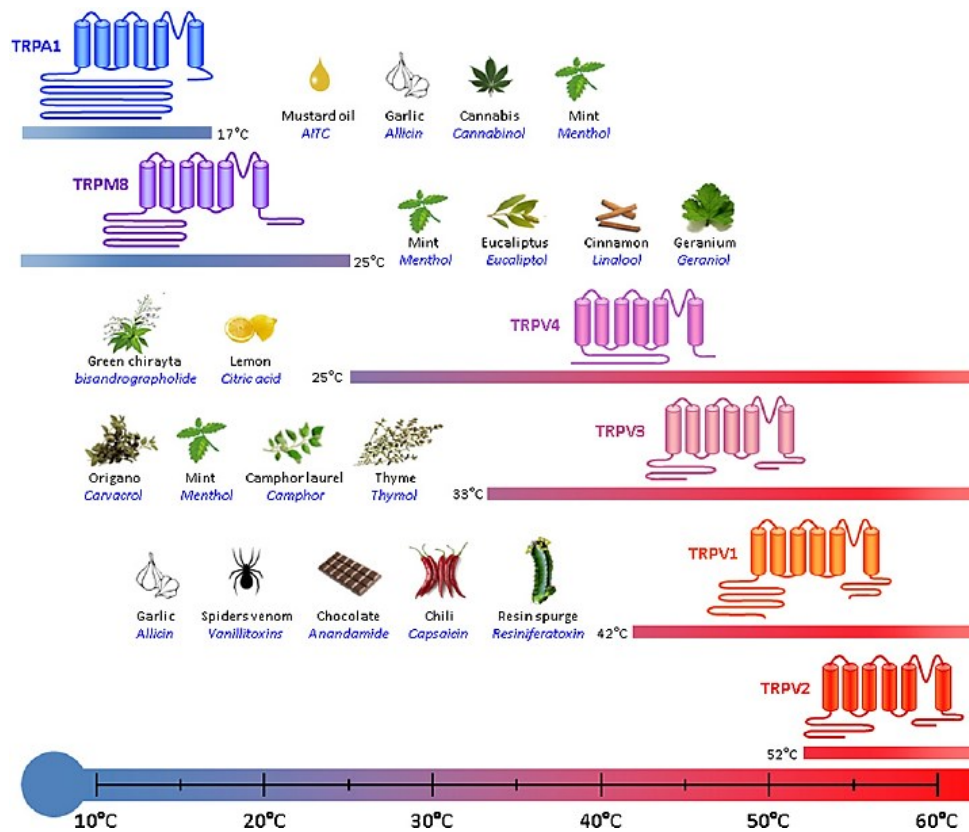
Figure 4. TRP channels act as thermosensors in sensory nerves. (Adapted from Belvisi *et al*., 2011).

1.2 TRPM8: structure and regulation

TRPM8 is a voltage-gated, nonselective cation cold sensing TRP channel that is activated by cooling temperatures below 25 °C, reaching a maximum response near 10 °C, and with its chemical ligands such as menthol, eucalyptol, and icilin.[16] These thermoreceptors are expressed by approximately 15% of all somatosensory neurons in the trigeminal and dorsal root ganglion (DRG). Accordingly, TRPM8-knockout mice have dramatically reduced cold-sensitive dorsal root ganglion neurons showing severe deficits in behavioral cool thermosensation.[17]

Electrophysiological studies have indicated that TRPM8 activation is followed in a large storage of intracellular Ca^{2+} levels through both Ca^{2+} entry from extracellular sites and Ca^{2+} release from intracellular calcium stores. Afterwards TRPM8 activation, extracellular calcium dependent desensitization has been found, presumably through TRPM8 dependent calcium influx.[18]

This process is dependent by depletion of phosphatidylinositol 4,5-bisphosphate (PIP2), associated either with the activation of Gq-coupled receptors or with the calcium-mediated activation of phospholipase Cβ (PLCβ).[19] PIP2 has been shown to stimulate TRPM8 interacting with positive charges in the C-terminal TRP domain (**Figures 4-5**). Its depletion decreases TRPM8 activity by shifting voltage towards more positive potentials inhibiting channel activity, reducing the cold- and menthol-activated currents.

Furthermore, also several signaling cascades are linked to the regulation of TRPM8 activity via protein kinase C (PKC) phosphorylation. Actually, activation of PLCβ leads, in addition to the PIP2 depletion, to PKC recruitment, which phosphorylates a large amount of TRPs including TRPM8. However, none of the putative PKC phosphorylation sites of TRPM8 is involved in channel modulation. Instead, PKC might have an indirect effect activating phosphatase calcineurin, indicating a dephosphorylation-induced desensitization process.[20,21]

Additionally, PKA is reported among the PKs as capable of modulating TRPM8.[22]

Other signaling pathways, besides PK and PIP2 modulate TRPM8 activity. Polyunsaturated fatty acids such as arachidonic acid generated by phospholipase A2 (PLA2) triggering, lead to the suppression of TRPM8 activity.[23]

The human TRPM8 channel consists of four identical subunits, and it is composed of 1104 amino acids with a molecular mass of 128 kDa.[24] Each subunit contains six transmembrane segments (S1-S6) and large intracellular amino and carboxyl terminal cytoplasmic residues (**Figure 4**). The first four helices (S1-S4) constitute the voltage sensor module and include the binding sites for menthol and icilin, even though they do not fully overlap, since most residues engaged in menthol recognition are in S2, whereas icilin interacts also with S3 residues.[25] S5 and S6 form the gate and selective pore. This is characterized by a highly conserved hydrophobic region and a conserved aspartate residue, whose deletion results in a non-functional channel.[24] TRPV1-TRPM8 chimeras showed that the C-terminus contains structural determinants crucial for temperature activation of the channel.[26] Indeed, it is involved in tetramer stabilization since some mutations within the coiled region of C-terminus (978-1104) markedly reduce the ability of the TRPM8 monomers to form oligomeric channels disrupting menthol and icilin sensitivity. On the other hand, N-terminus does not play a significant part

in tetramerization since the analysis of deletion mutants shows that the transmembrane domain for TRPM8 assembly into tetramers results satisfactory (**Figure 4**).[27]

The TRP box, a short hydrophobic sequence shared by TRPC, TRPV, and TRPM families, and a binding site for PIP2, are in C-terminal of S6 tail (**Figure 4**). Although the functional role of the TRP box is not entirely clear, the TRP box regions have recently been implicated in sensing PIP_2 levels. In addition, the TRP box could act as a coiled-coil zipper that holds the channel in a closed conformation.[28]

These thermoreceptors, apart from being expressed from primary afferent neurons, such as dorsal root and trigeminal ganglia, and in the nodose and geniculate ganglia in the peripheral nervous system, are localized on the cell surface membrane and endoplasmic reticulum of many tissues. In particular, TRPM8 are localized in the male urogenital organs, such as the prostate gland, testis, and urinary bladder, as well as the liver and lung. Above all, it is found in various cancers, including androgen-dependent prostate cancer, melanoma, colon, breast, and pancreatic cancer.
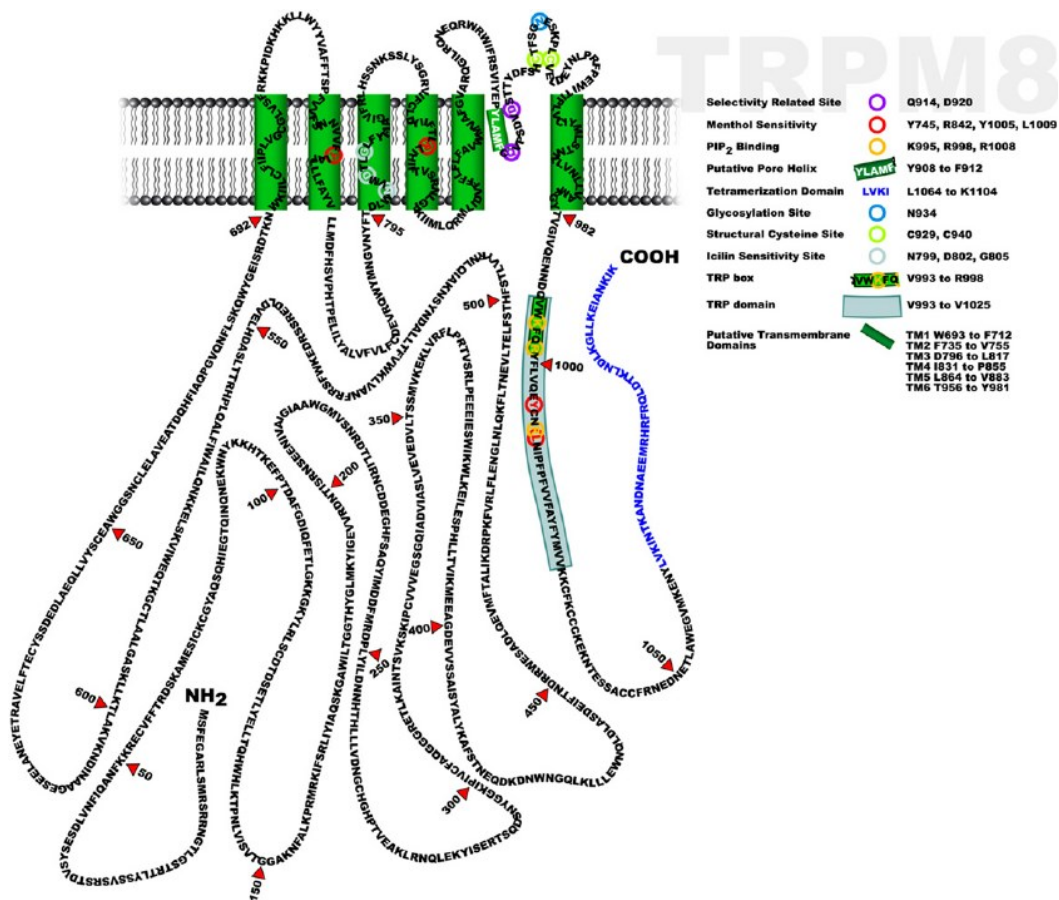
Figure 4. Schematic representation of TRPM8 protein. (Adapted from Latorre *et al*., 2011).
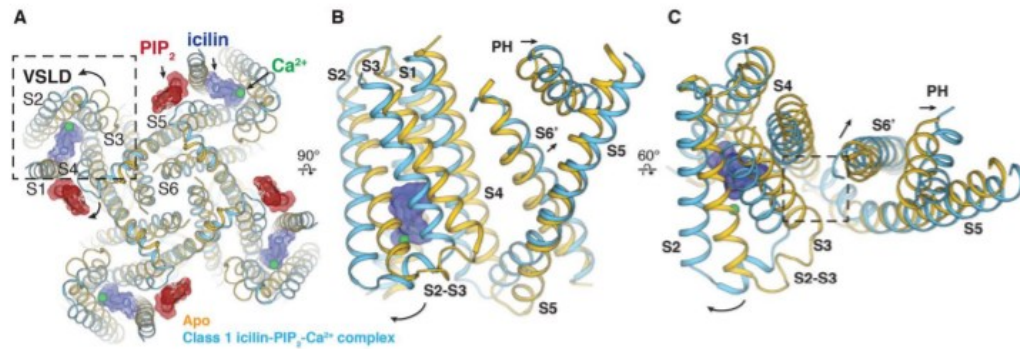
Figure 5. Structural rearrangements in response to the binding of PIP2 and agonists. (A) Viewed from the intracellular side. (B) Viewed from the membrane. (C) Viewed from the extracellular side. (Adapted from Yin *et al*., 2019).

1.3 TRPM8: physiopathological role

1.3.3 TRPM8 and cancer

A large body of evidence has demonstrated that TRPM8 is aberrantly expressed in a variety of malignant solid tumors and cell lines, revealing its important role in cancer cells survival, proliferation, and invasion (**Figure 6**).

Prostate cancer is the second most frequently diagnosed cancer in men and can easily evolve to more aggressive forms. Therefore, new approaches are needed for a better pharmacological management in prostate cancer patients with advanced disease. In this regard, TRPM8 expression is differentially regulated during prostate carcinogenesis, and it seems to be one of the most promising clinical targets.[32]

The proliferative effect of TRPM8 in cancers is also proved in osteosarcoma (MG-63 and U2OS), and colon cancer (Caco-2) cell lines. Anti-*TRPM8* siRNA administration reduced cellular proliferation and altered cell cycle progression with arrest in the G0/G1 phases.[33] In accord with these data, TRPM8 blockers inhibit proliferation.[34]

Consistent with TRPM8 role in tumor progression, pancreatic cancer cells with down-regulated expression of TRPM8 show typical characteristics of senescence. Morphological analysis revealed the presence of multiple nuclei, suggesting a defect in cell division. These findings indicate that TRPM8 is required for maintaining the uncontrolled proliferation of cancer cells through regulation of cell cycle progression and replicative senescence.[35]

Expression of TRPM8 has also been identified in other malignancies such as melanoma, lung and oral squamous carcinoma, glioblastoma multiforme, and neuroendocrine tumor. In more

details, TRPM8 has been found to be over-expressed in breast carcinoma, neuroblastoma, and osteosarcoma, as compared with the corresponding normal tissues. In this view, these findings suggest that TRPM8 channels play a pivotal role in the growth, development, and metastasis process of tumors.[36]
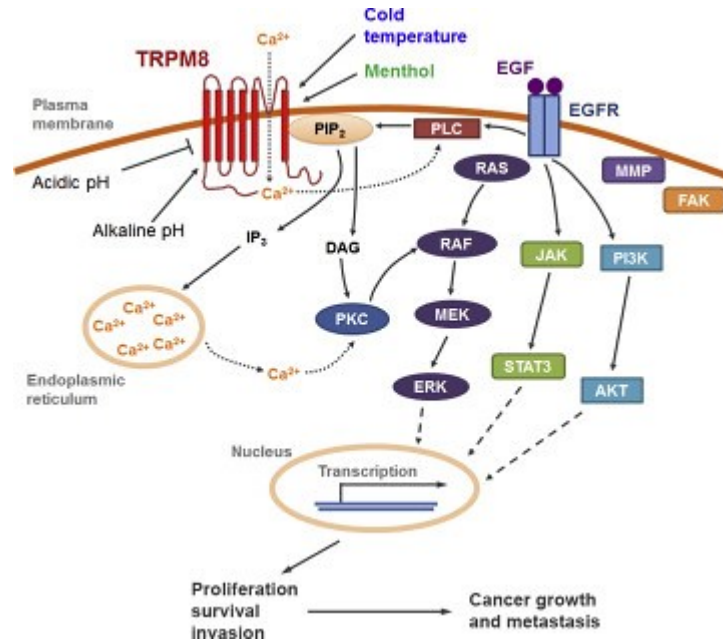
Figure 6. TRPM8 pathways involved in cancer. (Adapted from Yee *et al*., 2016).

1.3.4 *TRPM8 and pain*

Because of its function in detecting of temperature, TRPM8 provides to initiates signaling towards the central nervous system in according with its expression in a subpopulation of cold-sensitive DRG and in sensory nerves. Knockout mouse studies have in fact demonstrated the relevance of TRPM8 for sensation of a wide range of innocuous and noxious cold temperatures.[37]

Given its notable role in cold perception, neurons expressing TRPM8 represent an attractive target in the study of cold pain transduction.

A growing body of evidence demonstrates marked analgesic effects both by TRPM8 activators and antagonists in different models of neuropathic pain. This is because the channels show a desensitized state after long exposition of agonists, causing PIP2 depletion, which makes them incapable to conduct ions.[38]

Pharmacological studies in mice aimed to probe the role of TRPM8 in analgesia menthol-induced, showed the analgesic properties of the levo isomer, which is able to relieve pain caused by chemical stimuli due to capsaicin, acrolein, and acetic acid. These analgesic effects were completely reverted in mice with genetic deletion of TRPM8. This supports a crucial role of the receptors in menthol-induced analgesia. Moreover, a TRPM8 inhibitor, AMTB (*N*-(3-Aminopropyl)-2-[(3-methylphenyl)methoxy]-*N*-(2-thienylmethyl)benzamide hydrochloride), partially reverse counterirritant effects of menthol towards acrolein and other respiratory irritants in tobacco smoke. This result also supports a role of TRPM8 in menthol induced counterirritation in the respiratory system, which is innervated by sensory neurons, showing how TRP channel expression patterns is linked to nociceptors.[39,40]

Additionally, it is clearly the role of these thermoTRPs in pain management and in amplifying pain sensation after injury. This occurs due to their increasing, as well as mRNA levels, in different animal models such as neuropathy induced by oxaliplatin and by streptozotocin-induced diabetes.[41,42] TRPM8 inhibitors dramatically reduced cold and mechanical allodynia in acute and chronic pain models.[43]

Besides, inflammatory factors such as H^+, bradykinin and phospholipases can affect the activation of TRPM8.[44-46]
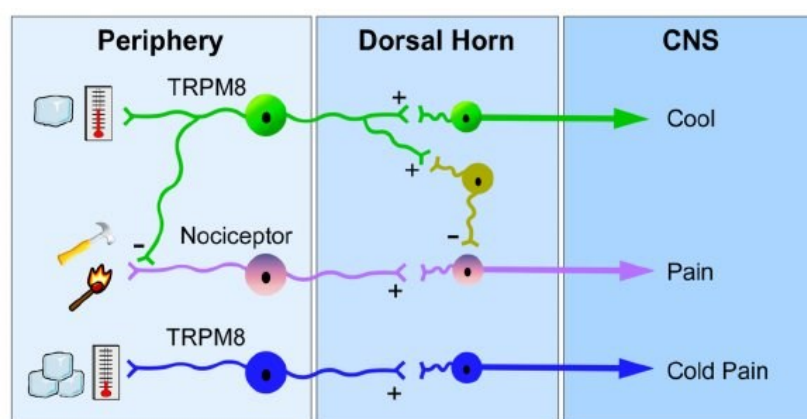
Figure 7. Model for TRPM8 neuronal function. (Adapted from Knowlton *et al*., 2013).

1.3.5 TRPM8 and genitourinary diseases

In the recent past, TRPM8 was found widely expressed in different human genitourinary tract tissues, including urinary bladder.[47]

The thermoTRPs in the urinary tract exhibit the same functional role as others found elsewhere in the body. Indeed, the body cooling is commonly associated with an increase in diuresis and thus the bladder cooling reflex plays a critical role in the relief of the bladder when it is under cooling stress.[48] Further studies in a variety of animal models have shown that intravesical menthol induced urination or increased bladder contraction frequency.[49]

Moreover, levels of TRPM8-immunoreactive nerve fibers in suburothelium and mRNA from patients with overactive bladder syndrome (OAB) and painful bladder syndrome (PBS) were significantly increased. Based on this positive correlation, TRPM8 may provide an additional target for future overactive and painful bladder syndromes pharmacotherapy.[50,51]

In accordance with above mentioned, intravenous administration of AMTB decreased the bladder contractions frequency and markedly attenuated responses to noxious urinary bladder distension.[52]

These observations suggest that a blocker of the TRPM8 channels may provide a new therapeutic opportunity for treatment of PBS and OAB.

1.4 TRPM8 modulation

1.4.1 TRPM8 activators

TRPM8 channels respond to a wide range of stimuli.

Among TRPM8 biological ligands, PIP2 is required for activation of the channel through interactions with positively charged residues from three regions of the same subunit (TRP domain, S4-S5 linker and preS1 segment).[53]

In addition, many studies have examined the role of PLA2 in the activation of TRPM8 given its ability to release polyunsaturated fatty acids (PUFAs) and a lysophospholipids (LPLs). These exert opposing effects: LPLs positively modulate TRPM8 while PUFAs, such as arachidonic, eicosapentaenoic, and docosahexaenoic acid, showed an inhibitory activity. Although the products act oppositely, the net balance of equimolar concentrations of the products is in favour of TRPM8 activation.[54]

Furthermore, numerous natural and synthetic chemotypes (**Figure 7**) have been identified in recent times and are used as tools to explore the pharmacological role of these channels, besides representing an interesting approach for potential treatment of obesity, type 2 diabetes, and related metabolic diseases.[55,56]

Among the natural products which act as TRPM8 activators can be found terpenes such as menthol (*Menta spp.*), eucalyptol (*Eucalyptus spp.*), borneol (*Dipterocarpus spp.*), cubebol (*Piper cubeba*), while icilin (AG-3-5) stand out from the most potent synthetic activators (~200-fold more potent than menthol).[57] Icilin activation mechanism differs from menthol one: Whereas menthol activates TRPM8 in the absence of extracellular calcium, icilin is inactive under the same conditions. In fact, icilin requires a coincident rise in cytoplasmic calcium, either via permeation through the channel or by release from intracellular stores, to evoke TRPM8 currents, suggesting that the channel can be opened by multiple mechanisms. In this regard, it is proposed a TRPM8 agonists classification into two groups: type I (menthol-like) and type II (allyl isothiocyanate-like). They provided different kinetic models; type I stabilizes the open channel, while type II destabilizes the closed channel.[58] This is an important point to take on board for future prospective of TRPM8 agonists operating.
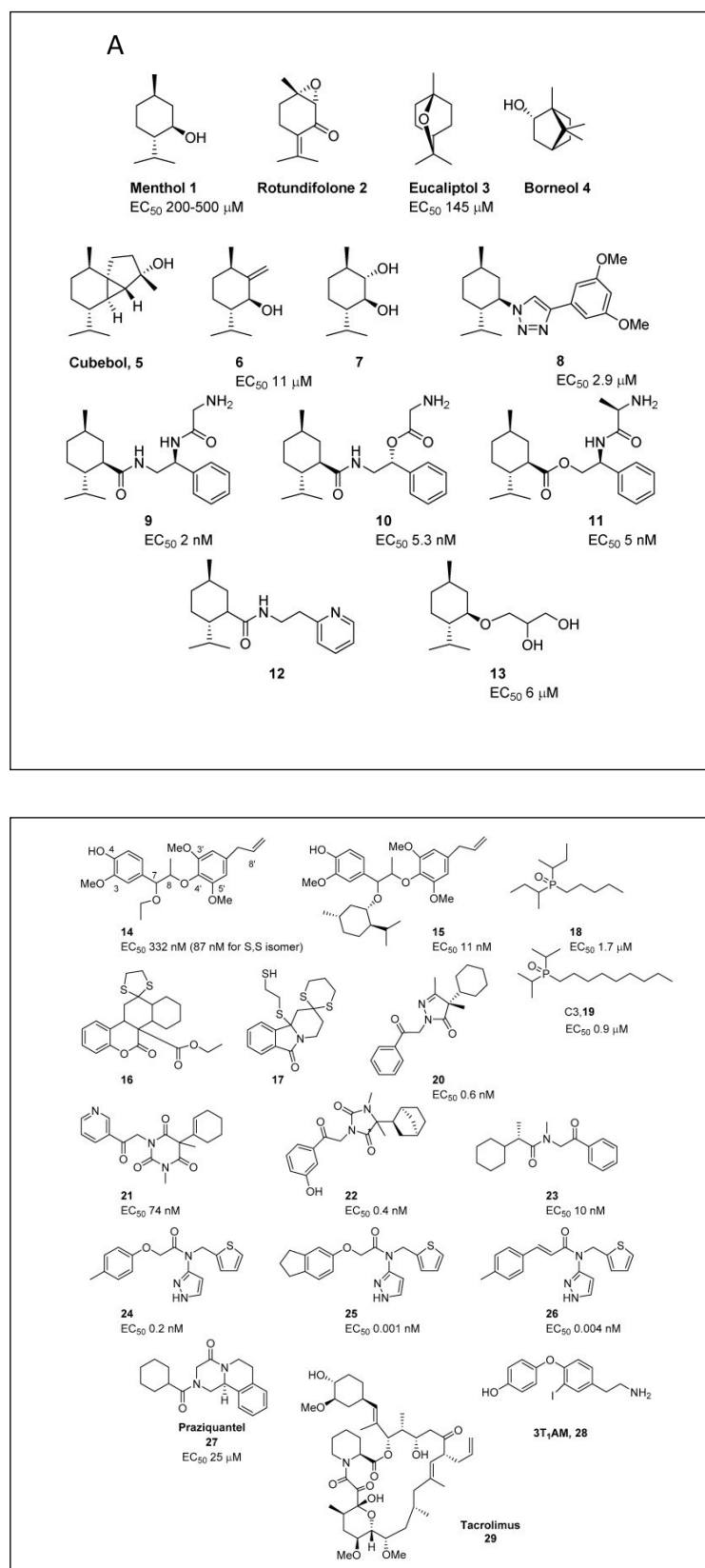
Figure 7. TRPM8 activators. (A) Menthol-derived. (B) Non-menthol chemotypes. (Adapted from González-Muñiz *et al*., 2019).

1.4.2 TRPM8 blockers

TRPM8 antagonists have been pursued over the recent time by many research groups and pharmaceutical companies.[59-61] Nevertheless, a lot of these displayed severe side effects mainly caused by poor selectivity towards TRPM8, interacting also with other subfamilies such as TRPV1 and TRPA1.[62,63]

At the present, only three compounds have been received approval for clinical trials (**Figure 8**): AMG-333 and PF-05105679, which have not passed phase I studies, and cannabidivarin, which is in phase II clinical assays.[64,65] Therefore, there is a need to discover potent and selective TRPM8 antagonists, thus also enabling an improving in the knowledge about their binding sites. This is now facilitated, among other things, by the determination of the first full-length TRPM8 cryo-electron microscopy structure from the collared flycatcher *Ficedula albicollis*.[66]

Most TRPM8 antagonists are reported as drugs for bladder pain, inflammation, migraine, and cancer. Since chemotherapy is associated with changes in TRPM8 expression,[67] in several studies TRPM8 is targeting to reversal chemotherapy-induced cold allodynia.[68,69] This neuropathy can be dose limiting causing the cessation of chemotherapy, enduring years beyond treatment, and for which there are currently no other therapies.[70,71]

Several structural classes of nanomolar TRPM8 antagonists have been described, including substituted 4-benzyloxy-phenylmethylamides (M8-B), benzyloxy-benzoic acid amides (AMTB), 1-phenylethyl-4-(benzyloxy)-3-methoxybenzyl(2-aminoethyl)carbamate (PBMC), BCTC (4-(3-Chloro-2-pyridinyl)-N-[4-(1,1-dimethylethyl)phenyl]-1 piperazinecarboxamide), thio-BCTC, (2R)-4-C3-chloro-2-pyridinyl)-2-methyl-N-[4-(trifluoromethyl)phenyl]-1-piperazinecarboxamide (CTPC), and capsazepine.[72] Many tryptamine derivatives also act as TRPM8 antagonists.[73,74] In addition, the antifungal drug clotrimazole has strong TRPM8 antagonistic activity, but also activates TRPV1 and TRPA1, actions consistent with the commonly reported side effects of irritation and burning.[75]

Some of these compounds are patented for the treatment of urological diseases, although there are no adequate data available on the *in vivo* efficacy. High affinity antagonists M8-B, AMTB and PBMC have been used as selective pharmacological tools of TRPM8 to explore its therapeutic applications, such as the regulation of deep body temperature, treatment of urological disorders and cold hypersensitivity associated with inflammatory and neuropathic conditions.[76]

Lastly, endogenous antagonists PKC-dependent, comprise bradykinin, a proinflammatory agent, are widely reported as TRPM8 blockers.[77,78]
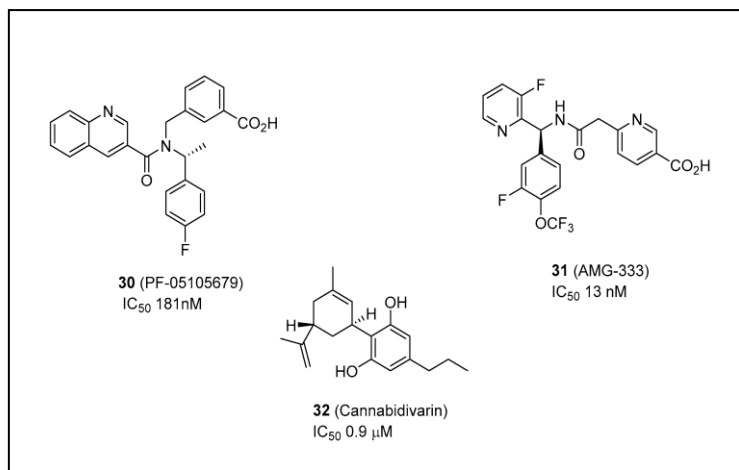
Figure 8. TRPM8 antagonists that have reached clinical trials. (Adapted from González-Muñiz *et al*., 2019).

2.1 Tryptophan-based derivatives as TRPM8 channel antagonists: Background

Considering all the above, therefore at the potential activity of these receptors in neuropathic pain, cancer, and other pathologies, the design and synthesis of new TRPM8 antagonists represented one of the goals of my PhD programme.

Recently, some indole compounds have been identified as potent and selective TRPM8 antagonists. Voacangine (compound **1**, **Figure 9**), an iboga-type indole alkaloid, is found in the root bark of *Voacanga africana* Stapf ex Scott-Elliot (*Apocynaceae*) and acts as modulator for TRPV1, TRPA1 and TRPM8. In particular, voacangine showed TRPA1 agonistic and remarkable TRPM8 antagonistic activity.[79]

Also 5-substituted tryptamines have been studied as TRPM8 blockers and a structure-activity study described some important determinants of TRPM8 activity. In more detail, the phenyl ring and ethylamine side chain were found to be crucial for the antagonist activity of 5-benzyloxytryptamine (compound **2**, **Figure 9**).[73]

Based on these findings, in a precedent work we chose the tryptamine nucleus as template for the design of a small library of TRPM8 modulators and considered of interest to introduce different substituents on the side chain of the starting tryptamine and to derivatize the N-1 position of the indole scaffold. Overall, this has led us to obtain compound **3** (**Figure 9**), a potent and selective TRPM8 antagonist (IC$_{50}$ = 367 ± 24 nM) with reduced scaffold complexity compared with ibogaine alkaloids.[74]

Starting from this result, a new small library of indole derivatives was designed, synthesized, and characterized, obtaining new structure-activity relationship (SAR) clues and a new potent tryptophan-based antagonist of TRPM8 channel (compound **4**, **Figure 9**) with significantly improved potency (IC$_{50}$ = 0.2 ± 0.2 nM) over the parent compound **3** and potent *in vivo* antinociceptive activity.[80]
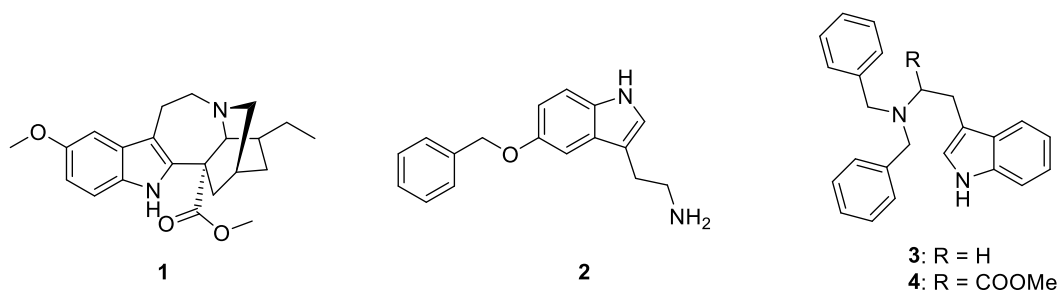
Figure 9. Indole-based TRPM8 antagonists.

Considering these achievements and due to resolution of the TRPM8 protein structure from the collared flycatcher *Ficedula albicollis* (TRPM8$_{FA}$) using cryoelectron microscopy,[66] we have used a homology model of human TRPM8 using the TRPM8$_{FA}$ structure as template to rationalize the potent antagonist activity showed by tryptamine (**3**) and tryptophan-based (**4**) TRPM8 antagonists.

In order to deepen the structural requirements necessary for the TRPM8 antagonist activity of these indol-based derivatives, we designed and synthesized a new series of conformationally restricted analogues of **4** pursuing a dual purpose:[81]

(a) to increase the metabolic stability of our lead compound by decreasing its amino acid character;

(b) to explore new TRPM8/antagonist interactions leading to the potential discovery of SAR clues.
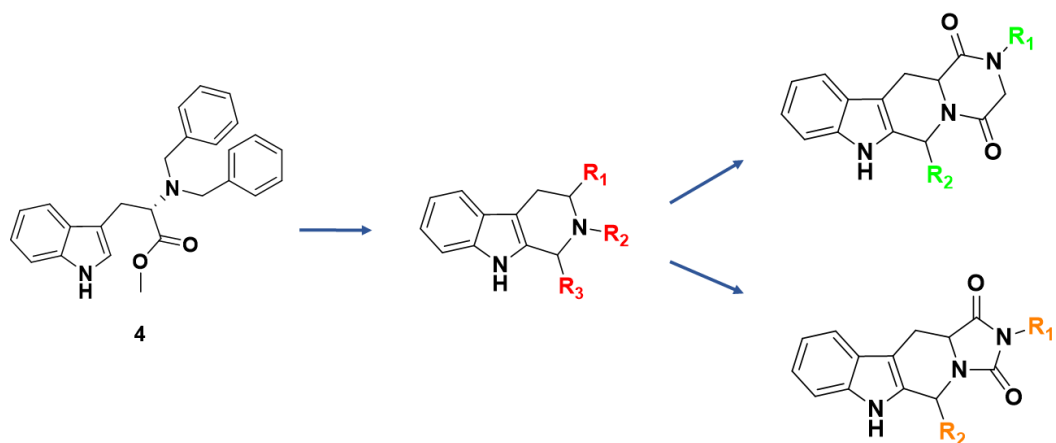
Figure 10. Rational design of three TRPM8 series of tryptophan-based restricted analogues of the lead compound **4**, namely tetrahydro-β-carbolines (THBCs), THBC-based diketopiperazines, and THBC-based hydantoin derivatives.

2.2 Synthesis of I series

THBCs **6a,b**, **9**, and **10-12a,b**, were synthesized as depicted in **Scheme 1** and **Scheme 2**, respectively. Starting from a microwave assisted Pictet-Spengler reaction of L-Trp-OMe with benzaldehyde and trifluoroacetic acid (TFA) in methanol, the THBC intermediates **5a,b** were obtained as diasteroisomeric mixtures (2:1 cis:trans), which were resolved by flash chromatography. N-benzylation reaction of the pure diastereoisomers with benzyl bromide, sodium iodide, and triethylamine (TEA) in THF using palladium acetate as catalyst and microwave irradiation led to the final trans-(**6a**) and cis-(**6b**) THBCs in 62% and 59% yields, respectively.
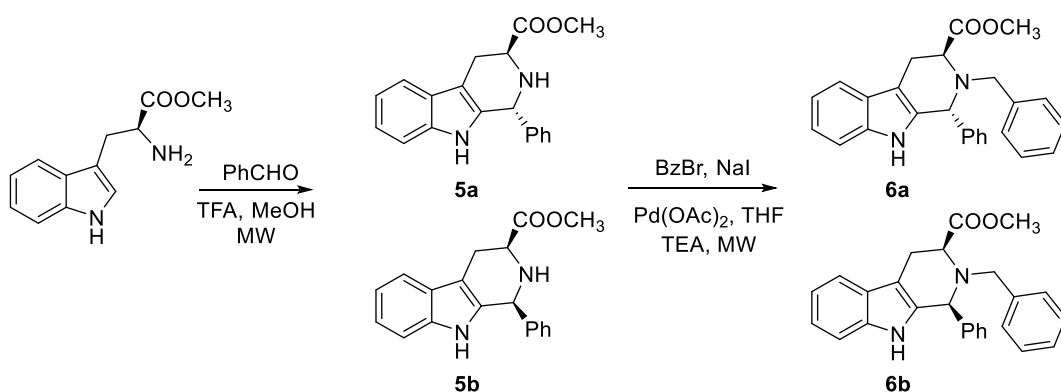
Scheme 1. Synthesis of the THBCs derivatives **6a,6b**.

The relative configuration for **6a** and **6b** was assigned by ROESY NMR spectra considering the cross peak between H1 and H3 that is present for **6b** (H1, δ 4.96 ppm; H3, δ 3.87 ppm, **Figure 12**), while it is missing in **6a** (H1, δ 5.39 ppm; H3, δ 3.87 ppm, **Figure 14**). Assuming that, the absolute configuration for the L-tryptophan moiety is maintained in the reaction conditions, the configuration at C1 was assigned accordingly. The same key correlation was used to assign the absolute configuration of the other THBCs derivatives (**10-12a,b**).

Figure 11. ^{1}H NMR spectrum of compound **6b**.

Figure 12. ROESY spectrum of compound **6b**.

Figure 13. ^{1}H NMR spectrum of compound **6a**.
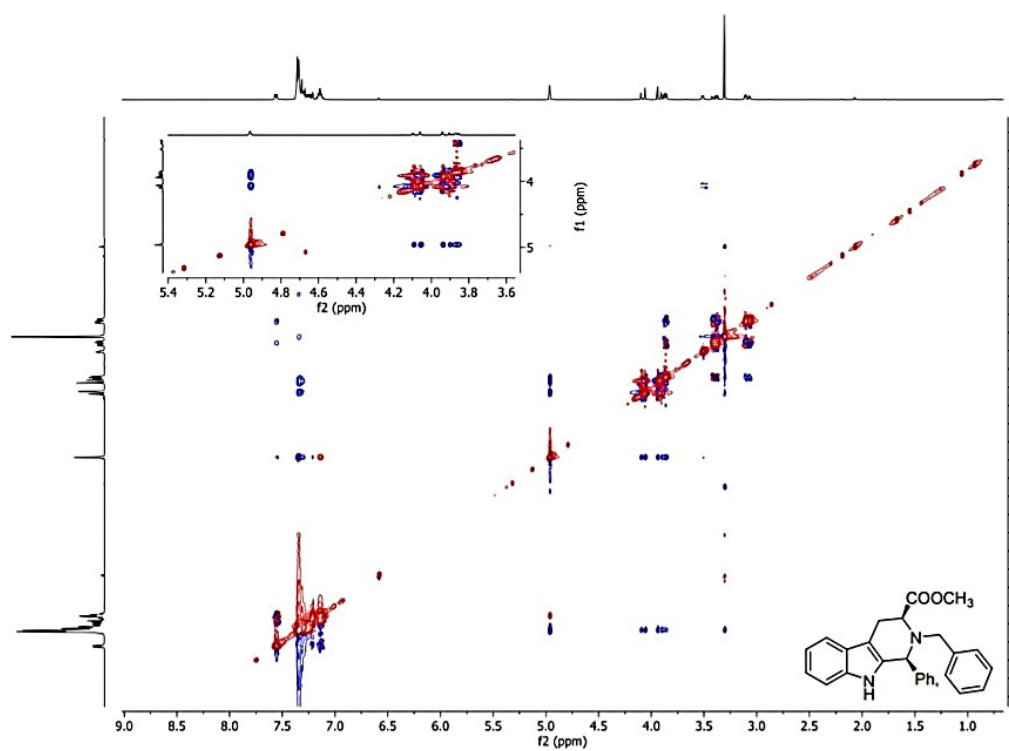
Figure 14. ROESY spectrum of compound **6a**.

Reaction of Boc-L-Trp-OH with 4-F-benzylamine, using HOBt and HBTU as coupling agents and DIPEA as base in a mixture of DCM/DMF, gave the amide intermediate **7**, which was then deprotected in DCM/TFA (3:1 v:v). The free amine **8** was subjected to a Pictet-Spengler reaction with formaldehyde or isovaleraldehyde or methyl-4-oxobutanoate or 4-oxobuthanoic acid in the above-described conditions, leading to the formation of THBC **9** (55% of yield) and the trans-cis mixtures **10-12a,b**. Flash chromatography allowed the separation of the corresponding trans **10-12a** (35-143% yields) and cis **10-12b** (33-43% yields) diastereoisomers. Based on 2D NMR correlations and considering the fixed configuration at C-3 as S, we assigned the configurations to the THBCs trans **10-12a** and cis **10-12b** as (1R,3S) and (1S,3S), respectively.

	R
9	H
10a,10b	$(CH_3)_2CHCH_2$-
11a,11b	$CH_3OCOCH_2CH_2$-
12a,12b	$HOCOCH_2CH_2$-
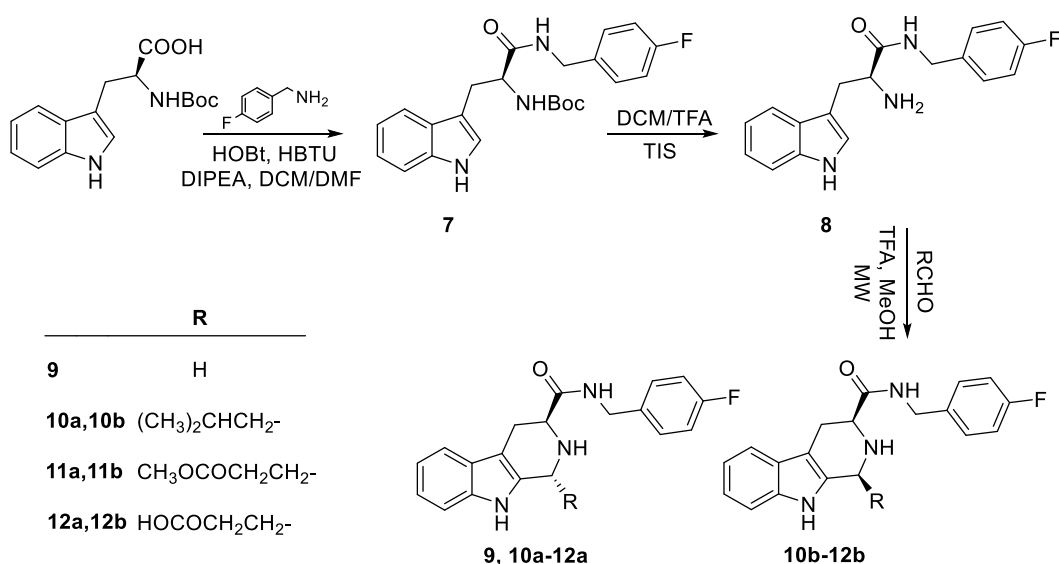
Scheme 2. Synthesis of the THBCs derivatives **9**, **10a-12a**, **10b-12b**.

2.3 Synthesis of II series

THBC derivatives **13**, **14a,b**, and **15a,b**, were obtained following the procedure described above by reaction of L-Trp-OMe with formaldehyde (**Scheme 3**), isovaleraldehyde, and 4-Cl-benzaldehyde (**Scheme 4**) respectively. Coupling of these intermediates with NHBoc-β-Ala-OH, NHBoc-Gly-OH, NHBoc-L-PheOH, or NHBoc-D-Phe-OH using HOBt, HBTU in DCM/DMF gave the pseudo dipeptide intermediates **16**, **18-20**, **24a,b**, and **26a,b** in 25-71% yields, respectively. Boc deprotection of the amino group in TFA acid medium of the derivatives **18-20**, **24a,b**, and **26a,b** followed by a spontaneous intramolecular cyclization provided the final THBC-based diketopiperazines **21-23**, **25a,b**, **27a,b** with 73-85% of yields. As expected, the treatment of **16** with TFA gave the unprotected derivative **17** in quantitative yield. To determine the relative configuration for the tetrahydropyrazino[1′,2′:1,6]pyrido[3,4-b]indole-1,4(6H,7H)- dione derivatives, the cross peak between H6 and H12a was investigated through ROESY NMR. For example, **27b** shows a cross peak between δ 6.16 ppm (H6) and δ 4.30 ppm (H12a, **Figure 16**) while this correlation is missing for the diastereoisomer **27a** (δ 6.67 ppm; δ 4.18 ppm, **Figure 18**). The absolute configuration was attributed considering the retention of the L-tryptophan chirality.
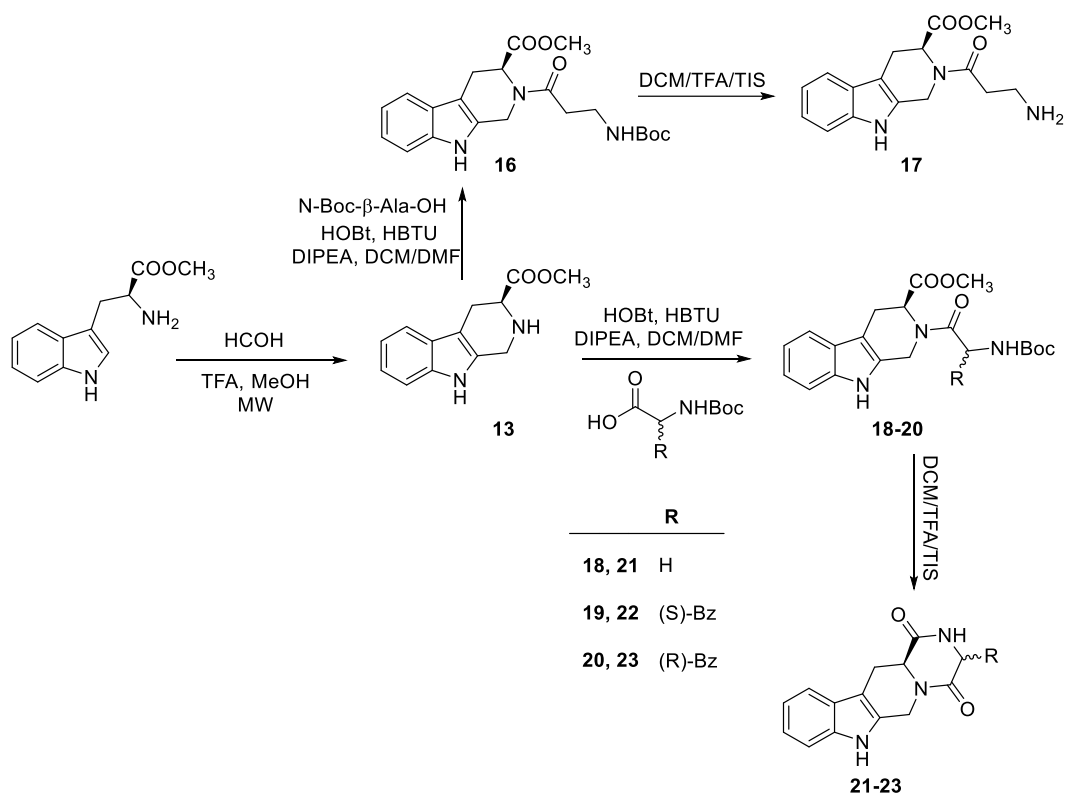
Scheme 3. Synthesis of the THBC derivative **17**, and THBC-based diketopiperazines derivatives **18-20**, **21-23**.
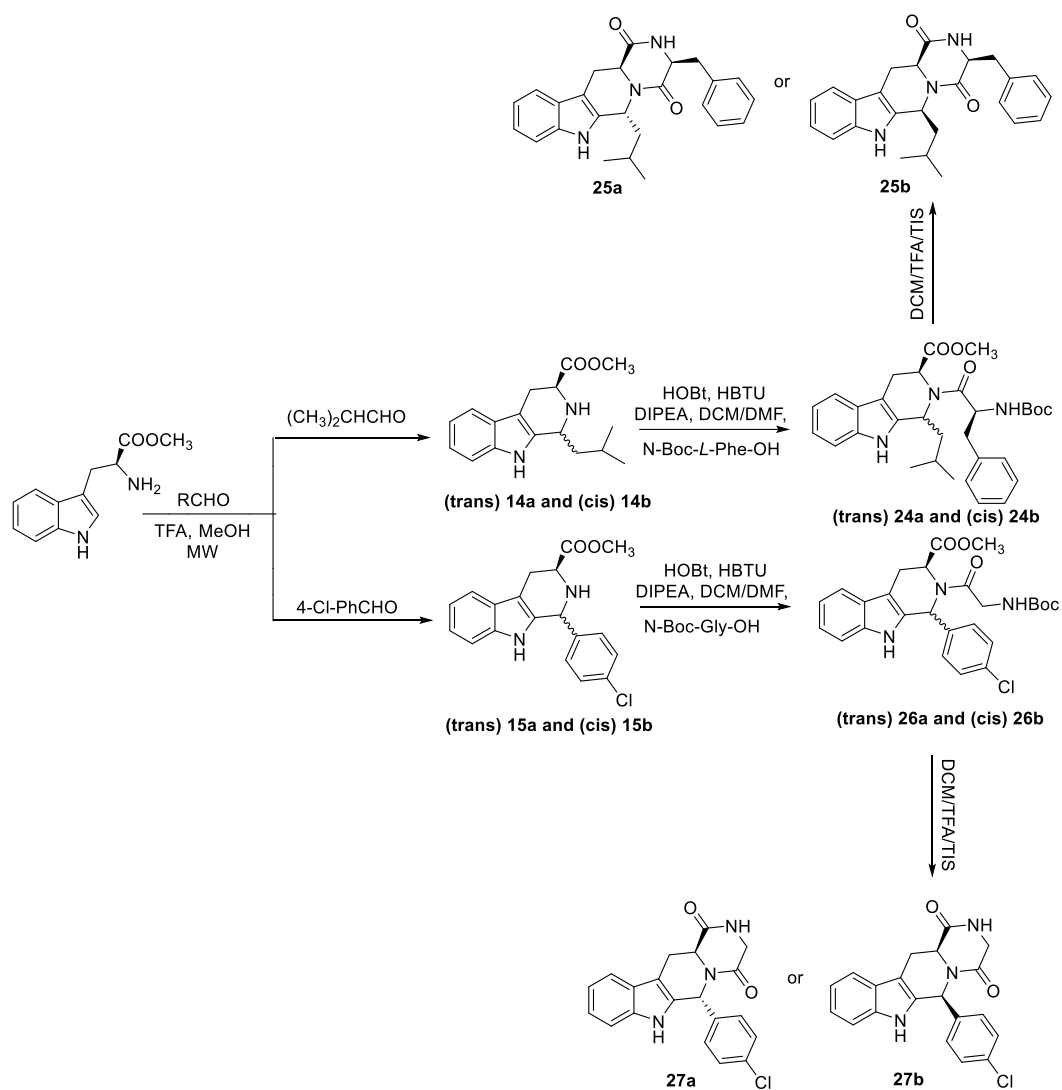
Scheme 4. Synthesis of the THBC-based diketopiperazines derivatives **25a-25b**, **27a-27b**.

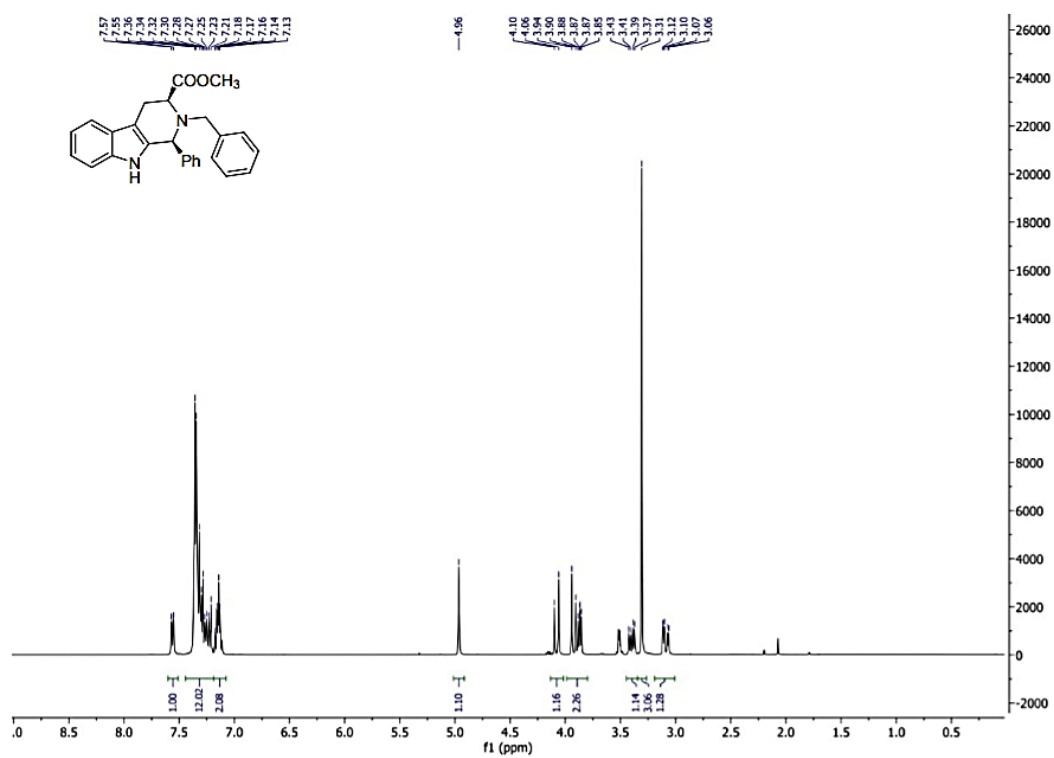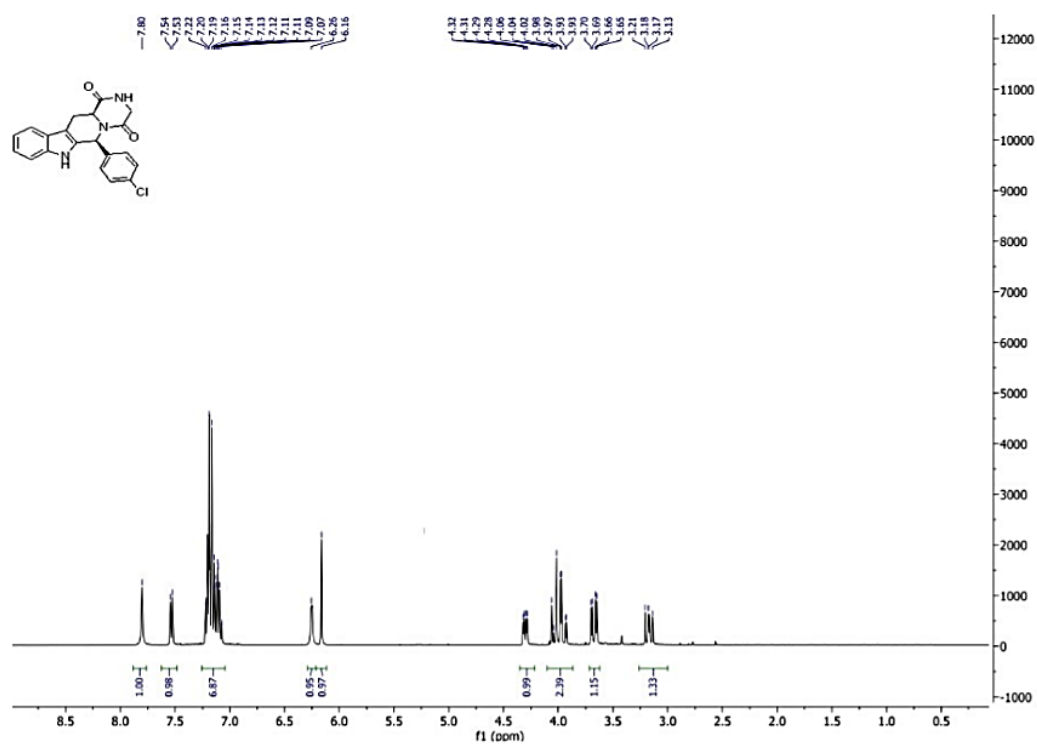**Figure 11.** ^{1}H NMR spectrum of compound **27b**.
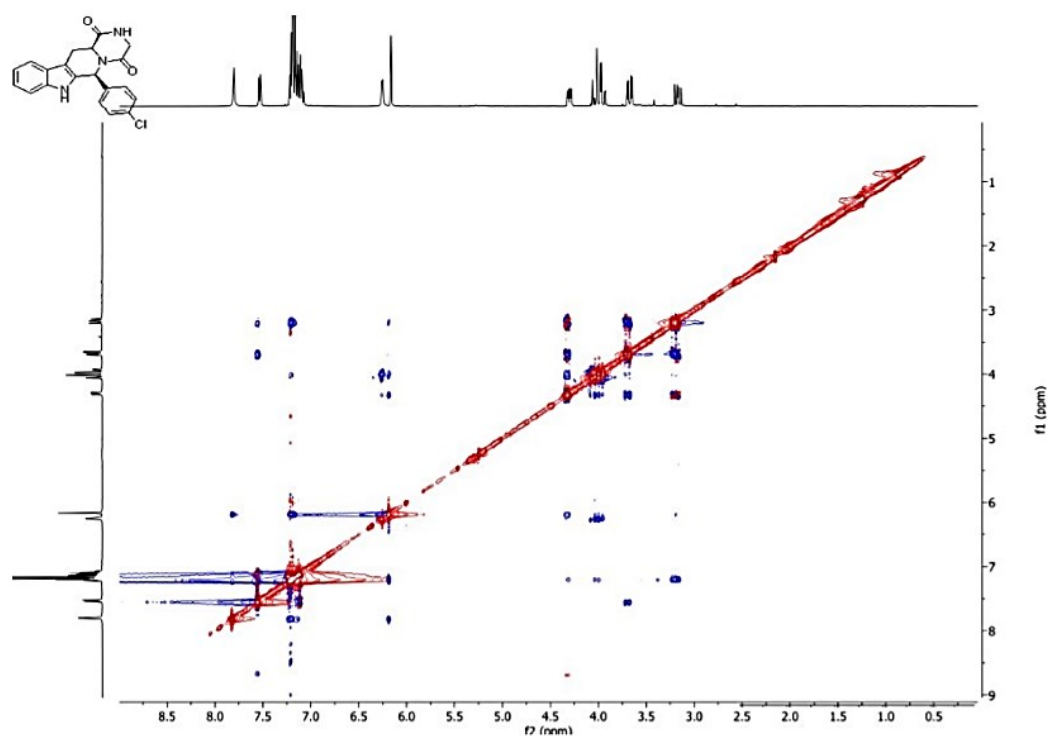
Figure 12. ROESY spectrum of compound **27b**.
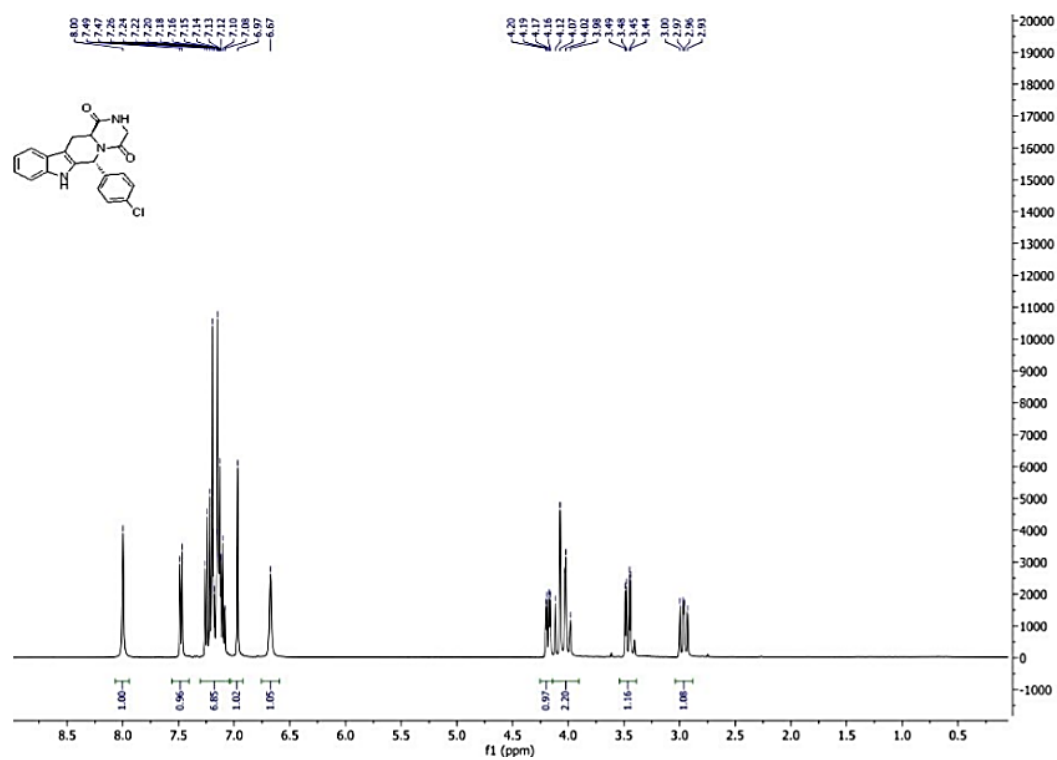
Figure 13. ^{1}H NMR spectrum of compound **27a**.
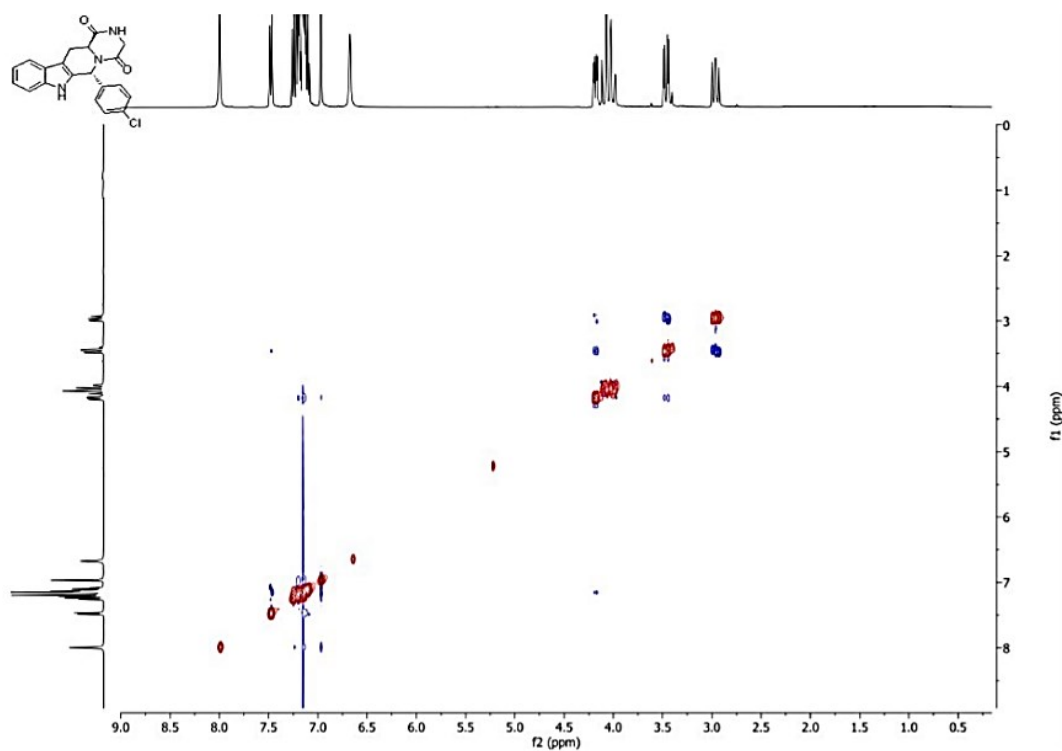
Figure 14. ROESY spectrum of compound **27a**.

2.4 Synthesis of III series

THBC-based hydantoin derivatives were obtained through the synthetic method reported in **Scheme 5**. Reaction of the starting THBCs **13**, **14a**, **14b**, **15a**, **15b** and the now synthesized **32a** and **32b** with triphosgene and different amines, such as 4-F, 4-OMe, 4-Me-benzylamine, benzylamine, and NHBoc propylendiamine in THF using TEA as base, led to the final hydantoin derivatives **28**, **29a-31a**, **29a′-31a′** (**Scheme 5**), and **33-34a**, **33-34a′** (**Scheme 6**) in one step with 35-62% yields. Removal of the Boc protecting group from **34a** and **34a′** using TFA and triisopopylsilane (TIS) in dichloromethane led to the final products **35a** and **35a′**, respectively (**Scheme 6**).
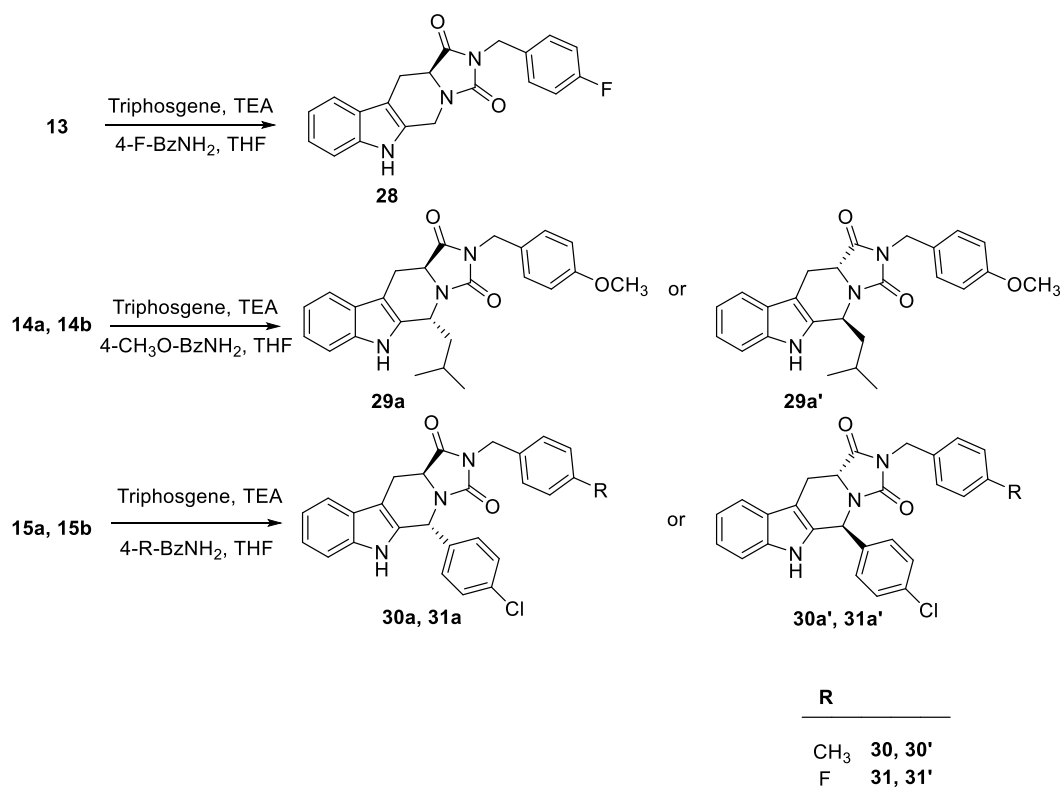
Scheme 5. Synthesis of the THBC-based hydantoin derivatives **28**, **29a-31a**, **29a′-31a′**.

R	
CH₃	30, 30'
F	31, 31'
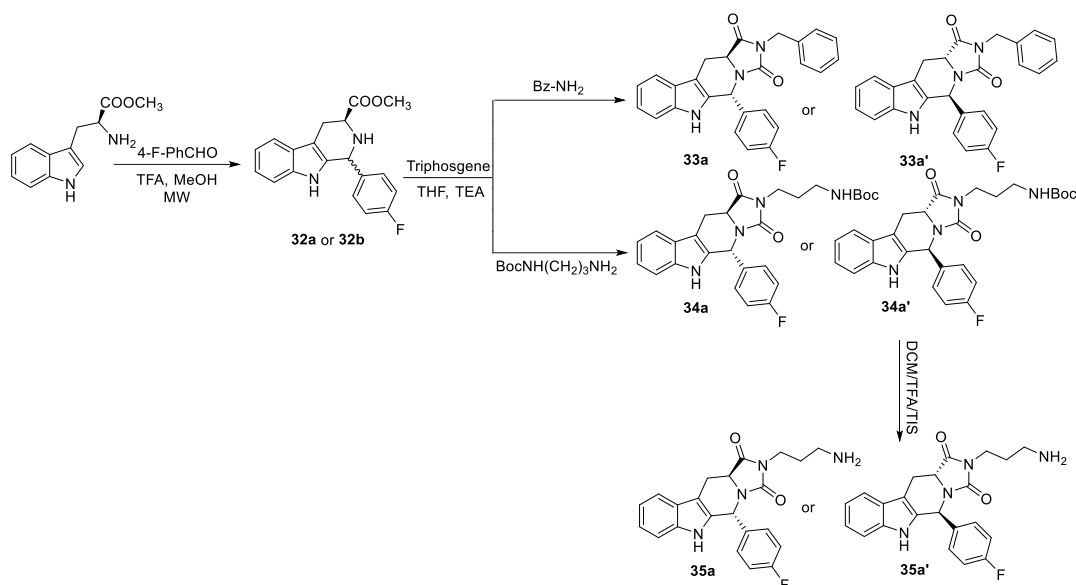
Scheme 6. Synthesis of the THBC-based hydantoin derivatives **33-34a**, **33-34a′**, **35a-35a′**.

NMR data, αD values, and circular dichroism experiments showed that the reaction of trans (1R,3S) THBCs **14a**, **15a**, and **32a** originated the trans derivatives (5R,11aS) **29a-31a**, **33a**, and **34a**, while the cyclization reaction from the cis analogues (1S,3S) **14b**, **15b**, and **32b** led to the formation of the trans enantiomers (5S,11aR) **29a′-1a′**, **33a′**, and **34a′**. For instance, the configuration of THBCs **15a** and **15b** was assessed by ROESY NMR, investigating the correlation between H3 and H1, assuming retention of configuration for the L-tryptophan moiety. As shown in **Figure 14**, only compound **15b** showed the investigated correlation (H1, δ 5.25 ppm; H3, δ 3.99 ppm). After cyclization reaction of **15b** to the hydantoin derivative (**30a′**) the cross peak between the same hydrogens (H11a δ 4.30 ppm, H5 δ 6.29 ppm) was not detected (**Figure 14**). This is in accordance with literature[82,83] that describes the epimerization at C-3 position of the (1S,3S) THBCs during the cyclization process, resulting in the formation of the most stable trans (5S,11aR) THBC-based hydantoin derivatives. Moreover, for all the THBC-based hydantoin enantiomeric couples, as expected, we observed the same NMR chemical shifts and opposite values for αD and specular circular dichroism spectra.
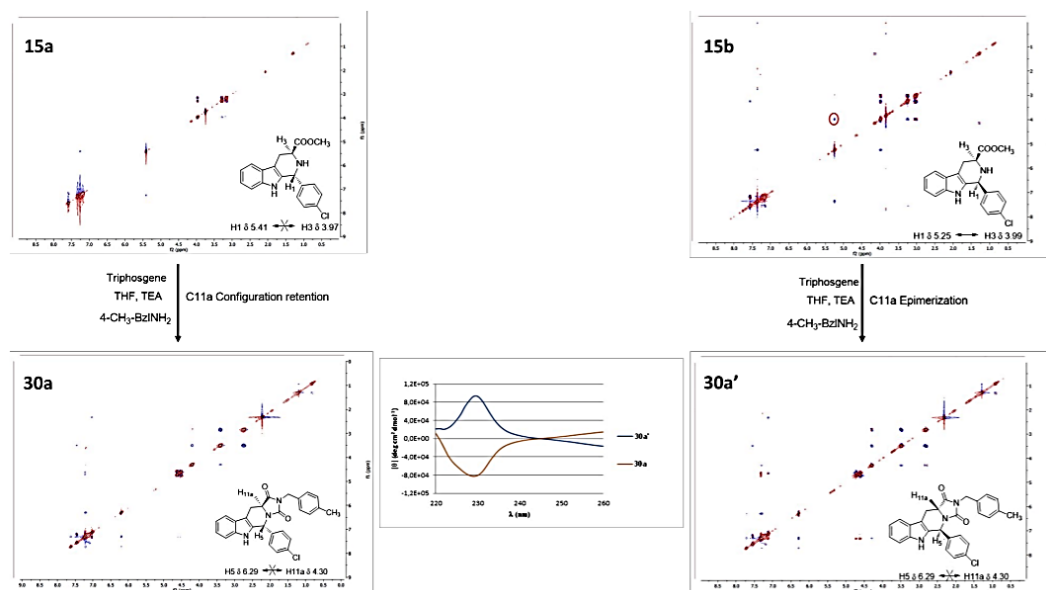
Figure 15. Attribution of the absolute configuration for derivatives **30a** and **30a'**.

On the other hand, **Scheme 7** reports the synthesis of the N-aryl hydantoin derivatives **36a-38a** and **36b-38b**. In this case, a different chemical approach is required because of the minor reactivity of anilines. Intermediates THBC **32a** and **32b** were coupled with 3-CF$_3$ or 2-F or 4-F-phenyl isocyanate in basic medium of TEA. In these conditions, we obtained the corresponding (5R,11aS) trans- and (5S,11aS) cis-hydantoins (**36a-38a** and **36b-38b**, respectively), which were isolated and characterized by 2D NMR spectroscopy. In particular, the cis configuration was evidenced by the correlation between H11a and H5, corresponding to δ 4.53 ppm and δ 5.86 ppm, respectively, for compound **36b** (**Figure 17**). Absolute configuration was determined as described above. In addition, the corresponding C-11a epimers **36a'-38a'** could be obtained directly by reaction of **32b** with the corresponding isocyanates and TEA at 60 °C for 30 min in 39-45% yields.
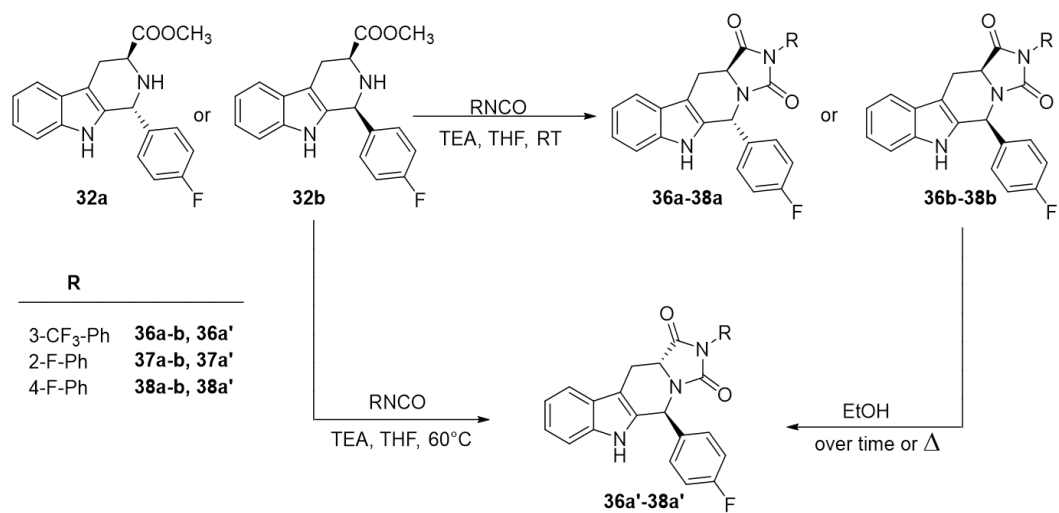
Scheme 7. Synthesis of the THBC-based hydantoin derivatives **36-38a**, **36-38b**, **36a'-38a′**.
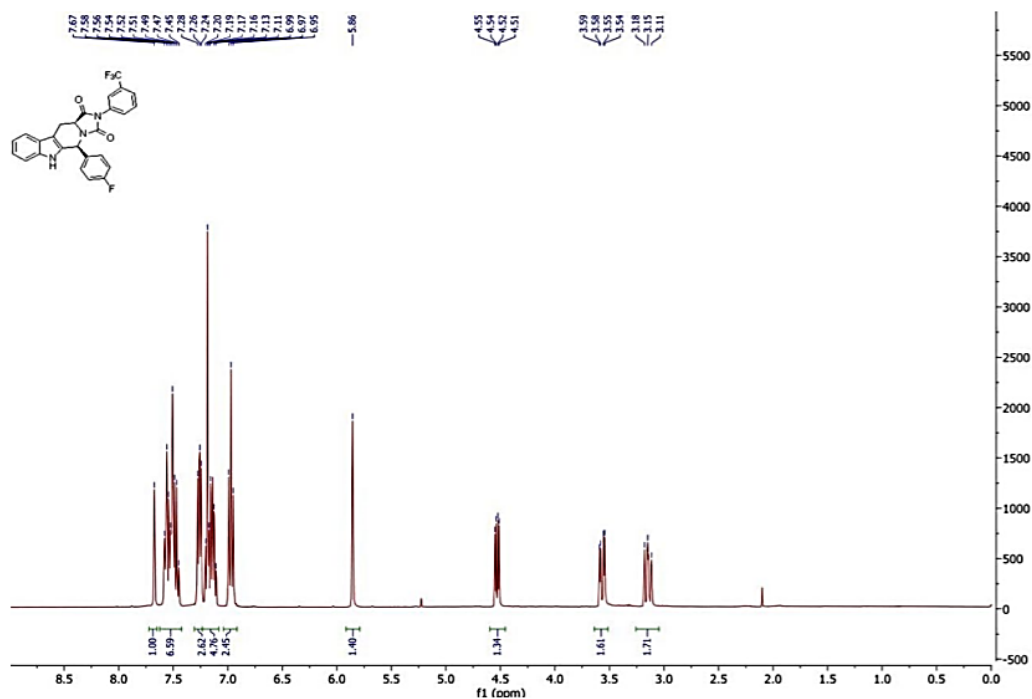
Figure 16. ^{1}H NMR spectrum of compound **36b**.
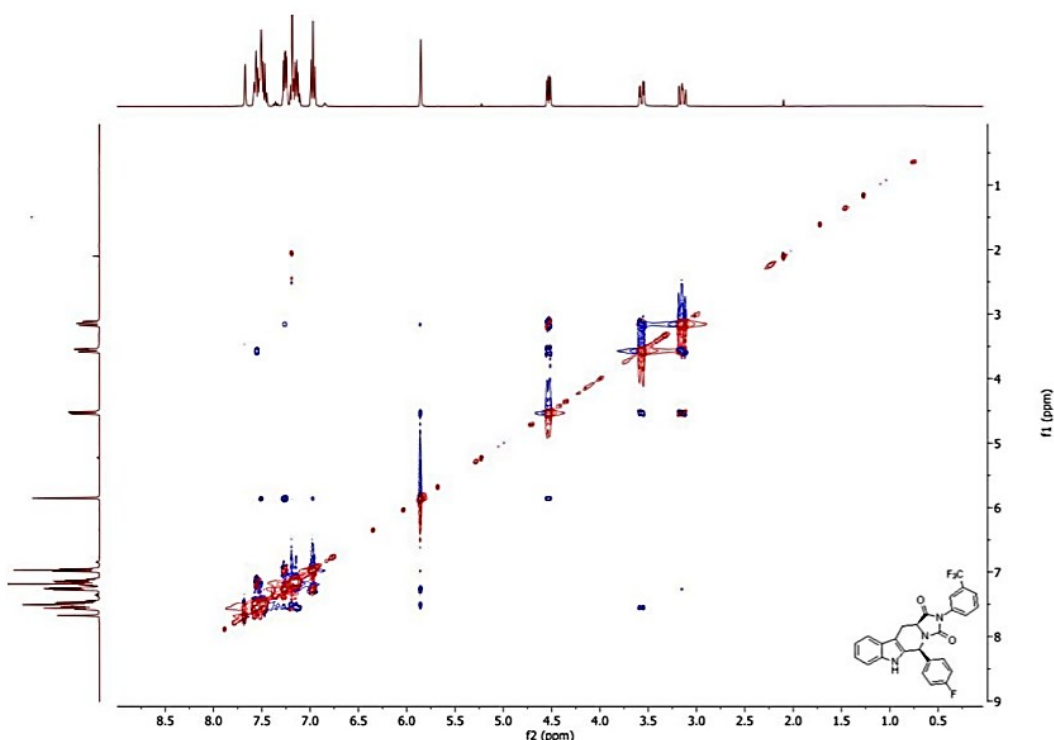
Figure 17. ROESY spectrum of compound **36b**.

The formation of the cis intermediates, which was not observed with the N-benzyl or N-alkyl analogs, can be explained by the increased stability of the kinetic control species due to the higher rigidity of this structure. However, C11a epimerization was not suppressed, and we noticed that the cis conformers converted to their thermodynamically more stable trans congeners (5S,11aR) **36a′-38a′**, with a conversion kinetic depending on experimental conditions. High temperatures and alcoholic solvents such as methanol and ethanol favored the conversion to the trans derivative, while in aqueous media at room temperature the cis conformers were more stable (**Figure 18**). Therefore, given the spontaneous trend of cis-hydantoins towards trans-conversion, we considered inappropriate the pharmacological testing of all the cis isomers and we decided to assay only **36b** for its pharmacological activity, due to its higher stability in water environment in comparison with its congeners **37b** and **38b**, which were almost fully converted to the trans isomers during 60 min regardless of the solvent used (**Figure 18**).
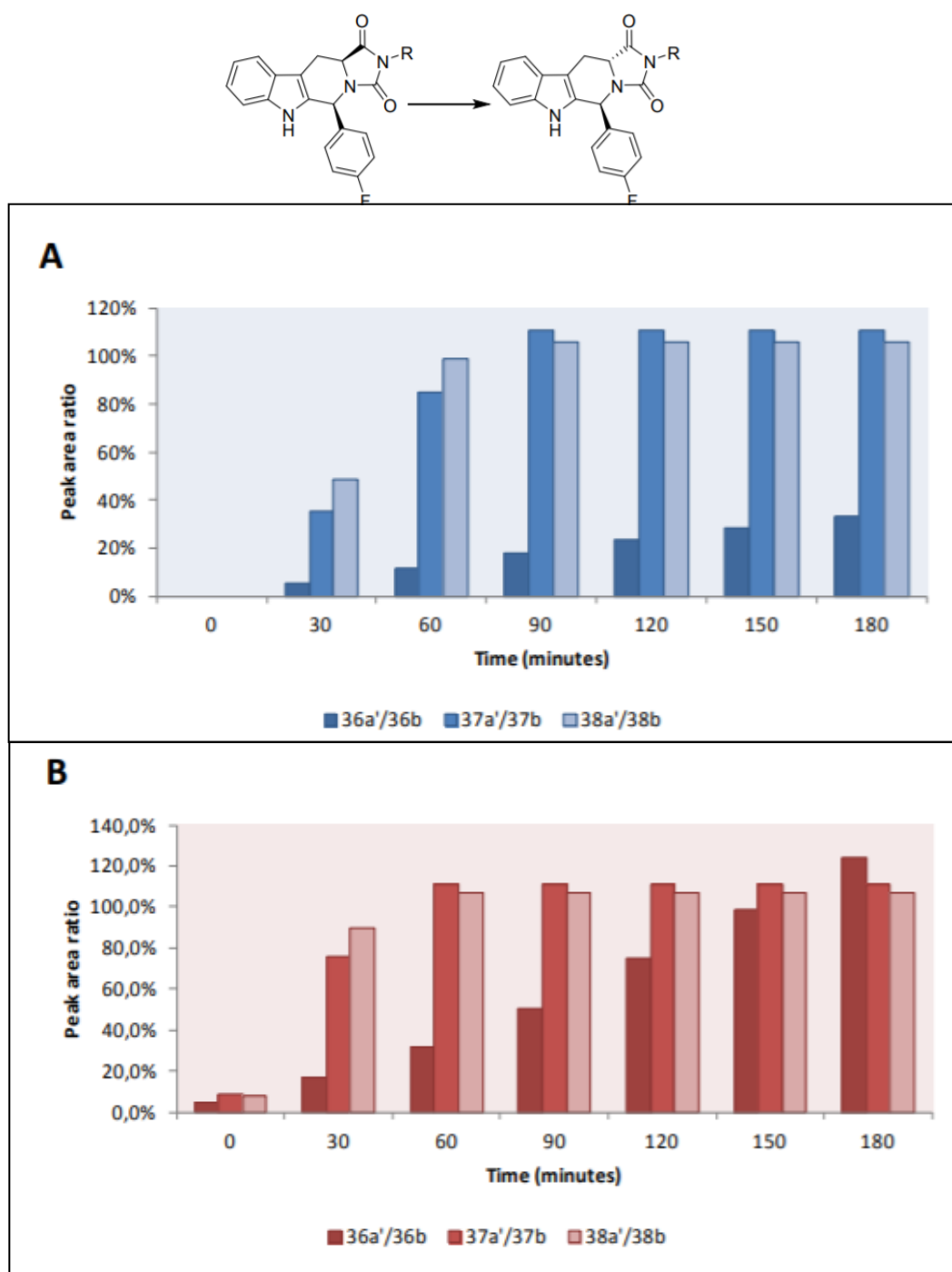
Figure 18. Time-course trans-(**36a'-38a'**)/cis-(**36b-38b**) HPLC peak area ratio in physiological buffer (PBS, panel A) and methanol (Panel B).

3.1 Activity evaluation of series I-III

3.1.1 Screening by Ca²⁺-imaging experiments

TRPM8 blocker activity of all synthesized compounds was tested by Ca^{2+} fluorimetric assays using HEK-293 cells stably expressing the rat isoform of TRPM8 channels, using menthol and AMTB as prototypical agonist and antagonist, respectively. All the compounds were tested by research group of Prof. Asia Fernandez Carvajal at the Institute of Molecular and Cellular Biology of University Miguel Hernández of Elche and showed an antagonist activity higher than the canonical TRPM8 antagonist AMTB, although lower than the lead compound **4** with IC_{50} values in the 100-0.3 μM range (**Table 1**). In the 1,2,3-substituted THBCs (**6, 9-12**, and **17**) series, the antagonist activity is conditioned by the relative configuration at position 1 when long and linear aliphatic chains are used. Thus, the trans derivatives (1R,3S) **11a** and **12a** are around 4 times more active than the corresponding cis diastereoisomers (1S,3S) **11b** and **12b** (IC_{50} = 1.1 μM and 3.0 μM for the **11a** and **11b**, respectively, and 5 μM and 22 μM for **12a** and **12b**, respectively). The influence of the configurational pattern was not observed for other diastereoisomer couples bearing bulkier alkyl or planar aryl substituents in C-1 (**6a/6b**, **10a/10b**). Indeed, the unsubstituted derivative at position C-1 (**9**) had an interesting antagonistic activity with an IC_{50} value of 0.9 μM, while the restricted pseudo dipeptide Trp-β-Ala **17**, bearing a polar 3-aminopropanoic chain in position 2, was completely inactive (IC_{50} > 100 μM). Further expansion of the structure from TBHCs to diketopiperazines (**21-23**, **25a/b**, **27a/ b**) retained the antagonist activity. The unsubstituted TBHC-based diketopiperazine **21**, for instance, maintained good potency (11.4 μM), but the introduction of a benzyl substituent at C-3 (**22**, **23**, and **25**) significantly increased activity with IC_{50} value in the range 4-0.4 μM. In this case, the configuration at position 3 did not significantly influence compound potencies that were comparable for the (3R,12aS) diastereoisomer **23** and its 3-epimer (3S,12aS) **22** (IC_{50} = 1.6 ± 0.7 μM and 0.4 ± 0.1 μM, respectively). The trans derivative **25a** (3S,6R,12aS) bearing the isobutyl moiety at C-6 was significantly less potent than its cis diastereoisomer **25b** (3S,6S,12aS) (IC_{50} = 4.1 ± 1.1 μM vs 1.3 ± 0.6 μM), while the introduction of the 4-Cl-phenyl moiety at position C-6 (**27**) was well tolerated and no differences in potency were evidenced between the 6R,12aS and the 6S,12aS isomers (**27a** and **27b**, IC_{50} = 1.5 ± 1.1 μM and 1.7 ± 0.8 μM, respectively). Finally, the diketopiperazines ring was simplified to the five membered hydantoin system. For this series (**28**, **29a-31a**, **33a**, **35a**, **36a-38a**, **36b** and their enantiomers **29a′-31a′**, **33a′**, **35a′-38a′**) the most active compounds **30a** and **31a**, with IC_{50} in the range 0.5-0.8 μM, feature an aromatic group at C-5 position and a benzyl group at N-2 and retain the trans configuration, 5R,11aS. The unsubstituted compound **28** and the C-6 alkyl derivative **29a**

showed reduced potency. On the other hand, the N-benzyl trans isomers (5S,11aR) **29a′-31a′**, **33a′, 35a′**, were less active than their corresponding trans 5R,11aS enantiomers. This difference was not statistically significant for the N-aryl derivatives (**37a/37a′** and **38a/38a′**) except for the compound **36a** (5R,11aS), containing a 3-trifluoromethyphenyl substituent at N2, which was about 3-fold more potent than its enantiomer **36a′** (5S,11aR) (IC$_{50}$ = 2.8 µM and 7.8 µM, respectively). Compound **36b**, the only tested cis derivative of this series, showed a remarkable higher potency (IC$_{50}$ = 0.2 µM) than its two trans analogues **36a** and **36a′**.

Table 1. IC$_{50}$ values for the compounds obtained by calcium imaging assay on HEK293 cells. Compound **4** and AMTB are used as references. [a] = Data are given as mean ± DS. Compounds more potent are in the boxes highlighted in red.

compd	R	R$_1$	R$_2$	configuration	IC$_{50}$ (μM)[a]
4					0.09 ± 0.08
6a	OCH$_3$	C$_6$H$_5$	CH$_2$C$_6$H$_5$	1R, 3S	1.3 ± 0.7
6b	OCH$_3$	C$_6$H$_5$	CH$_2$C$_6$H$_5$	1S,3S	1.6 ± 0.9
9	NHCH$_2$(4-F)Ph	H	H	3S	0.9 ± 0.4
10a	NHCH$_2$(4-F)Ph	CH$_2$CH(CH$_3$)$_2$	H	1R,3S	4.6 ± 1.3
10b	NHCH$_2$(4-F)Ph	CH$_2$CH(CH$_3$)$_2$	H	1S,3S	6.2 ± 1.2
11a	NHCH$_2$(4-F)Ph	CH$_2$CH$_2$COOCH$_3$	H	1R,3S	1.1 ± 0.5
11b	NHCH$_2$(4-F)Ph	CH$_2$CH$_2$COOCH$_3$	H	1S,3S	3.0 ± 1.2
12a	NHCH$_2$(4-F)Ph	CH$_2$CH$_2$COOH	H	1R,3S	5.0 ± 1.2
12b	NHCH$_2$(4-F)Ph	CH$_2$CH$_2$COOH	H	1S,3S	22.0 ± 1.4
17	OCH$_3$	H	COCH$_2$CH$_2$NH$_2$	3S	>100
21		H	H	12aS	11.4 ± 1.6
22		H	CH$_2$C$_6$H$_5$	3S,12aS	1.6 ± 0.7
23		H	CH$_2$C$_6$H$_5$	3R,12aS	0.4 ± 0.1
25a		CH$_2$CH(CH$_3$)$_2$	CH$_2$C$_6$H$_5$	3S,6R,12aS	4.1 ± 1.1
25b		CH$_2$CH(CH$_3$)$_2$	CH$_2$C$_6$H$_5$	3S,6S,12aS	1.3 ± 0.6
27a		4-Cl-C$_6$H$_4$	H	6R,12aS	1.5 ± 1.1
27b		4-Cl-C$_6$H$_4$	H	6S,12aS	1.7 ± 0.8
28		H	CH$_2$4-(F)-C$_6$H$_4$	11aS	17.8 ± 1.2
29a		CH$_2$CH(CH$_3$)$_2$	CH$_2$4-(OCH$_3$)C$_6$H$_4$	5R,11aS	2.8 ± 1.2
29a′		CH$_2$CH(CH$_3$)$_2$	CH$_2$4-(OCH$_3$)C$_6$H$_4$	5S,11aR	22.9 ± 1.4
30a		4-(Cl)C$_6$H$_5$	CH$_2$4-(CH$_3$)C$_6$H$_4$	5R,11aS	0.8 ± 0.4
30a′		4-(Cl)C$_6$H$_5$	CH$_2$4-(CH$_3$)C$_6$H$_4$	5S,11aR	2.3 ± 0.8
31a		4-(Cl)C$_6$H$_5$	CH$_2$4-(F)-C$_6$H$_4$	5R,11aS	0.5 ± 0.3
31a′		4-(Cl)C$_6$H$_5$	CH$_2$4-(F)C$_6$H$_4$	5S,11aR	>30
33a		4-(F)C$_6$H$_5$	CH$_2$C$_6$H$_4$	5R,11aS	6.4 ± 1.2
33a′		4-(F)C$_6$H$_5$	CH$_2$C$_6$H$_4$	5S,11aR	17.5 ± 1.4
35a		4-(F)C$_6$H$_5$	(CH$_2$)$_3$NH$_2$	5R,11aS	5.1 ± 1.2
35a′		4-(F)C$_6$H$_5$	(CH$_2$)$_3$NH$_2$	5S,11aR	27.2 ± 1.4
36a		4-(F)C$_6$H$_5$	3-(CF$_3$)C$_6$H$_4$	5R,11aS	2.8 ± 1.5
36a′		4-(F)C$_6$H$_5$	3-(CF$_3$)C$_6$H$_4$	5S,11aR	7.8 ± 2.4
36b		4-(F)C$_6$H$_5$	3-(CF$_3$)C$_6$H$_4$	5S,11aS	0.2 ± 0.2
37a		4-(F)C$_6$H$_5$	2-(F)C$_6$H$_4$	5R,11aS	4.4 ± 1.3
37a′		4-(F)C$_6$H$_5$	2-(F)C$_6$H$_4$	5S,11aR	5.1 ± 2.1
38a		4-(F)C$_6$H$_5$	4-(F)C$_6$H$_4$	5R,11aS	6.7 ± 1.2
38a′		4-(F)C$_6$H$_5$	4-(F)-C$_6$H$_4$	5S,11aR	7.2 ± 0.9
AMTB					7.3 ± 1.5
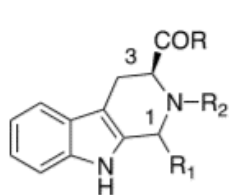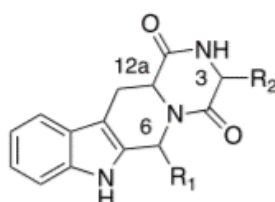
6a, 6b, 9, 10-12 a,b, 17   21-23, 25a,b, 27a,b   28-31,33,35-38, 29'-31',33', 35'-38'
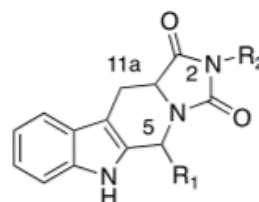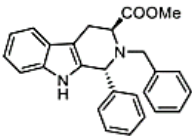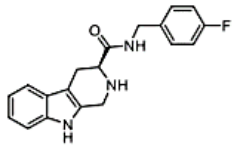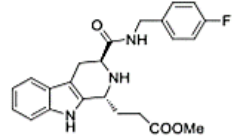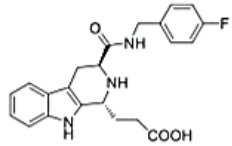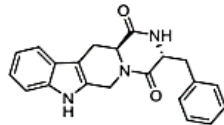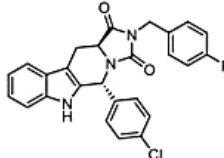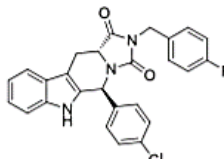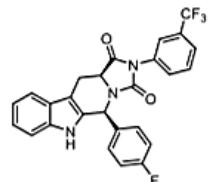
3.1.2 Patch-clamp electrophysiology

Functional assays were conducted by research group of Prof. Asia Fernandez Carvajal at the Institute of Molecular and Cellular Biology of University Miguel Hernández of Elche. There were identified derivatives **6a**, **9**, **11a**, **23**, **31a**, and **36b** to be among the most effective and potent TRPM8 antagonist compounds with IC_{50} values in the submicromolar range. To provide direct evidence for this activity, these derivatives were tested in HEK-293 cells transiently expressing the human TRPM8 isoform by whole-cell voltage clamp experiments. Moreover, we decided to perform whole-cell voltage clamp experiments also for compounds **12a** and **31a′** in order to further highlight the pharmacophoric properties of the ester group in **11a** and of the stereocenters of **31a**. As shown in **Table 2**, the well-known TRPM8 antagonist BCTC (300 nM), used as reference, produced a complete inhibition of menthol gated TRPM8 currents, with an IC_{50} of 501 nM. THBC-based diketopiperazine **23** and the hydantoin derivatives **31a** have concentration-dependent antagonistic activity, showing IC_{50} of 6.57 ± 1.21 nM and of 4.10 ± 1.52 nM, respectively. The THBC **6a** and **9** showed decreased potency. The propanoic ester derivative **11a**, identified as a potent inhibitor of menthol induced increase of intracellular Ca^{2+} levels (IC_{50} = 0.8 μM), antagonized the effect of menthol with an EC_{50} of 15.41 nM, while its acid free analogue **12a** inhibited only 34% of the menthol-induced current at the maximum concentration of 300 nM. To determine the role of the relative configuration at the stereocenters in the hTRPM8-blocking activity of compound **31a**, the pharmacological effect of its 5S,11aR enantiomer, namely, **31a′**, was also investigated. As shown in **Table 2**, **31a′** weakly inhibited menthol-induced currents showing very weak efficacy when compared to the 5R,11aS enantiomer, therefore confirming the crucial role of the configurations in the pharmacological properties of this series of compounds. The activity of compound **36b**, which proved to be a powerful antagonist of TRPM8 in Ca^{2+} fluorimetric assay, was confirmed by patch clamp experiment with an IC_{50} of 7.67 nM, and an inhibition efficacy of the menthol evoked currents of 59.4%. In light of the reported spontaneous epimerization of the cis isomer **36b** to its trans congener (**36a′**) we hypothesized that the cis-isomer contributed mainly to this pharmacological activity. Thus, **36b** was assayed in a time course stability test, and results confirmed that the percentage of epimerization was negligible during patch-clamp electrophysiology assays (**Figure 18**).

Table 2. I*n vitro* pharmacological characterization for selected compounds through patch-clamp assay. Data are given as mean ± DS.

Comp.	Structure	IC$_{50}$ Ca^{2+} (µM)	% Inhibition 300 µM menthol-evoked currents at 300 nM compounds	IC$_{50}$ (nM)
6a		0.9±1.9	62.5 ±2.3	12.30±4.21
9		0.9±0.4	59.4±6.6	36.85±8.04
11a		1.1 ±0.5	62.1±4.2	15.46±5.63
12a		5.0 ±1.2	34.1±9.6	n.a.
23		0.4 ±0.1	61.1±6.3	6.57±1.21
31a		0.6 ±1.2	61.7±8.7	4.10±1.52
31a'		>30	11.6±3.6	n.a
36b		0.2 ±0.2	59.4±9.7	7.67±1.74

3.1.3   Selectivity studies

Selectivity assays were conducted by research group of Prof. Asia Fernandez Carvajal at the Institute of Molecular and Cellular Biology of University Miguel Hernández of Elche. The most potent compounds identified by patch clamp studies (**6a**, **9**, **11a**, **23**, **31a**, and **36b**) were subjected to further in vitro characterization by assessment of their selectivity toward TRPV1, TRPA1, and $Na_{v1.7}$ channels by calcium fluorimetric experiments. All the derivatives were unable to modulate these channels, showing no activity as agonists or antagonists. Only compounds **6a** and **9** showed a negligible antagonistic activity over $Na_{v1.7}$ with $IC_{50} > 10$ μM.

3.1.4   In vitro metabolic studies

In vitro metabolic studies were conducted by my research group. The most potent compounds analyzed by patch-clamp electrophysiological assays were further characterized for their metabolic stability using human liver microsomes as *in vitro* model. Compound **4** was used as reference, considering that its main pitfall was represented by metabolic instability that the newly synthesized compounds were aimed in overcoming. As shown in **Figure 19**, almost all the compounds proved to be stable in the absence of metabolic cofactors (NADPH or UDP-GlcUA/NADPH) except for **11a**, showing unspecific metabolic liability. When the phase I metabolism conditions were mimicked, compound **4** was massively metabolized with a turnover percentage of $98.3 \pm 3.1\%$ (**Figure 19**), in accordance with our previously reported data.[80] Indeed, the newly synthesized analogues showed improved metabolic stability with a metabolic turnover in the range 1.1-72.0% under phase I metabolism conditions. In particular, compound **31a** with a phase I metabolic turnover of $26.5 \pm 3.9\%$ was the most stable compound. For these reasons, stability of derivative **31a** was further challenged using a different protocol that involved both phase I and phase II metabolic cofactors. As shown in **Figure 19**, **31a** proved to have a slow metabolic turnover ($46.0 \pm 2.3\%$) in the experimental conditions used and was then selected for the *in vivo* pharmacological assays.
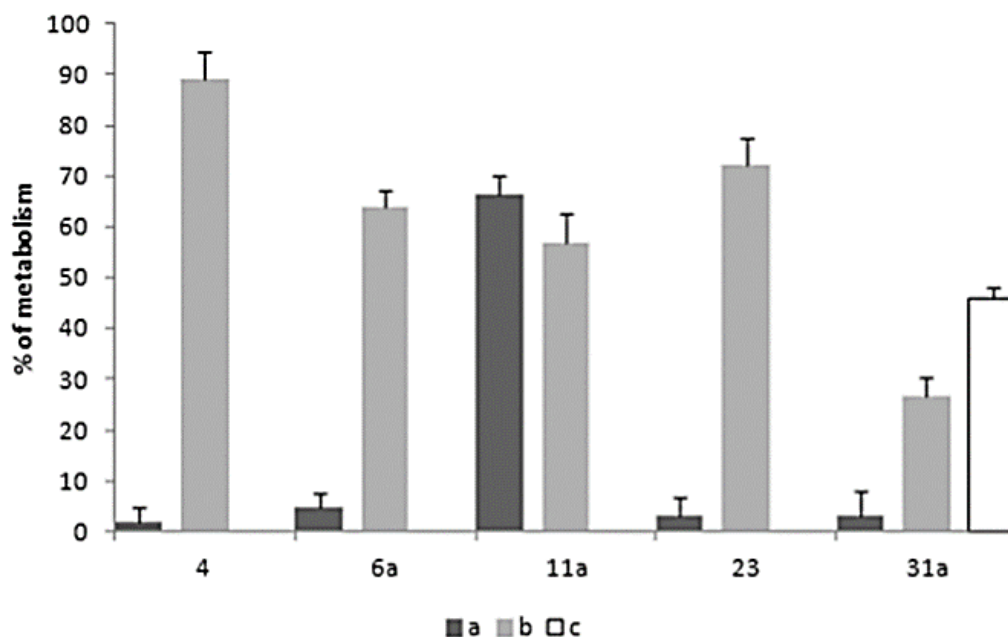
Figure 19. *In vitro* metabolic stability assays for the selected compounds: (a) compounds' unspecific metabolism in absence of cofactors calculated as ([ ]t60/[ ]t0) × 100, black bars; (b) compounds' metabolic stability under phase I metabolism (gray bars, protocol I; see materials and methods section); (c) compound **31a** metabolic stability under phase I + phase II metabolism.

3.1.5 In vivo studies
3.1.5.1 Icilin-induced WDS

Initially, we have evaluated the capability of TRPM8 antagonist **31a** in blocking the spontaneous wet-dog shake (WDS) induced by icilin in comparison with its precursor derivative **4** at equimolar doses. Icilin-induced WDS was conducted by research group of Prof. Roberto Russo (University of Naples "Federico II"). Due to the difference in metabolic stability, a prolonged pharmacological effect of **31a** was expected. For this purpose, **4** and **31** were administrated 30 min before the challenge with icilin (1 mg/kg ip) and WDS was recorded for 30 min. In the vehicle-treated group, a mean of about 128 shakes were counted (**Figure 20**, white column). As expected, from the metabolic stability experiments, the pretreatment with **4** (10 mg/kg ip) significantly decreased the number of icilin-induced WDS 0.5 h after the injection (Figure 5; **$p < 0.01$ vs vehicle treated mice); no effect was observed at 2 h. On the contrary, **31a** (11.5 mg/kg ip) showed a significant effect at both 0.5 and 2 h after the injection (Figure 5; *$p < 0.05$ and **$p < 0.01$ vs vehicle treated mice).
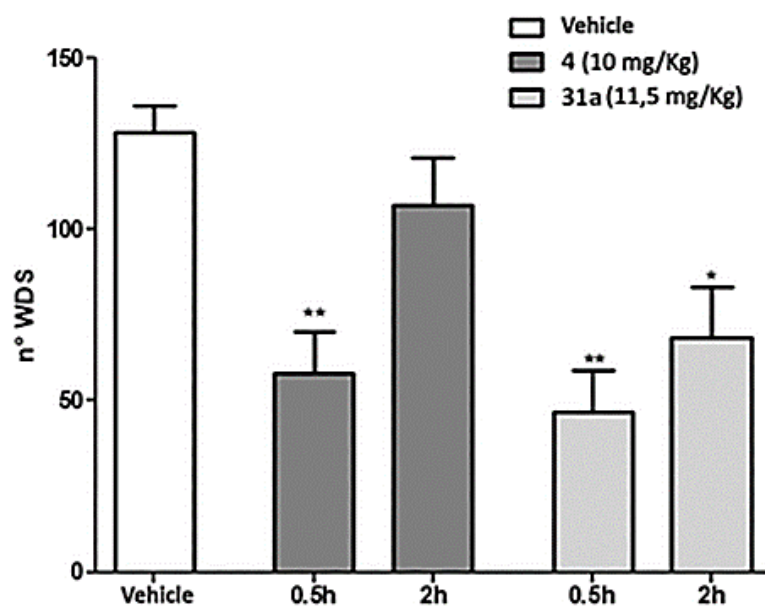
Figure 20. Comparative effect of **4** and **31a** on icilin-induced WDS in Swiss CD1 mice. After ip injection of icilin (10 mg/kg), the number of wet-dog shakes (WDS) were counted over 30 min. Data are given as the mean ± SEM n = 6, two-way ANOVA with Bonferroni post hoc test: $*p < 0.05$; $**p < 0.01$.

3.1.5.2 Oxaliplatin-induced neuropatic pain model

TRPM8 plays a critical role in mouse models of chemotherapy-induced neuropathic pain evoked by oxaliplatin (OXP), a condition mimicking cold hypersensitivity provoked by chemotherapy-induced peripheral neuropathy (CIPN). Both acute and chronic OXP-induced cold hypersensitivity has been reproduced in rats and correlated with TRPM8 expression and function. Mizoguchi *et al.*[84] reported that in a rodent model, acute cold allodynia after OXP injection was alleviated by the TRPM8 blockers N-(2-aminoethyl)-N-[4-(benzyloxy)-3-methoxybenzyl]-N′-(1S)-1-(phenyl)ethyl]urea and TC-I 2014. According to these findings, we investigated the effect of our antagonist **31a** in an OXP-induced cold allodynia model, using acetone for cooling stimulation. The assay was conducted by research group of Prof. Roberto Russo (Department of Pharmacy, University Federico II of Naples). Considering that the cold pain threshold is increased from ≈12 °C to ≈26 °C in OXP-treated patients, acetone stimulation is considered to evoke pain in OXP-treated mice. The activity of compound **31a** was evaluated 7 days after three intraperitoneal injections of OXP (6 mg/kg) in C57/BL6 mice, when cold allodynia had developed. As shown in **Figure 21**, a single subcutaneous administration of 1 μg of **31a** was not effective in inhibiting the (OXP)-induced cold allodynia, whereas injections of 10 and 30 μg of our compound showed a remarkable inhibitory effect, which was maximum

after 15 min. This effect was still evident 30 min after administration of a 30 µg dose (**Figure 21**). These data suggest that **31a** may be a viable therapeutic scaffold for the treatment of CIPN.
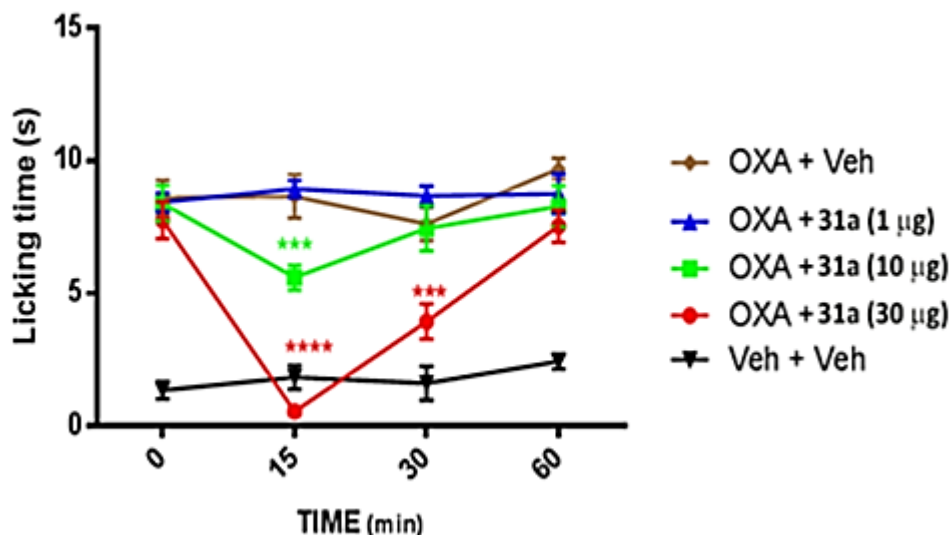
Figure 21. Dose-dependent inhibition of nocifensive paw licking given by compound **31a** (1, 10, and 30 µg, sc) in oxaliplatin-induced cold allodynia in C57/BL6 mice. Data are given as the mean ± SEM n = 6. Statistical analysis was two-way ANOVA followed by post hoc Bonferroni test by multiple comparison: ***$p < 0.001$, ****$p < 0.0001$.

3.1.5.3 Thermal ring assay

Further we investigated the efficacy of **31a** in a chronic constriction injury (CCI) model of neuropathic pain, using a thermal gradient ring assay. This assay deeply differs from the canonical reflexive measures of nociception, in which the end point is withdrawal to a noxious stimulus, a fact that has been questioned during the past years for their unsatisfactory translation.[85] In particular, this test integrates information on temperature perception distinguishing exploratory behavior from thermal preference behavior.[86a] Thus, we measured the thermal preference location of sham, CCI-mice, and CCI-mice treated intraperitoneally with **31a** in a thermal gradient assay equilibrated between 15 and 40 °C. The mean temperature to which the sham animal located during the observation time was 27.9 °C ± 0.35 °C (**Figure 22A**), and no statistical differences were evidenced at the different time points (**Figure 22B**). No effects on temperature preferences were observed after **31a** administration in sham mice (data not shown). This value slightly differs from the previously reported by Touska *et al*.[86a] but is consistent with gender, age, and strain differences within animals used. The same temperature preference was observed in CCI-mice 7 days after ligation (mean preferred

temperature 25.88 °C ± 1.08 °C, for CCI mice, p = 1.452 vs sham mice, **Figure 22A** and **Figure 22B**). However, 14 days after ligation, when the neuropathic pain and the related nociceptive disorders are well-known to occur,[86b,c] the CCI animals displayed a marked preference for colder areas (mean temperature = 22.80 °C ± 0.61 °C, *p < 0.05 vs sham mice, **Figure 22A**), which was most prominent during the first 45 min of exposure as shown in **Figure 22B** (**p < 0.01 vs sham mice) and extending to 60 min. This is in accordance with the cold-seeking behaviors reported during inflammatory states.[86d] Considering that thermosensation is mediated by the primary afferent Aδ and C fibers,[86e] where TRPM8 is particularly represented, its role in the cold seeking behaviors of CCI animal seems evident. In fact, intraperitoneal administration of the TRPM8 antagonist **31a** (11.5 mg/kg) significantly reverted this behavior to 33.30 °C ± 1.44 °C (**Figure 22A**; °p < 0.05 vs CCI 14 days). Similar enhanced thermal tolerance has been recently reported when the antihyperalgesic drug clonidine was administered in a CCI mouse model.[85] Moreover, the mice behavior is also in accordance with previous data that describe TRPM8 deficient mice (TRPM8−/−) as rather preferring warmer than colder areas.[86a] It should be noted that mice treated with **31a** immediately recognized warmer zones as preferable to colder areas compared to vehicle CCI-mice (Figure 7B; °°°p < 0.001 and °°°°p < 0.0001 vs CCI-mice) also showing a preference for an even warmer temperature than sham animals during the first 15 min (Figure 7B; # p < 0.05 vs sham mice). It is questionable why this transient effect was recorded, but it must be considered that TRPM8 antagonists are able to decrease the body temperature. This effect could probably account for the thermal preference expressed by animals treated with **31a** at 15 min. The efficacy and the rapid onset of action further confirm the efficacy of compound **31a** as TRPM8 antagonists.
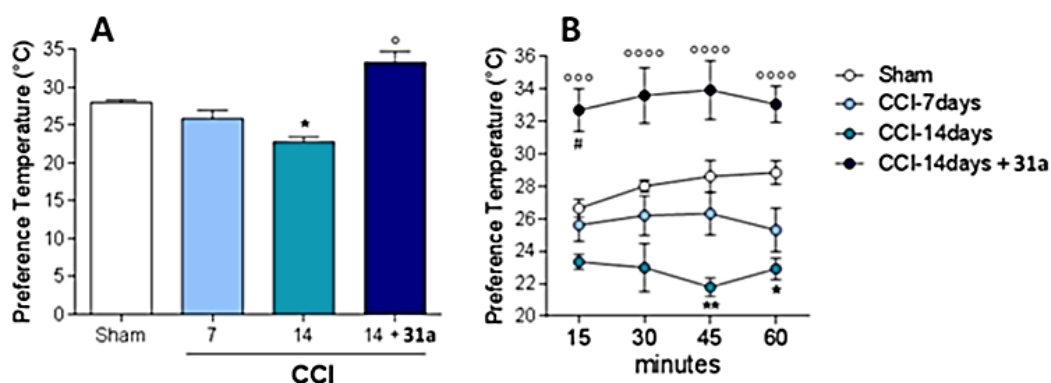
Figure 22. (A) Thermal preference behavior of Swiss CD1 mice 7 days (light blue bar) and 14 days (green bar) after CCI. The blue bar represents the effect of compound **31a** administration at 14 days of CCI. Data are given as the mean ± SEM, n = 6, two-way ANOVA with Bonferroni post hoc test: *p < 0,05 vs sham mice; °p < 0,05 vs 14 days CCI. (B) Time course thermal preference behavior of sham Swiss CD1 mice (white dots), CD1 mice 7 days (light blue dots), and 14 days (green dots) after CCI. The blue dots represent the time course effect of compound **31a** administration at 14 days of CCI. Data are given as the mean ± SEM n = 6, two-way ANOVA with Bonferroni post hoc test: *p < 0,05 and **p < 0.01 vs vehicle treated; °°°p < 0.001 and °°°°p < 0.0001 vs CCI-mice; # p < 0.05 vs sham mice.

43

4.1 Molecular modelling

Molecular modelling was performed by research group of Prof. Giuseppe Bifulco (Department of Pharmacy, University of Salerno). The TRPM8 three-dimensional structures complexed with the two antagonists AMTB and TC-I 2014 (PDB codes 6O6R and 6O72) released by Diver *et al.* in 2019 revealed new important details for developing potential modulators of this protein.[87] The preliminary analysis and superposition of both of the TRPM8 structures revealed a very similar protein architecture when bound with the two different antagonists. Starting from these premises, the binding mode of the lead compound **4** was first re-evaluated by considering the TC-I 2014-bound TRPM8 protein structure (PDB code 6O72), chosen as reference system since it featured a better resolution if compared with that originally complexed with AMTB (PDB code 6O6R). In particular, the obtained docking poses of the lead compound **4** revealed a binding mode different from what was reported in our precedent work,[80] in which a homology modeling structure of the protein was accounted. Indeed, in the TC-I 2014-bound protein structure (PDB code 6O72), compound **4** adopted a particular shape in which one aromatic function was in front of another one, establishing an intramolecular π-π stacking interaction. Specifically, the aromatic functions of **4** were π−π stacked with several residues stabilizing the ligand/protein complex and allowing a large set of additional interactions, such as H-bond contacts. Indeed, the indole function of **4** was involved in both π-π stacking (with Tyr736) and π-cation (with Arg998) interactions, whereas one benzyl function also established an edge-to-face π-π stacking with Phe729 Also, H-bonds were detected for compound **4** with Asn732 and Gln776 (**Figure 23**). In order to shed light about the possible mechanism of action of the reported β-carboline-based TRPM8 antagonists, molecular docking calculations (Glide software) were performed. Concerning compound **31a**, featuring four fused rings (tetrahydro-1H-imidazo[1′,5′:1,6]pyrido[3,4-b]indole1,3(2H)-dione scaffold), the presence of a substituent at C-5 determined a flip of the indole moiety, able to interact with Phe729 and Tyr995 through π-π stacking contacts. Also, the 4-Cl-phenyl substituent at C-5 determined further π-π interaction with Tyr736, whereas an H-bond contact was established with Arg998 (**Figure 24A**). On the other hand, the corresponding enantiomeric species of **31a**, which is **31a'**, showed a different occupation of the TRPM8 binding site due to the different stereo arrangements, especially for what concerns the position of the terminal substituted benzyl and aryl moieties, suggesting the poor consistency of this mode of binding that could explain the detected related decreases of antagonistic activity against TRPM8 (**Figure 24B**).
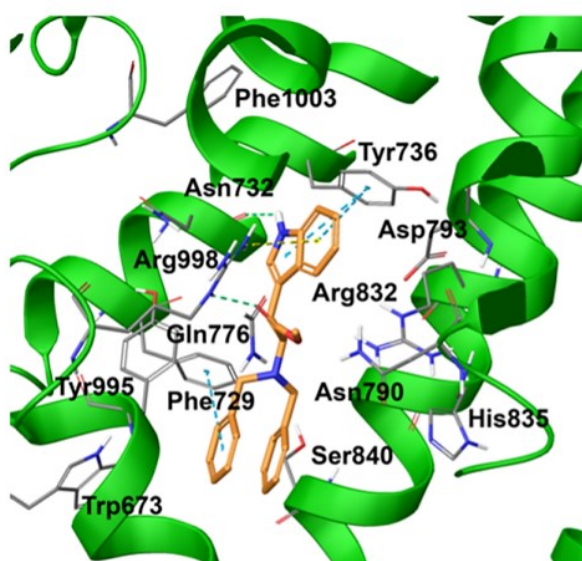
Figure 23. Compound **4** (colored by atom type; C orange, N blue, O red, polar H light gray) in docking with TRPM8 (represented in green ribbons; residues colored by atom type; C gray, N blue, O red, polar H light gray) in the TC-I 2014 ligand binding site. H bonds are represented with green dotted lines, π-cation interactions with yellow dotted lines, and π-π interactions with light blue dotted lines (PDB code 6O72).
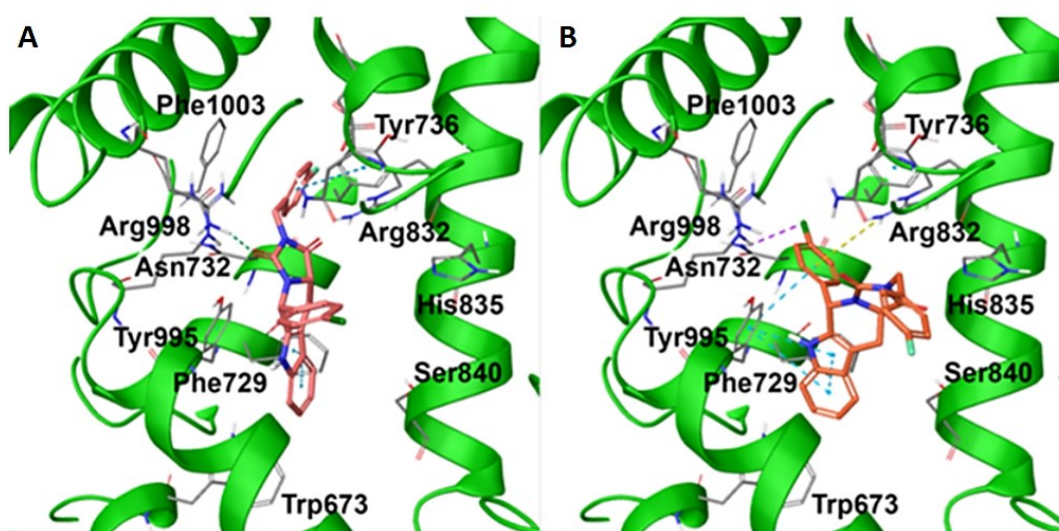
Figure 24. Predicted binding modes of (A) **31a** (colored by atom type, C pale red), (B) **31a′** (colored by atom type, C red-orange).

5.1 Conclusions

Following our interest in the TRPM8 modulation and taking into account the in vivo promising results obtained with a tryptophan-based TRPM8 antagonist (**4**), in this chapter it's reported the synthesis and the pharmacological characterization of different conformationally restricted analogues of this hit compound, designed with the dual objective of exploring the structural requirements for antagonizing TRPM8 at molecular level and improving the metabolic stability of our hit compound. Some of the synthesized compounds featuring tetrahydrocarboline, tetrahydropyrazino[1′,2′:1,6]pyrido[3,4- b]indole-1,4(6H,7H)-dione, and tetrahydro-1H-imidazo [1′,5′:1,6]pyrido[3,4-b]indole-1,3(2H)-dione chemical structures showed an efficient and potent TRPM8 antagonist activity in the nanomolar range. Using a new TRPM8 three-dimensional protein structure, we rationalized the SAR of this series of compounds. One of the synthesized compounds, the (5R,11aS)-5-(4-chlorophenyl)-2-(4-fluorobenzyl)-5,6,11,11atetrahydro-1H-imidazo[1′,5′:1,6]pyrido[3,4-b]indole-1,3(2H)- dione, **31a**, has a slow metabolic turnover and both overcomes TRPM8-mediated cold hypersensitivity over time, as measured in the WDS assay, and displays acute antinociceptive response 15 min after its application in an oxaliplatin-induced cold allodynia model. In addition, **31a** also shows remarkable analgesic activity in an animal model of CCI-induced hyperalgesia. Our results confirm the validity of the indole nucleus in the design of potent TRPM8 modulators, adding one more piece to the puzzle that composes the TRPM8's complex biology in the transmission and modulation of pain.

6.1 Experimental section
6.1.1 Chemistry

All reagents and solvents used were purchased from Sigma-Aldrich (Milan, Italy) unless otherwise stated. Reactions were performed under magnetic stirring in round-bottomed flasks unless otherwise noted. Moisture-sensitive reactions were conducted in oven-dried glassware under nitrogen stream, using freshly distilled solvents. TLC analysis of reaction mixtures was performed on precoated glass silica gel plates (F254, 0.25 mm, VWR International), while crude products were purified by the Isolera Spektra One automated flash chromatography system (Biotage, Uppsala, Sweden), using commercial silica gel cartridges (SNAP KP-Sil, Biotage). NMR spectra were recorded on a Bruker Avance 400 MHz apparatus, at room temperature. Chemical shifts were reported in δ values (ppm) relative to internal Me4Si for ^{1}H and ^{13}C NMR and to CFCl$_3$ for ^{19}F NMR. J values were reported in hertz (Hz). ^{1}H NMR and ^{19}F NMR peaks were described using the following abbreviations: s (singlet), d (doublet), t (triplet), and m (multiplet). HR-MS spectra were recorded by LTQ-Orbitrap-XL-ETD mass spectrometer (Thermo Scientific, Bremen, Germany), equipped with an ESI source. Analytical RP-HPLC analysis of final products was performed through a Nexera UHPLC system (Shimadzu, Kyoto, Japan) consisting of a CBM-20A controller, two LC-30AD pumps, a DGU20 A5R degasser, an SPD-M20A photodiode array detector, a CTO20AC column oven, a SIL-30AC autosampler, and a Kinetex C18 150 mm × 2.1 mm × 2.6 μm (100 Å) column (Phenomenex, Bologna, Italy). The optimal mobile phase consisted of 0.1% HCOOH/H$_2$O v/v (A) and 0.1% HCOOH/© v/v (B). Analysis was performed in gradient elution as follows: 0-13.00 min, 5-65% B; 13-14.00 min, 65-95% B; 14-15.00 min, isocratic to 95% B; then 3 min for column re-equilibration. Flow rate was 0.5 mL min^{-1}. Column oven temperature was set to 40°C. Injection volume was 5 μL of sample. The following PDA parameters were applied: sampling rate, 12.5 Hz; detector time constant, 0.160 s; cell temperature, 40 °C. Data acquisition was set in the range 190-800 nm, and chromatograms were monitored at 230 nm. Analytical RP-HPLC confirmed that all final compounds had a purity of >95%. For quantitative analysis, the calibration curve was obtained in a concentration range of 2.5-40 μM with five concentration levels and triplicate injections of each level were run. Peak areas were plotted against corresponding concentrations, and the linear regression was used to generate a calibration curve with R^2 values of ≥0.999. Stability analysis was performed using the same chromatographic conditions reported above but with the following elution gradient: 0-13.00 min, 15-65% B; 13-14.00 min, 65-95% B; 14-15.00 min, isocratic to 95% B; then 3 min for

column reequilibration. All circular dichroism spectra were recorded using a JASCO J810 spectropolarimeter at 25 °C in the range λ = 260-190 nm (1 mm path length, 1 nm bandwidth, four accumulations, and a scanning speed of 10 nm min^{-1}). Compounds were dissolved in methanol at a concentration of 0.100 mM. Spectra were corrected for the solvent contribution.

General Procedure A: Pictet-Spengler Reaction. 1 mmol of L-tryptophan methyl ester or (S)-2-amino-N-(4-fluorobenzyl)-3-(1H-indol-3-yl)propanamide (**8**) was dissolved in methanol and added with the proper aldehyde (1.5 eq) and trifluoroacetic acid (1.5 eq). The mixture was subjected to a microwave assisted closed vessel reaction for 45 min at 110 °C. The mixture was then evaporated in vacuo, and the residue was dissolved in dichloromethane and was washed three times with water. The organic phase was extracted, dried over Na$_2$SO$_4$, filtered, and concentrated under vacuum. The crude products were purified by flash chromatography using mixtures of n-hexane/ethyl acetate as mobile phase.

General Procedure B: Coupling Reactions. 1 mmol of the proper carboxylic acid was dissolved in dichloromethane/DMF (4:1 v/v) and added with HOBt (1.2 eq), HBTU (1.2 eq), DIPEA (2.4 eq), and the corresponding amine (1.2 eq) and stirred at room temperature overnight. Then, the solvent was evaporated in vacuum, and the residue was dissolved in dichloromethane and washed with water (3 times), a saturated solution of NaHCO$_3$ (3 times), and a solution of citric acid (10% w/w). The organic phase was extracted, dried over Na$_2$SO$_4$, filtered, and concentrated under vacuum. The crude products were purified by flash chromatography using mixtures of n-hexane/ethyl acetate as mobile phase.

General Procedure C: Boc Removal. The N-Boc protected intermediate (0.2 mmol) was dissolved in a mixture of TFA/DCM (1:3 v/v), and triisopropylsilane (TIS, 0.25 eq) was added. Reaction was stirred at room temperature for 2 h. Then, a solution of NaOH (2 N) was added dropwise until pH 7. The mixture was diluted with water and dichloromethane, and the organic phase was extracted, dried over Na$_2$SO$_4$, filtered, and concentrated under vacuum. The crude products were purified by flash chromatography using mixtures of n-hexane/ethyl acetate as mobile phase.

General Procedure D: Hydantoin Synthesis. Diastereoisomerically pure tetrahydro-β-carbolines (0.2 mmol) were dissolved in THF, and 0.4 equivalents of triphosgene was added. The pH was adjusted to 8 by addition of TEA, and the mixture was stirred at room temperature

for 10 min. Then, the proper amine (1.2 eq) was added, and the resulting mixture was refluxed for 1 h. After cooling to room temperature, the solvent was evaporated, the residue reconstituted in dichloromethane and washed with water (3 times). The organic phase was extracted, dried over Na_2SO_4, filtered, and concentrated under vacuum. The crude products were purified by flash chromatography using mixtures of n-hexane/ethyl acetate as mobile phase.

General Procedure E: Hydantoin Synthesis. Tetrahydro-β-carboline **32a** or **32b** (0.2 mmol) was dissolved in THF, and 1.2 equivalents of trimethylamine and 1.2 equivalents of the proper isocyanate were added. The mixture was stirred at room temperature for 30 min. The solvent was evaporated, the residue reconstituted in dichloromethane and washed with water (3 times). The organic phase was extracted, dried over Na_2SO_4, filtered, and concentrated under vacuum. The crude products were purified by flash chromatography using mixtures of n-hexane/ethyl acetate as mobile phase.

General Procedure F: Hydantoin Synthesis. Tetrahydro-β-carboline **32b** (0.2 mmol) was dissolved in THF, and 1.2 equivalents of trimethylamine and 1.2 equivalents of the proper isocyanate were added. The mixture was stirred at room temperature for 30 min and then refluxed for further 30 min. After cooling to room temperature, the solvent was evaporated, the residue reconstituted in dichloromethane and washed with water (3 times). The organic phase was extracted, dried over Na_2SO_4, filtered, and concentrated under vacuum. The crude products were purified by flash chromatography using mixtures of n-hexane/ethyl acetate as mobile phase.

(1R,3S)-Methyl 1-Phenyl-2,3,4,9-tetrahydro-1H-pyrido[3,4- b]indole-3-carboxylate (5a). Compound **7a** was obtained using general procedure A in 33% yield, using benzaldehyde as starting material. Spectral data were in accordance with literature.[88] FC in n-hexane/ethyl acetate 1/1, Rf = 0.37.

(1S,3S)-Methyl 1-Phenyl-2,3,4,9-tetrahydro-1H-pyrido[3,4- b]indole-3-carboxylate (5b). Compound **7b** was obtained using general procedure A in 41% yield, using benzaldehyde as starting material. Spectral data were in accordance with literature.[88] FC in n-hexane/ethyl acetate 1/1, Rf = 0.44.

(1R,3S)-Methyl 2-Benzyl-1-phenyl-2,3,4,9-tetrahydro-1Hpyrido[3,4-b]indole-3-carboxylate (6a).

Intermediate **5a** (0.2 mmol) was dissolved in THF and added with NaI (1.1 eq), Pd(CH3COO)$_2$ (10% mol), TEA (1.2 eq), and benzyl bromide (1.2 eq). The mixture was subjected to a microwave assisted closed vessel reaction for 45 min at 110 °C. After removal of the solvent, the residue was reconstituted in dichloromethane and was washed three times with water. The organic phase was extracted, dried over Na$_2$SO$_4$, filtered, and concentrated under vacuum. The crude products were purified by flash chromatography using n-hexane/ ethyl acetate 1/1, Rf = 0.35. White powder (62% yield). $[\alpha]^{25}_D$: −101.16 ± 0.17 (c = 0.10, MeOH). ^{1}H NMR (400 MHz, CDCl$_3$) δ: 3.14 (d, 2H, CH$_2$, J = 4.8 Hz); 3.55 (s, 3H, CH$_3$); 3.80 (d, 2H, CH$_2$, J = 11.8 Hz) 3.85-3.88 (m, 1H, CH); 5.39 (s, 1H, CH); 6.99-7.02 (m, 2H, aryl); 7.04 (d, 1H, aryl, J = 7.2 Hz); 7.10-7.28 (m, 8H, aryl); 7.39 (d, 2H, aryl, J = 7.8 Hz); 7.43 (d, 1H, aryl, J = 8.0 Hz). ^{13}C NMR (100 MHz, CDCl$_3$) δ 24.5, 51.4, 54.4, 56.1, 60.9, 106.4, 110.8, 118.2, 119.3, 121.6, 127.0, 127.1, 128.1, 128.4, 128.6, 128.8, 128.9, 135.0, 136.5, 139.4, 142.2, 173.6. HR-MS m/z calcd for C$_{26}$H$_{24}$N$_2$O$_2$ [(M + H)]$^+$: 397.1911; found 397.1918.

(1S,3S)-Methyl 2-Benzyl-1-phenyl-2,3,4,9-tetrahydro-1Hpyrido[3,4-b]indole-3-carboxylate (6b).

Final product **6b** was synthesized starting from **5b** and following the procedure described above for **6a**. FC in n-hexane/ethyl acetate 2/1, Rf = 0.40. White powder (59% yield). $[\alpha]^{25}_D$: 135.18 ± 0.25 (c = 0.10, MeOH). ^{1}H NMR (400 MHz, CDCl$_3$) δ: 3.08 (dd, 1H, CH$_{2a}$, J′ = 4.4, J″ = 15.6 Hz); 3.31 (s, 3H, CH$_3$); 3.40 (dd, 1H, CH$_{2b}$, J′ = 7.8, J″ = 15.6 Hz); 3.87 (t, 1H, J = 8.0 Hz, CH); 3.92 (d, 1H, CH$_{2a}$, J = 16.0 Hz); 4.08 (d, 1H, CH$_{2b}$, J = 16.0 Hz); 4.96 (s, 1H, CH); 7.13-7.23 (m, 2H, aryl); 7.25-7.36 (m, 11H, aryl); 7.56 (d, 1H, aryl, J = 7.6 Hz). ^{13}C NMR (100 MHz, CDCl3) δ 22.7, 51.4, 57.2, 61.0, 61.8, 107.2, 110.8, 118.4, 119.5, 121.8, 126.8, 127.1, 128.0, 128.5, 129.3, 133.2, 136.4, 138.2, 140.2, 173.5. HR-MS m/z calcd for C$_{26}$H$_{24}$N$_2$O$_2$ [(M + H)]$^+$: 397.1911; found 397.1920.

tert-Butyl (S)-(1-((4-Fluorobenzyl)amino)-3-(1H-indol-3-yl)- 1-oxopropan-2-yl)carbamate (7).

Synthesized according to the general procedure B, starting from N-Boc-L-tryptophan-OH and 4-fluorobenzylamine. FC in n-hexane/ethyl acetate 3/2, Rf = 0.6. yellowish oil (75% yield). ^{1}H NMR (400 MHz, CDCl$_3$) δ 1.42 (s, 9H, CH$_3$); 3.17-3.22 (m, 1H, CH$_{2a}$); 3.30-3.35 (m, 1H, CH$_{2b}$) 4.14-4.25 (m, 2H, CH$_2$); 4.49 (bs, 1H, CH); 5.27 (bs, 1NH); 6.20 (s, 1H, CH); 6.89-6.95

(m, 4H, aryl); 7.13 (t, 1H, aryl, J = 7.2 Hz); 7.21 (t, 1H, aryl, J = 7.6 Hz); 7.37 (d, 1H, aryl, J = 8.0 Hz); 7.66 (d, 1H, aryl, J = 7.6 Hz); 8.45 (bs, 1NH). HR-MS m/z calcd for $C_{23}H_{26}FN_3O_3$ [(M + H)]$^+$: 411.1958; found 411.1963.

(S)-2-Amino-N-(4-fluorobenzyl)-3-(1H-indol-3-yl51ecarbonateide (8).

Intermediate **8** was synthesized according to the general procedure C, starting from **7**. FC in ethyl acetate, Rf = 0.3. White powder (94% yield). ^{1}H NMR (400 MHz, CD$_3$OD) δ 3.06 (dd, 1H, CH$_{2a}$, J′ = 6.5, J″ = 14.1 Hz); 3.18 (dd, 1H, CH$_{2b}$, J′ = 7.0, J″ = 14.1 Hz); 3.69 (t, 1H, CH, J = 6.8 Hz); 4.18 (d, 1H, CH$_{2a}$, J = 14.9 Hz); 4.31 (d, 1H, CH$_{2b}$, J = 14.9 Hz); 6.89-6.98 (m, 3H, aryl); 7.01-7.06 (m, 2H, aryl); 7.13 (t, 1H, aryl, J = 7.8 Hz); 7.39 (d, 1H, aryl, J = 8.1 Hz); 7.63 (d, 1H, aryl, J = 7.9 Hz). HR-MS m/z calcd for $C_{18}H_{18}FN_3O$ [(M + H)]$^+$: 312,1507; found 311.1512.

(S)-N-(4-Fluorobenzyl)-2,3,4,9-tetrahydro-1H-pyrido[3,4-b]- indole-3-carboxamide (9).

Compound **9** was obtained using general procedure A, starting from intermediate **8** which was reacted with formaldehyde. Compound FC in ethyl acetate/acetone 9.8/0.2, Rf = 0.48. White powder (55% yield). ^{1}H NMR (400 MHz, DMSO): δ: 2.69 (dd, 1H, CH$_{2a}$, J′ = 9.7, J″ = 14.9 Hz); 2.90 (dd, 1H, CH$_{2b}$, J′ = 4.5, J″ = 15.2 Hz); 3.48-3.53 (m, 1H, CH); 3.95 (dd, 2H, CH$_2$, J′ = 17.4, J″ = 22.5 Hz); 4.32 (d, 2H, CH$_2$, J = 5.6, Hz); 6.94 (t, 1H, aryl, J = 7.1 Hz); 7.01 (t, 1H, aryl, J = 7.3 Hz); 7.17 (t, 2H, aryl, J = 8.8 Hz); 7.26-7.39 (m, 3H, aryl); 8.46 (t, 1H, aryl, J = 6.1 Hz); 10.68 (s, 1H, NH). ^{13}C NMR (100 MHz, DMSO) δ 25.4, 41.7, 42.3, 57.0, 106.9, 111.3, 115.3, 115.5, 117.7, 118.7, 120.9, 127.6, 129.6, 129.7, 134.3, 136.2, 136.32, 136.34, 160.4, 162.8, 173.2. ^{19}F NMR (DMSO, 376.3 MHz) δ: −(116.37) (s, 1F, CF). HR-MS m/z calcd for $C_{19}H_{18}FN_3O$ [(M + H)]$^+$: 324.1507; found 324.1516.

(1R,3S)-N-(4-Fluorobenzyl)-1-isobutyl-2,3,4,9-tetrahydro1H-pyrido[3,4-b]indole-3-carboxamide (10a).

Compound **10a** was obtained using general procedure A, starting from intermediate **8** which was reacted with isovaleraldehyde. FC in n-hexane/ethyl acetate 1/1, Rf = 0.46. White powder (35% yield). ^{1}H NMR (400 MHz, CDCl$_3$): δ: 0.90 (d, 3H, CH$_3$, J = 5.5 Hz); 0.93 (d, 3H, CH$_3$, J = 5.7 Hz); 1.40-1.48 (m, 1H, CH$_{2a}$); 1.56−1.68 (m, 1H, CH$_{2b}$); 1.85− 1.89 (m, 1H, CH); 2.78 (dd, 1H, CH2a, J′ = 8.3, J″= 17.2 Hz); 3.21 (dd, 1H, CH$_{2b}$, J′ = 5.0, J″= 15.9 Hz); 3.71 (dd, 1H, CH, J′ = 5.0, J″ = 7.9 Hz); 4.05 (dd, 1H, CH, J′ = 4.2, J″= 10.0 Hz); 4.36 (dd, 1H, CH$_{2a}$, J′ = 5.7, J″= 14.8 Hz); 4.43 (dd, 1H, CH$_{2b}$, J′ = 5.7, J″= 14.8 Hz); 6.95 (t, 2H, aryl, J = 8.7 Hz); 7.01-

7.11 (m, 2H, aryl); 7.18-7.24 (m, 2H, aryl); 7.39 (t, 1H, aryl, J = 5.8 Hz); 7.45 (d, 1H, aryl, J = 6.3 Hz); 7.62 (s, 1H, NH). ^{13}C NMR (100 MHz, CDCl$_3$) δ 22.0, 23.5, 24.6, 25.1, 42.5, 43.9, 49.5, 52.7, 108.4, 110.7, 115.4, 115.7, 118.3, 119.7, 121.9, 127.3, 129.7, 135.9, 136.4, 173.0. ^{19}F NMR (CDCl$_3$, 376.3 MHz) δ: −(115.17) (s, 1F, CF). HR-MS m/z calcd for C$_{23}$H$_{26}$FN$_3$O [(M + H)]$^+$: 380.2133; found 380.2139.

(1S,3S)-N-(4-Fluorobenzyl)-1-isobutyl-2,3,4,9-tetrahydro1H-pyrido[3,4-b]indole-3-carboxamide (10b).

Compound **10b** was obtained using general procedure A, starting from intermediate 8 which was reacted with isovaleraldehyde. FC in hexane/ethyl acetate 6/4, Rf = 0.44. White powder (43% yield). ^{1}H NMR (400 MHz, CDCl$_3$): δ: 0.92 (d, 3H, CH$_3$, J = 6.6 Hz); 0.96 (d, 3H, CH$_3$, J = 6.5 Hz); 1.41-1.48 (m, 1H, CH$_{2a}$); 1.61-1.68 (m, 1H, CH$_{2b}$); 1.95-1.97 (m, 1H, CH); 2.66 (dd, 1H, CH$_{2a}$, J′= 8.7, J″= 15.6 Hz); 3.29 (dd, 1H, CH$_{2a}$, J′ = 4.4, J″= 17.6 Hz); 3.52 (dd, 1H, CH, J′= 4.5, J″= 11.3 Hz); 4.08 (d, 1H, CH, J = 8.7 Hz); 4.42 (d, 2H, CH$_2$, J = 5.7, Hz); 6.96 (t, 2H, aryl, J = 8.6 Hz); 7.02-7.10 (m, 2H, aryl); 7.19-7.25 (m, 2H, aryl); 7.38 (t, 1H, aryl, J = 5.6 Hz); 7.43 (d, 1H, aryl, J = 7.5 Hz); 7.75 (s, 1H, NH). ^{13}C NMR (100 MHz, CDCl$_3$) δ 21.9, 23.8, 25.5, 30.9, 42.4, 44.2, 51.9, 57.9, 109.0, 110.8, 115.4, 115.7, 118.3, 119.7, 121.9, 127.4, 129.4, 134.4, 135.9, 136.5, 163.4, 172.9. ^{19}F NMR (CDCl$_3$, 376.3 MHz) δ: −(115.89) (s, 1F, CF). HR-MS m/z calcd for C$_{23}$H$_{26}$FN$_3$O [(M + H)]$^+$: 380.2133; found 380.2142.

Methyl   3-((1R,3S)-3-((4-Fluorobenzyl)carbamoyl)-2,3,4,9-   tetrahydro-1H-pyrido[3,4-b]indol-1-yl)propanoate (11a).

Compound **11a** was obtained using general procedure A, starting from intermediate **8** which was reacted with methyl-4-oxobutanoate. FC in dichloromethane/methanol 9.5/0.5, Rf = 0.44. White powder (43% yield). ^{1}H NMR (400 MHz, CDCl$_3$) δ: 1.98-2.14 (m, 2H, CH$_2$); 2.49-2.67 (m, 2H, CH$_2$); 2.80 (dd, 1H, CH$_{2a}$, J′= 15.6, J″= 19.8 Hz); 3.30 (dd, 1H, CH$_{2b}$, J′ = 4.6, J″= 19.4 Hz); 3.67 (s, 3H, CH$_3$); 3.73 (dd, 1H, CH, J′= 8.0, J″= 16.0 Hz); 4.06 (dd, 1H, CH, J′ = 4.4, J″= 12.2 Hz); 4.45 (dd, 1H, CH$_{2a}$, J′ = 7.8, J″= 18.8 Hz); 4.54 (dd, 1H, CH$_{2b}$, J′ = 7.8, J″= 18.8 Hz); 7.05 (t, 2H, aryl, J = 8.0 Hz); 7.09-7.18 (m, 2H, aryl); 7.21-7.39 (m, 3H, aryl); 7.53 (d, 1H, aryl, J = 8.0 Hz); 8.21 (s, 1H, NH). ^{13}C NMR (100 MHz, CDCl$_3$) δ: 24.7, 29.7, 31.4, 42.6, 51.3, 51.8, 52.6, 108.7, 110.8, 115.4, 115.7, 118.4, 119.6, 122.1, 127.1, 129.5, 134.3, 135.2, 136.0, 161.1, 163.4, 172.7, 174.4. HR-MS m/z calcd for C$_{23}$H$_{24}$FN$_3$O$_3$ [(M + H)]$^+$: 410.1874; found 410.1888.

Methyl 3-((1S,3S)-3-((4-Fluorobenzyl)carbamoyl)-2,3,4,9- tetrahydro-1H-pyrido[3,4-b]indol-1-yl)propanoate (11b).

Compound **11b** was obtained using general procedure A, starting from intermediate **8** which was reacted with methyl-4-oxobutanoate. FC in dichloromethane/methanol 9.5/0.5, Rf = 0.41. White powder (37% yield). ^{1}H NMR (400 MHz, CDCl$_3$): δ: 1.83-1.88 (m, 1H, CH$_{2a}$); 2.25−2.30 (m, 1H, CH$_{2b}$); 2.44-2.49 (m, 2H, CH$_2$); 2.64-2.72 (m, 1H, CH$_{2a}$); 3.25 (dd, 1H, CH$_{2b}$, J′ = 4.8, J″ = 12.0 Hz); 3.54-3.58 (m, 4H, CH$_3$ and CH); 4.12 (dd, 1H, CH, J′ = 4.2, J″ = 8.6 Hz); 4.36-4.45 (m, 2H, CH$_2$); 6.97 (t, 2H, aryl, J = 8.0 Hz); 7.04 (t, 1H, aryl, J = 8.0 Hz); 7.10 (t, 1H, aryl, J = 8.0 Hz); 7.19-7.26 (m, 3H, aryl); 7.43 (d, 1H, aryl, J = 8.0 Hz); 8.00 (s, 1H, NH). ^{13}C NMR (100 MHz, CDCl$_3$) δ 25.4, 29.2, 30.3, 42.5, 51.8, 53.5, 57.8, 109.5, 111.0, 115.5, 115.7, 118.4, 119.8, 122.2, 127.2, 129.5, 134.2, 134.5, 136.1, 155.3, 161.0, 163.5, 172.5, 174.2. HR-MS m/z calcd for C$_{23}$H$_{24}$FN$_3$O$_3$ [(M + H)]$^+$: 410.1874; found 410.1879.

3-((1R,3S)-3-((4-Fluorobenzyl)carbamoyl)-2,3,4,9-tetrahydro-1H-pyrido[3,4-b]indol-1-yl)propanoic Acid (12a).

Compound **11a** was dissolved in a mixture of NaOH 6 N/methanol (9/1 v/v) and stirred for 90 min at room temperature. The mixture was then buffered to pH 7 using HCl (6N) and extracted three times with ethyl acetate. The organic phases were collected, dried over Na$_2$SO$_4$, filtered, and concentrated in vacuo. The final product was purified using reverse phase preparative HPLC using a Synergi fusion column (4 μm, 80A, 150 mm × 21.2 mm, Phenomenex Torrence, CA, USA) as stationary phase and a gradient elution with acetonitrile 0.1% TFA (A) and water 0.1% TFA (B) (from 5% to 90% of A in 22 min). Flow rate was set at 20 mL/min. Retention time was 9.10 min. White powder (42% yield).

^{1}H NMR (400 MHz, CD$_3$OD): δ: 2.01-2.08 (m, 1H, CH$_{2a}$); 2.11-2.19 (m, 1H, CH$_{2b}$); 2.47 (t, 2H, CH$_2$, J = 7.0 Hz); 2.88 (dd, 1H, CH$_{2a}$, J′=9.2, J″= 15.2 Hz); 3.10 (dd, 1H, CH$_{2b}$, J′ = 4.6, J″= 15.3 Hz); 3.90 (dd, 1H, CH, J′= 4.7, J″= 9.3 Hz); 4.20 (dd, 1H, CH, J′ = 3.6, J″= 9.0 Hz); 4.45 (s, 2H, CH$_2$); 6.96-7.09 (m, 4H, aryl); 7.29-7.35 (m, 3H, aryl); 7.42 (d, aryl, 1H, J = 7.7 Hz). ^{13}C NMR (100 MHz, CD$_3$OD) δ: 24.4, 31.0, 34.8, 41.8, 51.2, 52.5, 106.1, 110.4, 114.6, 114.8, 117.1, 118.2, 120.7, 126.9, 128.9, 129.0, 134.7, 135.6, 136.5, 163.2, 174.1. HR-MS m/z calcd for C$_{22}$H$_{22}$FN$_3$O$_3$ [(M + H)]$^+$: 396.1718; found 396.1725.

3-((1S,3S)-3-((4-Fluorobenzyl)carbamoyl)-2,3,4,9-tetrahydro-1H-pyrido[3,4-b]indol-1-yl)propanoic Acid (12b).

Compound **12b** was synthesized and purified according to the procedure described for **12a**, using **11b** as starting material. Retention time in RP-HPLC was 8.98 min. The product was isolated as white powder (33% yield). ^{1}H NMR (400 MHz, CD$_3$OD): δ: 1.92-2.02 (m, 1H, CH$_{2a}$); 2.35-2.44 (m, 3H, CH$_2$); 2.71-2.78 (m, 1H, CH$_{2a}$); 3.09 (dd, 1H, CH$_{2b}$, J′ = 4.4, J″ = 15.0 Hz); 3.61 (dd, 1H, CH, J′= 4.2, J″= 11.2 Hz); 4.18 (d, 1H, CH, J = 8.2 Hz); 4.47 (s, 2H, CH$_{2a}$); 6.98 (t, 1H, aryl, J = 7.9 Hz); 7.04-7.09 (m, 3H, aryl); 7.31 (d, 1H, aryl, J = 8.0 Hz); 7.38-7.41 (m, 3H, aryl). ^{13}C NMR (100 MHz, CD$_3$OD): δ: 25.6, 30.8, 33.7, 41.8, 53.1, 57.8, 107.1, 110.6, 114.6, 114.8, 117.0, 118.3, 120.6, 127.1, 129.1, 134.8, 135.8, 136.6, 160.9, 163.3, 174.6, 181.2. ^{19}F NMR (CDCl$_3$, 376.3 MHz) δ: -(118.05) (s, 1F, CF). HRMS m/z calcd for C$_{22}$H$_{22}$FN$_3$O$_3$ [(M + H)]$^+$: 396.1718; found 396.1729.

(S)-Methyl 2,3,4,9-Tetrahydro-1H-pyrido[3,4-b]indole-3-carboxylate (13).

Intermediate **13** was synthesized in 89% yield according to the general procedure A starting from L-tryptophan methyl ester and formaldehyde. The product was isolated by filtration from the reaction mixture. Spectral data were in accordance with literature.[88]

(1R,3S)-Methyl 1-iIsobutyl-2,3,4,9-tetrahydro-1H-pyrido- [3,4-b]indole-3-carboxylate (14a).

Synthesized in 36% yield according to the general procedure A starting from tryptophan methyl ester and isovaleraldehyde. FC in n-hexane/ethyl acetate 1/1, Rf = 0.40. Spectral data were in accordance with literature.[89]

(1S,3S)-Methyl 1-Isobutyl-2,3,4,9-tetrahydro-1H-pyrido[3,4-b]indole-3-carboxylate (14b).

Synthesized in 40% yield according to the general procedure A starting from tryptophan methyl ester and isovaleraldehyde. FC in n-hexane/ethyl acetate 1/1, Rf = 0.44. Spectral data were in accordance with literature.[89]

(1R,3S)-Methyl 1-(4-Chlorophenyl)-2,3,4,9-tetrahydro-1Hpyrido[3,4-b]indole-3-carboxylate (15a).

Synthesized in 33% yield according to the general procedure A starting from tryptophan methyl ester and 4-chlorobenzaldehyde. FC in n-hexane/ethyl acetate 1/1, Rf = 0.45. Spectral data were in accordance with literature.[90]

(1S,3S)-Methyl 1-(4-Chlorophenyl)-2,3,4,9-tetrahydro-1H- pyrido[3,4-b]indole-3-carboxylate (15b).

Synthesized in 46% yield according to the general procedure A starting from tryptophan methyl ester and 4-chlorobenzaldehyde. FC in n-hexane/ethyl acetate 1/1, Rf = 0.51. Spectral data were in accordance with literature.[90]

(S)-Methyl 2-(3-((tert-Butoxycarbonyl)amino)propanoyl)- 2,3,4,9-tetrahydro-1H-pyrido[3,4-b]indole-3-carboxylate (16).

Synthesized in 71% yield according to the general procedure B starting from intermediate **13** and N-Boc-β-Ala-OH. FC ethyl acetate/n-hexa½1/2. Rf = 0.65. Spectral data were in accordance with literature.[83]

(S)-Methyl 2-(3-Aminopropanoyl)-2,3,4,9-tetrahydro-1H- pyrido[3,4-b]indole-3-carboxylate (17).

Synthesized from intermediate **16** using the general procedure C. FC in ethyl acetate, Rf = 0.60. White powder (91% yield). $[\alpha]^{25}_D$: +101.70 ± 0.03. ^{1}H NMR (CD$_3$OD, 400 MHz): δ: (A) 2.62-2.72 (m, 2H, CH$_2$); 2.86-2.92 (m, 3H, CH$_2$ and CH$_{2a}$); 3.35 (d, 1H, CH$_{2b}$, J = 15.6 Hz); 3.50 (s, 3H, CH$_3$); 4.64 (d, 1H, CH$_{2a}$, J = 15.4 Hz); 4.82 (d, 1H, CH$_{2b}$, J = 15.4 Hz); 5.15 (d, 1H, CH, J = 4.5 Hz); 6.90 (t, 1H, aryl, J = 7.2 Hz); 6.95-7.00 (m, 1H, aryl); 7.18 (t, 1H, aryl, J = 6.8 Hz); 7.31 (d, 1H, aryl, J = 7.8 Hz); ^{13}C NMR (CD$_3$OD, 100 MHz) δ: ^{1}H NMR (CD$_3$OD, 400 MHz). δ: (B) 2.49-2.56 (m, 2H, CH$_2$); 2.86-2.92 (m, 2H, CH$_2$); 3.01 (dd, 1H, CH$_{2a}$, J′ = 5.8 and J″ = 15.6 Hz); 3.42 (d, 1H, CH$_{2a}$, J = 15.3 Hz); 3.52 (s, 3H, CH$_3$); 4.24 (d, 1H, CH$_{2a}$, J = 17.1 Hz); 5.04 (d, 1H, CH$_{2b}$, J = 17.1 Hz); 5.74 (d, 1H, CH, J = 7.5 Hz); 6.90 (t, 1H, aryl, J = 7.2 Hz); 6.95-7.00 (m, 1H, aryl); 7.18 (t, 1H, aryl, J = 6.8 Hz); 7.31 (d, 1H, aryl, J = 7.8 Hz); ^{13}C NMR (CD$_3$OD, 100 MHz) (A + B) δ: 22.4, 23.2, 29.4, 35.4, 36.8, 37.0, 38.9, 41.2, 51.0, 51.6, 51.8, 55.2, 104.4, 105.0, 110.6, 117.2, 118.7, 121.1, 126.5, 128.6, 129.2, 137.0, 171.3, 171.7, 173.3, 173.5. HR-MS m/z calcd for C$_{16}$H$_{19}$N$_3$O$_3$, [(M + H)]$^+$: 302.1499; found 302.1503.

(S)-Methyl 2-(2-((tert-Butoxycarbonyl)amino)acetyl)-2,3,4,9- tetrahydro-1H-pyrido[3,4-b]indole-3-carboxylate (18).

Compound **18** was synthesized in 71% yield starting from intermediate **13** and N-Boc-Gly-OH following the general procedure B. FC in ethyl acetate/n-hexane 1/1, Rf = 0.25. Spectral data were in accordance with literature.[91]

(S)-Methyl 2-((S)-2-((tert-Butoxycarbonyl)amino)-3-phenylpropanoyl)-2,3,4,9-tetrahydro-1H-pyrido[3,4-b]indole-3-carboxylate (19).

Compound **19** was synthesized in 68% yield starting from intermediate **13** and N-Boc-L-Phe-OH following the general procedure B. FC in ethyl acetate/n-hexane 2/3, Rf = 0.30. Spectral data were in accordance with literature.[91]

(S)-Methyl 2-((R)-2-((tert-Butoxycarbonyl)amino)-3-phenylpropanoyl)-2,3,4,9-tetrahydro-1H-pyrido[3,4-b]indole-3-carboxylate (20).

Compound **20** was synthesized in 65% yield starting from intermediate **13** and N-Boc-D-Phe-OH following the general procedure B. FC in ethyl acetate/n-hexane 2/3, Rf = 0.30. Spectral data were in accordance with literature.[91]

(S)-2,3,6,7,12,12a-Hexahydropyrazino[1′,2′:1,6]pyrido[3,4- b]indole-1,4-dione (21).

Synthesized from **18** following the general procedure C. FC in ethyl acetate/n-hexane 3/1, Rf = 0.32. White powder (85% yield). $[\alpha]^{25}_D$: +37.40 ± 0.01. ^{1}H NMR (CD$_3$OD, 400 MHz): δ: 2.99 (t, 1H, CH$_{2a}$, J = 13.1 Hz); 3.32-3.41 (m, 1H, CH$_{2b}$); 4.05 (d, 1H, CH$_{2a}$, J = 18.0 Hz); 4.17 (d, 1H, CH$_{2b}$, J = 18.0 Hz); 4.27 (d, 1H, CH$_{2a}$, J = 16.6 Hz); 4.37 (dd, 1H, CH, J′ = 7.6, J″ = 11.8 Hz); 5.55 (d, 1H, CH$_{2b}$, J = 16.6 Hz); 7.03 (t, 1H, aryl, J = 7.8 Hz); 7.11 (t, 1H, aryl, J = 8.1 Hz); 7.33 (d, 1H, aryl, J = 8.1 Hz); 7.45 (d, 1H, aryl, J = 7.8 Hz). ^{13}C NMR (CD$_3$OD, 100 MHz) δ: 26.3, 39.7, 43.9, 56.5, 105.6, 110.6, 117.2, 118.8, 121.2, 128. HR-MS m/z: calcd. for C$_{14}$H$_{13}$N$_3$O$_2$, [(M + H)]$^+$: 256,1081; found 256.1087.

(3S,12aS)-3-Benzyl-2,3,12,12a-tetrahydropyrazino-[1′,2′:1,6]pyrido[3,4-b]indole-1,4(6H,7H)-dione (22).

Synthesized from **19** following the general procedure C. FC in ethyl acetate, Rf = 0.25. White powder (81% yield). $[\alpha]^{25}_D$: −68.000 ± 0.00108 (c = 0.10, MeOH). ^{1}H NMR (CD$_3$OD, 400 MHz): δ: 0.89 (t, 1H, CH$_{2a}$, J = 12.8 Hz); 2.73 (dd, 1H, CH$_{2b}$, J′ = 5.8, J″ = 15.1 Hz); 2.99 (dd, 1H, CH$_{2a}$, J′ = 4.8, J″ = 13.7 Hz); 3.37 (dd, 1H, CH$_{2b}$, J′ = 5.3, J″ = 13.7 Hz); 4.06-4.15 (m, 2H,

CH and CH$_{2a}$); 4.49 (t, 1H, CH, J = 4.0 Hz); 5.51 (d, 1H, CH$_{2b}$, J = 16.5 Hz); 6.98 (t, 1H, aryl, J = 7.0 Hz); 7.01-7.12 (m, 6H, aryl); 7.19 (d, 1H, aryl, J = 7.8 Hz); 7.29 (d, 1H, aryl, J = 8.1 Hz). ^{13}C NMR (CD$_3$OD, 100 MHz) δ: 25.8, 39.6, 56.1, 105.8, 110.5, 117.1, 118.6, 121.0, 126.9, 126.9, 127.9, 128.2, 130.1, 135.0, 136.5, 164.9, 167.9. HR-MS m/z: calcd. for C$_{21}$H$_{19}$N$_3$O$_2$, [(M + H)]$^+$: 346.1550; found 346.1556.

(3R,12aS)-3-Benzyl-2,3,12,12a-tetrahydropyrazino-[1′,2′:1,6]pyrido[3,4-b]indole-1,4(6H,7H)-dione (23).

Synthesized from **20** following the general procedure C. FC in ethyl acetate, Rf = 0.20. White powder (80% yield). [α]^{25}$_D$: −102.7 ± 0.2 (c = 0.10, MeOH). ^{1}H NMR (CDCl$_3$, 400 MHz): δ: 2.78 (t, 1H, CH$_{2a}$, J = 15.3 Hz); 3.02 (dd, 1H, CH$_{2b}$, J′ = 8.1, J″ = 13.8 Hz); 3.32-3.36 (m, 2H, CH$_{2a}$ and CH$_{2a}$); 3.67 (dd, 1H, CH, J′ = 4.3, J″ = 11.2 Hz); 4.04 (d, 1H, CH$_{2a}$, J = 16.8 Hz); 4.31 (dd, 1H, CH, J′ = 3.5, J″ = 7.9 Hz); 5.48 (d, 1H, CH$_{2b}$, J = 16.8 Hz); 5.79 (s, 1NH); 7.05 (t, 1H, aryl, J = 7.0 Hz); 7.12 (t, 1H, aryl, J = 7.1 Hz); 7.16-7.30 (m, 6H, aryl); 7.38 (d, 1H, aryl, J = 7.7 Hz); 7.81 (s, 1NH); 13C NMR (CDCl$_3$, 100 MHz) δ: 28.0, 41.4, 42.1, 56.8, 56.9, 108.4, 112.0, 119.3, 121.0, 123.4, 127.3, 128.7, 129.2, 130.2, 130.77, 136.1, 137.3, 163.9, 166.1. HR-MS m/z: calcd for C$_{21}$H$_{19}$N$_3$O$_2$, [(M + H)]$^+$: 346.1550; found 346.1541.

(1R,3S)-Methyl 2-((S)-2-((tert-Butoxycarbonyl)amino)-3- phenylpropanoyl)-1-isobutyl-2,3,4,9-tetrahydro-1H-pyrido- [3,4-b]indole-3-carboxylate (24a).

Compound **24a** was synthesized in 25% yield starting from intermediate **14a** and N-Boc-L-PheOH following the general procedure B. FC in ethyl acetate/n-hexane 1/2, Rf = 0.60. Spectral data were in accordance with literature.[91]

(1S,3S)-Methyl 2-((S)-2-((tert-Butoxycarbonyl)amino)-3-phenylpropanoyl)-1-isobutyl-2,3,4,9-tetrahydro-1H-pyrido[3,4-b]-indole-3-carboxylate (24b).

Compound **24b** was synthesized in 29% yield starting from intermediate **14b** and N-Boc-L-Phe-OH following the general procedure B. FC in ethyl acetate/n-hexa½1/2, Rf = 0.65. Spectral data were in accordance with literature.[91]

(3S,6R,12aS)-3-Benzyl-6-isobutyl-2,3,12,12a-tetrahydropyrazino[1′,2′:1,6]pyrido[3,4-b]indole-1,4(6H,7H)-dione (25a).

Obtained from **24a** following the general procedure C. FC in ethyl acetate/n-hexane 1/1, Rf = 0.32. White powder (78% yield). [α]^{25}$_D$: −201.40 ± 0.01. ^{1}H NMR (400 MHz, CDCl$_3$): δ: 1.02

(d, 3H, CH₃, J = 6.4 Hz); 1.14 (d, 3H, CH$_3$, J = 6.3 Hz); 1.62−1.84 (m, 4H, CH, CH$_{2a}$ and CH$_2$); 3.12 (dd, 1H, CH$_{2b}$, J′ = 4.6, J″ = 15.4 Hz); 3.18 (d, 2H, CH$_2$, J = 5.5 Hz); 4.30 (dd, 1H, CH, J′ = 4.5, J″ = 11.8 Hz); 4.43-4.46 (m, 1H, CH); 5.97-6.00 (m, 1H, CH); 6.26 (s, 1NH); 7.12-7.24 (m, 7H, aryl); 7.36 (t, 2H, aryl, J = 7.8 Hz); 7.84 (s, 1NH). ^{13}C NMR (100 MHz, CDCl$_3$) δ 18.5, 19.3, 21.3, 23.3, 37.7, 39.7, 43.9, 48.4, 53.0, 102.7, 106.9, 114.2, 116.0, 118.4, 122.5, 123.6, 125.1, 125.9, 128.8, 131.1, 132.0, 160.3, 163.6. HR-MS m/z calcd for C$_{25}$H$_{27}$N$_3$O$_2$ [(M + H)]$^+$: 402.2176; found 402.2189.

(3S,6S,12aS)-3-Benzyl-6-isobutyl-2,3,12,12a-tetrahydropyrazino[1′,2′:1,6]pyrido[3,4-b]indole-1,4(6H,7H)-dione (25b).

Obtained from **24b** following the general procedure C. FC in ethyl acetate/n-hexane 1/1, Rf = 0.38. White powder (73% yield). [α]$^{25}_D$: −122.36 ± 0.01. ^{1}H NMR (400 MHz, CDCl$_3$): δ: 0.78 (d, 3H, CH$_3$, J = 6.3 Hz); 1.02 (d, 3H, CH$_3$, J = 6.4 Hz); 1.49-1.55 (m, 2H, CH$_2$); 1.72-1.79 (m, 1H, CH); 2.81 (dd, 1H, CH$_{2a}$, J′ = 10.8, J″ = 14.8 Hz); 2.94 (dd, 1H, CH$_{2a}$, J′ = 11.7, J″ = 15.6 Hz); 3.51 (dd, 1H, CH$_{2b}$, J′ = 4.7, J″ = 15.7 Hz,); 3.63 (dd, 1H, CH$_{2b}$, J′ = 3.4, J″ = 14.4 Hz,); 3.98 (dd, 1H, CH, J′ = 4.5, J″ = 11.6 Hz); 4.14 (dd, 1H, CH, J′ = 3.4, J″ = 10.6 Hz); 5.45 (dd, 1H, CH, J′ = 4.0, J″= 9.2 Hz); 5.67 (s, 1NH); 7.07-7.16 (m, 2H, aryl); 7.19 (d, 2H, aryl, J = 5.6 Hz); 7.25 (d, 1H, aryl, J = 6.9 Hz); 7.31 (t, 3H, aryl, J = 7.9 Hz); 7.50 (d, 1H, aryl, J = 7.6 Hz); 7.95 (s, 1NH). ^{13}C NMR (100 MHz, CDCl$_3$) δ 17.7, 18.1, 19.9, 27.0, 33.3, 42.0, 47.3, 51.1, 52.2, 103.0, 107.2, 114.3, 116.2, 118.3, 122.2, 125.2, 125.4, 130.3, 131.8, 164.3, 165.2. HR-MS m/z calcd for C$_{25}$H$_{27}$N$_3$O$_2$ [(M + H)]$^+$: 402.2176; found 402.2190.

(1R,3S)-Methyl   2-(2-((tert-Butoxycarbonyl)amino)acetyl)-1-(4-chlorophenyl)-2,3,4,9-tetrahydro-1H-pyrido[3,4-b]indole3-carboxylate (26a).

Compound **26a** was synthesized in 62% yield starting from intermediate **15a** and N-Boc-Gly-OH following the general procedure B. FC in ethyl acetate/n-hexa½1/2, Rf = 0.35. Spectral data were in accordance with literature.[91]

(1S,3S)-Methyl   2-(2-((tert-Butoxycarbonyl)amino)acetyl)-1-(4-chlorophenyl)-2,3,4,9-tetrahydro-1H-pyrido[3,4-b]indole3-carboxylate (26b).

Compound **26b** was synthesized in 52% yield starting from intermediate **15b** and N-Boc-Gly-OH following the general procedure B. FC in ethyl acetate/n-hexa½1/2, Rf = 0.45. Spectral data were in accordance with literature.[91]

(6R,12aS)-6-(4-Chlorophenyl)-2,3,12,12a-tetrahydropyrazino[1′,2′:1,6]pyrido[3,4-b]indole-1,4(6H,7H)-dione (27a).

Obtained from **26a** following the general procedure C. FC in ethyl acetate/n-hexane 4/1, Rf = 0.33. White powder (82% yield). $[\alpha]^{25}_D$: −244.0 ± 0.2. ^{1}H NMR (CDCl$_3$, 400 MHz): δ: 2.96 (dd, 1H, CH$_{2a}$, J′ = 12.0, J″ = 16.6 Hz); 3.46 (dd, 1H, CH$_{2a}$, J′ = 4.2, J″ = 15.5 Hz); 4.02 (d, 1H, CH$_{2a}$, J = 17.7 Hz); 4.12 (d, 1H, CH$_{2b}$, J = 17.7 Hz); 4.18 (dd, 1H, CH, J′ = 4.2, J″ = 12.0 Hz); 6.67 (s, 1H, CH); 6.97 (s, 1NH); 7.08-7.26 (m, 7H, aryl); 7.48 (d, 1H, aryl, J = 7.7 Hz); 8.00 (s, 1NH). ^{13}C NMR (CDCl$_3$, 100 MHz) δ: 27.2, 44.8, 51.5, 52.3, 109.1, 111.2, 118.5, 120.3, 123.0, 126.2, 129.1, 129.2, 130.1, 135.0, 136.4, 136.7, 161.8, 167.5. HR-MS m/z calcd for C$_{20}$H$_{16}$ClN$_3$O$_2$, 366.1004; found 366.1011.

(6S,12aS)-6-(4-Chlorophenyl)-2,3,12,12a-tetrahydropyrazino[1′,2′:1,6]pyrido[3,4-b]indole-1,4(6H,7H)-dione (27b).

Obtained from **26b** following the general procedure C. FC in ethyl acetate/n-hexane 4/1, Rf = 0.37. White powder (76% yield). $[\alpha]^{25}_D$: −79 ± 0.01. ^{1}H NMR (CDCl$_3$, 400 MHz): δ: 3.17 (dd, 1H, CH2a, J′ = 10.3, J″ = 16.0 Hz); 3.67 (dd, 1H, CH$_{2b}$, J′ = 4.6, J″ = 16.0 Hz); 3.93-4.06 (m, 2H, CH$_2$); 4.30 (dd, 1H, CH, J′ = 4.5, J″ = 11.5 Hz); 6.16 (s, 1H, CH); 6.26 (s, 1NH); 7.07-7.22 (m, 7H, aryl); 7.53 (d, 1H, aryl, J = 8.4 Hz); 7.80 (s, 1NH). ^{13}C NMR (CDCl$_3$, 100 MHz) δ: 23.4, 45.3, 55.8, 56.3, 106.6, 111.3, 118.6, 120.3, 122.8, 126.1, 128.6, 128.9, 132.2, 133.7, 136.6, 139.8, 167.1, 168.5. HR-MS m/z calcd for C$_{20}$H$_{16}$ClN$_3$O$_2$ [(M + H)]$^+$: 366.1004; found 366.1009.

(S)-2-(4-Fluorobenzyl)-5,6,11,11a-tetrahydro-1H-imidazo-[1′,5′:1,6]pyrido[3,4-b]indole-1,3(2H)-dione (28).

Obtained from **13** and 4-fluorobenzylamine following the general procedure D. FC in n-hexane/ethyl acetate 3/2, Rf = 0.45. White powder (65% yield). ^{1}H NMR (400 MHz, CDCl$_3$): δ: 2.78 (dd, 1H, CH$_{2a}$, J′ = 12.8, J″ = 13.1 Hz); 3.41 (dd, 1H, CH$_{2b}$, J′= 5.3, J″= 15.1 Hz,); 4.25 (dd, 1H, CH, J′ = 5.5, J″ = 11.0 Hz); 4.40 (d, 1H, CH$_{2a}$, J = 16.1 Hz); 4.73 (s, 2H, CH$_2$); 5.10 (d, 1H, CH$_{2b}$, J = 16.1 Hz); 7.03 (t, 2H, aryl, J = 8.6 Hz); 7.17 (t, 1H, aryl, J = 7.4 Hz); 7.23 (t, 1H, aryl, J = 7.1 Hz); 7.34 (d, 1H, aryl, J = 8.0 Hz); 7.43-7.46 (m, 2H, aryl); 7.50 (d, 1H, aryl, J = 7.7 Hz); 8.15 (s, 1H, NH). ^{13}C NMR (100 MHz, CDCl$_3$) δ: 23.1, 37.8, 41.7, 55.3, 106.3, 111.0, 115.5, 115.7, 118.1, 120.2, 122.7, 126.4, 128.3, 130.6, 131.9, 136.5, 155.1, 161.3, 163.7, 172.5. HR-MS m/z calcd for C$_{20}$H$_{16}$FN$_3$O$_2$ [(M + H)]$^+$: 350.1299; found 350.1307.

(5R,11aS)-5-Isobutyl-2-(4-methoxybenzyl)-5,6,11,11a-tetrahydro-1H-imidazo[1′,5′:1,6]pyrido[3,4-b]indole-1,3(2H)-dione (29a).

Obtained from 14a and 4-methoxybenzylamine following the general procedure D. FC in n-hexane/ethyl acetate 1/1, Rf = 0.38. White powder (32% yield). $[\alpha]^{25}_D$: −92.360 ± 0.179 (c = 0.10, MeOH). ^{1}H NMR (400 MHz, CDCl$_3$) δ 0.98 (d, 3H, CH$_3$, J = 8.2 Hz); 1.17 (d, 3H, CH$_3$, J = 8.8 Hz); 1.68-1.77 (m, 2H, CH$_2$); 1.79-1.88 (m, 1H, CH); 2.75 (dd, 1H, CH$_{2a}$, J′ = 12.3, J″ = 17.4 Hz); 3.37 (dd, 1H, CH$_{2b}$, J′ = 6.8, J″= 19.4 Hz); 3.79 (s, 3H, CH$_3$); 4.30 (dd, 1H, CH, J′ = 7.8, J″ = 14.8 Hz); 4.62 (d, 1H, CH$_{2a}$, J = 18.5 Hz,); 4.75 (d, 1H, CH$_{2b}$, J = 18.5 Hz); 5.29-5.34 (m, 1H, CH); 6.87 (d, 2H, aryl, J = 10.0 Hz); 7.14 (t, 1H, aryl, J = 9.0 Hz); 7.24 (t, 1H, aryl, J = 9.0 Hz); 7.33-7.40 (m, 3H, aryl); 7.47 (d, 1H, aryl, J = 8.8 Hz); 7.89 (s, 1NH). ^{13}C NMR (100 MHz, CDCl$_3$) δ 22.2, 23.5, 23.6, 25.0, 41.8, 45.8, 46.9, 52.9, 55.2, 105.7, 111.0, 114.1, 118.2, 120.1, 122.6, 126.3, 128.5, 130.2, 133.2, 136.2, 155.3, 159.2, 172.9. HR-MS m/z calcd for C$_{25}$H$_{27}$N$_3$O$_3$ [(M + H)]$^+$: 418.2125; found 418.2139.

(5S,11aR)-5-Isobutyl-2-(4-methoxybenzyl)-5,6,11,11a-tetrahydro-1H-imidazo[1′,5′:1,6]pyrido[3,4-b]indole-1,3(2H)-dione (29a′).

Obtained from **14b** and 4-methoxybenzylamine following the general procedure D. FC in n-hexane/ethyl acetate 1/1, Rf = 0.44. White powder (43% yield). $[\alpha]^{25}_D$: +98.563 ± 0.158 (c = 0.10, MeOH). ^{1}H NMR (400 MHz, CDCl$_3$) δ 0.98 (d, 3H, CH$_3$, J = 8.7 Hz); 1.17 (d, 3H, CH$_3$, J = 8.7 Hz); 1.65-1.77 (m, 2H, CH$_2$); 1.80-1.88 (m, 1H, CH); 2.76 (dd, 1H, CH$_{2a}$, J′ = 14.5, J″ = 18.8 Hz); 3.37 (dd, 1H, CH$_{2b}$ J′ = 7.8, J″ = 20.4 Hz); 3.79 (s, 3H, CH$_3$); 4.30 (dd, 1H, CH, J′ = 7.7, J″ = 14.4 Hz); 4.62 (d, 1H, CH$_{2a}$, J = 19.2 Hz); 4.75 (d, 1H, CH$_{2b}$, J = 19.2 Hz); 5.30-5.34 (m, 1H, CH); 6.86 (d, 2H, aryl, J = 11.5 Hz); 7.15 (t, 1H, aryl, J = 9.3 Hz); 7.22 (t, 1H, aryl, J = 9.1 Hz); 7.28-7.40 (m, 3H, aryl); 7.47 (d, 1H, aryl, J = 10.4 Hz); 7.89 (s, 1NH). ^{13}C NMR (100 MHz, CDCl$_3$) δ 22.2, 23.5, 23.6, 25.0, 41.8, 45.8, 46.9, 52.9, 55.2, 105.7, 111.0, 114.1, 118.2, 120.1, 122.6, 126.3, 128.5, 130.0, 133.1, 136.2, 155.3, 159.3, 172.9. HR-MS m/z calcd for C$_{25}$H$_{27}$N$_3$O$_3$ [(M + H)]$^+$: 418.2125; found 418.2132.

(5R,11aS)-5-(4-Chlorophenyl)-2-(4-methylbenzyl)-5,6,11,11a-tetrahydro-1H-imidazo[1′,5′:1,6]pyrido[3,4-b]-indole-1,3(2H)-dione (30a).

Obtained from **15a** and 4-methylbenzylamine following the general procedure D. FC in dichloromethane/ethyl acetate 9.8/0.2, Rf = 0.42. White powder (38% yield). $[\alpha]^{25}_D$: −181.00 ± 0.10 (c = 0.10, MeOH). ^{1}H NMR (400 MHz, CDCl$_3$): δ: 2.32 (s, 3H, CH$_3$); 2.83 (dd, 1H, CH$_{2a}$, J′ = 11.3, J″ = 14.8 Hz); 3.49 (dd, 1H, CH$_{2b}$, J′= 5.3, J″ = 15.3 Hz); 4.30 (dd, 1H, CH, J′ = 5.3,

$J'' = 10.8$ Hz); 4.61 (d, 1H, CH$_{2a}$, J = 14.4 Hz); 4.71 (d, 1H, CH$_{2b}$, J = 14.4 Hz,); 6.29 (s, 1H, CH); 7.13 (d, 2H, aryl, J = 7.6 Hz); 7.18-7.36 (m, 9H, aryl); 7.55 (d, 1H, aryl, J = 7.6 Hz); 7.72 (s, 1NH). ^{13}C NMR (100 MHz, CDCl$_3$) δ: 21.1, 23.3, 42.2, 51.4, 53.2, 108.4, 111.2, 118.5, 120.3, 123.1, 126.1, 128.7, 129.4, 129.8, 133.0, 135.0, 136.6, 137.5, 137.8, 154.7, 172.2. HR-MS m/z calcd for C$_{27}$H$_{22}$ClN$_3$O$_2$ [(M + H)]$^+$: 456.1473; found 456.1480.

(5S,11aR)-5-(4-Chlorophenyl)-2-(4-methylbenzyl)-5,6,11,11a-tetrahydro-1H-imidazo[1′,5′:1,6]pyrido[3,4-b]- indole-1,3(2H)-dione (30a′).

Obtained from **15b** and 4-methylbenzylamine following the general procedure D. FC in dichloromethane/ethyl acetate 9.8/0.2, Rf = 0.42. White powder (41% yield). [α]^{25}$_D$: +175.00 ± 0.02 (c = 0.10, MeOH). ^{1}H NMR (400 MHz, CDCl$_3$): δ: 2.32 (s, 3H, CH$_3$); 2.84 (dd, 1H, CH$_{2a}$, J′ = 11.3, J″ = 14.8 Hz); 3.49 (dd, 1H, CH$_{2b}$, J′= 5.3, J″ = 15.3 Hz); 4.30 (dd, 1H, CH, J′ = 5.3, J″ = 10.8 Hz); 4.61 (d, 1H, CH$_{2a}$, J = 14.4 Hz); 4.71 (d, 1H, CH$_{2b}$, J = 14.4 Hz,); 6.29 (s, 1H, CH); 7.13 (d, 2H, aryl, J = 7.6 Hz); 7.20-7.35 (m, 9H, aryl); 7.54 (d, 1H, aryl, J = 7.6 Hz); 7.72 (s, 1NH). ^{13}C NMR (100 MHz, CD$_3$OD) δ: 21.1, 23.3, 42.2, 51.4, 53.2, 108.4, 111.2, 118.5, 120.3, 123.1, 126.0, 128.7, 129.8, 133.0, 135.0, 136.6, 137.5, 137.8, 154.7, 172.2. HR-MS m/z calcd for C$_{27}$H$_{22}$ClN$_3$O$_2$ [(M + H)]$^+$: 456.1473; found 456.1478.

(5R,11aS)-5-(4-Chlorophenyl)-2-(4-fluorobenzyl)-5,6,11,11a-tetrahydro-1H-imidazo[1′,5′:1,6]pyrido[3,4-b]- indole-1,3(2H)-dione (31a).

Obtained from **15a** and 4-fluorobenzylamine following the general procedure D. FC in dichloromethane/ethyl acetate 8/2, Rf = 0.40. White powder (33% yield). [α]^{25}$_D$: −105.00 ± 0.10 (c = 0.10, MeOH). ^{1}H NMR (400 MHz, CDCl$_3$): δ: 2.87 (t, 1H, CH$_{2a}$, J = 12.6 Hz); 3.51 (dd, 1H, CH$_{2b}$, J′= 4.2, J″ = 14.2 Hz); 4.31 (dd, 1H, CH, J′ = 4.9, J″ = 10.4 Hz); 4.60 (d, 1H, CH$_{2a}$, J = 14.5 Hz); 4.70 (d, 1H, CH$_{2b}$, J = 14.5 Hz,); 6.28 (s, 1H, CH); 7.00 (t, 2H, aryl, J = 8.1 Hz); 7.18-7.41 (m, 9H, aryl); 7.57 (d, 1H, aryl, J = 7.4 Hz); 7.84 (s, 1NH). ^{13}C NMR (100 MHz, CDCl$_3$) δ 23.3, 41.7, 51.4, 53.3, 108.4, 111.3, 115.5, 115.7, 118.5, 120.4, 123.2, 126.0, 129.4, 129.6, 129.7, 130.6, 131.8, 135.0, 136.6, 137.4, 154.6, 161.3, 163.7, 172.2. HR-MS m/z calcd for C$_{26}$H$_{19}$ClFN$_3$O$_2$ [(M + H)]$^+$: 460.1223; found 460.1218.

(5S,11aR)-5-(4-Chlorophenyl)-2-(4-fluorobenzyl)-5,6,11,11a-tetrahydro-1H-imidazo[1′,5′:1,6]pyrido[3,4-b]- indole-1,3(2H)-dione (31a′).

Obtained from **15b** and 4-fluorobenzylamine following the general procedure D. FC in dichloromethane/ethyl acetate 8/2, Rf = 0.40. White powder (41% yield). [α]^{25}$_D$: +97.00 ± 0.02

(c = 0.10, MeOH). ^{1}H NMR (400 MHz, CDCl$_3$): δ: 2.86 (dd, 1H, CH$_{2a}$, J′ = 11.1, J″ = 12.9 Hz); 3.50 (dd, 1H, CH2b, J′= 5.5, J″ = 15.4 Hz); 4.30 (dd, 1H, CH, J′ = 5.5, J″ = 11.0 Hz); 4.60 (d, 1H, CH$_{2a}$, J = 14.5 Hz); 4.69 (d, 1H, CH$_{2b}$, J = 14.5 Hz,); 6.28 (s, 1H, CH); 6.99 (t, 2H, aryl, J = 8.6 Hz); 7.16-7.41 (m, 9H, aryl); 7.55 (d, 1H, aryl, J = 7.6 Hz); 7.75 (s, 1NH). ^{13}C NMR (100 MHz, CDCl$_3$) δ: 23.3, 41.7, 51.5, 53.3, 108.4, 111.2, 115.5, 115.7, 118.5, 120.4, 123.2, 126.0, 129.4, 129.6, 129.7, 130.6, 131.8, 135.0, 136.6, 137.4, 154.6, 161.3, 163.7, 172.2. HR-MS m/z calcd for C$_{26}$H$_{19}$ClFN$_3$O$_2$ [(M + H)]$^+$: 460.1223; found 460.1215.

(1R,3S)-Methyl-1-(4-Fluorophenyl)-2,3,4,9-tetrahydro-1H-pyrido[3,4-b]indole-3-carboxylate (32a).

Synthesized in 35% yield from L-tryptophan methyl ester and 4-fluorobenzaldehyde following the general procedure A, as previously described.[85] FC in ethyl acetate/n-hexa½1/2, Rf = 0.36. Spectral data were in accordance with literature.

(1S,3S)-Methyl-1-(4-Fluorophenyl)-2,3,4,9-tetrahydro-1H-pyrido[3,4-b]indole-3-carboxylate (32b).

Synthesized in 44% yield from L-tryptophan methyl ester and 4-fluorobenzaldehyde following the general procedure A, as previously described.[85] FC in ethyl acetate/n-hexane 1/2, Rf = 0.41. Spectral data were in accordance with literature.

(5R,11aS)-2-Benzyl-5-(4-fluorophenyl)-5,6,11,11a-tetrahydro-1H-imidazo[1′,5′:1,6]pyrido[3,4-b]indole-1,3(2H)-dione (33a).

Obtained from **32a** and benzylamine following the general procedure D. FC in hexane/ethyl acetate 7/3, Rf = 0.48. White powder (36% yield). [α]^{25}$_D$: −113.529 ± 0.182 (c = 0.10, MeOH). ^{1}H NMR (400 MHz, CDCl$_3$): δ: 2.75 (dd, 1H, CH2a, J′ = 11.8, J″ = 16.0 Hz); 3.40 (dd, 1H, CH$_{2b}$, J′ = 5.5, J″ = 11.8 Hz); 4.22 (dd, 1H, CH, J′ = 5.5, J″ = 11.0 Hz); 4.61 (d, 1H, CH$_{2a}$, J = 14.5 Hz); 4.67 (d, 1H, CH$_{2b}$, J = 14.5 Hz,); 6.22 (s, 1H, CH); 6.96 (t, 2H, aryl, J = 8.6 Hz); 7.10-7.25 (m, 8H, aryl); 7.32 (d, 2H, aryl, J = 8.1 Hz); 7.46 (d, 1H, aryl, J = 7.7 Hz); 7.68 (s, 1NH). ^{13}C NMR (100 MHz, CDCl$_3$) δ: 23.4, 42.4, 51.4, 53.2, 108.3, 111.2, 116.0, 116.2, 118.5, 120.3, 123.1, 126.1, 128.0, 128.7, 130.1, 134.9, 136.0, 136.6, 154.7, 161.7, 164.2, 172.3. HR-MS m/z calcd for C$_{26}$H$_{20}$FN$_3$O$_2$ [(M + H)]$^+$: 426.1612; found 426.1619.

(5S,11aR)-2-Benzyl-5-(4-fluorophenyl)-5,6,11,11a-tetrahydro-1H-imidazo[1′,5′:1,6]pyrido[3,4-b]indole-1,3(2H)-dione (33a′).

Obtained from **32b** and benzylamine following the general procedure D. FC in hexane/ethyl acetate 7/3, Rf = 0.48. White powder (40% yield). $[\alpha]^{25}_D$: +124.615 ± 0.162. ^{1}H NMR (400 MHz, CDCl$_3$): δ: 2.79 (dd, 1H, CH$_{2a}$, J′ = 11.1, J″ = 15.3 Hz); 3.47 (dd, 1H, CH$_{2b}$, J′ = 5.4, J″ = 11.4 Hz); 4.30 (dd, 1H, CH, J′ = 5.5, J″ = 11.0 Hz); 4.63 (d, 1H, CH$_{2a}$, J = 14.5 Hz); 4.75 (d, 1H, CH$_{2b}$, J = 14.6 Hz); 6.30 (s, 1H, CH); 7.04 (t, 2H, aryl, J = 8.6 Hz); 7.17-7.35 (m, 8H, aryl); 7.41-7.44 (m, 2H, aryl); 7.54 (d, 1H, aryl, J = 7.7 Hz); 7.78 (s, 1NH). ^{13}C NMR (100 MHz, CDCl$_3$) δ: 23.3, 42.4, 51.3, 53.2, 108.3, 111.2, 116.0, 116.2, 118.5, 120.3, 123.1, 126.0, 128.0, 128.7, 130.1, 134.9, 136.0, 136.6, 154.6, 161.7, 164.1, 172.3. HR-MS m/z calcd for C$_{26}$H$_{20}$FN$_3$O$_2$ [(M + H)]$^+$: 426.1612; found 426.1621.

Tert-Butyl(3-((5R,11aS)-5-(4-Fluorophenyl)-1,3-dioxo11,11a-dihydro-1H-imidazo[1′,5′:1,6]pyrido[3,4-b]indol-2- (3H,5H,6H)-yl)propyl)carbamate (34a).

Synthesized from **32a** and N-Boc-diaminopropane following the general procedure D. FC in n-hexane/ethyl acetate 2/1, Rf = 0.55. White powder (49% yield). $[\alpha]^{25}_D$: −166.70 ± 0.35 (c = 0.10, MeOH). ^{1}H NMR (400 MHz, CDCl$_3$) δ 1.40 (s, 9H, CH$_3$); 1.73-1.80 (m, 2H, CH$_2$); 2.89 (dd, 1H, CH$_{2a}$, J′ = 11.5, J″ = 14.2 Hz,) 3.09-3.12 (m, 2H, CH$_2$); 3.51 (dd, 1H, CH$_{2b}$, J′ = 5.5, J″ = 15.5 Hz); 3.57-3.66 (m, 2H, CH$_2$); 4.28 (dd, 1H, CH, J′ = 5.4, J″ = 11.0 Hz); 5.19 (bs, 1NH); 6.31 (s, 1H, CH); 7.02 (t, 2H, aryl, J = 8.4 Hz); 7.19 (t, 1H, aryl, J = 7.1 Hz); 7.25 (t, 1H, aryl, J = 7.1 Hz); 7.31-7.35 (m, 3H, aryl); 7.55 (d, 1H, aryl, J = 7.7 Hz); 8.22 (bs, 1NH). HR-MS m/z calcd for C$_{27}$H$_{29}$FN$_4$O$_4$ [(M + H)]$^+$: 493.2246; found 493.2252.

Tert-Butyl(3-((5S,11aR)-5-(4-Fluorophenyl)-1,3-dioxo11,11a-dihydro-1H-imidazo[1′,5′:1,6]pyrido[3,4-b]indol-2- (3H,5H,6H)-yl)propyl)carbamate (34a′).

Synthesized from **32b** and N-Boc-diaminopropane following the general procedure D. FC in n-hexane/ethyl acetate 2/1, Rf = 0.55. White powder (57% yield). $[\alpha]^{25}_D$: +125.36 ± 0.40 (c = 0.10, MeOH). ^{1}H NMR (400 MHz, CDCl$_3$) δ 1.43 (s, 9H, CH$_3$); 1.75-1.81 (m, 2H, CH$_2$); 2.88 (dd, 1H, CH$_{2a}$, J′ = 11.3, J″ = 14.0 Hz) 3.08-3.11 (m, 2H, CH$_2$); 3.51 (dd, 1H, CH$_{2b}$, J′ = 5.6, J″ = 15.4 Hz); 3.55-3.67 (m, 2H, CH$_2$); 4.29 (dd, 1H, CH, J′ = 5.5, J″ = 11.1 Hz); 5.15 (bs, 1NH); 6.31 (s, 1H, CH); 7.04 (t, 2H, aryl, J = 8.6 Hz); 7.19 (t, 1H, aryl, J = 6.9 Hz); 7.24 (t, 1H, aryl, J = 7.0 Hz); 7.31-7.34 (m, 3H, aryl); 7.56 (d, 1H, aryl, J = 7.7 Hz); 8.24 (bs, 1NH). HR-MS m/z calcd for C$_{27}$H$_{29}$FN$_4$O$_4$ [(M + H)]$^+$: 493.2246; found 493.2250.

(5R,11aS)-2-(3-Aminopropyl)-5-(4-fluorophenyl)-5,6,11,11atetrahydro-1H-imidazo[1′,5′:1,6]pyrido[3,4-b]indole-1,3(2H)- dione (35a).

Synthesized according to the general procedure C starting from intermediate **34**. FC in dichloromethane/methanol 9/1, Rf = 0.47. White powder (35% yield). $[\alpha]^{25}_D$: -102.500 ± 0.075 (c = 0.10, MeOH). ^{1}H NMR (400 MHz, CD$_3$OD) δ 1.83-1.92 (m, 2H, CH$_2$); 2.81 (t, 2H, CH$_2$, J = 5.7 Hz) 2.90 (dd, 1H, CH$_{2a}$, J′ = 18.3, J″ = 20.0 Hz); 3.50 (dd, 1H, CH$_{2b}$, J′ = 7.4, J″= 20.0 Hz); 3.64 (t, 2H, J = 8.9 Hz, CH$_2$); 4.54 (dd, 1H, CH, J′ = 7.6, J″ = 14.7 Hz); 6.34 (s, 1H, CH); 7.05-7.17 (m, 4H, aryl); 7.29 (d, 1H, aryl, J = 10.0 Hz); 7.38-7.42 (m, 2H, aryl); 7.55 (d, 1H, aryl, J = 10.3 Hz). ^{13}C NMR (100 MHz, CD$_3$OD) δ 22.7, 30.7, 35.5, 38.1, 51.4, 53.2, 106.6, 110.9, 115.1, 115.3, 117.7, 119.0, 121.9, 126.0, 129.9, 130.3, 135.9, 137.2, 155.1, 161.5, 163.9, 173.6. HR-MS m/z calcd for C$_{22}$H$_{21}$FN$_4$O$_2$ [(M + H)]$^+$: 393.1721; found 393.1733.

(5S,11aR)-2-(3-Aminopropyl)-5-(4-fluorophenyl)-5,6,11,11atetrahydro-1H-imidazo[1′,5′:1,6]pyrido[3,4-b]indole-1,3(2H)- dione (35a′).

Synthesized according to the general procedure C starting from intermediate **34′**. FC in dichloromethane/methanol 9/1, Rf = 0.47. White powder (38% yield). $[\alpha]^{25}_D$: $+107.83 \pm 0.21$ (c = 0.10, MeOH). ^{1}H NMR (400 MHz, CD$_3$OD) δ 1.71-1.80 (m, 2H, CH$_2$); 2.61 (t, 2H, CH$_2$, J = 9.0 Hz,) 2.81 (dd, 1H, CH$_{2a}$, J′ = 14.9, J″ = 19.8 Hz,); 3.43 (dd, 1H, CH$_{2b}$, J′ = 7.4, J″ = 20.1 Hz); 3.60 (t, 2H, CH$_2$, J = 8.9 Hz,) 4.46 (dd, 1H, CH, J′ = 7.5, J″ = 14.7 Hz); 6.30 (s, 1H, CH); 7.03-7.15 (m, 4H, aryl); 7.28 (d, 1H, aryl, J = 10.7 Hz); 7.34-7.39 (m, 2H, aryl); 7.52 (d, 1H, aryl, J = 10.1 Hz). ^{13}C NMR (100 MHz, CD$_3$OD) δ: 22.7, 30.7, 35.5, 38.0, 51.4, 53.2, 106.6, 110.9, 115.1, 115.3, 117.7, 119.0, 121.9, 126.0, 129.9, 130.3, 135.9, 137.2, 155.1, 161.5, 163.9, 173.6. HR-MS m/z calcd for C$_{22}$H$_{21}$FN$_4$O$_2$ [(M + H)]$^+$: 393.1721; found 393.1729.

(5R,11aS)-5-(4-Fluorophenyl)-2-(3-(trifluoromethyl)phenyl)-5,6,11,11a-tetrahydro-1H-imidazo[1′,5′:1,6]pyrido[3,4-b]- indole-1,3(2H)-dione (36a).

Synthesized form **32a** and 3-trifluoromethylphenyl isocyanate following the general procedure E. FC in dichloromethane/n-hexane 8/2, Rf = 0.40. Yellowish powder (39% yield). $[\alpha]^{25}_D$: -159.00 ± 10.00 (c = 0.10, MeOH). ^{1}H NMR (CDCl$_3$, 400 MHz): δ: 3.01 (dd, 1H, CH$_{2a}$, J′ = 11.1, J″ = 15.4 Hz); 3.54 (dd, 1H, CH$_{2b}$, J′ = 5.5, J″ = 15.4 Hz); 4.41 (dd, 1H, CH, J′ = 5.5, J″ = 11.0 Hz); 6.32 (s, 1H, CH); 7.14 (t, 1H, aryl, J = 6.9 Hz); 7.18 (t, 1H, aryl, J = 6.8 Hz); 7.24-7.30 (m, 5H, aryl); 7.49-7.56 (m, 3H, aryl); 7.61 (d, 1H, aryl, J = 7.6 Hz); 7.71 (s, 1H, aryl); 7.78 (s, 1H, NH). ^{13}C NMR (CDCl$_3$, 100 MHz) δ: 23.6, 51.7, 53.1, 108.4, 111.3, 118.6, 120.5, 122.9, 123.3, 124.8, 126.0, 129.0, 129.5, 129.6, 129.8, 131.4, 131.8, 132.1, 135.3, 136.7, 137.1,

153.2, 170.9. ^{19}F NMR (CDCl$_3$, 376.3 MHz) δ: −(62.59) (s, 3F, CF$_3$); −(111.96) (s, 1F, CF). HR-MS m/z: calcd. for C$_{26}$H$_{17}$F$_4$N$_3$O$_2$, [(M + H)]$^+$: 480.1330; found 480.1338.

(5S,11aR)-5-(4-Fluorophenyl)-2-(3-(trifluoromethyl)phenyl)- 5,6,11,11a-tetrahydro-1H-imidazo[1′,5′:1,6]pyrido[3,4-b]- indole-1,3(2H)-dione (36a′).

Synthesized form **32b** and 3-trifluoromethylphenyl isocyanate following the general procedure F. FC in dichloromethane/n-hexane 8/2, Rf = 0.40. Yellowish powder (40% yield). [α]$^{25}_D$: +172.00 ± 10.00 (c = 0.10, MeOH). ^{1}H NMR (CDCl$_3$, 400 MHz): δ: 3.02 (dd, 1H, CH$_{2a}$, J′ = 11.3, J″ = 13.7 Hz); 3.56 (dd, 1H, CH$_{2b}$, J′ = 5.4, J″ = 15.3 Hz); 4.43 (dd, 1H, CH, J′ = 5.4, J″ = 10.8 Hz); 6.35 (s, 1H, CH); 7.01 (t, 2H, aryl, J = 8.5 Hz); 7.14-7.33 (m, 5H, aryl); 7.51-7.56 (m, 3H, aryl); 7.63 (d, 1H, aryl, J = 7.3 Hz); 7.74 (s, 1H, aryl); 7.80 (s, 1H, NH). ^{13}C NMR (CDCl$_3$, 100 MHz) δ: 23.6, 51.7, 53.0, 108.3, 111.3, 116.15, 116.36, 118.6, 120.5, 122.82, 122.86, 123.3, 124.8, 126.1, 129.0, 129.6, 129.8, 130.22, 130.31, 132.1, 134.5, 136.7, 153.2, 161.8, 164.3, 170.9. ^{19}F NMR (CDCl$_3$, 376.3 MHz) δ: −(62.67) (s, 3F, CF3); −(111.84) (s, 1F, CF). HR-MS m/z: calcd. for C$_{26}$H$_{17}$F$_4$N$_3$O$_2$, [(M + H)]$^+$: 480.1330; found 480.1335.

(5S,11aS)-5-(4-Fluorophenyl)-2-(3-(trifluoromethyl)phenyl)- 5,6,11,11a-tetrahydro-1H-imidazo[1′,5′:1,6]pyrido[3,4-b]- indole-1,3(2H)-dione (36b).

Synthesized form **32b** and 3-trifluoromethylphenyl isocyanate following the general procedure E. FC in dichloromethane/n-hexane 8/2, Rf = 0.35. Yellowish powder (42% yield). [α]$^{25}_D$: −1.00 ± 0.01 (c = 0.10, MeOH). ^{1}H NMR (CDCl$_3$, 400 MHz): δ: 3.15 (t, 1H, CH$_{2a}$, J = 13.5 Hz); 3.56 (dd, 1H, CH$_{2b}$, J′ = 4.4, J″ = 15.1 Hz); 4.54 (dd, 1H, CH, J′ = 4.5, J″ = 13.3 Hz); 5.86 (s, 1H, CH); 6.97 (t, 2H, aryl, J = 6.9 Hz); 7.11-7.20 (m, 3H, aryl); 7.26 (t, 2H, aryl, J = 6.8 Hz); 7.45-7.58 (m, 5H, aryl); 7.67 (s, 1H, NH). ^{13}C NMR (CDCl$_3$, 100 MHz) δ: 23.6, 51.7, 53.0, 108.3, 111.3, 116.1, 116.4, 118.6, 120.5, 122.8, 122.9, 123.3, 124.8, 126.1, 129.0, 129.6, 129.8, 130.2, 130.3, 132.1, 134.5, 136.7, 153.2, 161.8, 164.3, 170.9. ^{19}F NMR (CDCl$_3$, 376.3 MHz) δ: −(62.44) (s, 3F, CF3); −(112.08) (s, 1F, CF). HR-MS m/z: calcd for C$_{26}$H$_{17}$F$_4$N$_3$O$_2$, [(M + H)]$^+$: 480.1330; found 480.1341.

(5R,11aS)-2-(2-Fluorophenyl)-5-(4-fluorophenyl)-5,6,11,11a-tetrahydro-1H-imidazo[1′,5′:1,6]pyrido[3,4-b]- indole-1,3(2H)-dione (37a).

Synthesized from **32a** and 2-fluorophenyl isocyanate following the general procedure E. FC in dichloromethane/ethyl acetate 9.5/0.5, Rf = 0.52. Yellowish powder (42% yield). [α]$^{25}_D$: −154.00 ± 2.53 (c = 0.10, MeOH). ^{1}H NMR (CDCl$_3$, 400 MHz): δ: 3.11 (t, 1H, CH$_{2a}$, J = 12.7

Hz); 3.63 (dd, 1H, CH$_{2b}$, J$'$ = 5.4, J$''$ = 15.4 Hz); 4.52 (dd, 1H, CH, J$'$ = 5.2, J$''$ = 10.7 Hz); 6.41 (s, 1H, CH); 7.08 (t, 2H, aryl, J = 8.4 Hz); 7.23-7.45 (m, 9H, aryl); 7.62 (d, 1H, aryl, J = 7.4 Hz); 7.96 (s, 1H, NH). ^{13}C NMR (CDCl$_3$, 100 MHz) δ: 23.7, 51.6, 53.4, 108.3, 111.3, 116.1, 116.3, 116.7, 118.5, 119.1, 120.4, 123.2, 124.7, 126.1, 129.6, 129.9, 130.2, 131.0, 134.8, 136.7, 153.2, 156.5, 159.0, 161.8, 164.2, 170.9. ^{19}F NMR (CDCl$_3$, 376.3 MHz) δ: −(112.10) (s, 1F, CF). HR-MS m/z: calcd. for C$_{25}$H$_{17}$F$_2$N$_3$O$_2$, [(M + H)]$^+$: 430.1362; found 430.1370.

(5S,11aR)-2-(2-Fluorophenyl)-5-(4-fluorophenyl)-5,6,11,11a-tetrahydro-1H-imidazo[1′,5′:1,6]pyrido[3,4-b]- indole-1,3(2H)-dione (37a′).

Synthesized from **32b** and 2-fluorophenyl isocyanate following the general procedure F. FC in dichloromethane/ethyl acetate 9.5/0.5, Rf = 0.52. Yellowish powder (39% yield). [α]^{25}$_D$: +166.00 ± 2.53 (c = 0.10, MeOH). ^{1}H NMR (CDCl$_3$, 400 MHz): δ: 3.13 (t, 1H, CH$_{2a}$, J = 15.0 Hz); 3.64 (dd, 1H, CH$_{2b}$, J$'$ = 5.4, J$''$ = 15.4 Hz); 4.53 (dd, 1H, CH, J$'$ = 5.4, J$''$ = 11.0 Hz); 6.44 (s, 1H, CH); 7.10 (t, 2H, aryl, J = 8.5 Hz); 7.22-7.48 (m, 9H, aryl); 7.63 (d, 1H, aryl, J = 7.7 Hz); 7.88 (s, 1H, NH). ^{13}C NMR (CDCl$_3$, 100 MHz) δ: 23.7, 51.6, 53.4, 108.4, 111.3, 116.1, 116.3, 116.7, 116.9, 118.6, 120.4, 123.2, 124.7, 126.1, 129.6, 129.9, 130.2, 130.3, 130.87, 130.95, 134.7, 136.7, 153.2, 156.5, 159.0, 161.8, 164.3, 170.8. ^{19}F NMR (CDCl$_3$, 376.3 MHz) δ: −(119.22) (s, 1F, CF); −(112.05) (s, 1F, CF). HR-MS m/z: calcd for C$_{25}$H$_{17}$F$_2$N$_3$O$_2$, [(M + H)]$^+$: 430.1362; found 430.1355.

(5S,11aS)-2-(2-Fluorophenyl)-5-(4-fluorophenyl)-5,6,11,11a-tetrahydro-1H-imidazo[1′,5′:1,6]pyrido[3,4-b]- indole-1,3(2H)-dione (37b).

Synthesized from **32b** and 2-fluorophenyl isocyanate following the general procedure E. FC in dichloromethane/ethyl acetate 9.5/0.5, Rf = 0.48. Yellowish powder (40% yield). [α]^{25}$_D$: −14.00 ± 0.03 (c = 0.10, MeOH). ^{1}H NMR (CDCl$_3$, 400 MHz): δ: 3.15 (t, 1H, CH$_{2a}$, J = 13.1 Hz); 3.54 (dd, 1H, CH$_{2b}$, J$'$ = 4.2, J$''$ = 15.0 Hz); 4.55 (dd, 1H, CH, J$'$ = 3.8, J$''$ = 11.0 Hz); 5.83 (s, 1H, CH); 6.94 (t, 2H, aryl, J = 8.4 Hz); 7.11-7.32 (m, 8H, aryl); 7.53 (s, 2H, aryl). ^{13}C NMR (CDCl$_3$, 100 MHz) δ: 22.7, 56.4, 58.3, 107.3, 11.3, 115.8, 116.1, 116.6, 116.8, 118.6, 119.0, 120.4, 123.1, 124.5, 126.2, 129.8, 129.9, 130.8, 132.9, 134.0, 136.8, 153.1, 156.4, 158.9, 161.6, 164.0, 169.8. ^{19}F NMR (CDCl$_3$, 376.3 MHz) δ: −(119.00) (s, 1F, CF); −(112.68) (s, 1F, CF). HR-MS m/z: calcd. for C$_{25}$H$_{17}$F$_2$N$_3$O$_2$, [(M + H)]$^+$: 430.1362; found 430.1373.

(5R,11aS)-2,5-Bis(4-fluorophenyl)-5,6,11,11a-tetrahydro1H-imidazo[1′,5′:1,6]pyrido[3,4-b]indole-1,3(2H)-dione (38a).

Synthesized from **32a** and 4-fluorophenyl isocyanate following the general procedure E. FC in dichloromethane/n-hexane 8/2, Rf = 0.40. Yellowish powder (42% yield). $[\alpha]^{25}_D$: −164.00 ± 10.00 (c = 0.10, MeOH). ^{1}H NMR (CDCl$_3$, 400 MHz): δ: 2.99 (dd, 1H, CH$_{2a}$, J′ = 13.2, J″ = 16.9 Hz); 3.52 (dd, 1H, CH$_{2b}$, J′ = 5.5, J″ = 15.3 Hz); 4.39 (dd, 1H, CH, J′ = 5.5, J″ = 11.0 Hz); 6.33 (s, 1H, CH); 6.99 (t, 2H, aryl, J = 8.6 Hz); 7.07 (t, 2H, aryl, J = 8.7 Hz); 7.14-7.21 (m, 3H, aryl); 7.24-7.36 (m, 4H, aryl); 7.53 (d, 1H, aryl, J = 7.6 Hz); 7.76 (s, 1H, NH). ^{13}C NMR (CDCl$_3$, 100 MHz) δ: 23.6, 51.6, 53.0, 108.4, 111.3, 115.9, 116.3, 118.6, 120.4, 123.2, 126.1, 127.4, 127.9, 129.9, 130.9, 134.7, 136.7, 153.7, 160.7, 161.8, 163.2, 164.3, 171.3. ^{19}F NMR (CDCl$_3$, 376.3 MHz) δ: −(111.98) (s, 1F, CF); −(112.80) (s, 1F, CF). HR-MS m/z: calcd for C$_{25}$H$_{17}$F$_2$N$_3$O$_2$, [(M + H)]$^+$: 430.1362; found 430.1371.

(5S,11aR)-2,5-Bis(4-fluorophenyl)-5,6,11,11a-tetrahydro1H-imidazo[1′,5′:1,6]pyrido[3,4-b]indole-1,3(2H)-dione (38a′).

Synthesized from **32b** and 4-fluorophenyl isocyanate following the general procedure F. FC in dichloromethane/n-hexane 8/2, Rf = 0.40. Yellowish powder (45% yield). $[\alpha]^{25}_D$: +185.00 ± 10.00 (c = 0.10, MeOH). ^{1}H NMR (CDCl$_3$, 400 MHz): δ: 2.99 (dd, 1H, CH$_{2a}$, J′ = 11.5, J″ = 14.6 Hz); 3.53 (dd, 1H, CH$_{2b}$, J′ = 5.5, J″ = 15.4 Hz); 4.39 (dd, 1H, CH, J′ = 5.5, J″ = 11.0 Hz); 6.33 (s, 1H, CH); 6.99 (t, 2H, aryl, J = 8.5 Hz); 7.07 (t, 2H, aryl, J = 8.6 Hz); 7.12-7.19 (m, 3H, aryl); 7.24-7.36 (m, 4H, aryl); 7.53 (d, 1H, aryl, J = 7.8 Hz); 7.75 (s, 1H, NH). ^{13}C NMR (CDCl$_3$, 100 MHz) δ: 23.6, 51.6, 53.0, 108.4, 111.3, 115.9, 116.2, 118.6, 120.4, 123.3, 126.1, 127.4, 127.8, 129.9, 130.3, 134.7, 136.7, 153.7, 160.7, 161.8, 163.2, 164.3, 171.3. ^{19}F NMR (CDCl$_3$, 376.3 MHz) δ: −(111.97) (s, 1F, CF); −(112.80) (s, 1F, CF). HR-MS m/z: calcd. for C$_{25}$H$_{17}$F$_2$N$_3$O$_2$, [(M + H)]$^+$: 430.1362; found 430.1357.

(5S,11aS)-2,5-Bis(4-fluorophenyl)-5,6,11,11a-tetrahydro1H-imidazo[1′,5′:1,6]pyrido[3,4-b]indole-1,3(2H)-dione (38b).

Synthesized from **32b** and 4-fluorophenyl isocyanate following the general procedure E. FC in dichloromethane/n-hexane 8/2, Rf = 0.45. Yellowish powder (48% yield). $[\alpha]^{25}_D$: −8.03 ± 0.02 (c = 0.10, MeOH). ^{1}H NMR (CDCl$_3$, 400 MHz): δ: 3.22 (t, 1H, CH$_{2a}$, J = 11.7 Hz); 3.64 (dd, 1H, CH$_{2b}$, J′ = 3.2, J″ = 15.0 Hz); 4.59 (dd, 1H, CH, J′ = 4.4, J″ = 11.3 Hz); 5.92 (s, 1H, CH); 7.05 (t, 2H, aryl, J = 8.5 Hz); 7.12 (t, 2H, aryl, J = 8.6 Hz); 7.21-7.43 (m, 6H, aryl); 7.62-7.65 (m, 2H, aryl). ^{13}C NMR (CDCl$_3$, 100 MHz) δ: 22.7, 56.4, 57.9, 107.3, 111.3, 115.8, 116.1,

118.6, 120.4, 123.1, 126.2, 127.3, 127.8, 129.9, 132.9, 134.1, 136.8, 153.7, 160.0, 161.6, 163.1, 164.0, 170.2. ^{19}F NMR (CDCl$_3$, 376.3 MHz) δ: −(112.80) (s, 1F, CF); −(111.98) (s, 1F, CF). HR-MS m/z: calcd. for C$_{25}$H$_{17}$F$_2$N$_3$O$_2$, [(M + H)]$^+$: 430.1362; found 430.1370.

6.1.2 Pharmacology

Cell cultures

For measurement of the potency of the compounds, fluorimetric experiments were performed using HEK-293 cells (CRL-1573TM, American Type Culture Collection, LGC Promochem, Molsheim, France) that stably express rat TRPM8. The cells were seeded in 96-well plates (Corning Incorporated, Corning, NY) at a cell density of 40 000 cells 2 days before treatment. On the day of treatment, the medium was replaced with 100 μL of the dye loading solution Fluo-4 NW supplemented with probenecid 2.5 mM. For the assessment of selectivity of target compounds, fluorimetric experiments were performed using HEK-293 cells lines stably transfected with either hTRPA1 or hNav1.7 and CHO-K1 stably transfected with hTRPV1. HEK-293 cells were cultured in EMEM (MEM Eagle Earl's salts balanced salt solution, Lonza, Walkersville, USA), 5 mL of 200 mM Ultraglutamine1 (Lonza), 5 mL of 100× penicillin/streptomycin (Lonza), 50 mL of fetal bovine serum (Euroclone, Milan, Italy), 2 mL of 100 mg/mL G418 (InvivoGen, San Diego, USA). CHO-K1 cells were grown in DMEM F-12 (1:1) mixture (Lonza), 5 mL of 100 mM sodium pyruvate (Lonza), 25 mL of 7.5% sodium bicarbonate (Lonza), 6.5 mL of 1 M HEPES (Lonza), 5 mL of 100× penicillin/streptomycin (Lonza), 50 mL of fetal bovine serum (Euroclone), 0.25 mL of 10 mg/mL puromycin (InvivoGen), and 0.5 mL of 100 mg/mL zeocin (InvivoGen). For patch-clamp experiments, HEK-293/TRPM8 exon1 K3 cells were cultured in minimum essential medium with Earle's salts, without L-glutamine (Euroclone) supplemented with 5 mL of 200 mM Ultraglutamine 1 in 0.85% NaCl solution (Lonza), 5 mL of 100× penicillin/streptomycin (Lonza), 0.2 mL of 10 mg/mL puromycin (InvivoGen; final concentration 0.4 μg/mL), and 50 mL of fetal bovine serum (Sigma-Aldrich, Milan, Italy).

Fluorimetric assays

The tested molecules dissolved in DMSO were added at the desired concentrations, and the plates were incubated in darkness at 37 °C in a humidified atmosphere of 5% CO$_2$ for 60 min. The fluorescence was measured using instrument settings appropriate for excitation at 485 nm and emission at 535 nm (POLARstar Omega BMG LABtech). A baseline recording of four

cycles was recorded prior to stimulation with the agonist (100 μM menthol for TRPM8). The TRPM8 antagonist, 10 μM AMTB, was added to the medium containing the corresponding agonist to induce channel blockade. The changes in fluorescence intensity were recorded during 15 cycles more. The higher concentration of DMSO used in the experiment was added to the control wells. The cells' fluorescence was measured before and after the addition of various concentrations of test compounds. The fluorescence values obtained are normalized to that prompted by the corresponding agonist (for channel activating compounds) or upon agonist and antagonist coexposure (for channel blocker compounds).

Selectivity assays

The analysis was performed in 384-well clear bottom black walled polystyrene plates, (Thermo Scientific, Waltham, USA) for CHO-K1 cells and in 384-well clear bottom black polystyrene walled poly-D-Lys coated plates (TwinHelix, Rho, Italy) for HEK-293 cells. Compound dilution was performed in 96-well U bottom plates (Thermo Scientific), and then compounds were transferred into 384-well V bottom polypropylene barcoded plates (Thermo Scientific). To assess the activity of the selected compound over TRPA1 and TRPV1, cells were seeded in 384 MTP in complete medium (25 μL/well) at 10 000 cells/well concentration. 24 h after seeding, the culture medium was removed and cells were loaded with 20 μL/well of 0.5× calcium sensitive dye (Fluo-8 NW, AAT Bioquest, Sunnyvale, USA) in assay buffer. To assess the activity of the selected compound over $Na_{v1.7}$, cells were seeded at 15 000 cells/well in 384 MTP in complete medium (25 μL/well). 24 h after seeding, the culture medium was removed and cells were loaded with 20 μL/well of 0.5× membrane potential dye (FLIPR membrane potential assay kits Blue, Molecular Devices LLC, San Jose, USA) in assay buffer. Plates were incubated for 1 h at room temperature in the dark. Then, 10 μL/well of test compounds and controls were injected at 3× concentration, and the signal of the emitted fluorescence was recorded using FLIPRTETRA apparatus (ForteBio, Fremont, USA). Then, a second injection of 15 μL/well of 3× reference activator (at ~EC80) was performed analyzing the signal of the emitted fluorescence. Allyl isothiocyanate (AITC, Sigma-Aldrich), capsaicine (Sigma-Aldrich), and veratridine (Sigma-Aldrich) were used as reference agonists, while HC-030031 (Sigma-Aldrich), capasazepine (Sigma-Aldrich), and tetrodotoxine (Tocris bioscience, Bristol, U.K.) were used as reference antagonists for TRPA1, TRPV1, and Nav1.7 assaying, respectively.

Patch-clamp experiments

HEK-293/TRPM8exon 1 cells are seeded 72 or 96 h before experiment at a concentration of 4 and 2.5 million cells, respectively, onto a T225 flask. Just before the experiments, cells are washed twice with D-PBS without Ca2+/Mg2+ (Euroclone, Milan, Italy) and detached from the flask with trypsin− EDTA (Sigma-Aldrich, Milan, Italy; diluted 1/10). Cells are then resuspended in the suspension solution, 25 mL of EX-CELL ACF CHO medium (Sigma-Aldrich, Milan, Italy); 0.625 mL of HEPES (Lonza, Walkersville, USA); 0.25 mL of 100× penicillin/streptomycin (Lonza, Walkersville, USA), 0.1 mL of soybean trypsin inhibitor 10 mg/mL (Sigma-Aldrich, Milan, Italy), and placed on an automated patch-clamp platform (QPatch 16X, Sophion Bioscience, Ballerup, Denmark). Menthol was used as reference agonist, and a stock solution (1 M, 100% DMSO) was prepared the day of the experiment from the powder; an intermediate stock of 300 mM was prepared from the 1 M stock in 100% DMSO, and the final dilution was performed in the extracellular solution to obtain a working concentration of 300 μM (1:1000, 0.1% final DMSO concentration). Stock solutions of the testing compounds (10 mM; 100% DMSO; stored at −20 °C) were prepared the day of the experiment; an intermediate stock for each compound (300 μM) was prepared from the 10 mM stock in 100% DMSO, and the working dilutions were performed just before the experiments in the extracellular solution containing 300 μM menthol. The highest concentration tested was 300 nM, with serial dilutions (1:10) in the extracellular solution. DMSO was balanced to keep it constant throughout all the solutions in the same experiment (0.2% final DMSO concentration). Standard whole-cell voltage clamp experiments are performed at room temperature using the multihole technology. For the voltage clamp experiments on human TRPM8, data are sampled at 2 kHz. After establishment of the seal and the passage in the whole cell configuration, the cells are challenged by a voltage ramp (20 ms step at −60 mV; 100 ms ramp −60/+100 mV; 20 ms step at +100 mV; return to −60 mV) every 4 s. The potential antagonistic effect on human TRPM8 current of target compounds was evaluated after application of the agonist (menthol, 300 μM) alone and in the presence of the compound under investigation at increasing concentrations. Output: outward current evoked by the voltage ramp, measured in the step at +100 mV. The intracellular solution contained (mM) 135 CsCl, 10 BAPTA, 10 HEPES, 4 Na_2ATP (pH 7.2 with CsOH). The extracellular solution contained (mM) 145 NaCl, 4 KCl, 1 $MgCl_2$, 2 $CaCl_2$, 10 HEPES, 10 glucose (pH 7.4 with NaOH).

In vitro metabolic stability

Protocol I. Each sample (2.5 mM) was incubated with 100 mM phosphate buffer (pH 7.4) and 20 mg/mL of liver microsomes (Thermo Fisher Scientific, Bremen, Germany). After preincubation in water bath for 5 min, the mixture was incubated with 20 mM NADPH (protocol I) at 37 °C for 60 min in a Thermomixer comfort (Eppendorf, Hamburg, Germany). Protocol II. For the measurement of UGT activity the microsomes were preincubated with alamethicin, which forms pores in microsomal membranes, promoting access of substrate and cofactor to UGT enzymes. Subsequently, each sample was incubated with 100 mM phosphate buffer, 500 mM magnesium chloride, 10 mM NADPH, and 20 mM UDP-GlcUA at 37 °C for 60 min. Finally, the reactions from both protocols (protocols I and II) were stopped by the addition of 200 µL of ice-cold methanol, and then samples were centrifuged at 10 000 rpm at 25 °C for 5 min (Eppendorf microcentrifuge 5424, Hamburg, Germany). The supernatants were collected and injected in UHPLC-PDA. The control at 0 min was obtained by addition of the organic solvent immediately after incubation with microsomes. As the positive control, testosterone was used, while the negative controls were prepared by incubation up to 60 min without NADPH and UDPGlcUA/NADPH for protocols I and II, respectively. The negative control is essential to detect problems such as nonspecific protein binding or heat instability. The extent of metabolism is expressed as a percentage of the parent compound turnover.

Animals

C57-mice (males, 5 week old, ~30 g) (Harlan, The Netherlands) were used for the oxaliplatin-induced neuropathic pain study. All experiments were approved by the Institutional Animal and Ethical Committee of the Universidad Miguel Hernandez where experiments were conducted, and they were in accordance with the guidelines of the Economic European Community and the Committee for Research and Ethical Issues of the International Association for the Study of Pain. All parts of the study concerning animal care were performed under the control of veterinarians. The WDS was performed in Wistar male rats (300-350 g), and the thermal ring experiment was performed on male Swiss CD1 mice (30-35 g) purchased from Charles Rivers (Calco-Lecco-Italy) and then housed in the animal care facility of the Department Experimental of Pharmacology, University of Naples. The animals were acclimated to their environment for 1 week, and food and water were available ad libitum. All behavioral tests were performed between 9:00 am and 1:00 pm, and animals were used only once. Procedures involving animals and their care were conducted in conformity with international and national law and policies

(EU Directive 2010/63/ EU for animal experiments, ARRIVE guidelines, and the Basel declaration including the 3R concept). All procedures reported here were approved by the Institutional Committee on the Ethics of Animal Experiments (CVS) of the University of Naples "Federico II" and by "Ministero della Salute" under Protocol No. 851/2016. All efforts were made to minimize animal suffering, and at the end of all experiments, the animals were euthanized by CO_2 overdose.

Drug treatment

For the oxaliplatin-induced neuropathic pain assay, oxaliplatin (Tocris) was dissolved in water with gentle warming and was subcutaneously (sc) injected on days 1, 3, and 5 at a 6 mg/kg dose. The day 7 after administration, experiments were performed. Together with oxaliplatin injection, saline and a 5% mannitol solution were intraperitoneally injected to prevent kidney damage and dehydration. **31a** stock was prepared in DMSO (Sigma-Aldrich) and diluted in saline for injections. Compound **31a** at different doses (1 to 30 μg) was injected into the plantar surface (25 μL) of the right hind paw of mice. For the other in vivo assays, compound **4** and **31a** were dissolved in PEG 400 10% v/v, Tween 80 5% v/v, and sterile saline 85% v/v and injected once intraperitoneally at the equimolar doses of 10 mg/kg for 4 and 6.7 mg/kg for **31a**. Control group was only treated with vehicle.

Icilin-induced "wet-dog" shaking in rats

Icilin, a TRPM8 agonist, was used to induce shaking in mice. Animals were first habituated to the testing room for 30 min. After that they were randomized into treatment groups and treated with vehicle or TRPM8 antagonists. Icilin was administered intraperitoneally (ip) at 1 mg/kg dissolved in 1% Tween 80/H_2O 30 or 120 min after drugs. The number of intermittent but rhythmic "wet-dog-like" shakes (WDS) of neck, head, and trunk in each animal was counted for a period of 30 min following icilin administration.

Oxaliplatin-induced neuropatic pain model

Cold chemical thermal sensitivity was assessed using acetone drop method. Mice were placed in a metal mesh cage and allowed to habituate for approximately 30 min to acclimatize them. Freshly dispensed acetone drop (10 μL) was applied gently onto the mid-plantar surface of the hind paw. Cold chemical sensitive reaction with respect to paw licking was recorded as a positive response (nociceptive pain response). The responses were measured for 20 s with a

digital stopwatch. For each measurement, the paw was sampled twice, and the mean was calculated. The interval between each application of acetone was approximately 5 min.

Chronic constriction injury (CCI) model of neuropathic pain

Neuropathic pain behavior was induced by ligation of the sciatic nerve. Briefly, mice were first anesthetized with xylazine (10 mg/kg ip) and ketamine (100 mg/kg ip), and the left thigh was shaved and scrubbed with betadine, and then a small incision in the middle left thigh (2 cm in length) was performed to expose the sciatic nerve. The nerve was loosely ligated at two distinct sites (spaced at a 2 mm interval) around the entire diameter of the nerve using silk sutures (7-0). The surgical area was closed and finally scrubbed with betadine. In sham-operated animals, the nerve was exposed but not ligated. Drug effects were evaluated 7 and 14 days after ligation.

Thermal gradient ring

We utilized the thermal gradient ring from Ugo-Basile previously using a modified protocol.[89] The apparatus consists of a circular running track where each side of the ring is divided into 12 zones, in which the temperature is proportionally distributed from 15 to 40 °C, and each sector represents an increment of 2.27 °C. Before the experiment, on day 1, all mice were habituated to the apparatus for 30 min with the aluminum floor acclimatized to room temperature (22-24 °C). On day 2, mice were injected and 30 min after were placed in the apparatus and measured for 60 min using 15-40 °C. Data on preference temperature in time course were collected from the videotracking software Any-Maze connected to the apparatus.

Data analysis

Data are reported as the mean ± standard error of the mean (SEM) values of at least three independent experiments each in triplicate. Statistical analysis was performed by analysis of variance test, and multiple comparisons were made by Bonferroni's test by using Prism 5 (GraphPad Software, San Diego, CA, USA). p-values smaller than 0.05 were considered significant.

6.1.3 *Computational details*

3D structures of TRPM8 in complex with TC-I 2014 antagonist (PDB code: 6O72) were prepared using the Schrödinger Protein Preparation Wizard workflow. Specifically, water

molecules were deleted, cap termini were included, all hydrogen atoms were added, and bond orders were assigned. Finally, the .pdb files were converted to the .mae file. The grids for the subsequent molecular docking calculations were generated accounting the related position of TC-I 2014 on the receptor binding sites. In this way, the cocrystallized ligands were also automatically removed from the original binding sites. The library of investigated compounds was prepared using LigPrep software (Schrodinger Suite). Specifically, all the possible tautomers and protonation states at pH = 7.4 ± 1.0 were generated for each compound, and finally the structures were minimized using the OPLS 2005 force field. Molecular docking experiments were performed using Glide software (Schrödinger Suite), setting the Extra Precision [XP] mode. For this step, 20 000 poses were kept in the starting phase of docking, and 1200 poses for energy minimization were selected. The scoring window for keeping the initial poses was set to 400.0, and a scaling factor of 0.8 related to van der Waals radii with a partial charge cutoff of 0.15, based on a 0.5 kcal/mol rejection cutoff for the obtained minimized poses, was considered. In the output file, 10 poses for each compound were saved.

CHAPTER 2

Design, synthesis, and biological evaluation of neuronal K_{v7} channels activators

1.1   Potassium channels: an overview

Potassium channels are integral membrane proteins ubiquitously existing in practically all kingdoms of life, except for some parasites. They play a pivotal role in both excitable and non-excitable cells performing different functions. These include the monitoring and stabilization of the membrane potential, affecting the shape and duration of the action potential. This occurs by reducing the cell susceptibility to excitatory stimuli decreasing the frequency and the duration of the action potential.

Furthermore, K^+ channels are involved in regulation of hormonal secretion, epithelial function, as well as the control of cell survival, proliferation, and differentiation.[92-94]

Since their wide expression in both eukaryotic and prokaryotic cells, it's no wonder that about 70 K^+ channel genes are encoded, at present, in only mammals.[95]

Based on their structure and activation, K^+ channels may be categorized into three main families (**Figure 1**):[96]

I)   Channels with six transmembrane segments (6TMs).

It covers voltage-gated K^+ channels (K_v channels; K_{v1}-K_{v12}) and some calcium-dependent potassium channels as the small conductance Ca^{2+}- dependent K^+ channels (SK). Voltage-gated K^+ channels switch from a closed to open state in response to a membrane potential change, thus enabling potassium fluxes across the cell membranes.

II)   Channels with two transmembrane segments (2TMs).

This family is composed by the inward-rectifier channels (K_{ir1}-K_{ir7}), structurally homologous to the S5-S6 segments of the K_v channels. In contrast to voltage-gated K^+ channels, which require membrane depolarization to open, K_{ir} channels are active around the resting membrane potential, and decline their activity upon membrane depolarization. The mechanism underlying this steep voltage-dependence is blockade by intracellular polyamines and the lack of voltage sensor domain (VSD).[97,98]

III)   Channels with four transmembrane segments (4TM).

It includes at least 15 different genes (K2P1-K2P17), characterized by the tandem repetition of two pore domains. They are activated by different physical and chemical agents such as lipids, heat, oxygen, pH, and membrane tension.[99] They are the only one assemble as dimers except for others indicated above, which are tetramers.[100]
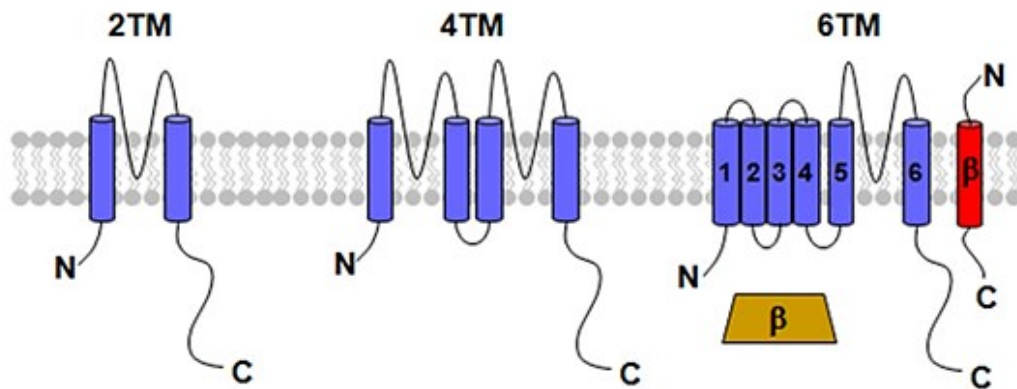
Figure 1. Topological representation of K⁺ channels.

Several voltage-gated potassium channels (VGKCs) interact with accessory β-subunits affecting gating, assembly, trafficking, and targeting of channels to different cellular compartments. β-subunits can be localised in cytosol or in membranes depending on their role. (Adapted from Miceli *et al*., 2015).

The K⁺ channels, independently of the belonging class, consist of two domains: the pore-forming domain and the regulatory domain. The pore-forming domain presents an extremely well conserved structure, and it is responsible for passage of potassium ions. The regulatory domain senses diverse stimuli and its structure differs among the classes.[97]

Since the basic organization of K⁺ channels in tetramers, each monomer includes one pore-forming domain. Four pore-forming domains comprise a pore through which potassium moves.[101]

The general structure of the pore-forming domain can be described by the transmembrane part of the first atomic structure of a prokaryotic potassium channel, a two TMs K⁺ channel from *Streptomyces lividans*, the so called KcsA.[102] The active site of K⁺ channels consists of four conserved signature sequences, TVGYG functioning as a selectivity filter to conduct very efficiently K⁺ ions (**Figure 2**). Simultaneously, K⁺ channels are highly selective and at least 10,000 times more permeant for K⁺ than Na⁺ ions. This is permitted by main chain carbonyl oxygen atoms which is held open by structural constraints to coordinate K⁺ ions but not smaller sodium ions. Thus K⁺ ions stabilize the conductive conformation of the selective filter, which in turn favors conduction of K⁺ ions. On the other side, Na⁺ ions may stabilize a nonconductive state, which has a distorted structure of the selective filter.[103] A similar structure is also observed for Li⁺ ions.[104]
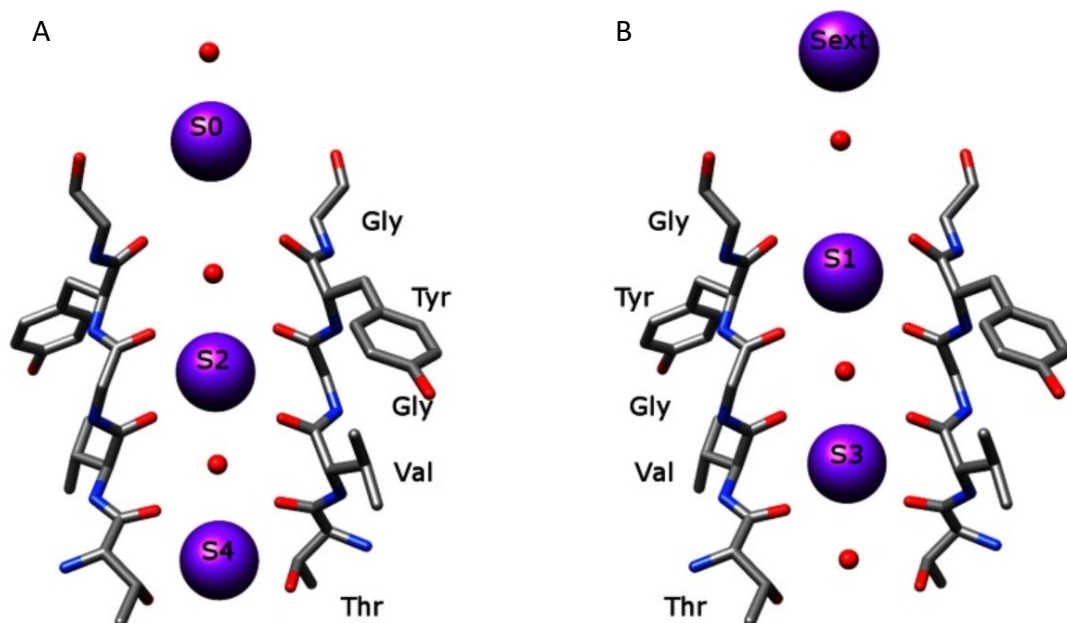
Figure 2. Enlarged view of the boxed area in the transmembrane part of KcsA.

The conducted K^+ ions are represented by purple balls with surrounding water molecules in red. The K^+ ions are in two configurations, either in S2 and S4 (A) or S1 and S3 (B) during conduction. The water molecules occupy the vacant ion positions in S1 and S3 (A) or in S2 and S4 (B). Other ions are in the extracellular entryway (Sext, B). For clarity, only two monomers opposite to each other are shown. (Adapted from Kuang *et al*., 2015).

1.2 K$_{v7}$ potassium channel family

Voltage-gated K$_v$ channels have a remarkable impact on physiology of neurons, cardiac myocytes, epithelial and smooth muscle cells. Since their highly heterogeneity, they are rank into different subfamilies, from K$_{v1}$ to K$_{v12}$. In this instance, K$_{v7}$ subfamily consists of 5 members, from K$_{v7.1}$ to K$_{v7.5}$, encoded by KCNQ genes (KCNQ1-5), showing distinct expression pattern and functional role.[105,106]

The K$_{v7.1}$ subunit, encoded by KCNQ1 gene, is mainly expressed in cardiomyocytes, where binds to the accessory proteins KCNE1. Thus, direct physical interaction generates the slowly activating delayed rectifying K$^+$ current (I$_{Ks}$) involved in ventricular repolarization. The I$_{Ks}$ current plays a key role in cardiac physiology. This is why mutations in the KCNQ1 genes cause the long QT syndrome, a hereditary arrhythmia characterized by delayed repolarization, syncopal episodes, and sudden death.[107,108]

These subunits are also co-expressed in the *stria vascularis* in the inner ear and are critical for hearing, probably controlling endolymph homeostasis.[109] In addition, K$_{v7.1}$ subunits are localized in the gastrointestinal tract, thyroid gland, pancreas, and assemble also with KCNE2 and KCNE3 ancillary subunits. In gastric parietal cells, K$_{v7.1}$/KCNE2 channels are involved in K$^+$ recycling coupled to the H$^+$-K$^+$-ATPase, essential for acid secretion, while in thyrocytes, regulates the synthesis of thyroid hormones.[110]

Unlike K$_{v7.1}$ channel, the K$_{v7.2}$-K$_{v7.5}$ subunits, encoded by KCNQ2-5, are very significant in the nervous system, as essential regulators of neuronal excitability by dampening repetitive action potential firing.[111] In more details, K$_{v7.2}$ and K$_{v7.3}$ are co-expressed in many areas of the brain, including the cerebral cortex, hippocampus, cerebellum, and thalamus, suggesting the formation of heteromeric K$_{v7.2/7.3}$ channels.[112] These generate a voltage-dependent K$^+$ current, the so called M-current (IKM) due to its sensitivity to muscarinic agonists. The M current is activated at a subthreshold membrane potential hyperpolarizing the cell membrane, and consequently reduces the firing of action potential. Its inhibition by acetylcholine or other agents such as cAMP, bradykinin, histamine, angiotensin, metabotropic glutamate, adrenergic, purinergic, substance P or opiate receptors leads to increased neuronal excitability.[113] Mutations in KCNQ2 or KCNQ3 genes have been associated to benign familial neonatal epilepsy (BFNE), a rare autosomal dominant idiopathic epilepsy of newborn infant.[114] This disorder is characterized by neonatal seizures, but development in these patients is generally normal. However, the risk of seizure recurrence in BFNE individuals is higher than the general population, and various degrees of developmental disability may be associated with this

pathology.[115] Moreover, mutations in KCNQ3 gene have also been associated with epileptic encephalopathy, and intellectual disability with seizures and cortical visual impairment.[116]

$K_{v7.4}$ (KCNQ4) was identified on the basal membrane of the outer hair cells of the inner ear and auditory nerves, with mutations to the channel associated with autosomal dominant deafness. The activation of KCNQ4 channels resembles M current, and it is likely that the function of the KCNQ4 channel is to regulate the subthreshold electrical activity of excitable cells.[117] $K_{v7.4}$ subunits are also expressed in the inner hair cells but at a lower level than the outer hair cells.[118] Mutations in the KCNQ4 gene cause deafness through a rare autosomal dominant disease in which hearing loss is caused by a slow degeneration of outer hair cells induced by their chronic depolarization.[119] Kv7.4 subunits have also been detected in skeletal muscle cells, as well as vascular and visceral smooth muscle, where they are involved in the control of basal tone and in response to myogenic stimuli.[120]

Lastly, $K_{v7.5}$ channel subunits, encoded by the KCNQ5 gene, are broadly expressed in the brain, and show an overlapping cellular pattern expression with $K_{v7.2}$ and $K_{v7.3}$ subunits. Instead, this subunit was identified as a molecular correlate of the M-current by forming heteromultimers with $K_{v7.3}$ and mutations in the KCNQ5 gene are associated with severe epilepsy conditions.[121,122] Further, this subunit is found in non-neuronal tissue, like skeletal and smooth muscle cells.[123] It is also involved in retinal disorders.[124]

1.3 K$_{v7}$: structure and regulation

The functioning of most ion channels is defined by the relationship between activation and inactivation gating. Activation is due to a large, hinged motion around the inner helix bundle, as observed in several K$^+$ channel structures.[125,126]

All K$_v$ channels exhibit a similar mechanism of activation. They can be present in three functional states: resting state (closed conformation) ↔ activated state (open conformation) ↔ inactivated state (**Figure 3**).[127]

Inactivation gating in eukaryotes can occur by two distinct molecular mechanisms: N-type inactivation, a fast, autoinhibitory process where an N-terminal inactivating peptide binds to the open pore, blocking conduction; and C-type inactivation, which originates from transitions at the selectivity filter. C-type inactivation often develops with much slower kinetics and is highly modulated by permeant ions and pore blockers.[127,128]
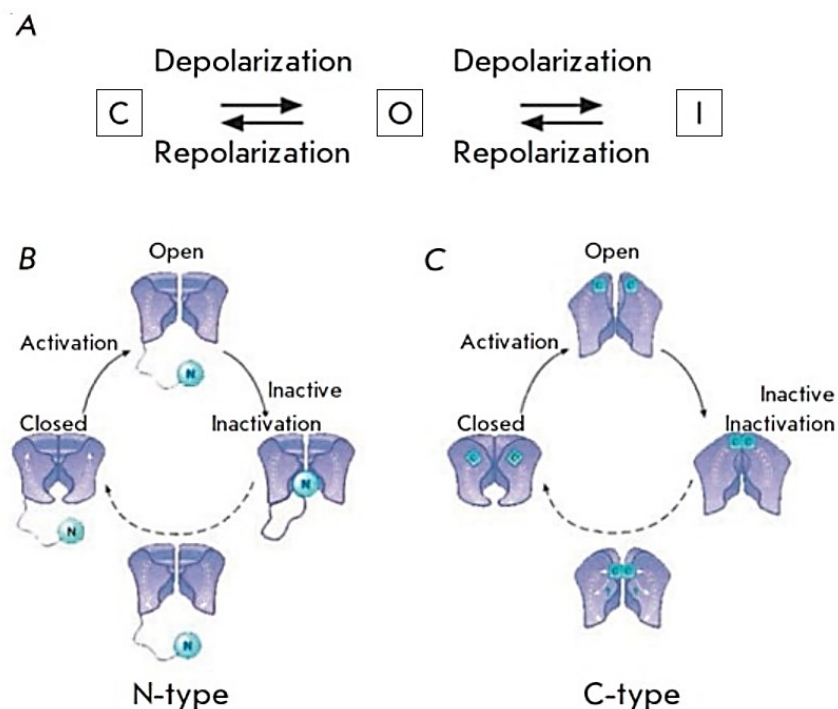
Figure 3. (A) Scheme of the conformational transitions in K$_v$ channels: C = closed channel; O = open channel; I = inactivated channel. (B) N-type inactivation. The inactivation peptide enters the pore and physically blocks the transfer of ions after the activation of the channel. (C) C-type inactivation. The selectivity filter acts as the second gate and closes, preventing the penetration of ions. The channels completely return to the closed conformation when the potential drops to the resting potential level.

K_{v7} channels assemble as tetramers of identical or compatible α subunits, with each α subunit consisting of six transmembrane segments (S1-S6) and cytoplasmic N- and C-terminal residues (**Figure 4**).[129] The transmembrane segments S1-S4 compose the voltage-sensing domain (VSD), where the S4 segment is crucial for channel gating as it contains from four to six positively charged arginines, each separated by non-polar residues. VSD can, therefore, shift position relative to the membrane electric field in response to membrane potential changes. The S5 and S6 segments and the interconnecting loop constitute the pore domain (PD).[130]
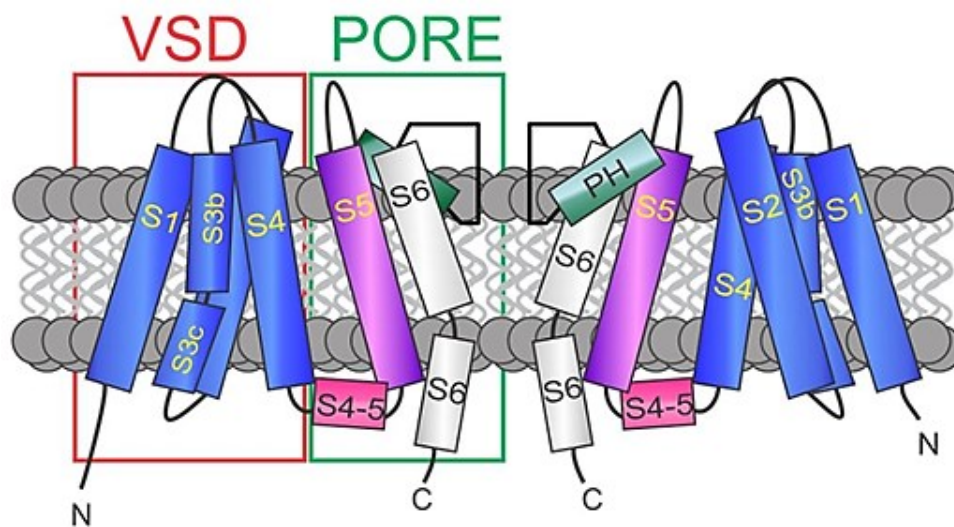
Figure 4. KCNQ channel architecture. VSD= voltage sensing domain; PH = pore helix. (Adapted from Abbott, 2020).

Because of depolarization, S4 moves outward, pulling the intracellular S4-S5 linker, which in turn transfers these mechanical forces to the distal region of S6 of a neighbor subunit, leading to pore opening (**Figure 5**). The most consolidated hypothesis that reports the movements of the VSD describes the stabilization of resting and activated states by hydrogen bonds occurring between the S4 positive residues and two clusters of highly conserved negatively charged residues: an external negative cluster consisting of S1 helix and S2 helix, and an internal negative cluster consisting of glutamate S0 helix, S2 helix, and S3a helix.[131] A major contribution to the formation of the so-called selectivity filter is given by the pore region that consists of about 20 amino acids and contains the molecular determinants of ion selectivity, the glycine-tyrosine-glycine (GYG) sequence, essential for discrimination between the various ionic species (**Figure 2**).[103]
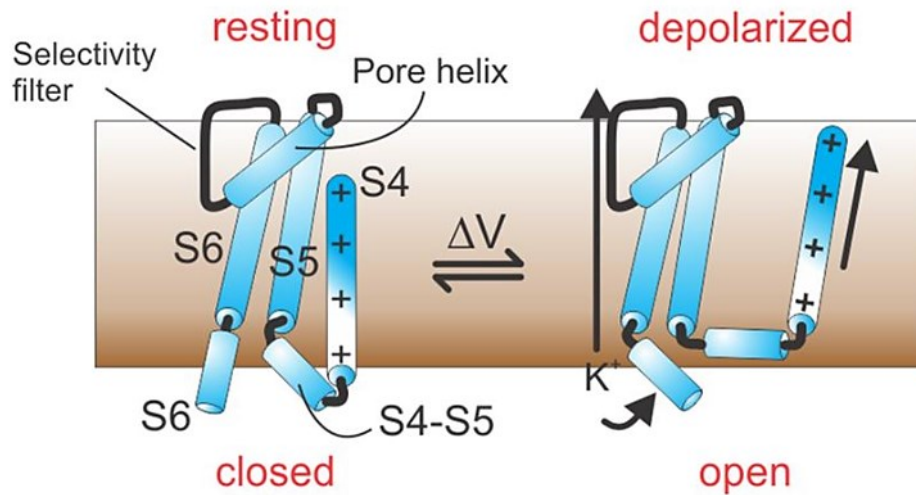
Figure 5. Cartoon of voltage gating depicting the S4-S6 portions of a K_v α subunit monomer and the types of conformational shifts that may occur upon membrane depolarization. (Adapted from Abbott, 2020).

K_{v7} channels are characterized by a long intracellular C-terminus, organized into four α-helical regions (called A-D helices), which are conserved in all K_{v7} family members. Moreover, they contain domains involved in binding and signal transduction activity by several regulators, such as PIP2, calmodulin (CaM), syntaxin, A-kinase-anchoring proteins, PKC, and ankyrin-G (**Figure 6**).[132]
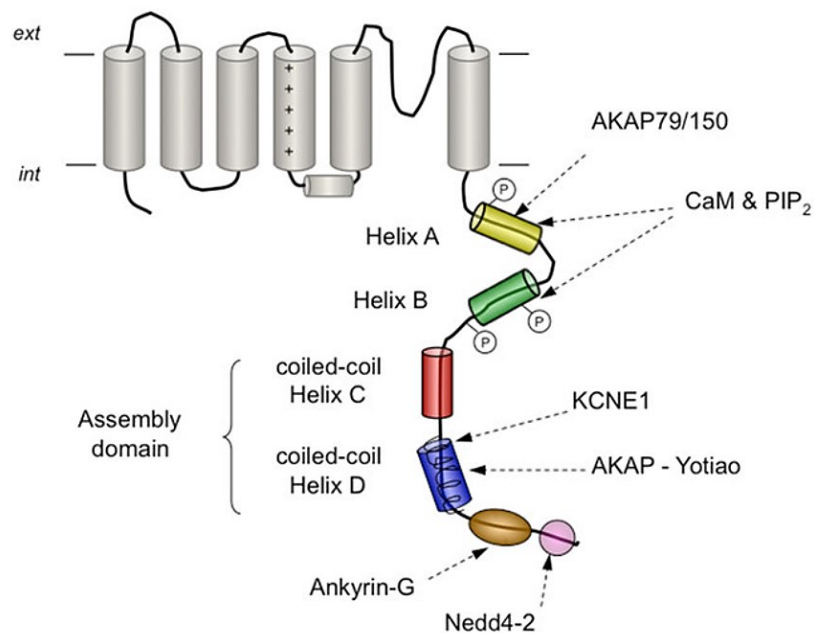
Figure 6. Schematic view of different structural and/or functional domains recognized at the cytoplasmic ends of K_v channels. (Adapted from Barros *et al.*, 2012).

In more details, PIP2 is a phospholipid negatively charged present in the intracellular edge of the plasmatic membrane essential for the activation of all KCNQ channels. Indeed, membrane depolarization opens the pore only in the presence of PIP2, although the voltage sensors gain an activated conformation independently.[133] In addition, PIP2 enhances the opening probability of both homomeric and heteromeric channels; differences in the single-channel open probability are dependent on their intrinsic affinities for PIP2.[134] Two binding sites have been revealed in the S2-S3/S4-S5 loops. Particularly, in $K_{v7.2}$ PIP2 binds S2-S3 loop in the closed state whereas, upon channel activation, PIP2 interacts with the S4-S5, modulating channel gating.[135] Moreover, the recently published cryo-EM structure of the hKCNQ1 showed that PIP2, also in this channel, could bind to S2-S3 and S4-S5 loops.[136]

Calmodulin is a small protein able to bind Ca^{2+} ions. All members of K_{v7} family subunits interact with CaM, which binds two different sites in the C-terminal domain located in helices A-B and is essential in the modulation of M-current.[137]

Further, phosphorylation of calmodulin by protein kinase CK2 (casein kinase 2) rapidly and reversibly modulates KCNQ2 current. CK2-mediated phosphorylation of calmodulin increases its binding to KCNQ2 channel and enhance the current amplitude.[138]

Ankyrin-G (AnkG) is an adaptor protein that allows localizing $K_{v7.2}$ and $K_{v7.3}$ subunits at the axon initial segment and in nodes of Ranvier, two neuronal sites crucially involved in the generation and propagation of action potentials. Ankyrin-G selectively interacts with $K_{v7.2}$ and $K_{v7.3}$ subunits, binding the distal part of the helix-D in C-terminus.[139]

1.4 **$K_{v7.2}$ and $K_{v7.3}$: physiopathological role**

The $K_{v7.2}$ and $K_{v7.3}$ subunits are highly expressed in both the central and peripheral nervous systems. In neuronal cells, K_{v7} channels are localized at key subcellular sites, including the perisomatic region, the axon initial segment, nodes of Ranvier, and synaptic terminals. According to their subcellular localization, K_{v7} channels regulate several aspects of neuronal excitability. Besides, their functions involve neuronal exocytosis and neurite formation, neuronal cell death, regulation of astrocyte Ca^{2+}, glial cell and glioma proliferation.[140,141]

Mutations in KCNQ2 are well known for their association to epilepsy, ranging from more benign forms, like benign familial neonatal seizures, to more severe forms, like the neonatal onset developmental and epileptic encephalopathy, such as early myoclonic encephalopathy (EME) and Ohtahara syndrome (OS), whose prognosis is very poor.[142,143]

BFNS is characterized by multifocal seizures starting on the first 7 day of life and remits by a few weeks or months. Generally, seizures episodes are brief, lasting one to two minutes, and the motor activity may be localized, migrate to other body regions, or generalize. The neuropsychological development is usually normal. Although the spontaneous remission, ever ~15% of affected children show seizures later in life.[144]

Two genetic conditions like BFNS have been described: Benign Familial Infantile Seizures (BFIS) and Benign Familial Neonatal-Infantile Seizures (BFNIS). This latter presents an intermediate phenotype between BFNS and benign familial infantile seizures BFIS.[145,146] Indeed, in BFIS, seizures start around 6 months of age, while in BFNIS, seizures display an intermediate age of onset between the neonatal and the infantile periods.

Like KCNQ2, mutations in the KCNQ3 gene are related to benign epilepsies with seizures starting in the neonatal (BFNS) or early infantile period (BFIS). However, KCNQ3 variants represent a relatively rare cause of BFNS, even in virtue of the smaller number of KCNQ3 mutations known, referred to those of KCNQ2.[147]

Additionally, more severe phenotypes have been associated with KCNQ3 mutations, such as autism spectrum disorders and cerebral visual impairment.[148,149]

In BFNS, mutations concern the full $K_{v7.2}$ sequence, causing a loss of channel activity, indicated with the term LoF (loss of function). The molecular mechanisms responsible for the decrease in IKM function can be related to mutations affecting residues located in the pore region reducing K^+ ion efflux,[150] whereas those affecting critical gating elements in the VSD may decrease voltage sensitivity of the channel, leading to a decreased opening probability and faster closing kinetics at each membrane voltage. This latter mechanism may to explain the functional

deficits demanded by the R207, the M208V, the D212G, the R213W/Q, and the R214W mutations; all affecting critical gating residues in the S4 segment of the VSD.[151-153]

More recently, in addition to the LoF mechanisms, heterozygous *de novo* missense variants which caused gain of function (GoF) effects were found. These include the R201C/H, the R144Q, and the R198Q.[154,155]

To understand the molecular basis of these two different effects, multistate structural modeling has been adopted. Activated VSD configuration is stabilized by hydrogen bonds established between arginine residues (R4, R5, R6) and an internal negative amino acid cluster mostly provided by E140 in S2 and D172 in S3, whereas R2 residue stabilizes the resting states by forming an elaborate network of electrostatic interactions with neighboring negatively charged residues. Thus, neutralization of the charge at R2 preferentially destabilized the resting VSD configuration, thereby causing constitutive channel activation, possibly explaining the observed GoF effects, while neutralization of the charge at R4, R5, R6 destabilizing the VSD-activated configuration and causing LoF effects (**Figure 7**).[156]
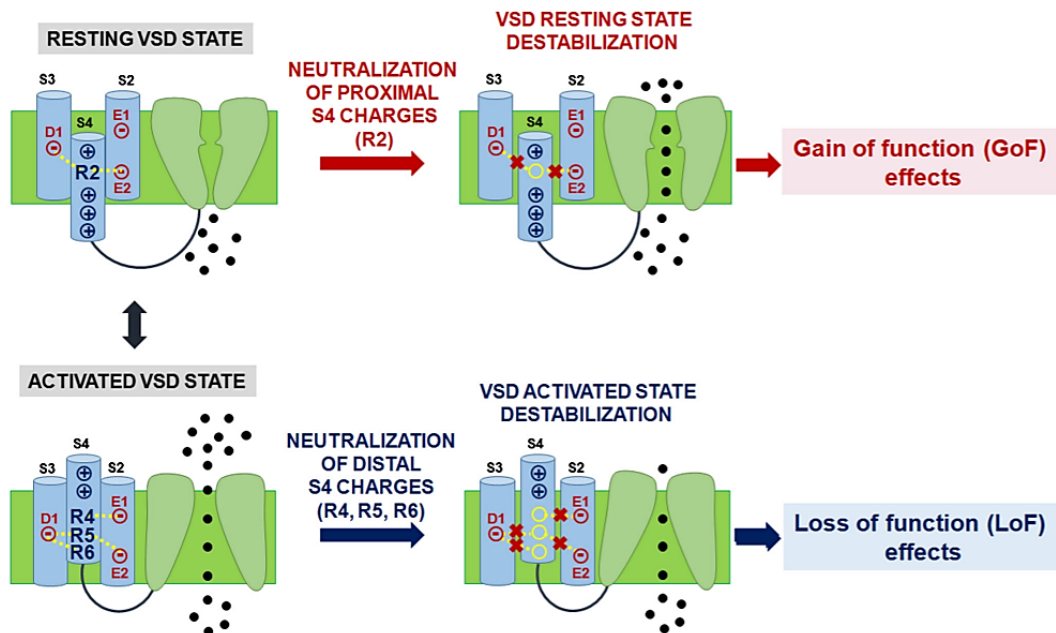
Figure 7. Representation of the differential role of ionized hydrogen bonds involving arginine (R) in the proximal (R2) and distal (R4, R5, R6) portions of the S4 transmembrane segment on VSD movement during K_{v7} channel gating (left panels). The right panels show the functional consequences of the neutralization of these Rs on VSD movement. (Adapted from Nappi *et al.*, 2020).

1.5 K_{v7} activators

1.5.1 Flupirtine, retigabine and derivatives

Developed as novel non-opioid centrally acting analgesic drug, flupirtine was marketed in Europe in 1981 and represents the first neuronal K_{v7} activator.[157] Flupirtine was submitted to the Antiepileptic Drug Development program at the National Institute of Healthy where it demonstrated good efficacy in pentylenetetrazol-induced seizures (PTZ) mice models, as well as in a small efficacy study in humans.[158] Using molecular modeling, an anticonvulsant pharmacophore was identified.[159] These studies revealed the phenyl ring, the basic nitrogen atom in the pyridine and their specific distance, as key elements for analgesic activity. The removal of the basic nitrogen atom enhances the antiepileptic activity, reducing at the same time analgesic activity. Out of this process was a despyridyl analogue of flupirtine, called retigabine (**Figure 8**).
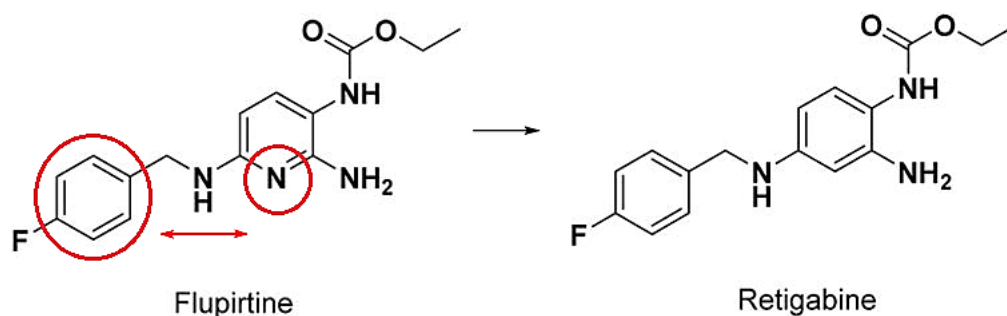
Figure 8. Pharmacophore modification of flupirtine and development of retigabine.

Retigabine showed an improved anticonvulsant activity, with a spectrum of action comparable to valproic acid, and low analgesic effects. Testing its in two heterozygous knock-in mice carrying BFNS causing mutations Y284C, A306T in KCNQ2, retigabine mitigated induced seizure activities in both mice models, more significantly than phenobarbital.[160] Considering this improved pre-clinical profile, retigabine was developed clinically as an anticonvulsant. In particular, it represents the first approved anticonvulsant drug acting on K_{v7} potassium channels.[161]

The principal effect is a hyperpolarizing shift in channel activation, together with an acceleration in channel activation and a slowing down of its deactivation.[162] Anyway, retigabine is a nonselective Kv7 channel opener and its effects on voltage-sensitivity depend on the K_{v7} family subtype. In more details, $K_{v7.1}$ channel is completely insensitive, while on $K_{v7.3}$

homomers the effect on voltage sensitivity is maximal (-43mV), intermediate for $K_{v7.2/3}$ heteromers (-30 mV) and $K_{v7.2}$ homomers (-24 mV) and very small for $K_{v7.4}$ homomers. In $K_{v7.5}$ retigabine does not change voltage sensitivity, but increases current amplitude.[163,164] Finally, on $K_{v7.2/3}$ heteromers retigabine increases the single channel opening by stabilizing the open conformation, without any significant change in channel conductance.[165]

Retigabine recognizes an intracellular hydrophobic pocket located between S5 and S6 in the pore domain. Within this cavity, a tryptophan residue (W236 in $K_{v7.2}$ and W265 in $K_{v7.3}$), present at the end of the S5 helix, appears crucial for the retigabine activity. Beside this residue, also other ones are involved in the binding of retigabine, like L243, L275, L299, and Gly301, but none of them seems to be critical as the tryptophan. The key role of this residue was confirmed by site-specific mutagenesis experiments; substitution of this residue with a leucine, resulted in a completely loss ability of retigabine to activate $K_{v7.2}$ currents.[166]

In 2009, Lange *et al.* hypothesized a generic hydrophobic interaction between retigabine and tryptophan residue, therefore the fluorophenyl ring of retigabine was in either the vicinity of the aromatic side chain of tryptophan.[167]

Recently, Kim *et al.* through a mutagenesis experiment using some non-natural amino acids, demonstrated that an H-bond interaction occurs between the carbamate group of retigabine and the tryptophan residue. In fact, the introduction of a non-natural isosteric H-bond-deficient Trp analogue abolishes channel potentiation. On the other side, substitution with fluorinated Trp analog (F_3-Trp), with increased H-bonding propensity, strengthens retigabine potency.

This evidence suggests a 'flip' bound conformation for retigabine compared to the original proposed by Lange *et al*. (**Figure 9**).[168]
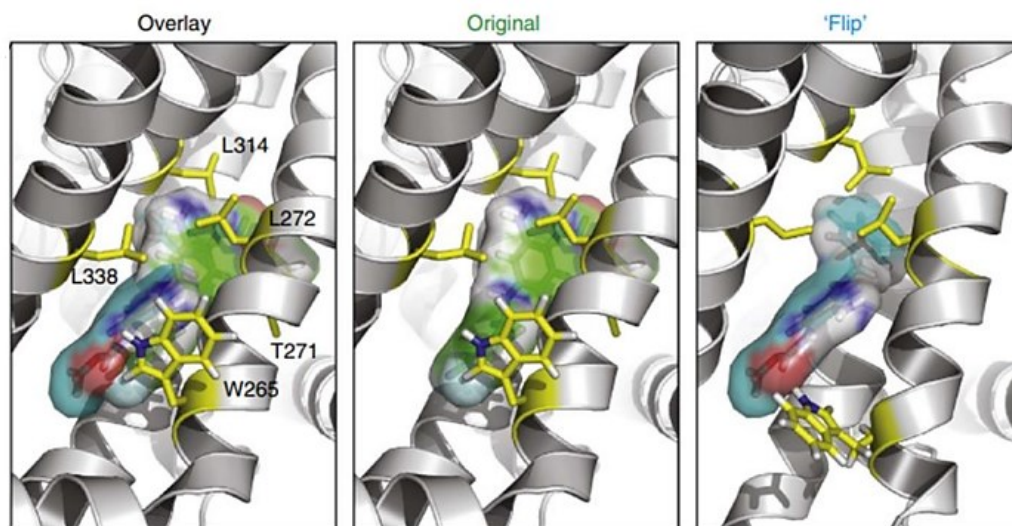
Figure 9. Docking of retigabine into a molecular model of the pore-forming domain of KCNQ3. Two orientations are shown with the carbamate group in either the vicinity of Leu314 (original model, proposed by Lange *et al*.) or Trp265 ('flip' model, proposed by Kim *et al*.). The two binding models are superimposed in the 'overlay', showing the similar space occupied by both drug orientations. (Adapted from Kim *et al*.).

Additionally, the hypothesis that retigabine forms a direct hydrogen bond with indole ring of tryptophan was validated in 2021 by the cryo-EM structures of the human KCNQ2 and KCNQ4 in complex with retigabine.[169,170]

In these models, further interaction sites were described (**Figure 10**); in both cases an H-bond interaction occurred between the primary aniline group of retigabine and serine residues. To corroborate the observations from the structural analysis, electrophysiological experiments were performed in $K_{v7.2}$ Ser303A mutants. A notable reduction of potentiation activity of retigabine was observed.[170]

Anyway, the exact structural basis for the activation mode remains unclear. Alignment of the apo structure of KCNQ2 and KCNQ2-retigabine complex, revealed that retigabine binding causes about 40 conformational changes mainly in the pore domain. On the contrary, the voltage sensor domain in KCNQ2-retigabine structure remained almost unchanged. These conformational changes caused by the binding of retigabine can provide a reasonable explanation for the activation mechanism on KCNQ channels, suggesting that retigabine acted as an allosteric modulator.
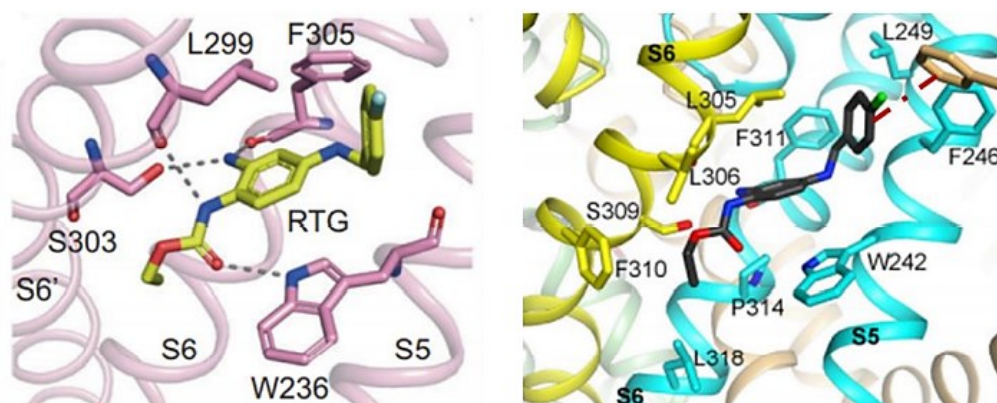
Figure 10. Binding of retigabine in KCNQ2 (right) and KCNQ4 (left). (Adapted from Li *et al*, and Xi *et al*.)

Retigabine has been approved in 2011 for clinical use of drug-resistant seizures in in people aged 18 or older. However, since 2017 because of its unfavorable risk/benefit ratio, retigabine was withdrawn from sale. Several negative sides are involved in the limited efficacy of the drug and can be summarized as follows: (a) poor selectivity for K_{v7} subtypes. Indeed, activation of $K_{v7.4/5}$ channels expressed in genitourinary smooth muscle cells seems responsible for urinary retention; (b) short half-life. Retigabine is metabolized by phase-II enzymes. Consequently, it requires dosing three times a day; (c) poor brain penetration. Because of its limited lipophilicity (log P = 3.08), the brain/plasma concentration ratio of retigabine is rather low, thus requiring posological schemes at relatively high doses; (d) chemical instability.[171-174] In this regard, one hypothesis is that light exposure may cause photodegradation and oxidation of retigabine's aniline ring, which may lead to phenazinium dimers as outlined in **Figure 11**.[175] Dimers formation can be rationalized through a concerted or stepwise conjugate addition pathway to form the two new C-N bonds of the hydrophenazine ring following by a second oxidation step to aromatize the hydrophenazine ring to the phenazinium cationic species and then phenazines.
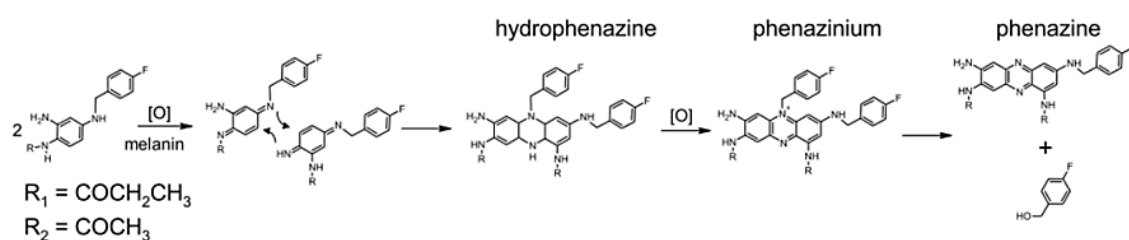
Figure 11. Proposed mechanism for the formation of phenazinium dimers. (Adapted from Groseclose *et al.*).

For these reasons, several companies and research groups are pursuing the synthesis of novel retigabine derivatives with improved chemical, pharmacokinetic, or pharmacodynamic properties.

In this regard, it was synthetized a fluroanilinic retigabine derivative (SF0034) obtained by introducing a fluorine atom at the 3- position of the aniline ring of retigabine. The compound appeared selective and 5-times more potent than retigabine on $K_{v7.2}$ and $K_{v7.3}$ channels showing an EC_{50} of 1.3 ± 0.3 µM and 6.5 ± 1.5 µM, respectively.[176]

Considering the structure of SF0034, Kumar *et al.* synthetized RL648-81, characterized by a CF_3-group at the 4-position of the benzylamine moiety, combined with the fluorine atom on the aniline ring. Compared to SF0034, RL648-81 has been reported to be 3-times more potent in activating $K_{v7.2}$ and $K_{v7.3}$ channels with an EC_{50} of 0.6 ± 0.02 µM and 0.19 ± 0.02 µM, respectively. As well as SF0034, RL648-81 showed a pair profile of selectivity, thus obtaining a compound more potent, selective, and stable than retigabine.[177] In any case, similarly to retigabine, conserved residue W236 is necessary for SF0034, and RL648-81 activity. In both cases, gating effect on KCNQ2 channels are abolished upon substitution of W236L suggesting that these analogues share the same binding site. Starting from RL648-81, new analogues are synthetized. The introducing of a propargyl group at the N position of the retigabine linker led to obtain P-retigabine, which showed an increased brain-to-plasma ratio compared to retigabine (2.30 versus 0.16), while electrophysiological experiment demonstrated that P-retigabine was more potent than retigabine on $K_{v7.2}$.[178]

Besides flupirtine and retigabine, other molecules are potent activators of K_{v7} channels, like compounds belonging to the class of the acrylamides (BMS-568274), benzamides (ICA-110381) and fenamates (diclofenac, mefenamic acid, NH-29). However, these compounds do not bind to retigabine site.[179-181]
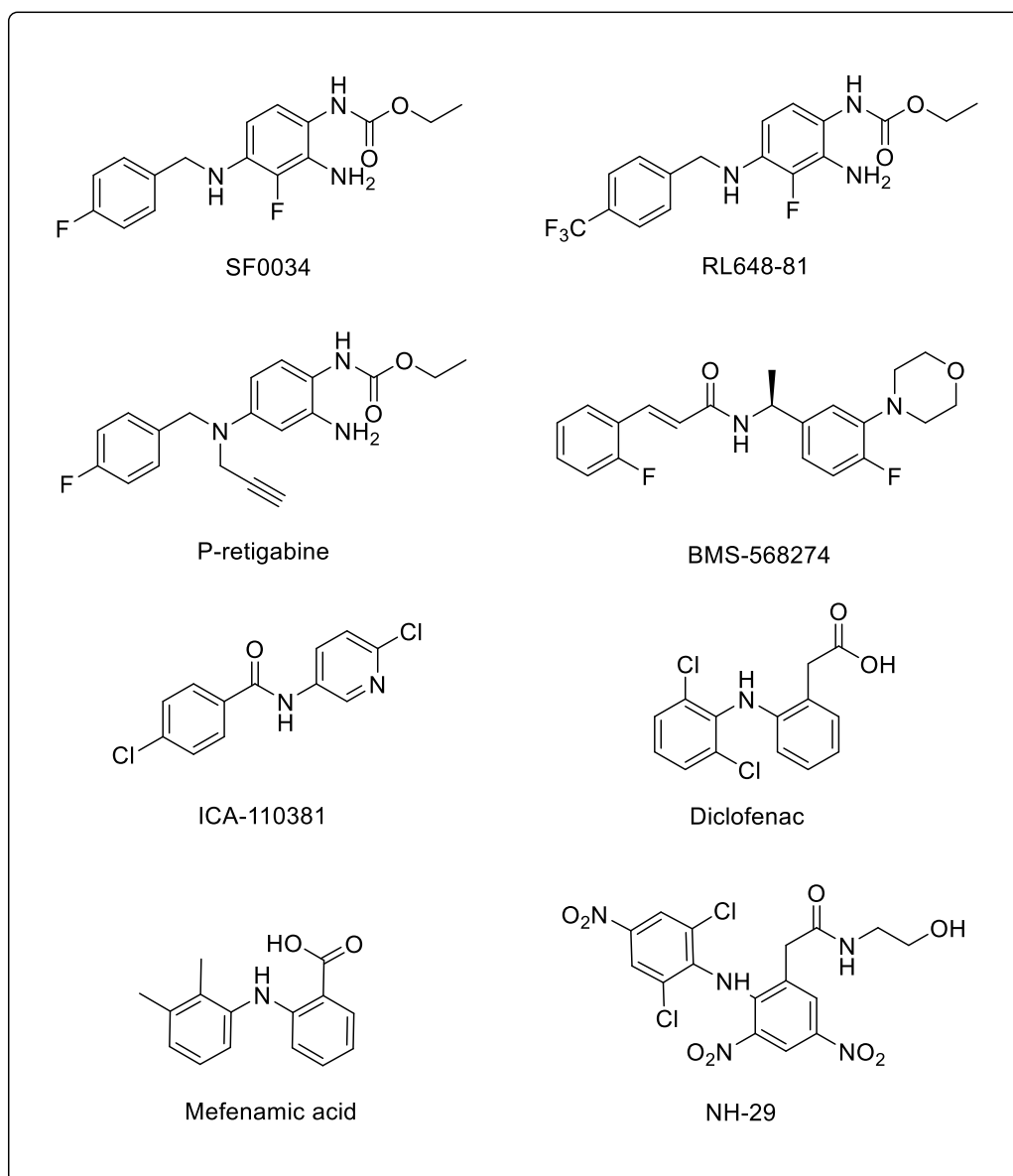
Figure 12. More potent retigabine derivatives and other K_{v7} activators.

2.1 Design of new conformationally restricted analogues of retigabine

Retigabine is very efficient in the treatment of many epileptic disorders, even though it presents some drawback such as short half-life, poor brain penetration and chemical instability. Besides, the poor selectivity of this drug causes $K_{v7.4}$ and $K_{v7.5}$ activation resulting in urinary retention. For these reasons, the identification of novel IKM modulators is more and more necessary. According to these premises, a further goal of my PhD programme was to develop a new library of $K_{v7.2}$ agonists synthesized introducing a conformational restriction of retigabine scaffold aimed at increasing the potency, the metabolic, and photochemical stability by blocking the labile 4-NH_2 and removing the 2-NH_2 of benzene-1,2,4-triamine scaffold.[182] By this strategy indoline, indole, and tetrahydronaphthalene (**A**, **B**, **C**, respectively. **Figure 13**) derivatives were designed and synthesized. Moreover, the designed structures allow extensive and chemically accessible modifications to investigate structure-activity relationships. The compounds were designed maintaining the substituted benzyl group at the N-1 position (series **A** and **B**, **Figure 13**) and C-5 position (series **C**, **Figure 13**) while varying the nature of both the R' chain and the linker X on the secondary amino group. At this position, we have chosen a series of linker groups characterized by different electrostatic potential, electron density distribution, and N-X rotation energy profiles, such as amide, sulphonamide, urea, thiourea and guanidine, which could mimic the retigabine pattern "HB (hydrogen bond) acceptor - HB donor - aromatic ring".
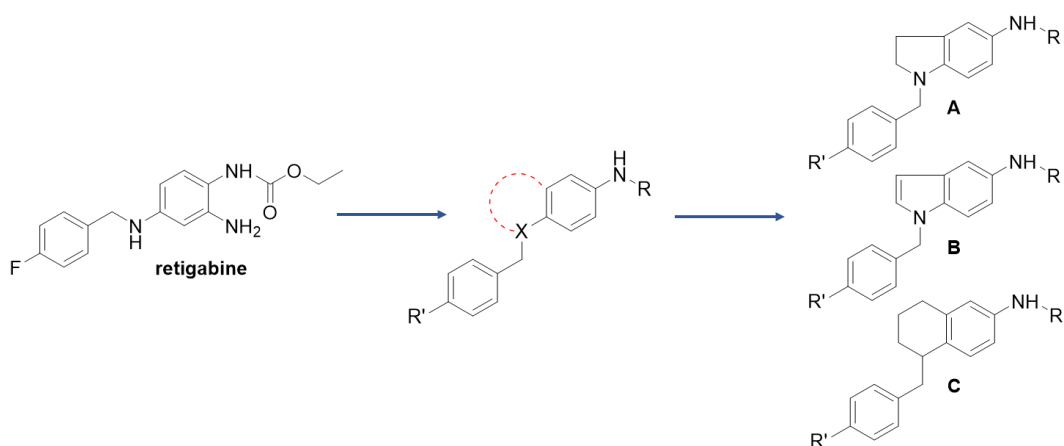
Figure 13. Structures of retigabine and its conformationally restricted proposed analogues.

2.2 Synthesis of I series

Starting from 5-nitroindoline (**1**), a reductive amination at the N-1 led to the corresponding 1-(4-fluorobenzyl)-5-nitroindoline (**2**) that, upon continuous flow hydrogenation to the corresponding amine (**3**), was used in the next steps. Reaction of **3** with ethyl or menthyl chloroformate in alkaline media gave the corresponding carbamate derivatives **4a** and **4b**. Urea derivatives **5a** and **5b** were prepared by one-pot reaction of **3** with triphosgene and 2,2-dimethylpropan-1-amine or cyclohexylamine, using DIPEA as base. On the other hand, treatment of **3** with CS_2 and 2,2-dimethylpropan-1-amine using TEA as base lead to the thiourea analogue of **5a** 1-(1-(4-fluorobenzyl)indolin-5-yl)-3-neopentylthiourea (**6**). Derivative **6** was converted to the corresponding carbodiimmide by reaction with HgO and then reacted with NH_4OH to give the guanidine derivative **7**. Finally, coupling of intermediate **3** with different sulfonyl chlorides and DBU led to the sulfonamide derivatives **8a-i**, while coupling with acyl chlorides using DIPEA as base led to the amide derivatives **9a-c**.
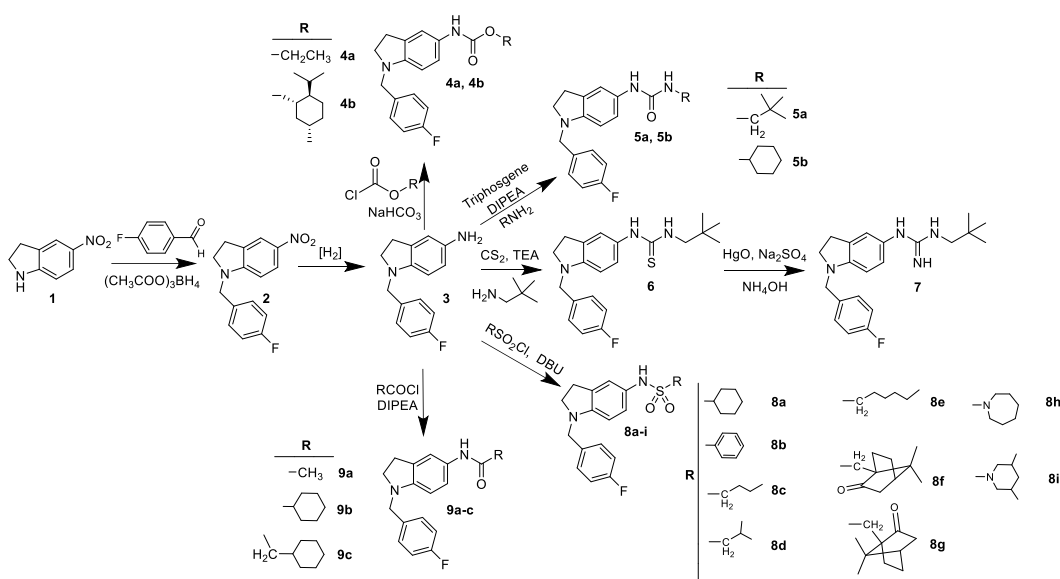
Scheme 1. Synthesis of 1-(4-fluorobenzyl)-5-substituted indoline derivatives **4a-b**, **5a-b**, **6**, **7**, **8a-i** and **9a-c**.

A second series of indoline analogues, investigating the influence of N-1 substituents on the pharmacological activity, was synthesized according to **Scheme 2** and **Scheme 3**.

5-nitroindoline (**1**) or 2-methyl-5-nitroindoline (**10**) were derivatized by reductive amination using different aldehydes, giving intermediates **11a-f**. Continuous flow hydrogenation of these intermediates led to the amines **12a-f** that were converted to the corresponding cyclohexylsulfonamides **13a-f**. Due to the lability of the 4-bromo-2-nitrobenzyl group to the hydrogenation conditions, final product **13g** was obtained using a different synthetic approach. In more detail, nitroindoline (**1**) was protected as tert-butoxycarbonyl derivative obtaining the intermediate tert-butyl 5-nitroindoline-1-carboxylate (**10b**). The nitro group of compound **10b** was reduced to the corresponding amine (**11g**) and coupled with cyclohexane sulfonyl chloride, as previously described, before removal of the Boc protecting group by trifluoroacetic acid (TFA). The intermediate **12g**, thus obtained, underwent to reductive amination using 4-bromo-2-nitrobenzaldehyde (**Scheme 2**).
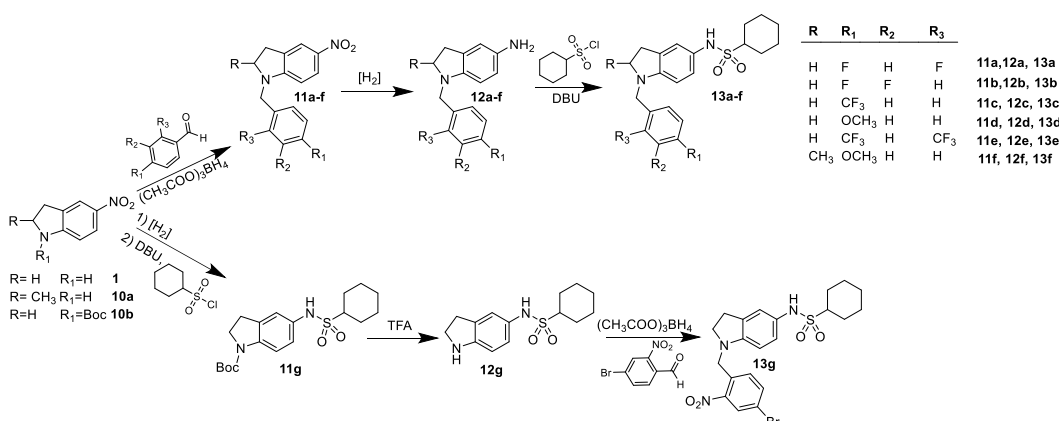
Scheme 2. Synthesis of 1-benzyl-5-cyclohexanesulfonamido indoline derivatives **13a-g.**

Functionalization of the N-1 was also attained by reaction of **1** with 4-chlorobenzoylchlorides, 2-(4-chlorophenyl)acetyl chloride and 1-(2-bromoethyl)-4-fluorobenzene to give intermediates **14a-b** and **17**. These intermediates were reduced by continuous flow hydrogenation and converted to the corresponding sulfonamides **16a-b** and **19** by coupling with cyclohexanesulfonyl chloride (**Scheme 3**).
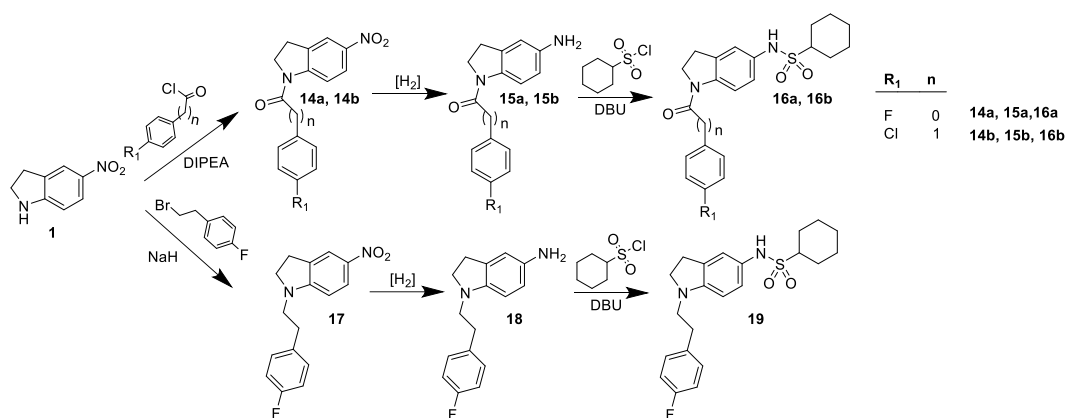
Scheme 3. Synthesis of 1-acyl-5-cyclohexanesulfonamido (**16a-b**) and 1-alkyl-5-cyclohexanesulfonamido (**19**) indoline derivatives.

2.3 Synthesis of II series

Indole analogues were synthesized according to **Scheme 4**. Intermediate **20b** was obtained starting from 4-hydroxybenzaldehyde, that reacted with methoxymethyl chloride (MOMCl) to give 4-(methoxymethoxy)benzaldehyde (**19a**). The protected aldehyde was reduced to the corresponding alcohol (**20a**) using $NaBH_4$ and then subjected to iodination affording 1-(iodomethyl)-4-(methoxymethoxy)benzene (**20b**). Nucleophilic displacements of **20** or commercially available 4-substitued benzyl halides by 5-nitroindole in strong basic medium provided the nitro intermediates **21a-d,** which were reduced to the corresponding substituted amino indole derivatives **22a-d**, as previously described. Coupling of these intermediates with acyl chlorides afforded the final alkyl amide derivatives **23a-b, 24a** and **25a**. Removal of the methoxymethyl group from derivative **23b** by TFA led to **24b**. On the other hand, reaction of amine intermediates **22a-d** with cyclohexanesulfonyl chloride gave final sulfonamides **23c**, **23d** and **26a**, while reaction with 2-cyclohexylethane-1-sulfonyl chloride (**20d**) led to the sulfonamide derivative **27a**. For the synthesis of **28a**, intermediate **22a** was reacted with chloroacetyl chloride and then subjected to nucleophilic displacement by n-butylamine. Alkylation of the secondary amine on the side chain by reductive amination with formaldehyde gave final product **29a**.
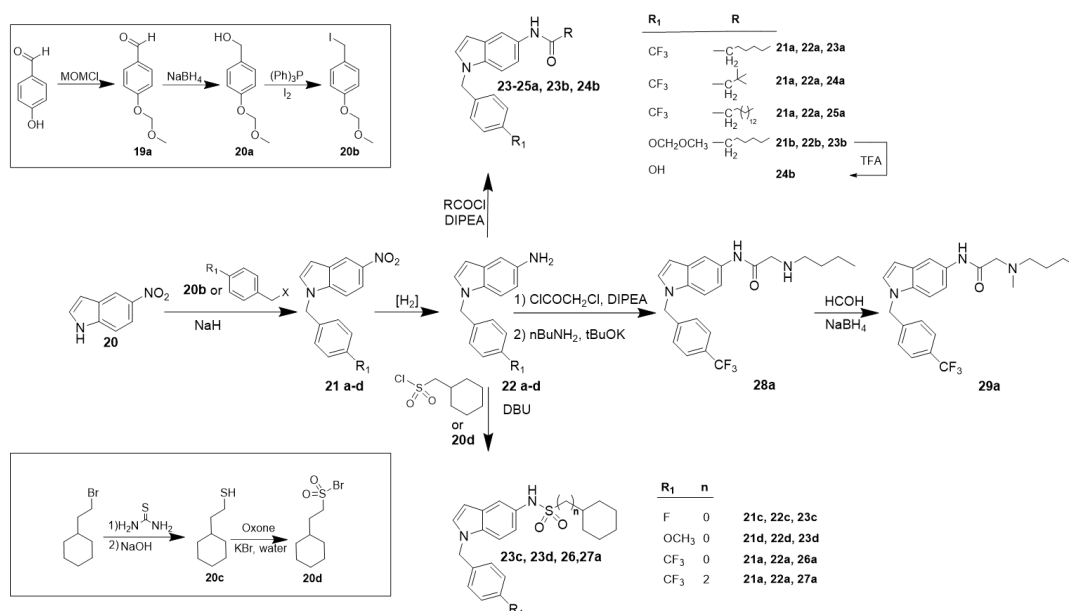
Scheme 4. Synthesis of 1-benzyl-5-amido (**23a-25a**, **23b-24b**, **28a-29a**) and 1-benzyl-5-cyclohexanesulfonamido (**23c-23d**, **26a-27a**) indole derivatives.

2.3 Synthesis of III series

Tetrahydronaphthalene analogues were synthesized as depicted in **Scheme 5**. Reaction of **30** with heptanoyl chloride and DIPEA, gave the amide intermediate **31**, which was reduced to the tetrahydronaphthol derivative **32** using NaBH$_4$ as reducing agent. Intermediate **32** was subjected to a modified Wittig reaction by formation of the corresponding phosphonium salt, followed by reaction with 4-(trifluoromethyl)benzaldehyde, giving the geometric isomers **33a** and **33b**.[183]   Their reduction using ammonium formate and Pd/C as catalyst gave final compound **34** as racemic mixture.
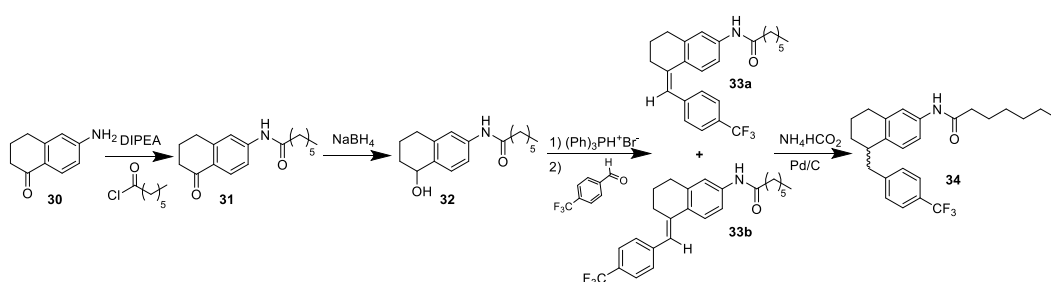
Scheme 5. Synthesis of (R,S)-N-(5-(4-(trifluoromethyl)benzyl)-5,6,7,8-tetrahydronaphthalen-2-yl)heptanamide (**34**).

2.5 Biological and photostability evaluation of series I-III

2.5.1 Whole-cell electrophysiology

To assess the effects of the derivatives on $K_{v7.2}$ currents, whole-cell patch-clamp electrophysiological experiments in CHO cells transiently transfected with $K_{v7.2}$ cDNA. Experiments were performed by research group of Prof. Maurizio Taglialatela (University of Naples "Federico II"). The effect of the synthesized compounds was investigated at a single concentration (10 µM), using a ramp protocol in which $K_{v7.2}$ currents were activated by a 3-second voltage ramps from -80 to +20 mV. Ramp-evoked currents were analysed by measuring the currents at -40 mV (a membrane potential value close to the activation threshold) and at 0 mV (a membrane potential value at which $K_{v7.2}$ conductance is almost completely saturated), and the effect of each compound was expressed as the ratio between current amplitude in the presence (A_2, B_2, I_{drug}) and absence (A_1, B_1, I_{CTL}) of the drug at these two membrane voltages (**Figure 14**). Using this method, drugs showing $I_{drug}/I_{CTL} > 1$ are considered as enhancers, drugs whose I_{drug}/I_{CTL} is < 1 are blockers and drugs whose I_{drug}/I_{CTL} is = 1 are considered ineffective.
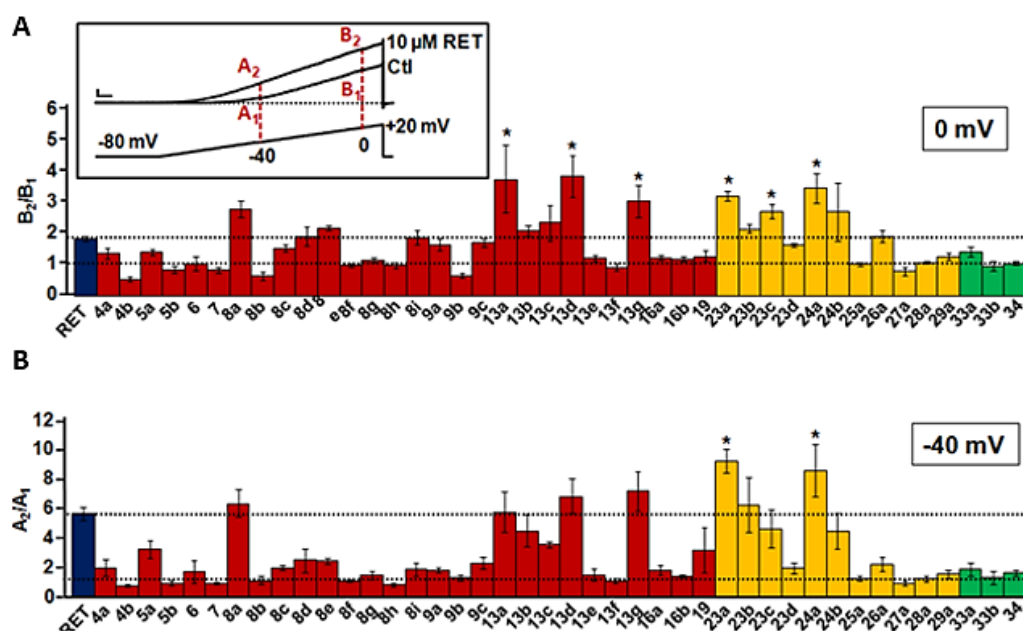
Figure 14. Effect of synthesized compounds on $K_{v7.2}$ current in comparison with retigabine. Representation of the ratio between current amplitude in the presence (A_2, B_2) and absence (A_1, B_1) of 10 µM drugs calculated at 0 mV (A) and at -40 mV (B). The inset shows the protocol used to evaluate drug activity on $K_{v7.2}$ currents. Current scale, 400 pA; time scale, 0.2 s. Histograms are colored according to the following scheme: blu represents retigabine, red represents indoline derivatives, yellow represents indole derivatives and green represents tetrahydronaphthalene derivatives. Each data point is the mean ± SEM. * indicates values significantly different (p < 0.05) from retigabine.

In this cellular assay, retigabine showed a ratio I_{drug}/I_{CTL} at -40 mV of about 6, whereas at 0 mV was about 2, suggesting that retigabine is more active at negative potentials than positive potentials, as previously described.[184,185] Of the 42 tested compounds at the single concentration of 10 μM, seven (**8a**, **13a**, **13d**, **13g**, **23a**, **23c**, and **24a**) were able to increase $K_{v7.2}$ currents more than retigabine (p<0.05) at 0 mV; among these, only two (**23a** and **24a**) also increased $K_{v7.2}$ currents more than retigabine at -40 mV (p<0.05) (**Figure 14**).

2.5.2 Characterization of the selectivity profile for channels formed by different K_{v7} subunits

Considering that I_{KM} is mainly formed by heteromeric assembly of $K_{v7.2}$ and Kv7.3 subunits, in subsequent experiments we evaluated the activity of **23a** and **24a** on $K_{v7.2}/K_{v7.3}$ heteromeric currents. Similarly to $K_{v7.2}$, **23a** and **24a** dose-dependently (0.01-10 μM) increased $K_{v7.2}/K_{v7.3}$ current with slower onset and offset kinetics and higher potency than retigabine (**Table 1**). Notably, when compared to retigabine, both **23a** and **24a** were more potent than their parent compounds in activating homomeric Kv7.4 channels.

In conclusion, the selectivity profile for **23a** was $K_{v7.2}=K_{v7.4}=K_{v7.2}/K_{v7.3}>>K_{v7.3}>>K_{v7.1}$; while for the **24a** was $K_{v7.4}> K_{v7.2}=K_{v7.2}/K_{v7.3}=K_{v7.3}>>K_{v7.1}$.

Table 1. EC_{50} and induced ΔV shift of retigabine and compounds **23a** and **24a** over different K_v channels. All three drugs were used at 10 μM concentration. * p<0.05 vs ΔV of retigabine on $K_{v7.3}$ channels; ** p<0.05 vs ΔV of retigabine on $K_{v7.4}$ channels; $ p<0.05 vs EC_{50} of retigabine; † p<0.05 vs EC_{50} of **23a** on $K_{v7.2}$ channels.

Target channel	ΔV (mV)			EC_{50} (μM)		
	RET	23a	24a	RET	23a	24a
$K_{v7.2}$	-25.37±1.23	-29.47±2.03	-30.01±3.81	0.93±0.43	0.08±0.04$	0.63±0.07
$K_{v7.2}/K_{v7.3}$	-26.81±1.93	-25.45±2.91	-20.00±2.48	1.72±0.41	0.21±0.14$	0.34±0.06$
$K_{v7.3}$	-39.88±5.13	-26.25±4.60	-21.40±6.18*	3.90±1.70	10.5±6.00†	0.92±0.64
$K_{v7.4}$	-15.19±1.97	-32.85±2.97**	-24.43±5.39	1.98±0.84	0.10±0.02$	0.08±0.20$

2.5.3 Photostability assays

All synthesized derivatives were subjected to photostability assays by our research group. Exposure to visible light led to a remarkable and significant photodegradation of retigabine; instead, about 47,33±4,03% of retigabine was degraded after 6 hours of drug exposition to artificial daylight lamp. Quantitatively similar results were obtained upon direct exposure of retigabine to natural solar light (43.5±4.3% degradation at 6 hours). We then decided to further investigate the photodegradative behaviour of retigabine by analysing the corresponding by-products. As shown in **Figure 15**, the HPLC profile of photodegraded retigabine batches is mainly characterized by the presence of two additional peak with a retention time of 5.98 and 14.39 minutes. Running HPLC/MS analysis of these peaks we were able to detect the mass spectra only for the late eluting peak (14.39 minutes), putatively identified as the retigabine adduct ethyl (2,4-bis((4-fluorobenzyl)amino)phenyl)carbamate (**Figure 15**). The peak eluting at 5.98 minutes was undetectable by mass spectrometry, in accordance with a previous paper reporting the existence of non-identified retigabine impurity at shorter retention times.[186] Thus, we decided to analyse the unknown peak using a GC/MS method, leading to the identification of 4-fluorobenzaldheyde as the main by-product in retigabine photodegradation. The result was further confirmed by comparison with the HPLC trace of pure 4-fluorobenzaldheyde and is consistent with a photooxidative C-N bond cleavage mechanism widely described in literature.[187]
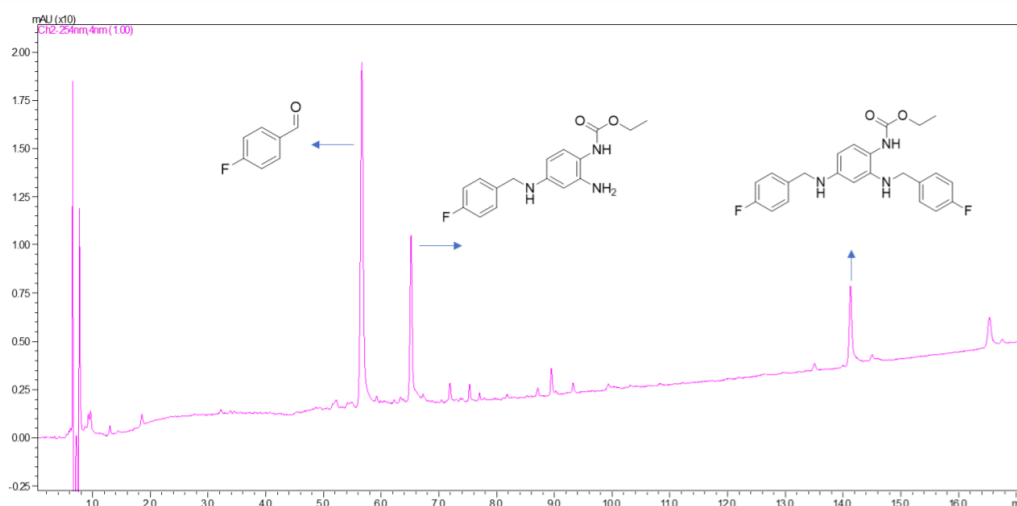
Figure 15. UHPLC profile of a retigabine batch after 6h visible light irradiation.

The proposed mechanism justifies the reason why visible light is more effective in inducing retigabine photodegradation and corroborate the hypothesis concerning the molecular structure of the peak eluting at 14.39 minutes. Considering that Groseclose and Castellino[188] found that the typical absorbance of retigabine photoinduced dimers is 550 nm, we decided to set the same wavelength for the UV detection, evidencing some additional byproducts corresponding to some of the previously reported phenazinium dimers.[188] Thereafter, the most active synthesized derivatives, namely derivatives **8a**, **13a**, **13d**, **23a** and **24a**, were subjected to the photostability assay. Results obtained are reported in **Table 2**.

Table 2. Photoinduced degradation of retigabine and its analogues under solar lighting. Results are expressed as percentage of degradation±SD.

Derivative	Time (h)		
	2	*4*	*6*
Retigabine	9.65±6.93%	25.16±7.31%	47.33±4.03%
8a	45.29±7.35%	86.87±10.54%	≥99%
13a	33.46±6.50%	81.72±1.12%	≥99%
13d	37.51±7.25%	84.66±4.12%	≥99%
23a	1.36±0.89%	5.82±2.05%	9.15±2.91%
23c	6.46±1.78%	15.78±1.97%	23.11±1.84%
24a	0.96±0.64%	6.62±2.17%	8.45±1.99%

Our results indicate that an increased photostability was attained turning to indole scaffold, probably due to the improved delocalization of the π-electrons of the indole ring. In particular, derivatives **23a** and **24a**, obtained by replacement of the sulfonamide with a carboxamide moiety, were the more photostable retigabine analogues, showing less than 10% of degradation after the 6 hours' time-course.

2.6   Molecular modelling

Pharmacophore modelling was generated by Dr. Nunzio Iraci (University of Messina) to get insight into the chemical features of K_{v7} channel activators. Using Phase on an active set (composed by molecules showing more than 4 I_{drug}/I_{ctl} at -40 mV) and on an inactive set, we obtained a pharmacophore model (**Figure 16**).
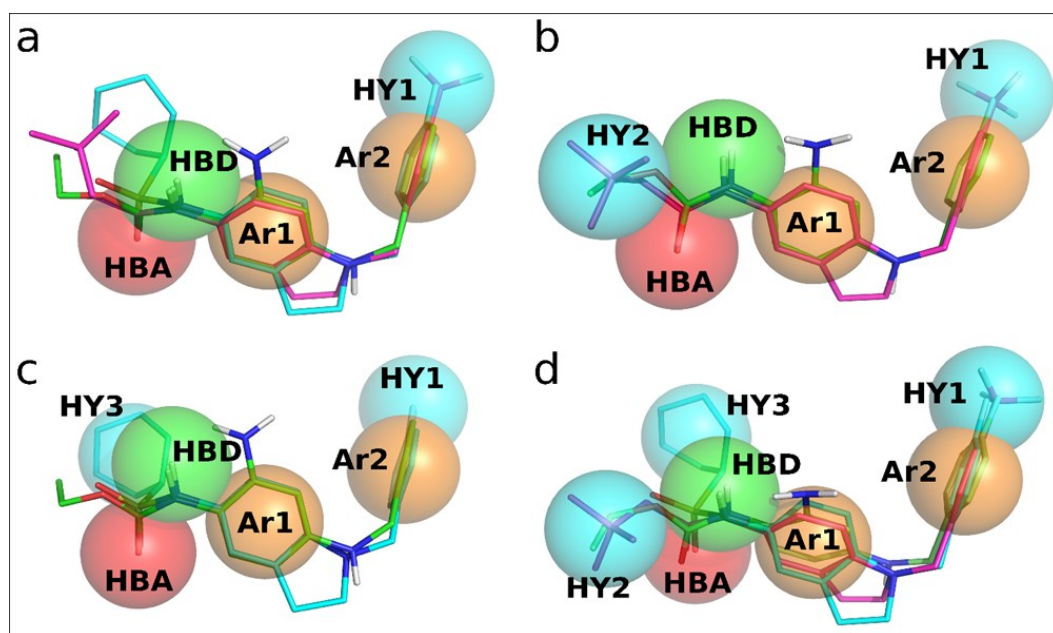
Figure 16. Pharmacophore models developed based on our novel K_{v7} channel activators. Pharmacophore features are color-coded as follows: Hydrophobic (HY – cyan), Aromatic (Ar – orange), Hydrogen Bond Donor (HBD – green), Hydrogen Bond Acceptor (HBA – red). a) Model A with compounds **24a** and **8a** depicted in magenta and cyan sticks, respectively. b) Model B with compound **24a** depicted in magenta sticks. c) Model C with compound **8a** depicted in cyan sticks. d) Model D with compounds **24a** and **8a** depicted in magenta and cyan sticks, respectively. Retigabine is depicted as reference, in every panel, in green sticks.

The model is composed by 5 pharmacophore features, a hydrogen bond acceptor (HBA), a hydrogen bond donor (HBD), a hydrophobic region (HY1) and two aromatic regions (Ar1 and Ar2). Despite the evident influence of the R substituent (**Figure 13**) on the activity, model A does not present any feature focused on these substituents. We thought this may be due to the different geometries of the sulphonamide and amide moieties of the molecules belonging to the active set. We thus developed two separate models for amides and sulphonamides. Removing the sulphonamide derivatives from the active set we obtained model B (**Figure 16b**). On the opposite, by keeping sulphonamides only we obtained model C (**Figure 16c**). The two models share features Ar1, Ar2, HY1, HBA and HBD, with almost identical coordinates. We

superimposed models B and C to model A to get model D (**Figure 16d**), that inherits Ar1, Ar2, HY1, HBA and HBD from model A, HY2 from model B and HY3 from model C. The hydrogen bond interaction with W236, whose importance has been proven for other channel modulators as well as for **23a** in this study, is represented in the models by the HBA feature. The finding of the two additional hydrophobic locations HY2 and HY3 could explain the great variety of substitutions tolerated at position 5, as well as the possibility of linking the HY2/3 substituent at 5-NH$_2$ with geometrically different linkers.

Indeed, despite the most potent molecules herein reported have an amide HBA-HBD moiety, the sulphonamide one results of great interest for this and for future investigations.

HY2 and HY3 could probably indicate a whole, larger, and flexible pocket on K$_{v7.2}$, where more flexible compounds could bind in different conformations, interacting with more protein residues. This may be achieved by the flexibility of the substituent in the case of **23a**, or of the sulphonamide linker in the case of **8a**. Homology modelling of the K$_{v7.2}$ 219-325 region agrees with the existence of two hydrophobic sites separated by W265; this critical residue appears indeed surrounded, on two sides, by several hydrophobic residues that could be the counterpart of HY1 and HY2/3 on the channel protein (**Figure 17**).

Addressing the binding mode of these derivatives, our next goal has been their optimization by structure-based drug design.
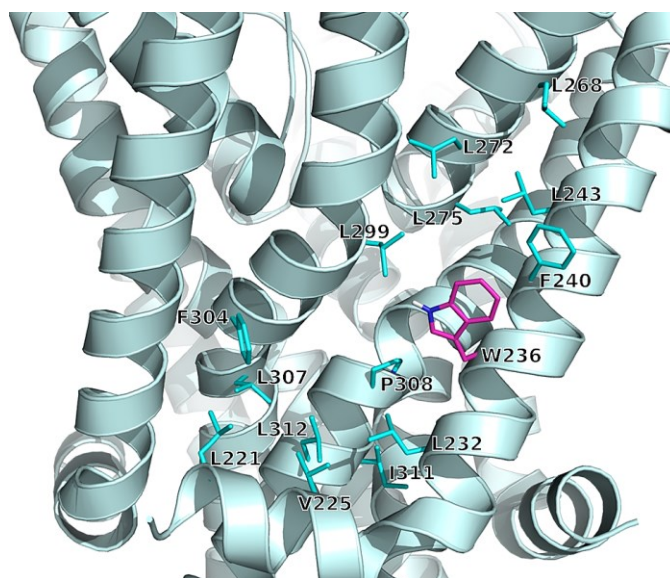
Figure 17. K$_{v7}$ modulators binding region modeled by homology with the Cryo-EM structure of Xenopus KCNQ1 channel (PDB id: 5vms). W236 (magenta sticks) is surrounded by several hydrophobic residues (cyan sticks) that could host chemical features HY1 and HY2/3.

3.1 Optimized agonists of Kv7.2 (series IV): Background and design

In the above work, we designed, synthesized, and evaluate the I-III series of conformationally restricted retigabine derivatives.

Through the use of pharmacophore modelling and homology modelling, we proposed the existence of a large and binding pocket formed by residues L221, V225, L232, F304, L307, I311 and L312.

Given the recent publication of experimental structure of $K_{v7.2}$ in complex with retigabine,[189] we performed molecular docking and molecular dynamics calculations to study the interactions of compounds **23a** and **24a** with $K_{v7.2}$ using retigabine as reference (**Figure 18A**).

Because of the size of the substituents at the amide carbonyl, **23a** and **24a** get to interact optimally with residues V225, F304 and L312, while retigabine does not, given the smaller size of its substituent.

In order to identify optimized agonists and to verify the hypothesis proposed by molecular modelling concerning the chemical space at the retigabine binding site, we conducted a structure-based drug design by performing modifications at three spots of the prototype agonist retigabine (**Figure 18B**). In particular, modifications at area 1 were meant to identify the most efficient substituents able to fit its pocket (pocket 1), which is not efficiently exploited by retigabine. Area 2 was investigated to challenge the importance of the H-bond established between the amino group at position 2 and the side chain of S303, and also the possibility of fitting larger substituents in the space lined by residues S303, V302, L299 and F305. Modifications at area 3 were mainly focused on the linker between the two phenyl ring and on the influence of the substitutions at the phenyl ring, that in our model shows π-stacking interaction with F240 and F305.
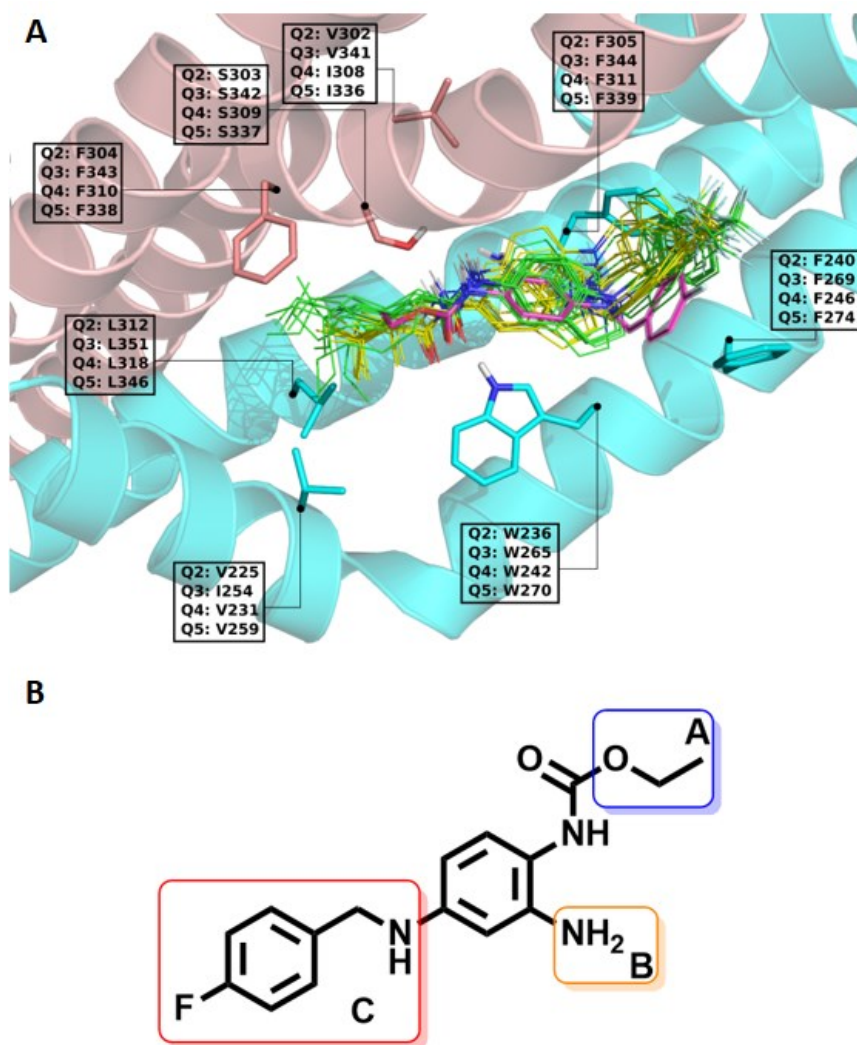
Figure 18. (A) Retigabine binding pocket on $K_{v7.2}$. $K_{v7.2}$ is depicted in sticks and cartoons, the two different monomers are colored in cyan and salmon. Bound conformations of **23a** (yellow) and **24a** (green) are shown in thin solid sticks. For each ligand, 12 bound conformations are represented. Experimentally solved bound conformation of retigabine (PDB ID: 7CR2) is shown in magenta thick transparent sticks. (B) Structural modifications of lead compound retigabine.

3.2 Synthesis of IV series

Derivatives **37**, **49-56**, **59-64** were prepared applying the synthetic route shown in **Scheme 6**. p-phenylenediamine, used as starting material for the synthesis of compound **37**, was subjected to N-acylation reaction using heptanoyl chloride and N,N-diisopropylethylamine, then N-4 alkylation was performed with 4-trifluoromethylbenzyl bromide. N-4 alkylated intermediate **39** was synthetized from starting material **38** using the procedure described above. The obtained compound was reacted with benzyl chloroformate under alkaline conditions leading to the protected intermediate **40**, which was derivatized at N-1 in basic medium using different commercially available acyl chlorides to yield intermediates **41-48**. Hydrogenation of intermediates **41-48** using ammonium formate and Pd/C under reflux gave the final derivatives **49-56**. Intermediate **39** was also used for the synthesis of final derivatives **59-64**. Reaction with Boc anhydride and triethylamine furnished the N-Boc protected intermediate **40'**, which was acylated at N-1 position using 3,3-dimethylbutanoyl chloride, yielding intermediate **41'**. Then, the nitro group of **41'** was subjected to reduction by ammonium formate and Pd/C, providing **42'**, which was reacted with 1,4-dibromobutane or 1,5-dibromopentane under basic conditions affording intermediates **57** and **58**, respectively. Deprotection by trifluoroacetic acid in dichloromethane led to the final products **59** and **60**. Compounds **49** and **53** were further derivatized at N-4 position: reductive amination reaction using formaldehyde or propionaldehyde in acid medium led to the N-4 alkyl derivatives **61-63**. On the other hand, derivative **64** was obtained by reaction of **49** with acetyl chloride under basic conditions.
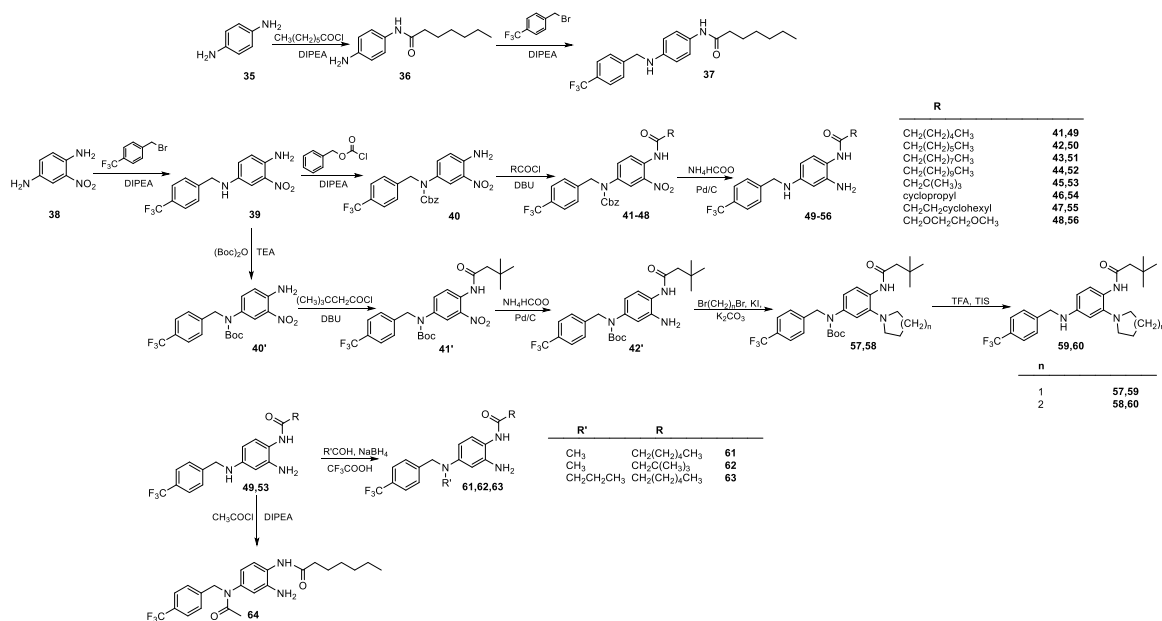
Scheme 6. Synthesis of 1,4-phenylenediamine (**37**), benzene-1,2,4-triamines (**49-56**), 2-(pyrrolidin-1-yl)benzene-1,4-diamine (**59**), 2-(piperidin-1-yl)benzene-1,4-diamine (**60**), N^4-alkylbenzene-1,2,4-triamines (**61-63**) and N-(3,4-diaminophenyl)acetamide (**64**) derivatives.

Derivative **68** was synthesized following the synthetic strategy shown in **Scheme 7**. 4-amino-3-nitrophenol was reacted with 4-trifluoromethylbenzyl bromide in alkaline media leading to the corresponding ether (**66**). Reaction of intermediate **66** with heptanoyl chloride under basic conditions furnished **67**, which was reduced using ammonium formate and Pd/C giving final product **68**.
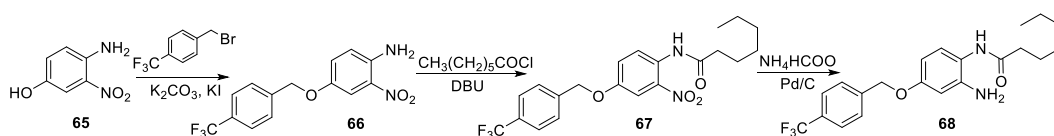
Scheme 7. Synthesis of 3,4-diaminophenol derivative **68**.

Derivatives **72**, **85-88**, **92**, **93**, and **99** were synthesized using an alternative synthetic route as described in **Scheme 8**. 2-nitro-1,4-phenylenediamine (**38**) was reacted with different commercially available alkyl halides in alcaline conditions to yield intermediates **73-76**, which were protected at N-4 by reaction with benzyl chloroformate furnishing intermediates **77-80**. The obtained compounds were acylated with heptanoyl chloride or 3,3-dimethylbutanoyl chloride affording **81-84**. Hydrogenation reaction was performed to provide the reduction of the nitro group and, at the same time, the removal of the Cbz protecting group leading to final derivatives **85-88**. The synthesis of **72** and its isomer **92** were performed using two alternative reaction procedures due to the different reactivity of 2-pyridinecarboxaldehyde and 4-pyridinecarboxaldehyde which were used as starting materials. Derivative **72** was synthetized from picolinaldehyde: reaction with 2-nitrobenzene-1,4-phenylendiamine in acid medium, followed by treatment with NaBH4 as reducing agent led to intermediate **69**. Then, **69** was coupled with benzyl chloroformate in alkaline conditions to give **70**, which was subjected to the same acylation and reduction reactions previously described yielding compound **72**. A different synthetic strategy was applied for the synthesis of compound **92**: 2-nitro-1,4-phenylendiamine was first protected at N-4 position using di-tert-butyl dicarbonate in alkaline media, then the obtained intermediate **89** was reacted with heptanoyl chloride affording **90**. The deprotection of the isolated intermediate using a mixture DCM/TFA led to N-(4-amino-2-nitrophenyl)heptanamide (**91**) which was reacted with 4-pyridinecarboxaldehyde under acid conditions, leading, at the same time, to the reduction of the NO2 group and to the final product

92. The synthesis of N-(2-amino-4-((2-fluorobenzyl)amino)phenyl)heptanamide (**93**) was performed using the same procedure and replacing 4-pyridinecarboxaldehyde with 2-fluorobenzaldehyde. Intermediate **91** was also used for the synthesis of derivative **99** as reported. N-(4-amino-2-nitrophenyl)heptanamide (**91**) was reacted in basic medium with (4-(iodomethyl)phenyl) carbonate (**97**) to yield compound **98**. Intermediate **97** was previously prepared starting from 4-hydroxybenzaldehyde, which was reacted with benzyl chloroformate to furnish **95**; reduction of the aldehyde function led to the alcohol **96**, which was converted to corresponding iodide **97** by reaction with iodine and triphenylphosphine. Hydrogenation of intermediate **98**, performed as described above, afforded final derivative **99**.
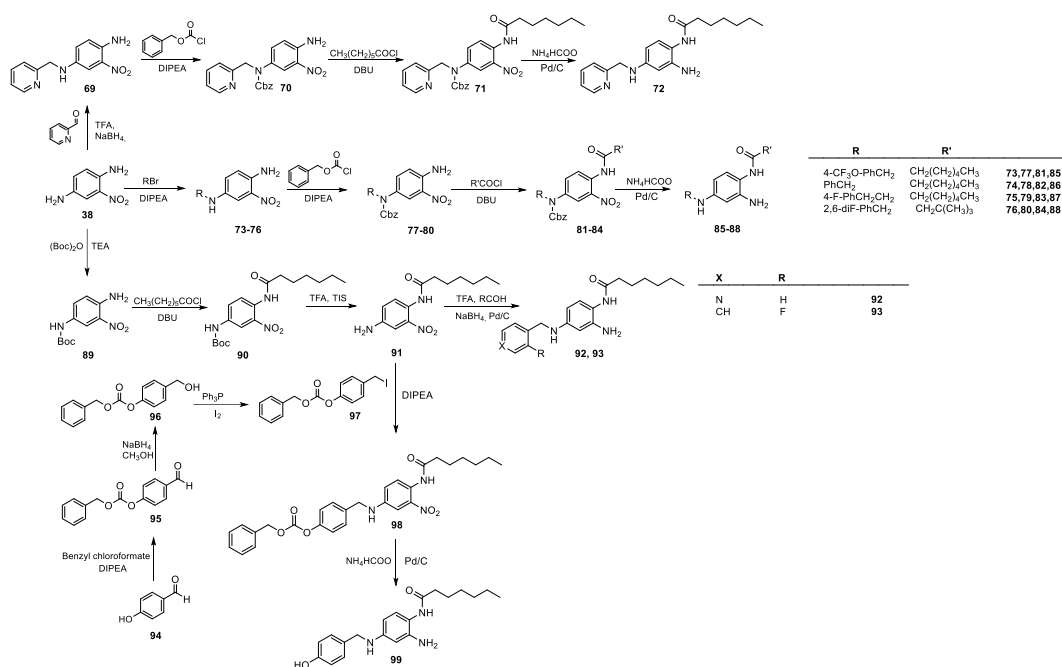
Scheme 8. Synthesis of benzene-1,2,4-triamine derivatives **72**, **85-88**, **92-93**, **99**.

In **Scheme 9** the synthetic route adopted for the synthesis of the fluorinated derivatives **103**, **106-110**, **112**, **117**, and **118** is shown. 2-fluoro-4-nitroaniline was used as starting material for the synthesis of compound **103**. N-alkylation was afforded by reaction with 4-fluorobenzyl bromide in basic medium. The subsequent hydrogenation reaction, performed using ammonium formate and Pd/C, followed by N-acylation with heptanoyl chloride and DIPEA yielded final amide **103**. The first step of the synthetic pathway which led to derivatives **106-110** and **112** involved the coupling of 2,3-difluoro-6-nitroaniline and 4-trifuloromethyl benzylamine by a iodine catalyzed Buchwald-Hartwig-type reaction.[190] The obtained intermediate **105** was, then, subjected to reduction using Zn and NH₄Cl and in situ coupling reaction with various acyl

chloride to furnish final derivatives **106-110**. On the other hand, intermediate **105** was alkylated with iodomethane and potassium tert-butoxide to give N-1-methyl derivative **111**. The subsequently one pot reduction-acylation reaction of **111** using 3,3-dimethylbutanoyl chloride provided final product **112**. Compounds **117** and **118** were prepared from 2,6-difluoro-4-nitroaniline, which was subjected to Pd/C catalyzed hydrogenation to give intermediate **114**. N-1 acylation using heptanoyl chloride or 3,3-dimethylbutanoyl chloride and DIPEA yielded intermediates **115** and **116**, respectively, which were further derivatized at N-4 position using 4-trifluorobenzyl bromide to afford final products **117** and **118**.
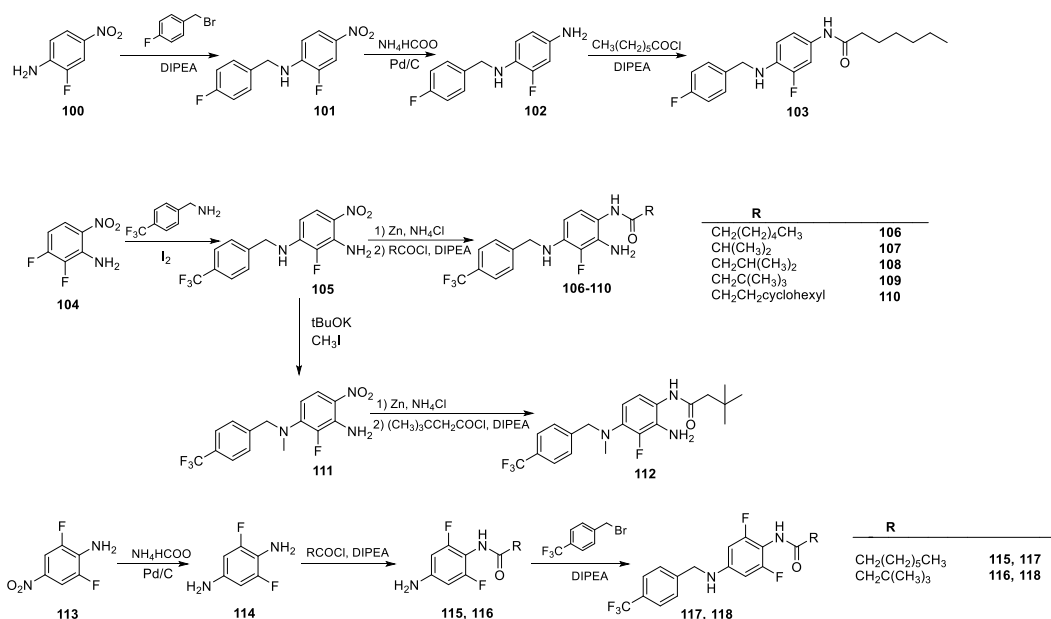
Scheme 9. Synthesis of N-(3-fluoro-4-((benzyl)amino)phenyl)amide **103**, N-(2-amino-3-fluoro-4-(benzyl)amino)phenyl)amide (**106-110**, **112**), and N-(2,6-difluoro-4-(benzyl)amino)phenyl)amide (**117**, **118**).

Derivatives **128** and **132** were prepared as described in **Scheme 10**. 4-nitrobenzaldehyde reacted with 4-trifluoromethylbenzyltriphenylphosphonium bromide by a Wittig-type reaction to furnish a mixture of *cis* and *trans* isomers of 1-nitro-4-(4-(trifluoromethyl)styryl)benzene (**120a** and **120b**). The reduction of the mixture of isomers by ammonium formate and Pd/C under reflux led to the corresponding 4-(4-(trifluoromethyl)phenethyl)aniline (**121**). N-1 acylation, performed using heptanoyl chloride or 3,3-dimethylbutanoyl chloride, led to intermediates **122** and **123**, respectively; the C-2 nitration by HNO$_3$ in acetic anhydride gave the N-(2-nitro-4-(4-(trifluoromethyl)phenethyl)phenyl)amide intermediates **124** and **125**, which were converted to the corresponding amines (**126** and **127**) by catalitic hydrogenation.

Finally, reaction with 1,4-dibromopentane in basic medium afforded 3,3-dimethyl-N-(2-(piperidin-1-yl)-4-(4-(trifluoromethyl)phenethyl)phenyl)butanamide (**128**) as final product. 2,4-dinitrobenzoic acid was used as starting material for the synthesis of derivative **132**. Coupling reaction with n-hexylamine, using PyBop as coupling agent and DIPEA as base, led to amide intermediate **130**, which was reduced to the corresponding diamino derivative (**131**) by catalytic hydrogenation procedure and then coupled with 4-trifluoromethylbenzyl bromide as previously described, to attain the final compound **132**.
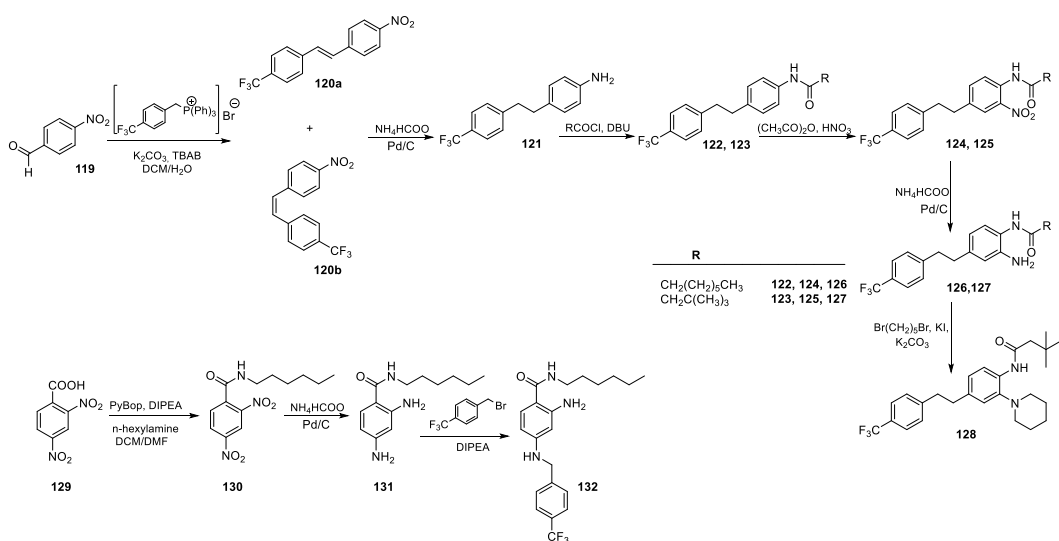
Scheme 10. Synthesis of N-(2-amino-4-(4-(trifluoromethyl)phenethyl)phenyl)amide (**126-127**) derivatives, 3,3-dimethyl-N-(2-(piperidin-1-yl)-4-(4-(trifluoromethyl)phenethyl)phenyl)butanamide (**128**) and 2-amino-N-hexyl-4-((4-(trifluoromethyl)benzyl)amino)benzamide (**132**).

4.1 Biological evaluation of series IV

4.1.1 Screening by thallium-based fluorometric assay

The activity screening of retigabine derivatives has been performed by research group of Prof. Maurizio Taglialatela (University of Naples "Federico II") on stable CHO cell lines co-expressing K_{v7} channel subunits of interest by using a fluorescence thallium-based assay. The analysis is based on the uses of Tl^+ as a surrogate for K^+ ions, recognized by a specific fluorogenic thallium-sensitive dye. During the assay, a small amount of thallium is added to the cells with a stimulus to open channels. Thallium then passes into cells through open potassium channels according to a strong inward driving force. Cell extrusion of dye is inhibited by the presence of probenecid, a blocker of the organic anion transporter.

Of the 35 tested compounds, thirteen derivatives result more efficient than retigabine in terms of both maximal fluorescence and slope of the fluorescent signal (**Figure 19**). Then these values are normalized as EC_{50} (**Table 3**).
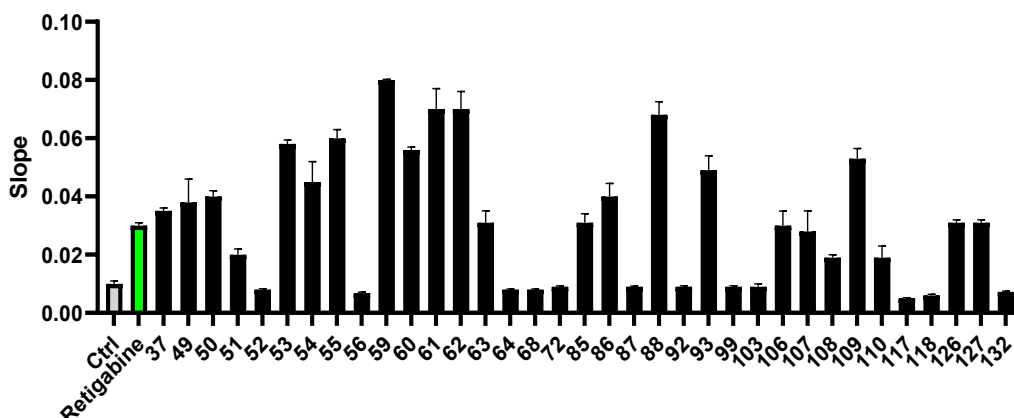
Figure 19. Effect of synthesized compounds in CHO cells on $K_{v7.2/7.3}$ current in comparison with retigabine. Two different parameters were calculated; the ratio between the maximal fluorescent signal and the fluorescent signal at time 0 (Fmax/F0), then the slope of the fluorescent curve calculated at 10". The derivatives synthesized were tested at the concentration of 10 μM. Data are given as mean ± DS.

4.1.2 Photostability assays

Compounds more potent than retigabine in the fluorometric assay were subjected to photostability assays, which were conducted by my research group. Initially, an UV quartz cuvette containing an aqueous solution of retigabine or tested compounds (10 μM) was irradiated by an UV lamp for 3 h. After exposure, aliquot of the solution was withdrawn and analyzed by HPLC to reveal the concentration of the starting materials and the formation of the

dimers. Exposure to UV light led to significant photodegradation of retigabine; about 63.3 ± 0.1 % was degraded after 3 h. Similar % of degradation was show by compound **55** whereas remarkable or almost complete degradation were obtained for derivatives **53, 59, 60, 62**, and **88**. Finally, derivatives **49, 86**, and **109** were the most photostable retigabine analogues (**Table 3**). We then decided to further investigate the photodegradative generation of dimeric by-products. Considering that the typical absorbance of retigabine photoinduced dimers is 550 nm, we decided to set the same wavelength for the UV detection. Compared to retigabine, the only derivatives which were not able to generate dimers were **59, 60, 61, 62**, and **109** suggesting that the structural modification at the aniline group or at NH-linker, that characterized these compounds, was able to reduce the dimerization reaction. This is in accordance with the mechanism we have previously identified for retigabine photooxidation, a photooxidative C-N bond cleavage that rapidly leads to the formation of the phenazine and phenazonium dimers, detected, *in-vivo*, by Castellino and Grosecloese.[187,188] In particular, compounds **59** and **60** are likely not amenable to dimer formation due to the lack of a reacting amino group in position 2 of the benzene-1,2,4-triamine core scaffold. Methyl derivatives **61** and **62** showed a remarkable agonist activity and inability to form dimers probably due to methyl group that interferes with intermediates stability after C-N photooxidative reaction (**Figure 20**). Moreover, the improved photostability of **86** could be justified in consideration of the lack of the electron-withdrawing fluorine at the benzyl moiety, responsible for an increased polarization of the C-N bond.

Among the compounds not able to form dimeric species, compound **109** shows also the lowest % of degradation. For these reasons, it has been selected for patch clamp electrophysiology studies, where it confirmed a potent *in vitro* activity on $K_{v7.2}$-$K_{v7.3}$ channels with 40-fold increased potency when compared with retigabine (EC_{50} = 0.12 ± 0.04 µM Vs retigabine EC_{50} = 4.80 ± 1.80 µM).

Table 3. % Degradation and EC_{50} values for the most active synthetized compounds obtained by fluorimetric assay on CHO cells. Retigabine is used for reference. Data are given as mean ± DS.

Compound	EC_{50}	% Degradation (3h, UV)	Dimers Formation
Retigabine	10.4±4.6	61.3±0.1	Yes
37	0.7±0.2	73.2±0.4	Yes
49	2.1±0.5	30.6 ± 2.2	Yes
53	0.2±0.8	79.8 ± 4.2	Yes
54	0.8±0.3	73.2 ± 1.7	Yes
55	2.2±0.5	64.8 ± 0.9	Yes
59	2.0±0.7	97.7± 1.0	No
60	0.9±0.2	79.8 ± 4.2	No
61	0.6±0.2	97.8± 2.1	No
62	0.7±0.4	99.5±0.1	No
88	0.8±0.3	98.4±0.2	Yes
86	7.1±0.5	19.5±4.7	Yes
93	5.1±0.1	74.9± 0.1	Yes
109	3.4±1.0	34.8± 1.8	No
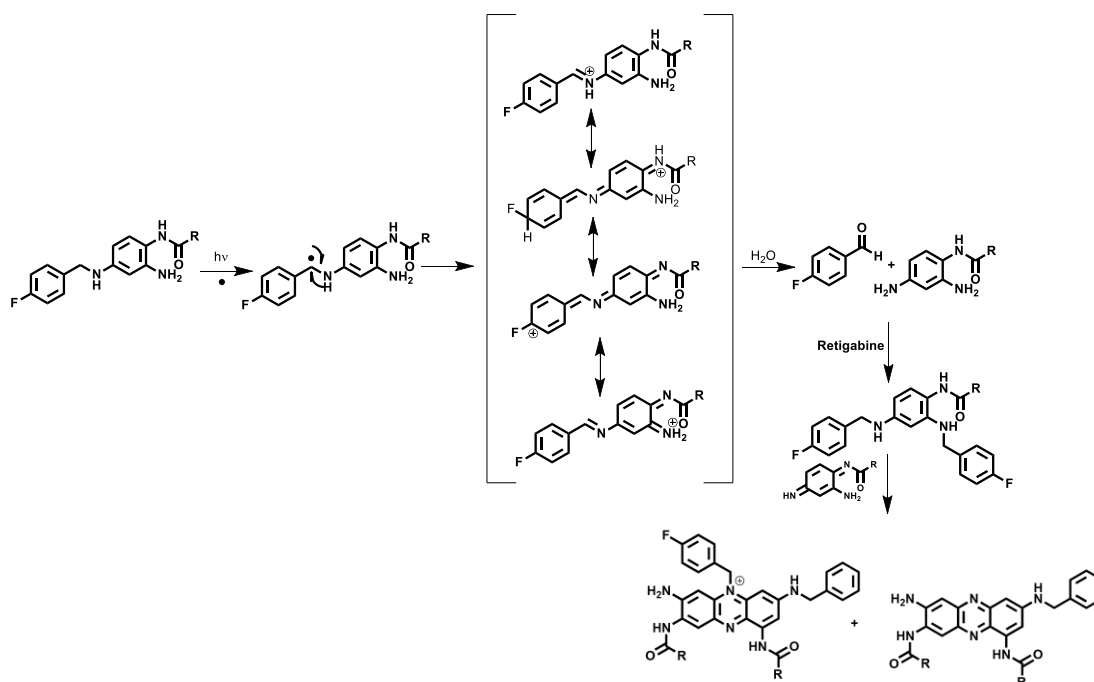
Figure 20. Proposed photooxidative mechanism of degradation of retigabine and its analogues.

4.1.3 Pharmacokinetics studies

The most potent compound (**109**) was tested to *in vitro* microsomal stability evaluating its towards liver first pass metabolism. A very remarkable stability was found for this derivative that demonstrated a metabolic profile comparable to retigabine both in phase I (8.2 ± 2.7% Vs 4.7 ± 0.4% of retigabine) and phase II (15.6 ± 0.3% Vs 17.4 ± 1.2% of retigabine) turnover simulated metabolism.

Furthermore, in order to explore the eligibility of this compound for *in vivo* administration, further pharmacokinetic experiments were performed to assess the brain concentration of **109**. The compound was administered via intraperitoneal injection in rats at a dose of 1 mg/Kg and, after 3 hours, time course, plasmatic concentration and brain concentration were assessed. Pharmacokinetic parameters were compared to those obtained with equal doses of retigabine. Compound **109** showed a brain accumulation of 726.6 ± 178.8 ng/mg of tissue, higher than retigabine (469.2 ± 142.8 ng/mg of tissue), with a brain-to-blood ratio 16 times higher.

For these founds, the compound was challenged in a pentetrazol-induced epilepsy mouse model.

4.1.4 In vivo studies

The pentylenetetrazol test, characterized by the chemical induction of acute convulsions, was adopted to evaluate the pharmacological effects of retigabine and compound **109** at different doses. These studies were performed by research group of Prof. Maurizio Taglialatela (University of Napoli "Federico II").

Seizures were induced by pentylenetetrazol at 100 mg/kg. Mice were pre-treated intraperitoneally with retigabine (3 mg/kg) and compound **109** (0.3, 1 mg/kg) 30 minutes before the induction of the seizures. When retigabine was unable to rescue by seizures, compound **109** at both dosages significantly reduced the seizure score (**Figure 21A**). Moreover, the same compound increased the latency to maximal seizures compared to control (**Figure 21B**). Finally, treatment with compound **109** markedly reduced pentylenetetrazol-induced mortality in mice, whereas retigabine was ineffective (**Figure 21C**).
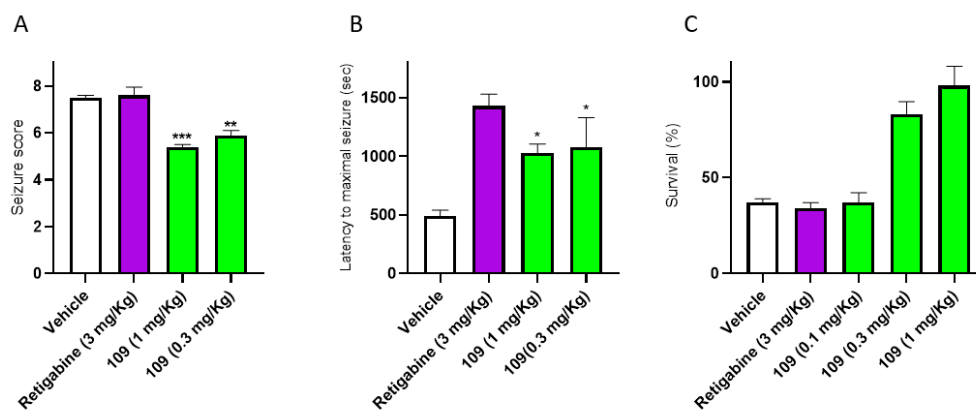
Figure 21. Data of *in vivo* studies on pentetrazol rat model. (A) indicates seizure score, (B) indicates latency to maximal seizure, and (C) depicts survival after the administration of the compound 109. Retigabine was used as reference. * $p < 0.05$, ** $p < 0.01$ and *** $p < 0.001$.

5.1 Conclusions

In this chapter it was reported the refinement of the retigabine binding site that allowed us to identify additional interaction sites and to develop rational design of a library of retigabine derivates. All the synthesized compounds were prior screened through fluorescence-based assays to evaluate the agonistic activity on K_{v7} channels. Subsequently, electrophysiological studies were performed to better understand the functional behavior of selected derivatives. The most active derivatives were further investigated to assess their photostability, considering chemical instability of retigabine. From these results it was found that compound **109** showed a remarkable potency and photostability compared to retigabine, over the lack of dimers formation involved in skin discoloration. For these reasons, additional studies were carried out to analyze pharmacokinetic properties and the *in vivo* anticonvulsant activity. **109** showed a metabolic profile comparable to retigabine with a brain accumulation 16 times higher than retigabine. In addition, the same compound was effective in reducing seizures score and the latency time to maximal seizures in a pentetrazol model at 1/10 dose than retigabine. Besides, a significant result is represented by the high survival rate of **109** (~90%), considering retigabine does not prevent death.

Hence, our results allowed to identify a potent and chemically stable K_{v7} channel activator with antiepilectic activity.

6.1 Experimental section
6.1.1 Chemistry

All reagents and solvents used were purchased from Sigma-Aldrich (Milan, Italy), unless otherwise stated. Reactions were carried out with magnetic stirring in round-bottomed flasks unless otherwise noted. Moisture-sensitive reactions were conducted in oven-dried glassware under nitrogen stream, using freshly distilled solvents. Pre-coated glass silica gel plates (F254, 0.25 mm, VWR International) were used for TLC analysis of reaction mixtures, while crude products were purified by an automated flash chromatography system (Isolera Spektra one, Biotage, Uppsala, Sweden) coupled with an APCI mass detector (Dalton 2000, Biotage), using pre-loaded silica gel cartridges (SNAP KP-Sil, Biotage). Continuous flow hydrogenation reactions were conducted using the H-cube hydrogenation reactor (ThalesNano, Budapest, Hungary) equipped with pre-loaded Pd/C 10% cartridges (30 mm, ThalesNano). NMR spectra were recorded on Varian Mercury 400 MHz and on a Bruker Avance 400 MHz and 300 MHz apparatus, at room temperature. Chemical shifts were reported in δ values (ppm) relative to internal Me_4Si, for ^1H and ^{13}C NMR, and $CClF_3$ for ^{19}F NMR. J values were reported in hertz (Hz). ^1H-NMR and ^{19}F NMR peaks were described using the following abbreviations: s (singlet), d (doublet), t (triplet) and m (multiplet). HR-MS spectra were recorded by LTQ-Orbitrap-XL-ETD mass spectrometer (Thermo Scientific, Bremen, Germany), equipped with an ESI source. Analytical RP-HPLC analysis of final products was performed to confirm ≥95% purity using the instrumentation and the UHPLC PDA conditions described below.

Analytical conditions

Purity assessment UHPLC runs were carried out on an EVO C18 150 × 2.1 mm × 2.6 μm (100 Å) column (Phenomenex, Bologna, Italy). The optimal mobile phase consisted of 0.1% $HCOOH/H_2O$ v/v (A) and 0.1 % HCOOH/ACN v/v (B). Analysis was performed in gradient elution as follows: 0-20.00 min, 5-95 % B; 20-25.00 min, 95-95 % B; 25-31.00 min, isocratic to 5 % B. Flow rate was 0.5 mL min^{-1}. Column oven temperature was set to 40 °C. Injection volume was 2 μL of sample. The following PDA parameters were applied: sampling rate, 12.5 Hz; detector time constant, 0.160 s; cell temperature, 40 °C. Data acquisition was set in the range 190-800 nm and chromatograms were monitored at 254 nm. Final compounds always showed a purity <95%.

HPLC/MS analysis

HPLC/MS analyses were conducted interfacing the UHPLC system described above with an IT-TOF hybrid mass spectrometer (ion trap-time of flight) equipped with an electrospray source (ESI) (Shimadzu, Kyoto, Japan). The LC−MS/MS data were processed by the LCMSsolution software (Version 3.50.346, Shimadzu). In detail, the analysis were conducted using a Kinetex EVO C18 150 × 2.1 mm (100 Å) column, having a 2.6 μm core−shell particulate (Phenomenex, Bologna, Italy). The flow of the mobile phases was set at 0.5 mL/min, and the oven temperature was set at 45 °C. The injection volume was 2 μL. The analysis were carried out employing as the mobile phase: (A) 10 mM $HCOONH_4$ in H_2O (pH = 6.3) and (B) ACN using the following elution gradient: 0.01−20.00 min, 5−95% B; 20.01−22.00 min, 95% isocratic B; and finally, 5 min for column re-equilibration. Data acquisition was set in the range of 190− 800 nm, and chromatograms were monitored at 254 and 550 nm. MS detection was operated in the positive ionization mode with the following parameters: 1.75 kV; CDL (curve desolvation line) temperature, 250 °C; block heater temperature, 250 °C; nebulizing gas flow (N_2), 1.5 L/min; drying gas pressure, 98 kPa. Full scan MS data were acquired in the range of 150−2000 m/z (ion accumulation time, 25 ms; IT, repeat = 3). MS/MS experiments were conducted in datadependent acquisition; precursor ions were acquired in the range 150− 2000 m/z; peak width, 3 Da; ion accumulation time, 50 ms; CID energy, 55%; collision gas, 50%; repeat = 1; execution trigger (BPC) intensity, at 70% stop level.

GC/MS analysis

GC/MS analysis was performed on a Shimadzu GC-2010 Plus gas chromatograph coupled to a 2010 Plus single quadrupole mass spectrometer (Shimadzu Corp., Kyoto, Japan). Chromatographic separation was carried out on an CP-Sil 8 CBfused silica capillary GC column (30 m × 0.25 mm i.d., 1.0 μm film thickness, Agilent, Santa Clara, CA). The operating conditions of GC were as follows: Helium (purity > 99.9999%) was used as carrier gas at a linear velocity of 39 cm/s, 2 μL of sample was injected in splitless mode via an autosampler (AOC-20s), and injector temperature (AOC-20i) was 280 °C. Oven temperature was programmed as follows: started from 100 °C (hold for 1 min) and increased to 320 °C at the rate of 6 °C/min (hold for 2 min). The mass spectrometer was operated in an electron-impact mode with 70 eV electrons. Interface and ion source temperatures were set at 320 and 200 °C, respectively. The quadrupoles were operated in the scan mode over the m/z range of 35−600 m/z with a solvent cut time of 2.9 min. The complete GC program duration was 40 min.

General procedures for I-III series

General procedure A: reductive amination reaction.

Reductive aminations were performed using 5-nitroindoline (**1**), 2-methyl-5-nitroindoline (**10**) or tert-butyl 5-nitroindoline-1-carboxylate (**10b**) as starting materials and commercially available aldehydes. Briefly, to a solution of the aldehyde (1.0 eq) in DCM:CH₃COOH (5:1 v/v) 2.0 equivalents of **1**, **10** or **10b** were added and the mixture was warmed to reflux for 1.5h. After addition of 1.8 equivalents of sodium triacetoxyborohydride the mixture was refluxed for further 3-5h. After cooling to room temperature, aqueous solution of NaOH (1N) was added. The organic layer was separated and further extracted with NaOH 1N. After drying over Na₂SO₄, the organic phase was concentrated in vacuo. Intermediates thus obtained were purified by flash chromatography using linear gradients of n-hexane/ethyl acetate as mobile phase.

General procedure B: Continuous flow hydrogenation.

Reduction of 5-nitroindoline and 5-nitroindole derivatives was achieved by continuous flow hydrogenation using the H-Cube hydrogenator and commercially available Pd/C 10% cartridges as catalyst. Starting material was dissolved in a mixture of THF/CH₃OH (1:1, v:v) at a final concentration of 0.1 M and was pumped at a flow rate of 1.0 mL/min. Temperature was set at 30 °C while the hydrogen inlet pressure was set at 10 bar. After completion, the reaction solution was evaporated *in vacuo* and the obtained products used in the following step without further purification.

General procedure C: Synthesis of sulfonamides.

Indolin-5-amino and 1H-indol-5-amino intermediates (1.0 eq) were dissolved in dry DCM under a nitrogen positive pressure. To this solution 1.2 equivalents of 1,5-diazabiciclo(5.4.0)undec-7-ene (DBU) were added. The reaction mixture was stirred at room temperature for 15 minutes, then 1.5 equivalents of the proper sulfonyl chloride were added. The mixture was stirred for further 2h. The reaction was then washed with a saturated solution of NaHCO₃ and brine. The organic phase was extracted, dried over anhydrous Na₂SO₄, filtered and concentrated *in vacuo*. Crude products were purified using a linear gradient of n-exane/ethyl acetate.

General procedure D: Synthesis of amides.

Indolin-5-amino and 1H-indol-5-amino intermediates (1.0 eq) were dissolved in dry DCM under a nitrogen positive pressure and added, under stirring, with 1.2 equivalents of N,N-Diisopropylethylamine (DIPEA). The mixture was cooled to 0 °C and added dropwise with a solution of the proper acyl chloride or acyl bromide (1.2 eq) in DCM. The solution was allowed to cool to room temperature and stirred for further 30 minutes. The reaction was then washed with a saturated solution of NaHCO$_3$ and brine. The organic phase was extracted, dried over anhydrous Na$_2$SO$_4$, filtered and concentrated in vacuo. Crude products were purified using a linear gradient of n-exane/ethyl acetate.

General procedure E: Synthesis of N-1 substitued 5-nitro indoline and 5-nitro-1H-indole derivatives.

The reactions were performed following the procedure described before.[80] Briefly, 5-nitroindoline (**1**) or 5-nitro-1H-indole (**20**) (1.0 eq) were dissolved in dry DCM/DMF (2/1 v/v) under stirring, at 0 °C. To this solution, 1.2 equivalents of NaH were added portionwise and the mixture stirred for 30 min at 0 °C. Then, a solution of of the proper alkyl halide (1.2 eq) in dry DCM was added dropwise. The mixture was warmed to room temperature and stirred for 12 h. After quenching by 10% aqueous solution of citric acid and washing with brine, the organic layer was separated, dried over anhydrous Na$_2$SO$_4$ and evaporated in vacuo. Crude products were purified by flash chromatography coupled to mass spectrometry, using a linear gradient of n-exane/ethyl acetate.

General procedures for IV series

General procedure A: N-acylation.

Starting material (1.0 eq) was dissolved in THF under magnetic stirring at room temperature. To this solution DIPEA (1.2 eq) and the proper acyl chloride (1.2 eq) were added and the mixture was stirred at room temperature for 1 hour. The reaction, then, was washed with water (3 x 20 mL), 10% aqueous solution of citric acid (3 x 20 mL) and saturated aqueous solution of sodium bicarbonate (3 x 20 mL). The combined organic layer was dried over anhydrous sodium sulfate, filtered, concentrated under vacuum and purified by flash chromatography using a linear gradient of n-exane/ethyl acetate.

General procedure B: N-acylation.

Starting material (1.0 eq), DBU (2 eq) and the proper acyl halide (2 eq) were dissolved in THF and the reaction mixture was heated to 140 °C for 60 min in a microwave reactor. The resulting mixture was then concentrated in vacuo, reconstituted in DCM and washed with a solution of K_2CO_3 and brine. The organic phase was extracted, dried over anhydrous Na_2SO_4, filtered and concentrated in vacuo. Crude products thus obtained were purified using a linear gradient of n-exane/ethyl acetate.

General procedure C: N-alkylation.

To a solution of the proper compound (1.0 eq) in DMF, 1.2 equivalents of the proper substituted benzyl bromide and 1.2 equivalents of DIPEA were added. The reaction mixture was refluxed under stirring for 3 hours. The resulting solution was then washed with a solution of K_2CO_3 and brine. The organic phase was extracted, dried over anhydrous Na_2SO_4, filtered and concentrated in vacuo. Crude product was purified using a linear gradient of n-exane/ethyl acetate.

General procedure D: Synthesis of N-protected derivatives (carbamates).

The proper amines (1.0 eq) were dissolved in THF, then benzyl chloroformate (1.2 eq) DIPEA (1.2 eq) or with Boc anhydride (1.2 eq) and TEA (1.2 eq) were added to obtain the N-Cbz or N-Boc protected derivatives, respectively. The reaction mixtures were stirred at room temperature till reaction completion (30-60 minutes) to give the corresponding N-protected intermediates. Afterward, the reaction mixture was evaporated to dryness, reconstituted in DCM, washed with K_2CO_3, dried over anhydrous Na_2SO_4, filtered and concentrated in vacuo. Crude products were purified by flash chromatography using a gradient of n-exane/ethyl acetate as mobile phase to furnish the corresponding N-protected derivatives.

General procedure E: Catalytic hydrogenation.

To a solution of starting material (1.0 eq) in THF/MeOH (1:1 v:v), ammonium formate (10 eq) and Pd/C (6% mol) were added. The reaction mixture was refluxed at 100°C for 1 hour. After completion, the reaction solution was filtered through Celite 503 (Merck Millipore, Burlington, USA), evaporated in vacuo, reconstituted with DCM and washed with a saturated aqueous solution of sodium bicarbonate (3 x 20 mL). The resulting intermediates were used in the following step without further purification, while final products obtained with this procedure were purified by flash chromatography.

General procedure F: Boc removal.

N-Boc protected compounds (1.0 eq) were dissolved in a mixture of DCM/TFA (3:1 v:v) and added with catalytic amounts of triethylsilane as radical scavenger. The resulting mixtures were stirred at room temperature till reaction completion, as evidenced by TLC. Then, the solution was diluted with DCM, quenched with a solution of K_2CO_3 and washed (3 x 20 mL). Organic layer was separated, dried over anhydrous Na_2SO_4, filtered, and evaporated in vacuo. Crude products were used in the in the following step without further purification. Instead, final products obtained with this procedure were purified by flash chromatography.

General procedure G: Reductive amination.

Starting compounds (1.0 eq) were dissolved in MeOH at room temperature. To this solution an amount of 1.2 equivalents of the proper aldehyde and TFA (1.0 eq) were added and the mixture was warmed to reflux for 3 h. Afterwards the reaction was cooled to 0°C and added with 3 equivalents of $NaBH_4$. After stirring for 20 minutes the solution was concentrated in vacuo and reconstituted in DCM, washed with a solution of K_2CO_3 and brine and dried over Na_2SO_4. Then, the organic phase was filtered, concentrated in vacuo purified using linear gradients of n-hexane/ethyl acetate as mobile phase.

General procedure H: one pot NO_2 reduction and selective acylation.

Starting compounds (1.0 eq) were dissolved in methanol and added with zinc powder (5 eq) and NH_4Cl (5 eq). The mixture was stirred at room temperature until disappearance of starting material assessed by TLC. Then different acyl halides (1.2 eq) and DIPEA (1.2 eq) were added and the reaction stirred at room temperature for further 45 minutes. The resulting mixture was concentrated under vacuum, reconstituted in DCM and extracted with an aqueous solution of K_2CO_3 and brine. The organic phase was separated, dried over Na_2SO_4, filtered, and concentrated in vacuo. The crude products were purified using linear gradients of n-hexane/ethyl acetate as mobile phase.

1-(4-fluorobenzyl)-5-nitroindoline (2).

Synthesized according to the general procedure A using 5-nitroindoline (**1**) and 4-fluorobenzaldehyde as reagents. Intermediate **2** was isolated as a yellow powder in 65% yield. ^{1}H NMR (CDCl$_3$, 400 MHz): δ: 3.12 (t, 2H, CH$_2$, J = 8.6 Hz); 3.63 (t, 2H, CH$_2$, J = 8.6 Hz); 4.42 (s, 2H, CH$_2$); 6.37 (d, 1H, aryl, J = 8.1 Hz); 7.04-7.09 (m, 2H, aryl); 7.24-7.28 (m, 2H,

aryl); 7.94 (s, 1H, aryl); 8.08 (d, 1H, aryl, J = 7.8 Hz). HR-MS m/z: calcd for $C_{19}H_{14}FN_2O_2$, $[(M+H)^+]$: 273.1034; found 273.1039.

1-(4-fluorobenzyl)indolin-5-amine (3).

Synthesized from intermediate **2** according to the general procedure B. The product was obtained as a grey powder in 98% yield. ^1H NMR (CDCl$_3$, 400 MHz): δ: 2.98 (t, 2H, CH$_2$, J = 8.7 Hz); 3.18 (t, 2H, CH$_2$, J = 8.7 Hz); 3.35 (bs, 2H, NH$_2$); 4.12 (s, 2H, CH$_2$); 6.38 (d, 1H, aryl, J = 8.1 Hz); 6.47 (d, 1H, aryl, J = 8.2 Hz); 6.60 (s, 1H, aryl); 6.99-7.07 (m, 2H, aryl); 7.34-7.39 (m, 2H, aryl). HR-MS m/z: calcd for $C_{15}H_{16}FN_2$, $[(M+H)^+]$: 243.1292; found 243.1301.

Ethyl (1-(4-fluorobenzyl)indolin-5-yl)carbamate (4a).

Intermediate **3** (1.0 eq) was dissolved in dry THF and stirred under nitrogen positive pressure. The solution was added with 1.1 equivalents of NaHCO$_3$ and the resulting suspension was cooled to 0°C in ice bath. To this suspension, 1.1 equivalents of ethyl chloroformate were added and the slurry was stirred at 0°C for further 30 minutes. After warming at room temperature, an equal volume of water was added, and the solution was extracted three times with ethyl acetate. Organic phases were dried over anhydrous Na$_2$SO$_4$, filtered and concentrated *in vacuo*. Final product was isolated as a white crystal in 72% yield and crystallized from n-hexane/diethyl ether. ^1H NMR (CDCl$_3$, 400 MHz): δ: 1.32 (t, 3H, CH$_3$, J = 7.1 Hz); 2.97 (t, 2H, CH$_2$, J = 8.2 Hz); 3.29 (t, 2H, CH$_2$, J = 8.2 Hz); 4.19-4.25 (m, 4H, CH$_2$); 6.37 (bs, 1H, NH); 6.45 (d, 1H, aryl, J = 8.3 Hz); 6.95 (d, 1H, aryl, J = 7.7 Hz); 7.04 (t, 2H, aryl, J = 8.4 Hz); 7.22 (bs, 1H, aryl); 7.32-7.36 (m, 2H, aryl). ^{13}C NMR (CDCl$_3$, 100 MHz) δ: 14.6; 28.6; 53.5; 53.9; 61.0; 107.0; 115.2; 115.4; 118.8; 119.3; 129.4; 131.0; 134.0; 149.3; 160.8; 163.3. ^{19}F NMR (CDCl$_3$, 376.3 MHz) δ: -(115.89-115.80) (m, 1F, CF). HR-MS m/z: calcd for $C_{18}H_{20}FN_2O_2$, $[(M+H)^+]$: 315.1503; found 315.1514.

(1S,2R,5S)-2-isopropyl-5-methylcyclohexyl(1-(4-fluorobenzyl)indolin-5-yl)carbamate (4b).

Final product **4b** was synthesized according to the same procedure described above for **4a**, using the commercially available (1S)-(+)-menthyl chloroformate as reagent. The product was obtained as a white wax in 63% yield. $[\alpha]^{25}_D$: 32.67 ± 0.04 (c = 0.15, MeOH). Final product **4b** was synthesized according to the same procedure described above for **4a**, using the commercially available (1S)-(+)-menthyl chloroformate as reagent. The product was obtained as a white wax in 63% yield. $[\alpha]^{25}_D$: 32.67 ± 0.04 (c = 0.15, MeOH). ^1H NMR (CDCl$_3$, 400

MHz): δ: 0.83 (d, 3H, CH$_3$, J = 7.0 Hz); 0.93 (d, 6H, CH$_3$, J = 7.1 Hz); 0.99-1.16 (m, 2H, CH$_2$); 1.27-1.41 (m, 1H, CH$_2$); 1.49-1.56 (m, 1H, CH); 1.67-1.74 (m, 2H, CH$_2$); 1.94-2.02 (m, 1H, CH); 2.09-2.16 (m, 1H, CH$_2$); 2.96 (t, 2H, CH$_2$, J = 8.4 Hz); 3.27 (t, 2H, CH$_2$, J = 8.4 Hz); 4.18 (s, 2H, CH$_2$); 4.61-4.70 (m, 1H, CH); 6.35 (bs, 1H, NH); 6.42 (d, 1H, aryl, J = 8.5 Hz); 6.95 (d, 1H, aryl, J = 8.2 Hz); 7.03 (t, 2H, aryl, J = 8.7 Hz); 7.25 (bs, 1H, aryl); 7.31-7.36 (m, 2H, aryl). ^{13}C NMR (CDCl$_3$, 100 MHz) δ: 16.5; 20.8; 22.1; 23.6; 26.3; 28.6; 31.4; 34.3; 41.5; 47.4; 53.5; 53.9; 74.8; 107.1; 115.2; 115.4; 117.4; 118.9; 129.1; 129.4; 129.5; 131.0; 134.0; 154.0; 160.8; 163.3. ^{19}F NMR (CDCl$_3$, 376.3 MHz) δ: -(115.82-115.74) (m, 1F, CF). HR-MS m/z: calcd for C$_{26}$H$_{34}$FN$_2$O$_2$, [(M+H)$^+$]: 425.2599; found 425.2608.

1-(1-(4-fluorobenzyl)indolin-5-yl)-3-neopentylurea (5a).

Triphosgene (1.0 eq) was dissolved in dry DCM, under nitrogen stream at 0 °C. To the resulting mixture, a solution of 1.25 equivalents of 1-(4-fluorobenzyl)indolin-5-amine (**3**) and 2.6 equivalents of DIPEA dissolved in DCM were added dropwise in 5 minutes. The solution was maintained under stirring for further 5 minutes. Then, a solution of 2,2-dimethylpropan-1-amine (2.5 eq) and DIPEA (2.6 eq) in DCM was added dropwise. The reaction mixture was allowed to warm at room temperature, maintained under stirring overnight and quenched by adding an equal volume of water. The organic phase was washed with a saturated solution of NaHCO$_3$ and then with brine, before being dried over anhydrous Na$_2$SO$_4$, filtered and evaporated to dryness. The crude product was isolated as white crystal in 69% yield and crystallized from ethyl acetate. ^{1}H NMR (CDCl$_3$, 400 MHz): δ: 0.89 (s, 9H, 3 CH$_3$); 2.99 (t, 2H, CH$_2$, J = 8.3 Hz); 3.05 (d, 2H, CH$_2$, J = 6.3 Hz); 3.35 (t, 2H, CH$_2$, J = 8.3 Hz); 4.23 (s, 2H, CH$_2$); 4.71 (t, 1H, NH, J = 5.6 Hz); 5.98 (s, 1H, NH); 6.45 (d, 1H, aryl, J = 8.2 Hz); 6.92 (d, 1H, aryl, J = 8.2 Hz); 7.02-7.07 (m, 3H, aryl); 7.32-7.35 (m, 2H, aryl). ^{13}C NMR (CDCl$_3$, 100 MHz) δ: 27.2; 28.4; 32.2; 51.4; 53.0; 53.7; 107.1; 115.3; 115.5; 122.8; 125.0; 127.7; 129.40; 129.45; 131.5; 133.7; 150.9; 157.5; 160.9; 163.3 ^{19}F NMR (CDCl$_3$, 376.3 MHz) δ: -(115.55-115.34) (m, 1F, CF). HR-MS m/z: calcd for C$_{21}$H$_{27}$FN$_3$O, [(M+H)$^+$]: 356.2133; found 356.2148.

1-cyclohexyl-3-(1-(4-fluorobenzyl)indolin-5-yl)urea (5b).

Final product **5b** was synthesized as described above for **5a**, using cyclohexylamine in place of 2,2-dimethylpropan-1-amine. Final product was obtained as a white crystal in 57% yield and crystallized from methanol. ^{1}H NMR (DMSO-d6, 400 MHz): δ: 1.08-1.34 (m, 5H, CH$_2$ and CH); 1.52-1.55 (m, 1H, CH); 1.63-1.67 (m, 2H, CH$_2$); 1.77-1.80 (m, 2H, CH$_2$); 2.82 (t, 2H,

CH$_2$, J = 8.2 Hz); 3.14 (t, 2H, CH$_2$, J = 8.2 Hz); 3.39-3.43 (m, 1H, CH); 4.16 (s, 2H, CH$_2$); 5.85 (d, 1H, NH, J = 7.9 Hz); 6.47 (d, 1H, aryl, J = 8.4 Hz); 6.90 (d, 1H, aryl, J = 8.4 Hz); 7.14-7.19 (m, 3H, aryl); 7.37-7.41 (m, 2H, aryl); 7.86 (s, 1H, NH). ^{13}C NMR (DMSO-d6, 100 MHz) δ: 24.9; 25.8; 28.7; 33.6; 48.0; 53.3; 53.8; 107.0; 115.4; 115.6; 116.6; 117.7; 130.4; 130.5; 132.1; 135.1; 147.6; 155.3; 160.5; 162.9. ^{19}F NMR (DMSO-d6, 376.3 MHz) δ: -(116.04-115.96) (m, 1F, CF). HR-MS m/z: calcd for C$_{22}$H$_{27}$FN$_3$O, [(M+H)$^+$]: 368.2133; found 368.2139.

1-(1-(4-fluorobenzyl)indolin-5-yl)-3-neopentylthiourea (6).

Starting from 1-(4-fluorobenzyl)indolin-5-amine (**3**), final compound **6** was obtained via isothiocyanate intermediate, followed by reaction with 2,2-dimethylpropan-1-amine slightly modifying a previously described procedure.[191] In our procedure, the use of benzene as solvent was avoided by replacing with dry toluene for the synthesis of the isothiocyanate intermediate, and dry DCM for the conversion of the isothiocyanate to thiourea. The final product was obtained as a grey powder in 54% yield and was crystallized form ethyl acetate. ^{1}H NMR (CDCl$_3$, 400 MHz): δ: 0.89 (s, 9H, CH$_3$); 2.99 (t, 2H, CH$_2$, J = 8.4 Hz); 3.39 (t, 2H, CH$_2$, J = 8.4 Hz); 3.48 (d, 2H, CH$_2$, J = 5.8 Hz); 4.25 (s, 2H, CH$_2$); 5.93 (t, 1H, NH, J = 7.4 Hz); 6.46 (d, 1H, aryl, J = 8.1 Hz); 6.90 (d, 2H, aryl, J = 9.4 Hz); 7.01-7.07 (m, 2H, aryl); 7.29-7.33 (m, 2H, aryl); 7.58 (s, 1H, NH). ^{13}C NMR (CDCl$_3$, 100 MHz) δ: 27.4; 28.2; 32.2; 52.5; 53.4; 56.4; 107.0; 115.3; 115.6; 123.3; 125.2; 126.1; 129.3; 132.0; 133.3; 152.1; 160.5; 163.7; 181.7. ^{19}F NMR (CDCl$_3$, 376.3 MHz) δ: -(115.25-115.18) (m, 1F, CF). HR-MS m/z: calcd for C$_{21}$H$_{27}$FN$_3$S, [(M+H)$^+$]: 372.1904; found 372.1911.

1-(1-(4-fluorobenzyl)indolin-5-yl)-3-neopentylguanidine (7).

Final compound **7** was obtained from **6** via carbodiimide intermediate followed by reaction with 2,2-dimethylpropan-1-amine, using the procedure described by Plsikova *et al.*[192] The final product was obtained as white crystal in 40% yield and crystallized from methanol. ^{1}H NMR (CDCl$_3$, 400 MHz): δ: 0.97 (s, 9H, 3 CH$_3$); 2.93 (t, 2H, CH$_2$, J = 8.1 Hz); 2.99 (s, 2H, CH$_2$); 3.25 (t, 2H, CH$_2$, J = 8.1 Hz); 4.18 (s, 2H, CH$_2$); 6.47 (d, 1H, aryl, J = 8.1 Hz); 6.67 (d, 1H, aryl, J = 7.8 Hz); 6.77 (s, 1H, aryl); 7.04 (t, 2H, aryl, J = 8.5 Hz); 7.34-7.37 (m, 2H, aryl). ^{13}C NMR (CDCl$_3$, 100 MHz) δ: 27.3; 28.7; 53.5; 53.9; 54.1; 107.9; 115.1; 115.4; 120.8; 122.1; 129.5; 129.6; 131.5; 134.3; 148.5; 160.8; 163.2. ^{19}F NMR (CDCl$_3$, 376.3 MHz) δ:-(115.86-115.78) (m, 1F, CF). HR-MS m/z: calcd for C$_{21}$H$_{28}$FN$_4$, [(M+H)$^+$]: 355.2293; found 355.2300.

N-(1-(4-fluorobenzyl)indolin-5-yl)cyclohexanesulfonamide (8a).

Final product **8a** was obtained from 1-(4-fluorobenzyl)indolin-5-amine (**3**) and cyclohexanesulfonyl chloride following the general procedure C. The product was isolated in 67% yield as a grey powder that crystallizes from n-hexane/diethyl ether. ^{1}H NMR (CDCl$_3$, 400 MHz): δ: 1.10-1.21 (m, 3H, CH$_2$ and CH); 1.47-1.60 (m, 3H, CH$_2$ and CH); 1.80-1.82 (m, 2H, CH$_2$); 2.08-2.11 (m, 2H, CH$_2$); 2.83-2.91 (m, 3H, CH$_2$ and CH); 3.25 (t, 2H, CH$_2$, J = 8.3 Hz); 4.12 (s, 2H, CH$_2$); 5.96 (s, 1H, NH); 6.31 (d, 1H, aryl, J = 8.2 Hz); 6.81 (d, 1H, aryl, J = 8.3 Hz); 6.93-6.98 (m, 3H, aryl); 7.22-7.25 (m, 2H, aryl). ^{13}C NMR (CDCl$_3$, 100 MHz) δ: 25.1; 26.4; 28.4; 53.0; 53.7; 59.3; 106.9; 115.3; 115.5; 121.4; 123.3; 126.5; 129.3; 129.4; 131.4; 133.7; 151.0; 160.9; 163.33. ^{19}F NMR (CDCl$_3$, 376.3 MHz) δ: -(114.71-114.63) (m, 1F, CF). HR-MS m/z: calcd for C$_{21}$H$_{26}$FN$_2$O$_2$S, [(M+H)$^+$]: 389.1694; found 389.1699; [(M+Na)$^+$]: 411.1513; found 411.1520.

N-(1-(4-fluorobenzyl)indolin-5-yl)benzenesulfonamide (8b).

Final product **8b** was obtained from 1-(4-fluorobenzyl)indolin-5-amine (**3**) and benzenesulfonyl chloride following the general procedure C. The product was isolated in 70% yield as a grey powder that crystallizes from n-hexane/ethyl acetate. ^{1}H NMR (CDCl$_3$, 400 MHz): δ: 2.92 (t, 2H, CH$_2$, J = 8.0 Hz); 3.31 (t, 2H, CH$_2$, J = 8.0 Hz); 4.18 (s, 2H, CH$_2$); 6.20 (s, s, 1H, NH); 6.29 (d, 1H, aryl, J = 8.2 Hz); 6.61 (d, 1H, aryl, J = 6.8 Hz); 6.87 (s, 1H, aryl); 7.03 (t, 2H, aryl, J = 8.4 Hz); 7.28-7.31 (m, 3H, aryl); 7.46 (t, 2H, aryl, J = 7.3 Hz); 7.56 (t, 1H, aryl, J = 7.1 Hz); 7.74 (d, 2H, aryl, J = 7.4 Hz). ^{13}C NMR (CDCl$_3$, 100 MHz) δ: 28.2; 52.8; 53.6; 106.6; 115.3; 115.5; 122.6; 124.7; 125.7; 127.4; 128.8; 129.3; 129.4; 131.1; 132.6; 133.6; 139.4; 151.4; 160.9; 163.3. ^{19}F NMR (CDCl$_3$, 376.3 MHz) δ: -(115.53-115.46) (m, 1F, CF). HR-MS m/z: calcd for C$_{21}$H$_{20}$FN$_2$O$_2$S, [(M+H)$^+$]: 383.1224; found 383.1230.

N-(1-(4-fluorobenzyl)indolin-5-yl)butane-1-sulfonamide (8c).

Final product **8c** was obtained from 1-(4-fluorobenzyl)indolin-5-amine (**3**) and butanesulfonyl chloride following the general procedure C. The product was isolated in 72% yield as an off-white powder that crystallizes from n-hexane/diethyl ether. ^{1}H NMR (CDCl$_3$, 400 MHz): δ: 0.94 (t, 3H, CH$_3$, J = 7.3 Hz); 1.38-1.49 (m, 2H, CH$_2$); 1.78-1.88 (m, 2H, CH$_2$); 2.95-3.06 (m, 4H, 2 CH$_2$); 3.34 (t, 2H, CH$_2$, J = 7.9 Hz); 4.21 (s, 2H, CH$_2$); 6.28 (s, 1H, NH); 6.40 (d, 1H, aryl, J = 8.2 Hz); 6.91 (d, 1H, aryl, J = 8.1 Hz); 7.02-7.07 (m, 3H, aryl); 7.30-7.35 (m, 2H, aryl). ^{13}C NMR (CDCl$_3$, 100 MHz) δ: 13.6; 21.5; 25.5; 28.3; 50.6; 52.9; 53.7; 106.9; 115.3; 115.5; 121.7; 123.7; 126.2; 129.3; 129.4; 131.5; 133.6; 151.2; 160.5; 163.7. ^{19}F NMR (CDCl$_3$, 376.3

MHz) δ: -(113.51-113.43) (m, 1F, CF). HR-MS m/z: calcd for $C_{19}H_{24}FN_2O_2S$, $[(M+H)^+]$: 363.1537; found 363.1545.

N-(1-(4-fluorobenzyl)indolin-5-yl)-2-methylpropane-1-sulfonamide (8d).

Final product **8d** was obtained from 1-(4-fluorobenzyl)indolin-5-amine (**3**) and 2-methylpropane-1-sulfonyl chloride following the general procedure C. The product was isolated in 71% yield as an off-white powder that crystallizes from n-hexane/diethyl ether. ^1H NMR (CDCl$_3$, 400 MHz): δ: 1.08 (d, 6H, CH$_3$, J = 6.6 Hz); 2.26-2.31 (m, 1H, CH); 2.90 (d, 2H, CH$_2$ J = 6.3 Hz); 2.96 (t, 2H, CH$_2$, J = 8.2 Hz); 3.32 (t, 2H, CH$_2$, J = 8.2 Hz); 4.19 (s, 2H, CH$_2$); 6.18 (s, 1H, NH); 6.38 (d, 1H, aryl, J = 7.8 Hz); 6.88 (d, 1H, aryl, J = 7.4 Hz); 7.00-7.04 (m, 3H, aryl); 7.29-7.32 (m, 2H, aryl). ^{13}C NMR (CDCl$_3$, 100 MHz) δ: 21.3; 24.6; 27.6; 48.5; 53.9; 58.6; 58.8; 115.6; 115.8; 116.5; 118.7; 119.2; 126.5; 132.7; 132.8; 136.4; 136.7; 139.6; 162.4; 164.9. ^{19}F NMR (CDCl$_3$, 376.3 MHz) δ: -(114.75-114.68) (m, 1F, CF). HR-MS m/z: calcd for $C_{19}H_{24}FN_2O_2S$, $[(M+H)^+]$: 363.1537; found 363.1545.

N-(1-(4-fluorobenzyl)indolin-5-yl)hexane-1-sulfonamide (8e).

Final product **8e** was obtained from 1-(4-fluorobenzyl)indolin-5-amine (**3**) and hexanesulfonyl chloride following the general procedure C. The product was isolated in 67% yield as a grey powder that crystallizes from ethyl acetate. ^1H NMR (CD$_3$OD, 400 MHz): δ: 0.91 (t, 3H, CH$_3$, J = 7.9 Hz); 1.28-1.34 (m, 4H, CH$_2$); 1.36-1.46 (m, 2H, CH$_2$); 1.75-1.82 (m, 2H, CH$_2$); 3.13-3.18 (m, 4H, 2 CH$_2$); 3.91 (t, 2H, CH$_2$, J = 8.2 Hz); 4.70 (s, 2H, CH$_2$); 7.18-7.27 (m, 3H, aryl); 7.33-7.35 (m, 2H, aryl); 7.49-7.52 (m, 2H, aryl). ^{13}C NMR (CD$_3$OD, 100 MHz) δ: 12.9; 22.0; 23.2; 27.6; 31.0; 51.1; 53.4; 53.9; 58.9; 115.8; 116.3; 118.9; 119.3; 126.1; 133.0; 135.7; 137.0; 140.2; 162.5; 165.0. ^{19}F NMR (CDCl$_3$, 376.3 MHz) δ: -(113.17-113.10) (m, 1F, CF). HR-MS m/z: calcd for $C_{21}H_{28}FN_2O_2S$, $[(M+H)^+]$: 391.1850; found 391.1862.

1-((1S,4R)-7,7-dimethyl-2-oxobicyclo[2.2.1]heptan-1-yl)-N-(1-(4-fluorobenzyl)indolin-5-yl)methanesulfonamide (8f).

Final product **8f** was obtained from 1-(4-fluorobenzyl)indolin-5-amine (**3**) and (1S)-(+)-10-camphorsulfonyl chloride following the general procedure C. The product was isolated in 57% yield as a grey powder that crystallizes from n-hexane/ethyl acetate. $[α]^{25}_D$: 37.50 ± 0.05 (c = 0.12, MeOH). ^1H NMR (CDCl$_3$, 400 MHz): δ: 0.92 (s, 3H, CH$_3$); 0.99 (s, 3H, CH$_3$); 1.47-1.52 (m, 1H, CH); 1.98-2.20 (m, 4H, CH$_2$ and 2 CH); 2.44-2.51 (m, 1H, CH); 2.81 (d, 1H, CH·, J = 15.3 Hz); 2.98 (t, 2H, CH$_2$, J = 8.3 Hz); 3.28-3.36 (m, 4H, 2 CH$_2$); 3.44 (d, 1H, CH, J = 15.2

Hz); 4.21 (s, 2H, CH$_2$); 6.41 (d, 1H, aryl, J = 8.3 Hz); 6.94 (d, 1H, aryl, J = 8.3 Hz); 7.04 (t, 2H, aryl J = 8.7 Hz); 7.10 (s, 1H, aryl); 7.31-7.35 (m, 2H, aryl); 7.45 (s, 1H, NH). ^{13}C NMR (CDCl$_3$, 100 MHz) δ: 19.4; 19.9; 27.1; 27.8; 28.4; 42.9; 43.1; 48.1; 49.1; 53.0; 53.7; 59.8; 106.8; 115.3; 115.5; 121.9; 123.5; 127.7; 129.3; 129.4; 131.3; 133.8; 151.1; 160.9; 163.3; 217.5. ^{19}F NMR (CDCl$_3$, 376.3 MHz) δ: -(115.58-115.50) (m, 1F, CF). HR-MS m/z: calcd for C$_{25}$H$_{30}$FN$_2$O$_3$S, [(M+H)$^+$]: 457.1986; found 457.2001.

1-((1R,4S)-7,7-dimethyl-2-oxobicyclo[2.2.1]heptan-1-yl)-N-(1-(4-fluorobenzyl)indolin-5-yl)methanesulfonamide (8g).

Final product **8g** was obtained from 1-(4-fluorobenzyl)indolin-5-amine (**3**) and (1R)-(−)-10-camphorsulfonyl chloride following the general procedure C. The product was isolated in 50% yield as a grey powder that crystallizes from n-hexane/ethyl acetate. [α]^{25}$_D$: -38.10 ± 0.06 (c = 0.12, MeOH). ^{1}H NMR (CDCl$_3$, 300 MHz): δ : 0.92 (s, 3H, CH$_3$); 0.98 (s, 3H, CH$_3$); 1.47-1.52 (m, 1H, CH); 1.97-2.22 (m, 5H, 2 CH$_2$ and CH); 2.44-2.52 (m, 1H, CH); 2.80 (d, 1H, CH, J = 15.6 Hz); 2.97 (t, 2H, CH$_2$, J = 8.6 Hz); 3.32 (t, 2H, CH$_2$, J = 8.6 Hz); 3.43 (d, 1H, CH, J = 16.0 Hz); 4.21 (s, 2H, CH$_2$); 6.41 (d, 1H, aryl, J = 8.4 Hz); 6.93 (d, 1H, aryl, J = 8.4 Hz); 7.01-7.10 (m, 3H, aryl); 7.30-7.35 (m, 2H, aryl); 7.47 (s, 1H, NH). ^{13}C NMR (CDCl$_3$, 75 MHz) δ: 19.4; 20.0; 27.1; 27.7; 28.4; 42.9; 43.1; 48.1; 49.1; 53.0; 53.7; 59.8; 106.8; 115.3; 115.56; 121.8; 123.5; 127.7; 129.40; 129.44; 131.3; 133.8; 151.1; 160.9; 163.3; 217.5. ^{19}F NMR (CDCl$_3$, 376.3 MHz) δ: -(115.89-115.82) (m, 1F, CF). HR-MS m/z: calcd for C$_{25}$H$_{30}$FN$_2$O$_3$S, [(M+H)$^+$]: 457.1986; found 457.1995.

N-(1-(4-fluorobenzyl)indolin-5-yl)azepane-1-sulfonamide (8h).

Final product **8h** was obtained from 1-(4-fluorobenzyl)indolin-5-amine (**3**) and azepane-1-sulfonyl chloride following the general procedure C. The product was isolated in 69% yield as an off-white powder that crystallizes from n-hexane/diethyl ether. ^{1}H NMR (CDCl$_3$, 400 MHz): δ: 1.56-1.59 (m, 4H, 2 CH$_2$); 1.68-1.70 (m, 4H, 2 CH$_2$); 2.97 (t, 2H, CH$_2$, J = 8.3 Hz); 3.29-3.34 (m, 6H, 3 CH$_2$); 4.21 (s, 2H, CH$_2$); 6.27 (s, 1H, NH); 6.41 (d, 1H, aryl, J = 8.3 Hz); 6.90 (d, 1H, aryl, J = 8.2 Hz); 7.02-7.06 (m, 3H, aryl); 7.31-7.34 (m, 2H, aryl). ^{13}C NMR (CDCl$_3$, 100 MHz) δ: 26.9; 28.4; 29.1; 48.9; 53.1; 53.7; 106.8; 115.2; 115.5; 121.4; 123.5; 127.4; 129.4; 129.5; 131.1; 133.8; 150.8; 160.9; 163.3. ^{19}F NMR (CDCl$_3$, 376.3 MHz) δ: -(115.58-115.51) (m, 1F, CF). HR-MS m/z: calcd for C$_{21}$H$_{27}$FN$_3$O$_2$S, [(M+H)$^+$]: 404.1803; found 404.1876.

N-(1-(4-fluorobenzyl)indolin-5-yl)-3,5-dimethylpiperidine-1-sulfonamide (8i).

Final product **8i** was obtained as a conformers mixture (A:B, 4:1) from 1-(4-fluorobenzyl)indolin-5-amine **(3)** and 3,5-dimethylpiperidine-1-sulfonyl chloride following the general procedure C. The product was isolated in 65% yield as an off-white powder that crystallizes from ethyl acetate. ^{1}H NMR (CD$_3$OD, 400 MHz): δ: **(A)** = 0.60-0.69 (m, 1H, CH); 0.88 (s, 3H, CH$_3$); 0.90 (s, 3H, CH$_3$); 1.56-1.60 (m, 2H, CH$_2$,); 1.75 (d, 2H, CH$_2$, J = 12.9 Hz); 2.24 (t, 2H, CH$_2$, J = 11.7 Hz); 3.12 (bs, 2H, CH$_2$); 3.66-3.69 (m, 2H, CH$_2$); 3.86 (bs, 2H, CH$_2$); 4.66 (s, 2H, CH$_2$); 7.17-7.24 (m, 5H, aryl); 7.46-7.49 (m, 2H, aryl). **(B)** = 0.88 (s, 3H, CH$_3$); 0.90 (s, 3H, CH$_3$); 1.37 (t, 2H, CH$_2$, J = 5.7 Hz); 1.75 (d, 2H, CH$_2$, J = 12.9 Hz); 1.89-1.91 (m, 2H, CH$_2$); 2.83-2.88 (m, 2H, CH$_2$); 3.12 (bs, 2H, CH$_2$); 3.22-3.26 (m, 2H, CH$_2$); 3.86 (bs, 2H, CH$_2$); 4.66 (s, 2H, CH$_2$); 7.17-7.24 (m, 5H, aryl); 7.46-7.49 (m, 2H, aryl). ^{13}C NMR (CD$_3$OD, 100 MHz) δ: **(A + B)** = 17.2; 17.8; 26.7; 27.6; 30.8; 38.0; 41.3; 52.4; 52.6; 53.9; 58.7; 58.8; 115.6; 115.8; 118.4; 118.8; 132.8; 132.9; 136.5; 162.5; 164.9. ^{19}F NMR (CDCl$_3$, 376.3 MHz) δ: -(116.04-116.12) (m, 1F, CF). HR-MS m/z: calcd for C$_{22}$H$_{29}$FN$_3$O$_2$S, [(M+H)$^{+}$]: 418.1959; found 418.1964.

N-(1-(4-fluorobenzyl)indolin-5-yl)acetamide (9a).

Final product **9a** was obtained from 1-(4-fluorobenzyl)indolin-5-amine **(3)** and acetyl chloride following the general procedure D. The product was isolated in 84% yield as a white powder that crystallizes from n-hexane/diethyl ether. ^{1}H NMR (CD$_3$OD, 400 MHz): δ: 2.09 (s, 3H, C*H$_3$*); 2.91 (t, 2H, C*H$_2$*, *J* = 8.2 Hz); 3.24 (t, 2H, CH$_2$, J = 8.2 Hz); 4.20 (s, 2H, CH$_2$); 6.50 (d, 1H, aryl, J = 8.4 Hz); 7.04-7.12 (m, 3H, aryl); 7.27 (s, 1H, aryl); 7.37-7.40 (m, 2H, aryl). ^{13}C NMR (CD$_3$OD, 100 MHz) δ: 22.2; 28.0; 52.9; 53.5; 106.8; 114.6; 114.8; 118.0; 119.9; 129.3; 129.5; 130.5; 134.32; 134.35; 149.5; 160.9; 163.3; 169.9. ^{19}F NMR (CD$_3$OD, 376.3 MHz) δ: -(117.98-118.06) (m, 1F, CF). HR-MS m/z: calcd for C$_{17}$H$_{18}$FN$_2$O, [(M+H)$^{+}$]: 285.1398; found 285.1405.

N-(1-(4-fluorobenzyl)indolin-5-yl)cyclohexanecarboxamide (9b).

Final product **9b** was obtained from 1-(4-fluorobenzyl)indolin-5-amine **(3)** and cyclohexanecarbonyl chloride following the general procedure D. The product was isolated in 79% yield as a white powder that crystallizes from ethyl acetate. ^{1}H NMR (CDCl$_3$, 400 MHz): δ: 1.22-1.38 (m, 3H, CH$_2$); 1.50-1.71 (m, 3H, CH$_2$); 1.84-1.87 (m, 2H, CH$_2$); 1.95-1.98 (m, 2H, CH$_2$); 2.18-2.24 (m, 1H, CH); 2.96 (t, 2H, CH$_2$, J = 8.2 Hz); 3.28 (t, 2H, CH$_2$, J = 8.2 Hz); 4.19 (s, 2H, CH$_2$); 6.42 (d, 1H, aryl, J = 8.3 Hz); 7.01-7.06 (m, 4H, aryl); 7.31-7.35 (m, 2H, aryl);

7.39 (s, 1H, NH). ^{13}C NMR (CDCl$_3$, 100 MHz) δ: 25.8; 28.6; 29.8; 46.4; 53.3; 53.8; 106.8; 115.2; 115.4; 118.4; 119.8; 129.0; 129.5; 133.97; 134.0; 149.5; 160.8; 163.3;174.1. ^{19}F NMR (CDCl$_3$, 376.3 MHz) δ: -(115.73-115.81) (m, 1F, CF). HR-MS m/z: calcd for C$_{22}$H$_{26}$FN$_2$O, [(M+H)$^+$]: 353.2024; found 353.2031.

2-cyclohexyl-N-(1-(4-fluorobenzyl)indolin-5-yl)acetamide (9c).

Final product **9c** was synthesized starting from 1-(4-fluorobenzyl)indolin-5-amine **(3)** and 2-cyclohexylacetyl chloride following the general procedure D. The product was isolated in 81% yield as a white powder that crystallizes from methanol. ^{1}H NMR (DMSO-d6, 400 MHz): δ: 0.92-1.00 (m, 2H, CH$_2$); 1.11-1.27 (m, 3H, CH$_2$); 1.60-1.74 (m, 5H, CH$_2$); 2.11 (d, 2H, CH$_2$, J = 7.0 Hz); 2.85 (t, 2H, CH$_2$, J = 8.3 Hz); 3.18 (t, 2H, CH$_2$, J = 8.3 Hz); 4.20 (s, 2H, CH$_2$); 6.51 (d, 1H, aryl, J = 8.4 Hz); 7.12-7.19 (m, 3H, aryl); 7.34-7.40 (m, 3H, aryl); 9.48 (s, 1H, NH). ^{13}C NMR (DMSO-d6, 100 MHz) δ: 26.1; 26.4; 28.6; 33.0; 35.4; 44.6; 52.8; 53.5; 107.3; 115.4; 115.6; 117.5; 119.0; 130.2; 130.4; 130.5; 130.7; 134.90; 134.92; 148.7; 160.5; 163.0; 170.0. ^{19}F NMR (CDCl$_3$, 376.3 MHz) δ: -(115.99-115,91) (s, 1F, CF). HR-MS m/z: calcd for C$_{23}$H$_{28}$FN$_2$O, [(M+H)$^+$]: 367.2186; found 367.2195.

Tert-butyl 5-nitroindoline-1-carboxylate (10b).

5-nitroindoline (**1**, 1.0 eq) was dissolved in DCM and added with 2.0 equivalents of TEA and 2.0 equivalents of di-tert-butyl dicarbonate. The mixture was refluxed overnight under stirring. Upon cooling to room temperature, the mixture was extracted three times with aqueous 2N HCl. The organic phase was dried over anhydrous Na$_2$SO$_4$, filtered and evaporated under vacuum. Crude product was purified by silica gel chromatography using a linear gradient of n-hexane/ethyl acetate as mobile phase. After flash-chromatographic purification, tert-butyl 5-nitroindoline-1-carboxylate (**10b**) was obtained as an orange crystal in 64% yield. ^{1}H NMR (CDCl$_3$, 400 MHz): δ: 1.47 (s, 9H, Boc); 2.93 (t, 2H, CH$_2$, J = 8.0 Hz); 3.76-3.90 (m, 4H, CH$_2$ and NH$_2$); 6.42-6.47 (m, 2H, aryl); 7.57 (bs, 1H, aryl). HR-MS m/z: calcd for C$_{13}$H$_{19}$N$_2$O$_2$, [(M+H)$^+$]: 235.1441; found 235.1452.

1-(2,4-difluorobenzyl)-5-nitroindoline (11a).

Synthesized according to the general procedure A using 5-nitroindoline (**1**) and 2,4-difluorobenzaldehyde as reagents. Intermediate **11a** was obtained as a yellow powder in 72% yield. ^{1}H NMR (CDCl$_3$, 400 MHz): δ: 3.12 (t, 2H, CH$_2$, J = 8.4 Hz); 3.66 (t, 2H, CH$_2$, J = 8.4 Hz); 4.45 (s, 2H, CH$_2$); 6.40 (d, 1H, aryl, J = 8.5 Hz); 6.85-6.91 (m, 2H, aryl); 7.21-7.28 (m,

1H, aryl); 7.93 (s, 1H, aryl); 8.08 (d, 1H, aryl, J = 6.5 Hz). HR-MS m/z: calcd for $C_{15}H_{13}F_2N_2O_2$, [(M+H)$^+$]: 291.0940; found 291.0951.

1-(3,4-difluorobenzyl)-5-nitroindoline (11b).

Synthesized according to the general procedure A using 5-nitroindoline (**1**) and 3,4-difluorobenzaldehyde as reagents. Intermediate **11b** was obtained as a yellow powder in 60% yield. ^{1}H NMR (CDCl$_3$, 400 MHz): δ: 3.14 (t, 2H, CH$_2$, J = 8.4 Hz); 3.64 (t, 2H, CH$_2$, J = 8.4 Hz); 4.40 (s, 2H, CH$_2$); 6.35 (d, 1H, aryl, J = 8.6 Hz); 7.00-7.22 (m, 3H, aryl); 7.96 (s, 1H, aryl); 8.08 (d, 1H, aryl, J = 6.2 Hz). HR-MS m/z: calcd for $C_{15}H_{13}F_2N_2O_2$, [(M+H)$^+$]: 291.0940; found 291.0952.

5-nitro-1-(4-(trifluoromethyl)benzyl)indoline (11c).

Synthesized according to the general procedure A using 5-nitroindoline (**1**) and 4-(trifluoromethyl)benzaldehyde as reagents. Intermediate **11c** was obtained as a yellow powder in 76% yield. ^{1}H NMR (CDCl$_3$, 400 MHz): δ: 3.14 (t, 2H, CH$_2$, J = 8.5 Hz); 3.67 (t, 2H, CH$_2$, J = 8.5 Hz); 4.51 (s, 2H, CH$_2$); 6.33 (d, 1H, aryl, J = 8.3 Hz); 7.41 (d, 2H, aryl, J = 12.0 Hz); 7.63 (d, 2H, aryl, J = 12.0 Hz); 7.92 (s, 1H, aryl); 8.03 (d, 1H, aryl, J = 6.5 Hz). HR-MS m/z: calcd for $C_{16}H_{14}F_3N_2O_2$, [(M+H)$^+$]: 323.1002; found 323.1010.

1-(4-methoxybenzyl)-5-nitroindoline (11d).

Synthesized according to the general procedure A using 5-nitroindoline (**1**) and p-anisaldehyde as reagents. Intermediate **11d** was isolated as a yellow powder in 72% yield. ^{1}H NMR (CDCl$_3$, 400 MHz): δ: 3.07 (t, 2H, CH$_2$, J = 8.4 Hz); 3.62 (t, 2H, CH$_2$, J = 8.4 Hz); 3.83 (s, 3H, CH$_3$); 4.39 (s, 2H, CH$_2$); 6.37 (d, 1H, aryl, J = 8.4 Hz); 6.90 (d, 2H, aryl, J = 9.8 Hz); 7.20 (d, 2H, aryl, J = 9.8 Hz); 7.93 (s, 1H, aryl); 8.08 (d, 1H, aryl, J = 6.6 Hz). HR-MS m/z: calcd for $C_{16}H_{17}N_2O_3$, [(M+H)$^+$]: 285.1234; found 285.1284.

1-(2,4-bis(trifluoromethyl)benzyl)-5-nitroindoline (11e).

Synthesized according to the general procedure A using 5-nitroindoline (**1**) and 2,4-bis(trifluoromethyl)benzaldehyde as reagents. Intermediate **11e** was obtained as a yellow powder in 58% yield. ^{1}H NMR (CDCl$_3$, 400 MHz): δ : 3.22 (t, 2H, CH$_2$, J = 8.4 Hz); 3.75 (t, 2H, CH$_2$, J = 8.4 Hz); 4.70 (s, 2H, CH$_2$); 6.25 (d, 1H, aryl, J = 8.6 Hz); 7.61 (d, 1H, aryl, J = 8.6 Hz); 7.81 (d, 1H, aryl, J = 8.9 Hz); 7.97-8.05 (m, 3H, aryl). HR-MS m/z: calcd for $C_{17}H_{13}F_6N_2O_2$, [(M+H)$^+$]: 391.0876; found 391.0884.

1-(4-methoxybenzyl)-2-methyl-5-nitroindoline (11f).

Synthesized according to the general procedure A using 2-methyl-5-nitroindoline (**10a**) and p-anisaldehyde as reagents. Intermediate **11f** was isolated as a yellow powder in 72% yield. ^{1}H NMR (CDCl3, 400 MHz): δ: 1.33 (d, 3H, CH_3, J= 7.4 Hz); 2.67-2.75 (m, 1H, CH); 3.20-3.28 (m, 1H, CH); 3.81-3.91 (m, 4H, CH and CH_3); 4.20 (d, 1H, CH, J=14.7 Hz), 4.43 (d, 1H, CH, J=14.7 Hz); 6.88 (d, 2H, aryl, J=10.1 Hz); 7.10 (s, 1H, aryl); 7.51 (d, 2H, aryl, J=12.0 Hz); 7.84 (d, 2H, aryl, J=8.5 Hz). HR-MS m/z: calcd for $C_{17}H_{19}N_2O_3$, [(M+H)$^+$]: 299.1390; found 299.1401.

Tert-butyl 5-(cyclohexanesulfonamido)indoline-1-carboxylate (11g).

Tert-butyl 5-nitroindoline-1-carboxylate (**10b**), synthesized according to the procedure described in supplementary materials, was reduced to the corresponding tert-butyl 5-aminoindoline-1-carboxylate by the general procedure B. The amine intermediate was reacted, without further purification, with cyclohexanesulfonyl chloride, following the general procedure C and giving **11g** in 54% yield as a grey solid. ^{1}H NMR (CDCl3, 400 MHz): δ: 1.12-1.26 (m, 3H, CH$_2$ and CH); 1.27-1.74 (m, 12H, Boc and CH$_2$); 1.83-1.90 (m, 2H, CH$_2$); 2.07-2.17 (m, 2H, CH$_2$); 2.86-2.95 (m, 1H, CH); 3.07 (t, 2H, CH$_2$, J = 8.6 Hz); 3.96 (t, 2H, CH$_2$, J = 8.6 Hz); 6.99-3.07 (m, 1H, aryl); 7.14 (s, 1H, aryl); 7.37 (bs, 1H, aryl); 7.76 (bs, 1H, NH). HR-MS m/z: calcd for $C_{19}H_{29}N_2O_4S$, [(M+H)$^+$]: 381.1843; found 381.1849.

1-(2,4-difluorobenzyl)indolin-5-amine (12a).

Synthesized according to the general procedure B. Intermediate **12a** was isolated as a grey powder in 97% yield. ^{1}H NMR (CDCl3, 400 MHz): δ: 2.92 (t, 2H, CH$_2$, J = 8.7 Hz); 3.23-3.32 (m, 4H, CH$_2$ and NH$_2$); 4.18 (s, 2H, CH$_2$); 6.41 (d, 1H, aryl, J = 6.4 Hz); 6.49 (d, 1H, aryl, J = 6.4 Hz); 6.61 (s, 1H, aryl); 6.81-6.90 (m, 2H, aryl); 7.40-7.48 (m, 1H, aryl). HR-MS m/z: calcd for $C_{15}H_{15}F_2N_2$, [(M+H)$^+$]: 261.1198; found 261.1205.

1-(3,4-difluorobenzyl)indolin-5-amine (12b).

Synthesized according to the general procedure B. Intermediate **12b** was isolated as an off-white powder in 98% yield. ^{1}H NMR (CDCl3, 400 MHz): δ: 2.93 (t, 2H, CH$_2$, J = 8.5 Hz); 3.03 (bs, 2H, NH$_2$); 3.20 (t, 2H, CH$_2$, J = 8.5 Hz); 4.11 (s, 2H, CH$_2$); 6.28 (d, 1H, aryl, J = 6.4 Hz); 6.35 (d, 1H, aryl, J = 7.2 Hz); 6.51 (s, 1H, aryl); 7.09-7.27 (m, 3H, aryl). HR-MS m/z: calcd for $C_{15}H_{15}F_2N_2$, [(M+H)$^+$]: 261.1198; found 261.1205.

1-(4-(trifluoromethyl)benzyl)indolin-5-amine (12c).

Synthesized according to the general procedure B. Intermediate **12c** was isolated as a white powder in 95% yield. ^{1}H NMR (CDCl$_3$, 400 MHz): δ: 2.94 (t, 2H, CH$_2$, J = 8.6 Hz); 3.21-3.27 (m, 4H, CH$_2$ and NH$_2$); 4.21 (s, 2H, CH$_2$); 6.35 (d, 1H, aryl, J = 8.9 Hz); 6.48 (d, 1H, aryl, J = 8.9 Hz); 6.63 (s, 1H, H-4); 7.54 (d, 2H, aryl, J = 5.7 Hz); 7.62 (d, 2H, aryl, J = 6.1 Hz). HR-MS m/z: calcd for C$_{16}$H$_{16}$F$_3$N$_2$, [(M+H)$^+$]: 293.1260; found 293.1269.

1-(4-methoxybenzyl)indolin-5-amine (12d).

Synthesized according to the general procedure B. Intermediate **12d** was isolated as a grey powder in 98% yield. ^{1}H NMR (CDCl$_3$, 400 MHz): δ: 2.88 (t, 2H, CH$_2$, J = 8.3 Hz); 3.17-3.23 (m, 4H, CH$_2$ and NH$_2$); 3.83 (s, 3H, CH$_3$); 4.10 (s, 2H, CH$_2$); 6.41 (d, 1H, aryl, J = 8.2 Hz); 6.47 (d, 1H, aryl, J = 9.2 Hz); 6.61 (s, 1H, aryl); 6.89 (d, 2H, aryl, J = 8.7 Hz); 7.31 (d, 2H, aryl, J = 8.7 Hz). HR-MS m/z: calcd for C$_{16}$H$_{19}$N$_2$O, [(M+H)$^+$]: 255.1492; found 255.1501.

1-(2,4-bis(trifluoromethyl)benzyl)indolin-5-amine (12e).

Synthesized according to the general procedure B. Intermediate **12e** was isolated as a white powder in 94% yield. ^{1}H NMR (CDCl$_3$, 400 MHz): δ: 2.71 (t, 2H, CH$_2$, J = 8.5 Hz); 3.37 (t, 2H, CH$_2$, J = 8.5 Hz); 3.50 (bs, 2H, NH$_2$); 4.40 (s, 2H, CH$_2$); 6.20 (d, 1H, aryl, J = 7.5 Hz); 6.48 (d, 1H, aryl, J = 7.4 Hz); 6.56 (s, 1H, aryl); 7.58 (d, 1H, aryl, J = 6.2 Hz); 7.95-8.02 (m, 2H, aryl). HR-MS m/z: calcd for C$_{17}$H$_{15}$F$_6$N$_2$, [(M+H)$^+$]: 361.1134; found 361.1140.

1-(4-methoxybenzyl)-2-methylindolin-5-amine (12f).

Synthesized according to the general procedure B. Intermediate **12f** was isolated as an off-white powder in 96% yield. ^{1}H NMR (CDCl$_3$, 400 MHz): δ: 1.33 (d, 3H, CH$_3$, J= 7.3 Hz); 2.52-2.62 (m, 1H, CH); 3.02-3.11 (m, 1H, CH); 3.35 (bs, 2H, NH$_2$); 3.84 (s, 3H, CH$_3$); 4.12 (d, 1H, CH$_2$, J=15.4 Hz), 4.30 (d, 1H, CH$_2$, J=15.4 Hz); 5.76 (d, 1H, aryl, J=3.8 Hz); 6.00 (d, 1H, aryl, J= 8.2 Hz); 6.82-6.90 (m, 3H, aryl) 7.29 (d, 2H, aryl, J=8.0 Hz); HR-MS m/z: calcd for C$_{17}$H$_{21}$N$_2$O, [(M+H)$^+$]: 269.1348; found 269.1351.

N-(indolin-5-yl)cyclohexanesulfonamide (12g).

Intermediate **11g** was dissolved in a solution of TFA in DCM (20% v:v) and stirred at room temperature for 45 minutes. The reaction was then diluted with DCM and extracted with water and saturated solution of NaHCO$_3$. The organic phase was dried over anhydrous Na$_2$SO$_4$, filtered and evaporated under vacuum. Purification by flash chromatography gave **12g** as a grey

solid in 90% yield ^{1}H NMR (CD$_3$OD, 400 MHz): δ: 1.18-1.31 (m, 2H, CH$_2$); 1.48-1.70 (m, 4H, 2 CH$_2$); 1.85-1.89 (m, 2H, CH$_2$); 2.11-2.17 (m, 2H, CH$_2$); 2.99-3.08 (m, 1H, CH); 3.31 (t, 2H, CH$_2$, J = 8.9 Hz); 3.86 (t, 2H, CH$_2$, J = 8.9 Hz); 7.28 (d, 1H, aryl, J = 6.8 Hz); 7.41-7.43 (m, 2H, aryl). HR-MS m/z: calcd for C$_{14}$H$_{21}$N$_2$O$_2$S, [(M+H)$^+$]: 281.1318; found 281.1326.

N-(1-(2,4-difluorobenzyl)indolin-5-yl)cyclohexanesulfonamide (13a).

Final product **13a** was synthesized according to the general procedure C. It was isolated in 71% yield as an off-white powder that crystallizes from n-hexane/ethyl acetate. ^{1}H NMR (CDCl$_3$, 400 MHz): δ: 1.21-1.26 (m, 3H, CH$_2$); 1.55-1.71 (m, 3H, CH$_2$); 1.88-1.91 (m, 2H, CH$_2$); 2.17-2.20 (m, 2H, CH$_2$); 2.95-3.02 (m, 3H, CH$_2$ and CH); 3.40 (t, 2H, CH$_2$, J = 8.3 Hz); 4.26 (s, 2H, CH$_2$); 6.21 (s, 1H, NH); 6.43 (d, 2H, aryl, J = 8.3 Hz); 6.82-6.93 (m, 3H, aryl); 7.07 (s, 1H, aryl); 7.34-7.40 (m, 1H, aryl). ^{13}C NMR (CDCl$_3$, 100 MHz) δ: 25.1; 26.4; 28.4; 46.5; 53.7; 59.3;103.6; 103.9; 104.1; 106.8; 111.13; 111.17; 111.34; 111.38; 115.0; 116.5; 120.75; 120.79; 120.90; 120.94; 121.29; 123.19; 123.23; 126.61; 126.71; 126.75; 130.72; 130.78; 130.81; 130.87; 131.3; 150.6; 159.63; 159.75; 160.98; 161.10; 162.1; 162.2; 163.45; 163.57. ^{19}F NMR (CDCl$_3$, 376.3 MHz) δ: -(113.98-113.91) (m, 1F, CF); -(115.54-115.46) (m, 1F, CF). HR-MS m/z: calcd for C$_{21}$H$_{25}$F$_2$N$_2$O$_2$S, [(M+H)$^+$]: 407.1599; found 407.1611; [(M+Na)$^+$]: 429.1419; found 429.1427.

N-(1-(3,4-difluorobenzyl)indolin-5-yl)cyclohexanesulfonamide (13b).

Final product **13b** was synthesized according to the general procedure C. It was isolated in 68% yield as an off-white powder that crystallizes from n-hexane/ethyl acetate. ^{1}H NMR (CDCl$_3$, 400 MHz): δ: 1.20-1.31 (m, 3H, CH$_2$); 1.56-1.72 (m, 3H, CH$_2$); 1.89-1.92 (m, 2H, CH$_2$); 2.17-2.21 (m, 2H, CH$_2$); 2.92-2.96 (m, 1H, CH); 3.01 (t, 2H, CH$_2$, J = 8.3 Hz); 3.37 (t, 2H, CH$_2$, J = 8.3 Hz); 4.19 (s, 2H, CH$_2$); 6.02 (s, 1H, NH); 6.36 (d, 1H, aryl, J = 8.3 Hz); 6.89 (d, 1H, aryl, J = 10.3 Hz); 7.08-7.23 (m, 4H, aryl). ^{13}C NMR (CDCl$_3$, 100 MHz) δ : 25.11; 25.14; 26.4; 28.4; 52.9; 53.9; 59.4; 106.9; 116. 4; 116.6; 117.2; 117.4; 121.4; 123.29; 123.39; 123.43; 123.46; 123.49; 126.8; 131.4; 150.7; ^{19}F NMR (CDCl$_3$, 376.3 MHz) δ: -(1137.54-137.43) (m, 1F, CF); -(139.98-139.87) (m, 1F, CF). HR-MS m/z: calcd for C$_{21}$H$_{25}$F$_2$N$_2$O$_2$S, [(M+H)$^+$]: 407.1599; found 407.1612; [(M+Na)$^+$]: 429.1419; found 429.1426.

N-(1-(4-(trifluoromethyl)benzyl)indolin-5-yl)cyclohexanesulfonamide (13c).

Final product **13c** was synthesized according to the general procedure C. It was isolated in 68% yield as a white powder that crystallizes from n-hexane/ethyl acetate. ^{1}H NMR (CDCl$_3$, 400

MHz): δ: 1.20-1.31 (m, 3H, CH$_2$); 1.56-1.62 (m, 3H, CH$_2$); 1.70-1.72 (m, 2H, CH$_2$); 2.18-2.21 (m, 2H, CH$_2$); 2.92-2.98 (m, 1H, CH); 3.02 (t, 2H, CH$_2$, J = 8.3 Hz); 3.39 (t, 2H, CH$_2$, J = 8.3 Hz); 4.30 (s, 2H, CH$_2$); 6.14 (s, 1H, NH); 6.37 (d, 1H, aryl, J = 8.2 Hz); 6.91 (d, 1H, aryl, J = 8.2 Hz); 7.09 (s, 1H, aryl); 7.50 (d, 2H, aryl, J = 8.0 Hz); 7.63 (d, 2H, aryl, J = 8.0 Hz). ^{13}C NMR (CDCl$_3$, 100 MHz) δ : 20.36; 20.40; 21.6; 23.7; 48.7; 49.3; 54.6; 102.12; 116.6; 118.5; 120.74; 120.77; 120.81; 120.85; 122.1; 123.2; 124.7; 125.0; 126.6; 137.6; 146.1; ^{19}F NMR (CDCl$_3$, 376.3 MHz) δ: -63.21 (s, 3F, CF$_3$). HR-MS m/z: calcd for C$_{22}$H$_{26}$F$_3$N$_2$O$_2$S, [(M+H)$^+$]: 439.1662; found 439.1677; [(M+Na)$^+$]: 461.1481; found 461.1490.

N-(1-(4-methoxybenzyl)indolin-5-yl)cyclohexanesulfonamide (13d).

Final product **13d** was synthesized according to the general procedure C. It was isolated in 68% yield as a grey powder that crystallizes from n-hexane/ethyl acetate. ^{1}H NMR (CDCl$_3$, 400 MHz): δ: 1.22-1.28 (m, 3H, CH$_2$); 1.57-1.72 (m, 3H, CH$_2$); 1.89-1.93 (m, 2H, CH$_2$); 2.17-2.21 (m, 2H, CH$_2$); 2.94-2.99 (m, 3H, H-3 and CH); 3.34 (t, 2H, H-2, J = 8.3 Hz); 3.83 (s, 3H, CH$_3$); 4.19 (s, 2H, CH$_2$); 5.93 (s, 1H, NH); 6.43 (d, 1H, H-7, J = 8.3 Hz); 6.88-6.92 (m, 3H, H-6 and aryl); 7.05 (s, 1H, H-4); 7.28 (d, 2H, aryl, J = 8.6 Hz). ^{13}C NMR (CDCl$_3$, 100 MHz) δ: 25.13; 25.15; 26.4; 28.4; 53.0; 53.5; 55.3; 59.2; 106.8; 113.9; 121.5; 123.5; 126.2; 129.1; 130.0; 131.5; 151.2; 158.9. HR-MS m/z: calcd for C$_{22}$H$_{29}$F$_3$N$_2$O$_3$S, [(M+H)$^+$]: 401.1893; found 401.1902; [(M+Na)$^+$]: 423.1718; found 423.1724.

N-(1-(2,4-bis(trifluoromethyl)benzyl)indolin-5-yl)cyclohexanesulfonamide (13e).

Final product **13e** was synthesized according to the general procedure C. It was isolated in 65% yield as a white powder that crystallizes from n-hexane/ethyl acetate. ^{1}H NMR (CDCl$_3$, 400 MHz): δ: 1.20-1.31 (m, 3H, CH$_2$); 1.56-1.72 (m, 3H, CH$_2$); 1.90-1.92 (m, 2H, CH$_2$); 2.19-2.21 (m, 2H, CH$_2$); 2.93-2.99 (m, 1H, CH); 3.09 (t, 2H, H-3, J = 8.3 Hz); 3.50 (t, 2H, H-2, J = 8.3 Hz); 4.49 (s, 2H, CH$_2$); 6.17 (s, 1H, NH); 6.24 (d, 1H, H-7, J = 8.3 Hz); 6.89 (d, 1H, H-6, J = 9.2 Hz); 7.13 (s, 1H, H-4); 7.80 (d, 1H, aryl, J = 8.1 Hz); 7.87 (d, 1H, aryl, J = 8.1 Hz); 7.96 (s, 1H, aryl). ^{13}C NMR (CDCl$_3$, 100 MHz) δ: 25.10; 25.14; 26.4; 28.6; 50.3; 54.5; 59.5; 106.7; 121.2; 121.4; 122.3; 123.1; 123.2; 123.31; 123.35; 125.0; 127.2; 128.5; 128.8; 128.9; 129.0; 129.5; 129.7; 130.0; 131.2; 141.7; 150.4; ^{19}F NMR (CDCl$_3$, 376.3 MHz) δ: -60.57 (s, 3F, CF$_3$), -62.80 (s, 3F, CF$_3$). HR-MS m/z: calcd for C$_{23}$H$_{25}$F$_6$N$_2$O$_2$S, [(M+H)$^+$]: 507.1535; found 507.1541; [(M+Na)$^+$]: 529.1355; found 529.1362.

(S,R)-N-(1-(4-methoxybenzyl)-2-methylindolin-5-yl)cyclohexanesulfonamide (13f).

Final product **13f** was synthesized according to the general procedure C. It was isolated in 65% yield as a yellowish wax and was not crystallized. ^{1}H NMR (CDCl$_3$, 400 MHz): δ: 1.17-1.28 (m, 3H, CH$_2$); 1.33 (d, 3H, CH$_3$, J=8.0 Hz); 1.53-1.68 (m, 3H, CH$_2$); 1.84-1.86 (m, 2H, CH$_2$); 2.07-2.10 (m, 2H, CH$_2$); 2.60-2.66 (m, 1H, CH); 2.89-2.97 (m, 1H, CH); 3.10-3.16 (m, 1H, CH); 3.74-3.81 (m, 4H, CH and CH$_3$); 4.12 (d, 1H, CH, J=15.7 Hz), 4.36 (d, 1H, CH, J=15.7 Hz); 6.06 (s, 1H, NH); 6.23 (s, 1H, aryl); 6.39 (d, 1H, aryl, J=7.7 Hz); 6.87 (d, 2H, aryl, J= 8.7 Hz); 6.94 (d, 1H, aryl, J=7.7 Hz); 7.27 (d, 2H, aryl, J=8.7 Hz); ^{13}C NMR (CDCl$_3$, 100 MHz) δ: 19.55; 25.04; 26.29; 36.69; 49.64; 55.23; 59.62; 60.28; 99.67; 109.12; 113.89; 124.45; 125.65; 128.70; 130.24; 136.48; 153.47; 158.71. HR-MS m/z: calcd for C$_{23}$H$_{31}$N$_2$O$_3$S, [(M+H)$^+$]: 415.2050; found 415.2059; [(M+Na)$^+$]: 437.1869; found 437.1874.

N-(1-(4-bromo-2-nitrobenzyl)indolin-5-yl)cyclohexanesulfonamide (13g).

The final product **13g** was synthesized from **12g** and 4-bromo-2-nitrobenzaldehyde following the general procedure A. It was isolated in 71% yield as a yellowish solid that crystallizes form n-hexane/ethyl acetate ^{1}H NMR (CDCl$_3$, 400 MHz): δ: 1.20-1.31 (m, 3H, CH$_2$ and CH); 1.58-1.72 (m, 3H, CH$_2$ and CH); 1.89-1.93 (m, 2H, CH$_2$); 2.17-2.20 (m, 2H, CH$_2$); 2.91-2.99 (m, 1H, CH); 3.06 (t, 2H, CH$_2$, J = 8,3 Hz); 3.46 (t, 2H, H-2, J = 8.3 Hz); 4.54 (s, 2H, CH$_2$); 5.99 (s, 1H, NH); 6.26 (d, 1H, aryl, J = 8.3 Hz); 6.87 (d, 1H, aryl, J = 8.2 Hz); 7.10 (s, 1H, aryl); 7.59 (d, 1H, aryl, J = 8.3 Hz); 7.74 (d, 1H, aryl, J = 10.3 Hz); 8.21 (s, 1H, aryl). ^{13}C NMR (CDCl$_3$, 100 MHz) δ: 25.10, 25.13; 26.4; 28.5; 51.6; 54.7; 59.4; 106.8; 121.2; 121.4; 123.3; 127.2; 128.0; 131.2; 133.5; 136.5; 148.8; 150.4. HR-MS m/z: calcd for C$_{21}$H$_{25}$BrN$_3$O$_4$S, [(M+H)$^+$]: 494.0744; found 494.0755; [(M+Na)$^+$]: 516.0563; found 516.0570.

(4-fluorophenyl)(5-nitroindolin-1-yl)methanone (14a).

To a solution of 5-nitro indoline (**1**, 1.0 eq) and DIPEA (1.2 eq) stirred at 0 °C under nitrogen stream, a solution of 4-fluorobenzoyl chloride (1.2 eq) was added dropwise in DCM. The resulting mixture was allowed to warm to room temperature and stirred for further 2h. Then, the reaction was quenched by adding a saturated solution of NaHCO$_3$. The organic phase was extracted two more times with aqueous HCl 2N, dried over anhydrous Na$_2$SO$_4$, filtered and evaporated under vacuum. Crude product was purified by flash chromatography giving **14a** as a yellowish solid in 81% yield. ^{1}H NMR (CDCl$_3$, 400 MHz): δ: 3.24 (t, 2H, CH_2, J = 8.5 Hz); 4.21 (t, 2H, CH_2, J = 8.5 Hz); 7.16-7.19 (m, 2H, aryl); 7.60-7.64 (m, 2H, aryl); 7.79 (bs, 1H,

aryl); 8.10-8.14 (m, 2H, aryl). HR-MS m/z: calcd for $C_{15}H_{12}FN_2O_3$, $[(M+H)^+]$: 287.0826; found 287.0833.

2-(4-chlorophenyl)-1-(5-nitroindolin-1-yl)ethan-1-one (**14b**).

Intermediate **14b** was synthesized using the same procedure described above for **14a**, starting from 5-nitro indoline (**1**) and 2-(4-chlorophenyl)acetyl chloride. Flash chromatographic purification gave **14b** as a dark yellow solid in 79% yield. ^{1}H NMR (CDCl$_3$, 400 MHz): δ: 3.29 (t, 2H, CH$_2$, J = 8.3 Hz); 3.82 (s, 2H, CH$_2$);4.23 (t, 2H, CH$_2$, J = 8.3 Hz); 7.24 (d, 2H, aryl, J = 8.5 Hz); 7.36 (d, 2H, aryl, J = 8.5 Hz); 8.04 (s, 1H, aryl); 8.12 (d, 1H, aryl, J = 6.8 Hz); 8.33 (d, 1H, aryl, J = 7.2 Hz). HR-MS m/z: calcd for $C_{16}H_{14}ClN_2O_3$, $[(M+H)^+]$: 317.0687 and $[(M+H)^++2]$: 319.0658; found 319.0690 and 319.0663.

(5-aminoindolin-1-yl)(4-fluorophenyl)methanone (**15a**).

Prepared from **14a** using the general procedure B. After purification the product was isolated in 94% yield as a white solid. ^{1}H NMR (CDCl$_3$, 400 MHz): δ: 3.05 (t, 2H, CH$_2$, J = 8.6 Hz); 3.59 (bs, 2H, NH$_2$); 4.01 (t, 2H, CH$_2$, J = 8.6 Hz); 6.57-6.62 (m, 2H, aryl); 7.10-7.16 (m, 2H, aryl); 7.55-7.59 (m, 2H, aryl); 8.02 (bs, 1H, aryl). HR-MS m/z: calcd for $C_{15}H_{14}FN_2O$, $[(M+H)^+]$: 257.1085; found 257.1094.

1-(5-aminoindolin-1-yl)-2-(4-chlorophenyl)ethanone (**15b**).

Prepared from **14b** using the general procedure B. After purification the product was isolated in 89% yield as a white solid. ^{1}H NMR (CDCl$_3$, 400 MHz): δ: 3.09 (t, 2H, CH$_2$, J = 8.4 Hz); 3.43 (bs, 2H, NH$_2$); 3.63 (s, 2H, CH$_2$); 4.09 (t, 2H, CH$_2$, J = 8.3 Hz); 7.20 (d, 2H, aryl, J = 8.3 Hz); 7.31 (d, 2H, aryl, J = 8.3 Hz); 7.49-7.54 (m, 2H, aryl); 7.73 (d, 1H, aryl, J = 6.9 Hz). HR-MS m/z: calcd for $C_{16}H_{16}ClN_2O$, $[(M+H)^+]$: 287.0946; found 287.0954.

N-(1-(4-fluorobenzoyl)indolin-5-yl)cyclohexanesulfonamide (**16a**).

Synthesized by coupling intermediate **15a** with cyclohexylsulfonyl chloride as for the general procedure C. After purification, **16a** was obtained in 61% yield as a white solid that crystallizes from ethyl acetate. ^{1}H NMR (DMSO-d6, 400 MHz): δ: 1.06-1.24 (m, 3H, CH$_2$); 1.36-1.45 (m, 2H, CH$_2$); 1.58-1.60 (m, 1H, CH$_2$); 1.75-1.78 (m, 2H, CH$_2$); 2.00-2.03 (m, 2H, CH$_2$); 2.89-2.97 (m, 1H, CH); 3.07 (t, 2H, CH$_2$, J = 8.2 Hz); 4.00 (t, 2H, CH$_2$, J = 8.2 Hz); 7.04 (bs, 1H, aryl); 7.15 (s, 1H, aryl); 7.32 (t, 1H, aryl, J = 8.8 Hz);7.65-7.68 (m, 2H, aryl); 7.95 (bs, 1H, aryl); 9.65 (s, 1H, NH). ^{13}C NMR (DMSO-d6, 100 MHz) δ: 24.8; 25.2; 26.4; 28.3; 50.9; 59.1; 115.8; 116.0;

117.3; 118.9; 130.0; 130.1; 133.9; 134.5; 134.9; 139.4; 162.1; 164.6; 167.2; ^{19}F NMR (DMSO-d6, 376.3 MHz) δ: -(117.14-117.21) (m, 1F, CF). HR-MS m/z: calcd for $C_{21}H_{24}FN_2O_3S$, [(M+H)$^+$]: 403.1486; found 403.1495; [(M+Na)$^+$]: 425.1306; found 425.1316.

N-(1-(2-(4-chlorophenyl)acetyl)indolin-5-yl)cyclohexanesulfonamide (16b).

Synthesized by coupling intermediate **15b** with cyclohexanesulfonyl chloride as for the general procedure C. After purification, **16b** was obtained in 57% yield as an off-white solid that crystallizes from ethyl acetate. ^{1}H NMR (DMSO-d6, 400 MHz): δ: 1.05-1.24 (m, 3H, CH$_2$); 1.34-1.43 (m, 2H, CH$_2$); 1.56-1.58 (m, 1H, CH); 1.73-1.76 (m, 2H, CH$_2$,); 1.98-2.01 (m, 12H, CH$_2$); 2.86-2.93 (m, 1H, CH); 3.14 (t, 2H, CH$_2$, J = 8.2 Hz); 3.83 (d, 2H, CH$_2$, J = 6.0 Hz); 4.16 (t, 2H, CH$_2$, J = 8.2 Hz); 6.99 (d, 1H, aryl, J = 8.6 Hz); 7.12 (s, 1H, aryl); 7.25-7.33 (m, 3H, aryl); 7.38 (d, 1H, aryl, J=8.4 Hz); 7.94-7.98 (m, 1H, aryl); 9.59 (s, 1 H, NH). ^{13}C NMR (DMSO-d6, 100 MHz) δ: 24.8; 25.2; 26.4; 27.9; 41.5; 48.2; 59.1; 116.7; 117.41; 117.4; 119.1; 126.9; 128.6; 128.7; 129.9; 131.7; 132.0; 133.5; 134.4; 134.7; 135.6; 139.8; 162.8; 169.2. HR-MS m/z: calcd for $C_{22}H_{26}ClNO_3S$, [(M+H)$^+$]: 433.1347 and [(M+H)$^+$+2]: 435.1318; found 433.1342 and 435.1323.

1-(4-fluorophenethyl)-5-nitroindoline (17).

Synthesized from 5-nitroindoline (**1**) following the general procedure E. The product was isolated in 68% yield as a yellowish solid. ^{1}H NMR (CDCl$_3$, 400 MHz): δ: 2.89 (t, 2H, CH$_2$, J = 6.7 Hz); 3.06 (t, 2H, CH$_2$, J = 8.4 Hz); 3.48 (t, 2H, CH$_2$, J = 6.7 Hz); 3.62 (t, 2H, CH$_2$, J = 8.4 Hz); 6.20 (d, 1H, CH$_2$, J = 8.6 Hz); 6.98-7.04 (m, 2H, aryl); 7.16-7.20 (m, 2H, aryl); 7.89 (s, 1H, aryl); 8.05 (d, 1H, aryl, J = 8.3 Hz). HR-MS m/z: calcd for $C_{16}H_{16}FN_2O_2$, [(M+H)$^+$]: 287.1190; found 287.1200.

1-(4-fluorophenethyl)indolin-5-amine (18).

Prepared from **17** using the general procedure B for continuous flow hydrogenation. The intermediate was isolated in 92% yield as a white solid. ^{1}H NMR (CDCl$_3$, 400 MHz): δ: 2.79-2.96 (m, 4H, 2 CH$_2$); 3.26-3.49 (m, 6H, 2 CH$_2$ and NH$_2$); 6.23 (d, 1H, aryl, J = 8.5 Hz); 6.95-7.05 (m, 2H, aryl); 7.13-7.28 (m, 4H, aryl). HR-MS m/z: calcd for $C_{16}H_{18}FN_2$, [(M+H)$^+$]: 257.1449; found 257.1453.

N-(1-(4-fluorophenethyl)indolin-5-yl)cyclohexanesulfonamide (19).

Obtained by coupling of **18** with cyclohexane sulfonyl chloride as for the general procedure C. The final product was isolated in 57% yield as an off-with solid that crystallizes in n-hexane/diethyl ether. ^{1}H NMR (CDCl$_3$, 400 MHz): δ: 1.19-1.30 (m, 3H, CH$_2$ and CH); 1.56-1.71 (m, 3H, CH$_2$ and CH); 1.89-1.92 (m, 2H, CH$_2$); 2.17-2.20 (m, 2H, CH$_2$); 2.85-3.00 (m, 5H, CH and 2 CH$_2$); 3.30 (t, 2H, CH$_2$, J = 7.9 Hz); 3.42 (t, 2H, CH$_2$, J = 8.3 Hz); 5.99 (s, 1H, NH); 6.35 (d, 1H, aryl, J = 8.3 Hz); 6.90 (d, 1H, aryl, J = 8.3 Hz); 6.99-7.04 (m, 3H, aryl); 7.20-7.23 (m, 2H, aryl). ^{13}C NMR (CDCl$_3$, 100 MHz) δ: 25.1; 26.4; 28.4; 32.8; 50.89; 50.90; 53.2; 59.2; 106.4; 115.19; 115.2; 115.4; 121.5; 123.5; 126.0; 130.0; 131.2; 135.3; 150.8; 160.3; 162.8. ^{19}F NMR (CDCl$_3$-d6, 376.3 MHz) δ: -(115.51-115.59) (m, 1F, CF). HR-MS m/z: calcd for C$_{22}$H$_{28}$FN$_2$O$_2$S, [(M+H)$^+$]: 403.1850; found 403.1862; [(M+Na)$^+$]: 425.1669; found 425.1675.

4-(methoxymethoxy)benzaldehyde (19a).

4-hydroxybenzaldehyde (1.0 eq) was dissolved in dry dimethylformamide (DMF) and added with 1.2 equivalents of potassium tert-butoxide. After 5 minutes stirring at room temperature a solution of methoxymethyl chloride (MOMCl, 1.2 eq) in DMF was added dropwise. The mixture was stirred for 4h before being quenched by aqueous 2N HCl. The aqueous phase was extracted three times with DCM. The organic phases were collected, dried over anhydrous Na$_2$SO$_4$, filtered and evaporated. Purification of the crude product by flash chromatography gave **33** in 76% yield. ^{1}H NMR (CDCl$_3$, 400 MHz) δ: 3.44 (s, 3H, CH$_3$), 5.22 (s, 2H, CH$_2$), 7.12 (d, 2H, aryl, J= 8.0 Hz), 7.80 (d, 2H, aryl, J= 8.0 Hz l); 9.87 (s, 1H, OCH).

(4-(methoxymethoxy)phenyl)methanol (20a).

The reaction was A solution of **19a** (1.0 eq) in methanol was cooled in an ice bath and added portionwise with 3 equivalents of NaBH$_4$. The reaction warmed to room temperature and was maintained under stirring for 15 minutes. Aqueous 2N HCl was then slowly added to quench the excess of hydride. The aqueous phase was extracted with ethyl acetate and the resulting organic phase washed two times with brine, dried over anhydrous Na$_2$SO$_4$, filtered and evaporated in vacuo. After flash chromatographic purification, **20a** was obtained in 86% yield. ^{1}H NMR (CDCl$_3$, 400 MHz): δ: 2.83 (bs, 1H, OH), 3.48 (s, 3H, CH$_3$); 4.57 (s, 2H, CH$_2$), 5.16 (s, 2H, CH$_2$); 7.02 (d, 2H, aryl, J= 8.0 Hz); 7.27 (d, 2H, aryl, J= 8.0 Hz).

1-(iodomethyl)-4-(methoxymethoxy)benzene (20b).

Synthesized according to the procedure previously described.[74] Iodine (1.5 eq) was dissolved in dry DCM and added with 1.5 equivalents of triphenylphosphine. The solution was stirred for 1.5 hours and then added with 1.5 equivalents of imidazole, stirring for further 1 hour. Then alcohol **20a** was added to the resulting slurry, maintaining under stirring overnight. Then a saturated aqueous solution of $Na_2S_2O_3$ was added and the organic layer was further washed with brine. The organic layer was dried over Na_2SO_4, filtered, and concentrated in vacuo. Compound **20b** was obtained in 67% yield after purification of the crude product by flash-chromatography using a linear gradient of n-hexane/ethyl acetate as mobile phase. ^{1}H NMR (CDCl$_3$, 400 MHz) δ: 3.50 (s, 3H, CH$_3$); 4.49 (s, 2H, CH$_2$), 5.19 (s, 2H, CH$_2$); 6.99 (d, 2H, aryl, J= 8.0 Hz); 7.34 (d, 2H, aryl, J= 8.0 Hz). HR-MS m/z: calcd for C$_9$H$_{11}$IO$_2$, [(M+H)$^+$]: 277.9804; found 277.9812.

2-cyclohexylethane-1-thiol (20c).

2-cyclohexylethane-1-thiol (**20c**) was synthesized according to Thuo *et al.*[193] from (2-bromoethyl)cyclohexane (2.0 mmol) that was dissolved in 20 mL of ethanol, added with thiourea (2.4 mmol) and heated to reflux overnight. Removal of the solvent led to an oil that was mixed with aqueous NaOH (6.0 mmol in 20 mL) and refluxed under magnetic stirring for 2 hours. After cooling to room temperature the resulting solution was extracted three times with diethyl ether. The organic phases were collected, dried over Na$_2$SO$_4$, and concentrated in vacuo. After purification by flash chromatography eluting with n-hexane, intermediate 20c was isolated in 65% yield. ^{1}H NMR (CDCl$_3$, 400 MHz): δ: 0.79-088 (m, 2H, CH$_2$), 1.06-1.22 (m, 4H, 2 CH$_2$), 1.46 (q, 2H CH$_2$, J$_1$=7.2 Hz, J$_2$=15.2 Hz); 1.56-1.65 (m, 5H, CH and CH$_2$), 2.60 (t, 2H, CH$_2$, J=7.7 Hz).

2-cyclohexylethane-1-sulfonyl bromide (20d).

Compound **20c** was prepared in 75% yield as previously described.[194] Briefly, **20b** (1 mmol) was suspended in 5 mL of water and added with 1.0 mmol of KBr and 2.5 mmol of oxone. The reaction was stirred for 20 minutes and then extracted two times with ethyl acetate. The organic layers were collected, dried over Na$_2$SO$_4$ and concentrated in vacuo. Crude product was purified by flash chromatography using n-hexane as eluent. ^{1}H NMR (CDCl$_3$, 400 MHz): δ: 0.79-0.95 (m, 2H, CH$_2$), 1.10-1.24 (m, 4H, 2 CH$_2$), 1.54-1.70 (m, 5H, CH and 2 CH$_2$), 1.76 (q, 2H, CH$_2$, J$_1$=6.7 Hz, J$_2$=16.1 Hz), 3.88 (q, 2H, CH$_2$, J$_1$=7.8 Hz, J$_2$=10.2 Hz). HR-MS m/z: calcd for C$_8$H$_{15}$BrO$_2$S, [(M+H)$^+$]: 253.9976; found 253.9984.

5-nitro-1-(4-(trifluoromethyl)benzyl)-1H-indole (21a).

Synthesized according to the general procedure E, starting from 5-nitro-1H-indole (**20**) and commercially available 1-(bromomethyl)-4-(trifluoromethyl)benzene. The intermediate was obtained in 71% yield as an orange solid. ^{1}H NMR (CDCl$_3$, 400 MHz): δ: 5.44 (s, 2H, CH$_2$); 6.75 (d, 1H, aryl, J = 3.2 Hz); 7.18 (d, 2H, aryl, J = 8.4 Hz); 7.24 (d, 1H, aryl, J = 8.3 Hz); 7.31 (d, 1H, aryl, J = 4.0 Hz); 7.56 (d, 2H, aryl, J = 8.5 Hz); 8.04 (d, 1H, aryl, J = 8.2 Hz); 8.58 (s, 1H, aryl). HR-MS m/z: calcd for C$_{16}$H$_{12}$F$_3$N$_2$O$_2$, [(M+H)$^+$]: 321.0845; found 321.0254.

1-(4-(methoxymethoxy)benzyl)-5-nitro-1H-indole (21b).

Synthesized according to the general procedure E, starting from 5-nitro-1H-indole (**20**) and 1-(iodomethyl)-4-(methoxymethoxy)benzene. The intermediate was obtained in 65% yield as a yellowish solid. ^{1}H NMR (CDCl$_3$, 400 MHz): δ: 3.48 (s, 3H, CH$_3$); 5.17 (s, 2H, CH$_2$), 5.32 (s, 2H, CH$_2$); 6.73 (d, 1H, aryl, J= 3.5 Hz); 7.02 (d, 2H, aryl, J= 8.3 Hz); 7.09 (d, 2H, aryl, J= 8.4 Hz); 7.28 (d, 1H, aryl, J= 4.7 Hz); 7.34 (d, 1H, aryl, J= 8.2 Hz); 8.09 (d, 1H, aryl, J= 8.5 Hz); 8.61 (s, 1H, aryl). HR-MS m/z: calcd for C$_{17}$H$_{17}$N$_2$O$_4$, [(M+H)$^+$]: 313.1183; found 313.1201.

1-(4-fluorobenzyl)-5-nitro-1H-indole (21c).

Synthesized according to the general procedure E, starting from 5-nitro-1H-indole (**20**) and commercially available 1-(bromomethyl)-4-fluorobenzene. The intermediate was obtained in 74% yield as an orange solid. ^{1}H NMR (CDCl$_3$, 400 MHz): δ: 5.36 (s, 2H, CH$_2$); 6.75 (d, 1H, aryl, J = 3.7 Hz); 7.01-7.13 (m, 4H, aryl); 7.28 (d, 2H, aryl, J = 4.2 Hz); 8.10 (d, 2H, aryl, J = 8.6 Hz); 8.63 (s, 1H, aryl). HR-MS m/z: calcd for C$_{15}$H$_{12}$FN$_2$O$_2$, [(M+H)$^+$]: 271.0805; found 271.0811.

1-(4-methoxybenzyl)-5-nitro-1H-indole (21d).

Synthesized according to the general procedure E, starting from 5-nitro-1H-indole (**20**) and commercially available 1-(bromomethyl)-4-methoxybenzene. The intermediate was obtained in 64% yield as a dark yellow solid. ^{1}H NMR (CDCl$_3$, 400 MHz): δ: 3.80 (s, 3H, CH$_3$); 5.32 (s, 2H, CH$_2$); 6.73 (d, 1H, aryl, J = 4.0 Hz); 6.88 (d, 2H, aryl, J = 8.2 Hz); 7.09 (d, 2H, aryl, J = 8.3 Hz); 7.31-7.35 (m, 2H, aryl); 8.10 (d, 1H, aryl, J = 8.6 Hz); 8.62 (s, 1H, aryl). HR-MS m/z: calcd for C$_{16}$H$_{15}$N$_2$O$_3$, [(M+H)$^+$]: 283.1077; found 283.1085.

1-(4-(trifluoromethyl)benzyl)-1H-indol-5-amine (22a).

Synthesized form **21a** using general procedure B. The intermediate was obtained in 93% yield as an off-white solid. ^{1}H NMR (CDCl$_3$, 400 MHz): δ: 3.71 (bs, 2H, NH$_2$); 5.32 (s, 2H, CH$_2$); 6.43 (d, 1H, aryl, J = 3.7 Hz); 6.67 (d, 1H, aryl, J = 8.4 Hz); 7.00-7.09 (m, 3H, aryl); 7.18 (d, 2H, aryl, J = 8.6 Hz); 7.55 (d, 2H, aryl, J = 8.6 Hz). HR-MS m/z: calcd for C$_{16}$H$_{14}$F$_3$N$_2$, [(M+H)$^+$]: 291.1104; found 291.1111.

1-(4-(methoxymethoxy)benzyl)-1H-indol-5-amine (22b).

Synthesized form **21b** using general procedure B. The intermediate was obtained in 91% yield as a grey solid. ^{1}H NMR (CDCl$_3$, 400 MHz): δ: 3.48 (s, 3H, CH$_3$); 5.16 (s, 2H, CH$_2$), 5.21 (s, 2H, CH$_2$); 6.36 (d, 1H, aryl, J= 3.9 Hz); 6.66 (d, 1H, aryl, J= 7.9 Hz); 6.96-7.00 (m, 3H, aryl); 7.06-7.12 (m, 4H, aryl). HR-MS m/z: calcd for C$_{17}$H$_{19}$N$_2$O$_2$, [(M+H)$^+$]: 283.1441; found 283.1498.

1-(4-fluorobenzyl)-1H-indol-5-amine (22c).

Synthesized form **21c** using general procedure B. The intermediate was obtained in 94% yield as a dark grey solid. ^{1}H NMR (CDCl$_3$, 400 MHz): δ: 3.50 (bs, 2H, NH$_2$); 5.24 (s, 2H, CH$_2$); 6.38 (d, 1H, aryl, J = 4.1 Hz); 6.65 (d, 1H, aryl, J = 8.4 Hz); 6.97-7.10 (m, 7H, aryl). HR-MS m/z: calcd for C$_{15}$H$_{14}$FN$_2$, [(M+H)$^+$]: 241.1136; found 241.1144.

1-(4-methoxybenzyl)-1H-indol-5-amine (22d).

Synthesized form **21d** using general procedure B. The intermediate was obtained in 92% yield as a brown solid. ^{1}H NMR (CDCl$_3$, 400 MHz): δ: 3.03 (bs, 2H, NH$_2$); 3.79 (s, 3H, CH$_3$); 5.20 (s, 2H, CH$_2$); 6.36 (d, 1H, aryl, J = 3.8 Hz); 6.65 (d, 1H, aryl, J = 8.6 Hz); 6.85 (d, 2H, aryl, J = 8.4 Hz); 6.96 (s, 1H, aryl); 7.05-7.12 (m, 4H, aryl). HR-MS m/z: calcd for C$_{16}$H$_{17}$N$_2$O, [(M+H)$^+$]: 253.1335; found 253.1344.

N-(1-(4-(trifluoromethyl)benzyl)-1H-indol-5-yl)heptanamide (23a).

Synthesized from **22a** and heptanoyl chloride following general procedure D. The final product was obtained in 80% yield as a white solid that crystallizes in n-hexane/diethyl ether. ^{1}H NMR (CDCl$_3$, 400 MHz): δ: 0.92 (t, 3H, CH$_3$, J = 6.5 Hz); 1.34-1.44 (m, 6H, 3 CH$_2$); 1.73-1.79 (m, 2H, CH$_2$); 2.39 (t, 2H, CH$_2$, J = 7.6 Hz); 5.38 (s, 2H, CH$_2$); 6.56 (d, 1H, aryl, J = 2.7 Hz); 7.15-7.23 (m, 6H, aryl); 7.56 (d, 2H, aryl, J = 8.0 Hz); 7.90 (s, 1H, NH). ^{13}C NMR (CDCl$_3$, 100 MHz) δ: 14.0; 22.5; 25.8; 29.0; 31.6; 37.8; 49.8; 102.4; 109.6; 113.2; 116.4; 125.8; 126.8;

129.0; 130.5; 133.6; 141.5; 171.5. ^{19}F NMR (CDCl$_3$, 376.3 MHz) δ: -62.61 (s, 3F, CF$_3$). HR-MS m/z: calcd for C$_{23}$H$_{26}$F$_3$N$_2$O, [(M+H)$^+$]: 403.1992; found 403.2003; [(M+Na)$^+$]: 425.1811; found 425.1820.

N-(1-(4-(methoxymethoxy)benzyl)-1H-indol-5-yl)heptanamide (23b).

Synthesized from **22b** and heptanoyl chloride following general procedure D. The final product was obtained in 76% yield as a grey wax that was not crystallized. ^{1}H NMR (CDCl$_3$, 400 MHz): δ: 0.92 (t, 3H, CH$_3$, J = 6.6 Hz); 1.28-1.43 (m, 6H, 3 CH$_2$); 1.72-1.80 (m, 2H, CH$_2$); 2.38 (t, 2H, CH$_2$, J= 7.6 Hz); 3.48 (s, 3H, CH$_3$); 5.16 (s, 2H, CH$_2$), 5.24 (s, 2H, CH$_2$); 6.50 (d, 1H, aryl, J= 3.0 Hz); 6.96 (d, 2H, aryl, J= 8.6 Hz); 7.05 (d, 2H, aryl, J= 8.6 Hz); 7.11 (d, 1H, aryl, J=3.0 Hz); 7.19-7.22 (m, 2H, aryl); 7.30 (s, 1H, aryl); 7.85 (s, 1H, NH). ^{13}C NMR (CDCl$_3$, 100 MHz) δ: 14.1; 22.5; 25.8; 29.0; 31.6; 37.8; 49.7; 56.0; 94.4; 101.7; 109.8; 112.9; 116.1; 116.5; 128.1; 128.9; 129.0; 130.4; 130.7; 133.7; 156.7; 171.2. HR-MS m/z: calcd for C$_{24}$H$_{31}$N$_2$O$_3$ [(M+H)$^+$]: 395.2329; found 395.2391.

N-(1-(4-fluorobenzyl)-1H-indol-5-yl)cyclohexanesulfonamide (23c).

Synthesized from **22c** and cyclohexanesulfonyl chloride following general procedure C. The final product was obtained in 71% yield as an off-white solid that crystallizes in n-hexane/ethyl acetate ^{1}H NMR (CDCl$_3$, 400 MHz) δ: 1.19-1.29 (m, 3H, CH$_2$); 1.61-1.68 (m, 3H, CH$_2$); 1.86-1.88 (m, 2H, CH$_2$); 2.19-2.22 (m, 2H, CH$_2$); 2.95-3.03 (m, 1H, CH); 5.29 (s, 2H, CH$_2$); 6.41 (s, 1H, NH); 6.55 (d, 1H, aryl, J = 2.8 Hz); 7.00-7.04 (m, 2H, aryl); 7.08-7.13 (m, 3H, aryl). 7.16 (d, 1H, aryl, J = 3.2 Hz); 7.22 (d, 1H, aryl, J = 8.7 Hz); 7.56 (d, 1H, aryl, J = 1.7 Hz). ^{13}C NMR (CDCl$_3$, 100 MHz) δ: 25.09; 25.11; 26.4; 49.7; 59.3; 102.0; 110.3; 115.3; 115.7; 115.9; 118.1; 128.5; 128.6; 129.0; 129.2; 129.4; 132.84; 132.88; 134.4; 161.1; 163.5. ^{19}F NMR (CDCl$_3$, 376.3 MHz) δ: -115.82 (s, 1F, CF). HR-MS m/z: calcd for C$_{21}$H$_{24}$FN$_2$O$_2$S, [(M+H)$^+$]: 387.1537; found 387.1548; [(M+Na)$^+$]: 409.1356; found 409.1362.

N-(1-(4-methoxybenzyl)-1H-indol-5-yl)cyclohexanesulfonamide (23d).

Synthesized from **22d** and cyclohexanesulfonyl chloride following general procedure C. The final product was obtained in 65% yield as dark grey solid that crystallizes in n-hexane/ethyl acetate. ^{1}H NMR (CDCl$_3$, 400 MHz): δ: 1.20-1.28 (m, 3H, CH$_2$); 1.58-1.68 (m, 3H, CH$_2$); 1.87-1.90 (m, 2H, CH$_2$); 2.19-2.22 (m, 2H, CH$_2$); 2.95-3.02 (m, 1H, CH); 3.80 (s, 3H, CH$_3$); 5.26 (s, 2H, CH$_2$); 6.21 (s, 1H, NH); 6.53 (d, 1H, aryl, J = 3.0 Hz); 6.86 (d, 2H, aryl, J = 8.6 Hz); 7.06-7.11 (m, 3H, aryl); 7.16 (d, 1H, aryl, J = 3.0 Hz); 7.26 (d, 1H, aryl, J = 8.8 Hz); 7.55 (d, 1H,

aryl, J = 2.0 Hz). ^{13}C NMR (CDCl$_3$, 100 MHz) δ: 25.1; 26.4; 49.9; 55.3; 59.2; 101.7; 110.5; 114. 2; 115.3; 118.0; 128.3; 128.7; 129.06; 129.16; 129.4; 134.5; 159.2. HR-MS m/z: calcd for C$_{22}$H$_{27}$N$_2$O$_3$, [(M+H)$^+$]: 399.1737; found 399.1745; [(M+Na)$^+$]: 421.1556; found 421.1566.

3,3-dimethyl-N-(1-(4-(trifluoromethyl)benzyl)-1H-indol-5-yl)butanamide (24a).

Synthesized from **22a** and 3,3-dimethylbutanoyl chloride following general procedure D. The final product was obtained in 74% yield as a white solid that crystallizes in n-hexane/diethyl ether. ^{1}H NMR (CDCl$_3$, 400 MHz): δ: 1.13 (s, 9H, CH$_3$); 2.24 (s, 2H, CH$_2$); 5.35 (s, 2H, CH$_2$); 6.54 (d, 1H, aryl, J = 3.0 Hz); 7.10-7.20 (m, 6H, aryl); 7.54 (d, 2H, aryl, J = 8.1 Hz); 7.88 (s, 1H, NH). ^{13}C NMR (CDCl$_3$, 100 MHz) δ: 29.9; 31.3; 49.7; 51.6; 102.4; 109.6; 113.1; 113.3; 116.5; 125.7; 126.8; 128.9; 129.0; 130.1; 130.5; 130.6; 133.6; 141.6; 170.1. ^{19}F NMR (CDCl$_3$, 376.3 MHz) δ: -61.85 (s, 3F, CF$_3$). HR-MS m/z: calcd for C$_{22}$H$_{24}$F$_3$N$_2$O, [(M+H)$^+$]: 389.1835; found 389.1901.

N-(1-(4-hydroxybenzyl)-1H-indol-5-yl)heptanamide (24b).

Compound **23b** was dissolved in a mixture of solution of TFA in DCM (15% v:v) and stirred at room temperature for 1.5h. The reaction was then diluted with DCM and extracted with a saturated solution of NaHCO$_3$ and brine. The organic phase was dried over anhydrous Na$_2$SO$_4$, filtered and evaporated under vacuum. After purification of the crude product, **24b** was obtained in 87% yield as a white solid that crystallizes from n-hexane/ethyl acetate. ^{1}H NMR (CD$_3$OD, 400 MHz): δ: 0.93 (t, 3H, CH$_3$, J = 6.6 Hz); 1.30-1.43 (m, 4H, CH$_2$); 1.68-1.75 (m, 2H, CH$_2$); 2.37 (t, 2H, CH$_2$, J = 7.6 Hz); 4.87 (s, 2H, CH$_2$); 6.42 (d, 1H, aryl, J = 3.0 Hz); 6.71 (d, 2H, aryl, J = 8.4 Hz); 6.99 (d, 2H, aryl, J = 8.4 Hz); 7.16-7.20 (m, 2H, aryl); 7.26 (d, 1H, aryl, J = 8.8 Hz); 7.77 (s, 1H, aryl). ^{13}C NMR (CD$_3$OD, 100 MHz) δ: 13.0; 22.2; 25.7; 28.7; 31.4; 36.6; 49.1; 100.8; 109.5; 112.9; 115.0; 115.9; 128.0; 128.7; 128.9; 130.2; 133.8; 156.5; 173.3. HR-MS m/z: calcd for C$_{22}$H$_{26}$N$_2$O$_2$ [(M+H)$^+$]: 351.2067; found 351.2073.

N-(1-(4-(trifluoromethyl)benzyl)-1H-indol-5-yl)palmitamide (25a).

Synthesized from **22a** and palmitoyl chloride following general procedure D. The final product was obtained in 66% yield as a white wax that did not crystallize. ^{1}H NMR (CDCl$_3$, 400 MHz): δ: 0.90 (t, 3H, CH$_3$, J = 7.0 Hz); 1.28-1.42 (m, 24H, CH$_2$); 1.73-1.80 (m, 2H, CH$_2$); 2.38 (t, 2H, CH$_2$, J = 7.6 Hz); 5.38 (s, 2H, CH$_2$), 6.56 (d, 1H, aryl, J = 3.0 Hz); 7.14-7.23 (m, 6H, aryl); 7.56 (d, 2H, aryl, J = 8.1 Hz); 7.89 (s, 1H, NH); ^{13}C NMR (CDCl$_3$, 100 MHz) δ: 14.1; 22.7; 25.8; 29.33; 29.36; 29.4; 29.5; 29.66; 29.68; 29.70; 31.9; 37.8; 49.8; 102.4; 109.6; 113.1; 116.3;

125.8; 125.8; 126.8; 128.96; 129.03; 130.6; 133.6; 141.5; 171.3. ^{19}F NMR (CDCl$_3$, 376.3 MHz) δ: -62.54 (s, 3F, CF$_3$). HR-MS m/z: calcd for C$_{33}$H$_{44}$F$_3$N$_2$O, [(M+H)$^+$]: 529.3400; found 529.3392.

N-(1-(4-(trifluoromethyl)benzyl)-1H-indol-5-yl)cyclohexanesulfonamide (26a).
Synthesized from **22a** and cyclohexane sulfonyl chloride following general procedure C. The final product was obtained in 69% yield as a grey solid that crystallizes in n-hexane/ethyl acetate. ^{1}H NMR (CDCl$_3$, 400 MHz): δ: 1.20-1.28 (m, 3H, CH$_2$); 1.58-1.68 (m, 3H, CH$_2$); 1.87-1.91 (m, 2H, CH$_2$); 2.20-2.23 (m, 2H, CH$_2$); 2.95-3.02 (m, 1H, CH); 5.39 (s, 2H, CH$_2$); 6.24 (s, 1H, NH); 6.58 (d, 1H, aryl, J = 2.7 Hz); 7.08 (d, 1H, aryl, J = 8.7 Hz); 7.17-7.22 (m, 5H, aryl); 7.58 (d, 2H, aryl, J = 8.7 Hz). ^{13}C NMR (CDCl$_3$, 100 MHz) δ: 25.1; 26.4; 49.9; 59.4; 102.4; 110.2; 115.4; 118.3; 125.85; 125.88; 125.92; 126.9; 129.19; 129.22; 129.50; 130.0; 130.3; 134.4; 141.2. ^{19}F NMR (CDCl$_3$, 376.3 MHz) δ: -61.89 (s, 3F, CF$_3$). HR-MS m/z: calcd for C$_{22}$H$_{24}$F3N$_2$O$_2$S, [(M+H)$^+$]: 437.1505; found 437.1513; [(M+Na)$^+$]: 459.1325; found 459.1333.

2-cyclohexyl-N-(1-(4-(trifluoromethyl)benzyl)-1H-indol-5-yl)ethane-1-sulfonamide (27a).
Synthesized, following general procedure C, from **22a** and 2-cyclohexylethane-1-sulfonyl bromide. The final product was obtained in 64% yield as an off-white solid that crystallizes in n-hexane/ethyl acetate. ^{1}H NMR (CDCl$_3$, 400 MHz): δ: 0.85-0.93 (m, 2H, CH$_2$); 1.11-1.33 (m, 4H, CH$_2$); 1.63-1.78 (m, 7H, CH and 3 CH$_2$); 3.05-3.09 (m, 2H, CH$_2$), 5.30 (s, 2H, CH$_2$); 6.48 (s, 1H, NH); 6.55 (d, 1H, aryl, J = 3.1 Hz), 7.01 (t, 2H, aryl, J = 8.6 Hz); 7.07-7.12 (m, 3H, aryl); 7.17 (d, 1H, aryl, J = 3.1 Hz); 7.22 (d, 1H, aryl, J = 8.7 Hz); 7.56 (d, 1H, aryl, J = 1.6 Hz). ^{13}C NMR (CDCl$_3$, 100 MHz) δ: 26.0; 26.3; 30.7; 32.8; 36.6; 48.9; 49.7; 102.1; 110.4; 115.7; 115.83; 115.89, 118.4; 128.4; 128.5; 128.7; 129.2; 129.5; 132.9; 134.6; 161.1; 163.5. ^{19}F NMR (CDCl$_3$, 376.3 MHz) δ: -62.01 (s, 3F, CF$_3$). HR-MS m/z: calcd for C$_{24}$H$_{28}$F$_3$N$_2$O$_2$S, [(M+H)$^+$]: 465,1818; found 465.1820.

2-(butylamino)-N-(1-(4-(trifluoromethyl)benzyl)-1H-indol-5-yl)acetamide (28a).
Intermediate **22a** was reacted with chloroacetyl chloride following the general procedure D. After work up the obtained 2-chloro-N-(1-(4-(trifluoromethyl)benzyl)-1H-indol-5-yl)acetamide crystallized from DCM at 0°C and, than filtration, was used without further purification. 2-chloro-N-(1-(4-(trifluoromethyl)benzyl)-1H-indol-5-yl)acetamide (1.0 eq) was then dissolved in DMF and added with 2.6 equivalents of potassium tert-butoxyde and 2.6 equivalents of n-butylamine. The reaction was stirred under reflux overnight. Then, water was

added and the mixture was extracted four times with DCM. The organic phases were collected, dried over anhydrous Na_2SO_4, filtered and concentrated *in vacuo*. After purification by flash chromatography, final product **28a** was obtained in 57% yield as a white solid that crystallized from n-hexane/ethyl acetate.

2-chloro-N-(1-(4-(trifluoromethyl)benzyl)-1H-indol-5-yl)acetamide.

^{1}H NMR (CDCl$_3$, 400 MHz): δ: 4.15 (s, 2H, CH$_2$), 5.30 (s, 2H, CH$_2$), 6.50 (d, 1H, aryl, J= 3.7 Hz), 7.08-7.19 (m, 5H, aryl); 7.48 (d, 2H, aryl, J= 8.0 Hz); 7.82 (s, 1H, aryl); 8.19 (bs, 1H, NH). HR-MS m/z: calcd for $C_{18}H_{14}ClF_3N_2O$, [(M+H)$^+$]: 367.0820; found 367.0824.

2-(butylamino)-N-(1-(4-(trifluoromethyl)benzyl)-1H-indol-5-yl)acetamide.

^{1}H NMR (CD$_3$OD, 400 MHz): δ: 1.03 (t, 3H, CH$_3$ J = 7.3 Hz); 1.42-1.51 (m, 2H, CH$_2$); 1.71-1.79 (m, 2H, CH$_2$), 3.12 (t, 2H, CH$_2$, J = 8.0 Hz); 3.99 (s, 2H, CH$_2$) 5.50 (s, 2H, CH$_2$), 6.54 (d, 1H, aryl, J = 2.9 Hz), 7.22-7.29 (m, 5H, aryl); 7.36 (d, 1H, aryl, J = 2.9 Hz); 7.59 (d, 2H, aryl, J = 8.0 Hz); 7.90 (s, 1H, NH). ^{13}C NMR (CD$_3$OD, 100 MHz) δ: 12.5; 19.4; 27.7; 48.2; 49.0; 101.5; 109.6; 112.6; 115.5; 125.1; 126.9; 129.0; 129.5; 129.8; 133.9; 142.7; 162.9. ^{19}F NMR (CDCl$_3$, 376.3 MHz) δ: -61.33 (s, 3F, CF$_3$). HR-MS m/z: calcd for $C_{22}H_{24}F_3N_3O$ [(M+H)$^+$]: 404,1944; found 404,2000.

2-(butyl(methyl)amino)-N-(1-(4-(trifluoromethyl)benzyl)-1H-indol-5-yl)acetamide (29a).

Compound **28a** (1.0 eq) was dissolved in dry methanol and the solution was added with 1.5 equivalents of formaldehyde. The reaction was stirred at room temperature under positive nitrogen pressure overnight. Then, 3 equivalents of $NaBH_4$ were added and the reaction mixture was stirred for further 3h. Water was added to quench the excess of hydride, and the aqueous solution was extracted four times with DCM. The organic phases were washed with brine, dried over anhydrous Na_2SO_4, filtered and concentrated. Purification by flash chromatography gave **29a** in 81% yield as a white solid that crystallized from n-hexane/ethyl acetate. ^{1}H NMR (CDCl$_3$, 400 MHz): δ: 0.88 (t, 3H, CH$_3$, J = 7.2 Hz); 1.30-1.38 (m, 2H, CH$_2$); 1.42-1.49 (m, 2H, CH$_2$); 2.59 (t, 2H, CH$_2$, J = 7.5 Hz); 3.40 (s, 3H, CH$_3$); 4.52 (s, 2H, CH$_2$); 5.30 (s, 2H, CH$_2$), 6.49 (d, 1H, aryl, J = 3.1 Hz), 7.06-7.13 (m, 4H, aryl); 7.30-7.32 (m, 1H, aryl); 7.47 (d, 2H, aryl, J = 8.2 Hz); 7.60 (d, 1H, aryl, J = 2.0 Hz). ^{13}C NMR (CDCl$_3$, 100 MHz) δ: 13.9; 20.4; 30.2; 49.8; 54.9; 57.4; 72.2; 102.5; 109.9; 113.3; 116.2; 125.8; 126.8; 128.8; 129.3; 130.2; 134.0; 141.4; 170.2. ^{19}F NMR (CDCl$_3$, 376.3 MHz) δ: -62.14 (s, 3F, CF$_3$). HR-MS m/z: calcd for $C_{23}H_{26}F_3N_3O$ [(M+H)$^+$]: 418,2101; found 418,2114.

N-(5-oxo-5,6,7,8-tetrahydronaphthalen-2-yl)heptanamide (31).

Intermediate **31** was synthesized in 84% yield, using 6-amino-3,4-dihydronaphthalen-1(2H)-one (**30**) and heptanoyl chloride as starting materials and following the general procedure D. ^{1}H NMR (CDCl$_3$, 400 MHz): δ: 0.90 (t, 3H, CH$_3$, J= 9.8 Hz); 1.27-1.27 (m, 6H, 3 CH$_2$); 1.69-1.78 (m, 2H, CH$_2$); 2.08-2.17 (m, 2H, CH$_2$); 2.40 (t, 2H, CH$_2$, J= 12.1 Hz); 2.64 (t, 2H, CH$_2$, J= 12.1 Hz); 2.94 (t, 2H, CH$_2$, J= 8.5 Hz), 7.23 (d, 1H, aryl, J= 11.6 Hz); 7.62 (bs, 1H, NH); 7.76 (s, 1H, aryl), 8.00 d (1H, H-4, J=11.5 Hz). HR-MS m/z: calcd for C$_{17}$H$_{24}$NO$_2$, [(M+H)$^+$]:274.1802; found 274.1810.

N-(5-hydroxy-5,6,7,8-tetrahydronaphthalen-2-yl)heptanamide (32).

Alcohol **32** was synthesized in 90% yield by reduction of the ketone precursor **31** as already described.[11] ^{1}H NMR (CDCl$_3$, 400 MHz) δ: 0.90 (t, 3H, CH$_3$, J= 9.5 Hz); 1.28-1.36 (m, 6H, 3 CH$_2$); 1.68-1.76 (m, 4H, 2 CH$_2$); 1.95-2.00 (m, 2H, CH$_2$); 2.36 (t, 2H, CH$_2$, J= 11.7 Hz); 2.65-2.86 (m, 2H, CH$_2$); 4.76 (t, 1H, H-5, J=3.6 Hz); 7.18 (bs, 1H, NH); 7.24 (d, 1H, aryl, J= 11.4 Hz); 7.36-7.39 (m, 2H, aryl). HR-MS m/z: calcd for C$_{17}$H$_{26}$NO$_2$, [(M+H)$^+$]:276.1958; found 276.1949.

(Z)-N-(5-(4-(trifluoromethyl)benzylidene)-5,6,7,8-tetrahydronaphthalen-2-yl)heptanamide (33a).

Final compound **32a** was synthesized from **31** as described by Ulmschneider *et al.*[195] After purification, **32a** was isolated in 32% yield as a white solid that crystallized from petroleum ether. The geometry of the double bond was assigned by bidimensional NMR experiments (please see supplementary material file). ^{1}H NMR (CDCl$_3$, 400 MHz): δ: 0.91 (t, 3H, CH$_3$, J=6.8 Hz); 1.28-1.40 (m, 8H, 3 CH$_2$); 1.68-1.76 (m, 2H, CH$_2$); 1.99-2.05 (m, 2H, CH$_2$); 2.34 (t, 2H, CH$_2$, J=7.6 Hz); 2.52-2.55 (m, 2H, CH$_2$); 2.90 (t, 2H, CH$_2$, J=6.6 Hz); 6.39 (s, 1H, C$_{sp2}$H); 6.81-6.84 (m, 1H aryl); 7.03 (d, 1H aryl, J=8.5 Hz); 7.08 (s, 1H, NH); 7.33 (d, 2H, aryl, J= 8.2 Hz); 7.46 (d, 2H, aryl, J=8.2 Hz); 7.55 (s, 1H, aryl). ^{13}C NMR (CDCl$_3$, 100 MHz) δ: 14.0; 22.5; 23.9; 25.6; 28.9; 29.7; 31.6; 34.9; 37.9; 116.1; 119.6; 122.4; 125.1; 125.7; 127.9; 128.3; 129.2; 129.5; 130.3; 137.4; 139.8; 140.2; 142.5; 171.3. ^{19}F NMR (CDCl$_3$, 376.3 MHz) δ: -62.51 (s, 3F, CF$_3$). HR-MS m/z: calcd for C$_{25}$H$_{29}$ F$_3$NO, [(M+H)$^+$]: 416.2193; found 416.2198.

(E)-N-(5-(4-(trifluoromethyl)benzylidene)-5,6,7,8-tetrahydronaphthalen-2-yl)heptanamide (33b).

Final compound **32b** was synthesized from **31** as described by Ulmschneider *et al.*[195] After purification, **32a** was isolated in 51% yield as a white solid that crystallized from petroleum ether. The geometry of the double bond was assigned by bidimensional NMR experiments (please see supplementary material file). ^{1}H NMR (CDCl$_3$, 400 MHz): δ: 0.92 (t, 3H, CH$_3$, J=6.7 Hz); 1.28-1.43 (m, 8H, 3 CH$_2$); 1.72-1.79 (m, 2H, CH$_2$); 1.82-1.89 (m, 2H, CH$_2$); 2.38 (t, 2H, CH$_2$, J=7.6 Hz); 2.76-2.80 (m, 2H, CH$_2$); 2.85 (t, 2H, CH$_2$, J= 6.2 Hz); 7.00 (s, 1H, C$_{sp2}$H); 7.19 (s, 1H, NH); 7.31 (d, 1H, aryl, J=8.5 Hz); 7.46 (d, 3H, aryl, J=7.8 Hz); 7.62 (d, 2H, aryl, J= 8.2 Hz); 7.68 (d, 1H, aryl, J= 8.6 Hz). ^{13}C NMR (CDCl$_3$, 100 MHz) δ: 14.0; 22.5; 23.5; 25.6; 28.0; 28.9; 30.4; 31.6; 37.9; 117.7; 119.7; 121.3; 123.0; 125.2; 125.7; 128.0; 128.3;129.5; 131.7; 137.5; 138.9; 139.2; 141.8; 171.4. ^{19}F NMR (CDCl$_3$, 376.3 MHz) δ: -62.37 (s, 3F, CF$_3$). HR-MS m/z: calcd for C$_{25}$H$_{29}$ F$_3$NO, [(M+H)$^+$]: 416.2193; found 416.2201.

N-(5-(4-(trifluoromethyl)benzyl)-5,6,7,8-tetrahydronaphthalen-2-yl)heptanamide (34).

Compounds **33b** (1.0 eq) was dissolved in methanol and added with a catalytic amount of Pd/C 10% and ammonium formate (10.0 eq). The reaction was refluxed under stirring. After 40 minutes, the mixture was cooled to room temperature and filtered through celite. The resulting solution was evaporated and reconstituted in DCM. The organic phase was washed with water (three times) and brine (two times) before being dried over anhydrous Na$_2$SO$_4$, filtered and concentrated at the rotary evaporator. After purification, product **34** was obtained in 86% yield as a white was unable to crystallize. [α]^{25}$_D$: +11.0 ± 0.03 (c = 0.05, MeOH). ^{1}H NMR (CDCl$_3$, 400 MHz) δ: 0.92 (t, 3H, CH$_3$, J=6.8 Hz); 1.28-1.42 (m, 6H, 3 CH$_2$); 1.56-1.78 (m, 5H, CH$_2$); 1.81-1.92 (m, 1H, CH); 2.36 (t, 2H, CH$_2$, J=7.86Hz); 2.72-2.83 (m, 3H, CH$_2$ and CH); 3.04-3.15 (m, 2H, CH$_2$); 7.10-7.14 (m, 2H, aryl and NH); 7.23-7.25 (m, 1H, aryl); 7.31 (d, 2H, aryl, J= 8.0 Hz); 7.35 (s, 1H, aryl); 7.57 (d, 2H, aryl, J=8.0 Hz). ^{13}C NMR (CDCl$_3$, 100 MHz) δ: 14.0; 19.2; 22.5; 25.6; 26.8; 28.9; 29.8; 31.6; 37.8; 39.0; 43.1; 117.5; 120.3; 123.0; 125.16; 125.19; 125.5; 125.4; 128.2; 128.5; 129.1; 129.5; 135.7; 135.9; 137.9; 145.0; 171.3. ^{19}F NMR (CDCl$_3$, 376.3 MHz) δ: -62.21 (s, 3F, CF$_3$). HR-MS m/z: calcd for C$_{25}$H$_{31}$ F$_3$NO, [(M+H)$^+$]: 418.2352; found 418.2361.

N-(4-aminophenyl)heptanamide (36).

Synthesized from 1,4-phenylenediamine following general procedure A (yield 88%). ^{1}H NMR (CDCl$_3$, 400 MHz): δ: 0.91 (t, 3H, C*H*$_3$, J=6.8 Hz); 1.28-1.40 (m, 6H, 3 C*H*$_2$); 1.70-1.74 (m,

2H, CH$_2$); 2.32 (t, 2H, CH$_2$, J=7.7 Hz); 3.61 (bs, 2H, NH); 6.65 (d, 2H, aryl, J=8.6 Hz); 7.14 (bs, 1H, CONH); 7.28 (d, 2H, aryl, J=8.6 Hz). HR-MS *m/z*: calcd for C$_{13}$H$_{21}$N$_2$O, [(M+H)$^+$]: 221.1654; found 221.1658.

N-(4-((4-(trifluoromethyl)benzyl)amino)phenyl)heptanamide (37).

Synthesized from **36** following the general procedure C (yield 72%). ^{1}H NMR (CD$_3$OD, 400 MHz): δ: 0.92 (t, 3H, CH$_3$, J=6.9 Hz); 1.32-1.40 (m, 6H, 3 CH$_2$); 1.64-1.71 (m, 2H, CH$_2$); 2.31 (t, 2H, CH$_2$, J=7.6 Hz); 4.40 (s, 2H, CH$_2$); 6.58 (d, 2H, aryl, J=8.9 Hz); 7.23 (d, 2H, aryl, J=8.8 Hz); 7.53-7.61 (m, 4H, aryl); ^{13}C NMR (CD$_3$OD, 100 MHz) δ: 13.0; 22.2; 25.7; 28.6; 31.3; 36.4;112.6; 122.1; 124.9; 127.3; 128.2; 128.5; 128.8; 145.1; 145.5; 173.0. ^{19}F NMR (CDCl$_3$, 376.3 MHz) δ: -62.44 (3F, CF$_3$). HR-MS *m/z*: calcd for C$_{21}$H$_{25}$F$_3$N$_2$O, [(M+H)$^+$]: 379.1997; found 379.2001.

3-nitro-N^1-(4-(trifluoromethyl)benzyl)benzene-1,4-diamine (39).

Synthesized from 2-nitrobenzene-1,4-diamine following the general procedure C (yield 69%). ^{1}H NMR (CDCl$_3$, 400 MHz): δ: 4.40 (s, 2H, CH$_2$); 5.67 (bs, 2H, NH$_2$); 6.73 (d, 1H, aryl, J=8.7 Hz); 6.88 (dd, 1H, aryl, J$_1$=6.5 Hz, J$_2$=2.5 Hz); 7.28 (s, 1H, aryl); 7.51 (d, 2H, aryl, J=7.5 Hz); 7.63 (d, 2H, aryl, J=7.5 Hz). HR-MS *m/z*: calcd for C$_{14}$H$_{13}$F$_3$N$_3$O$_2$, [(M+H)$^+$]: 312.0960; found 312.0957.

Benzyl (4-amino-3-nitrophenyl)(4-(trifluoromethyl)benzyl)carbamate (40).

Synthesized from **39** following the general procedure D for the synthesis of Cbz protected derivatives (yield 84%). ^{1}H NMR (CDCl$_3$, 400 MHz): δ: 4.90 (s, 2H, CH$_2$); 5.20 (s, 2H, CH$_2$); 6.16 (bs, 2H, NH$_2$); 6.72 (d, 1H, aryl, J=8.6 Hz); 7.26 (dd, 1H, aryl, J$_1$=6.5 Hz, J$_2$=2.3 Hz); 7.33-7.36 (m, 7H, aryl); 7.56 (d, 2H, aryl, J=7.6 Hz); 7.94 (s, 1H, aryl). HR-MS *m/z*: calcd for C$_{22}$H$_{19}$F$_3$N$_3$O$_4$, [(M+H)$^+$]: 446.1328; found 446.1332.

Tert-butyl (4-amino-3-nitrophenyl)(4-(trifluoromethyl)benzyl)carbamate (40').

Synthesized from **39** following the general procedure D for the synthesis of Boc protected derivatives (yield 79%). ^{1}H NMR (CDCl$_3$, 400 MHz): δ: 1.45 (s, 9H, 3 CH$_3$); 4.86 (s, 2H, CH$_2$); 6.72 (d, 1H, aryl, J=8.9 Hz); 7.13 (bs, 1H, aryl); 7.37 (d, 2H, aryl, J=7.9 Hz); 7.59 (d, 2H, aryl, J=7.9 Hz); 7.93 (s, 1H, aryl). HR-MS *m/z*: calcd for C$_{19}$H$_{21}$F$_3$N$_3$O$_4$, [(M+H)$^+$]: 412.1484; found 412.1488.

Benzyl (4-heptanamido-3-nitrophenyl)(4-(trifluoromethyl)benzyl)carbamate (41).

Synthesized from **40** and heptanoyl chloride following the general procedure B (yield 65%). ^{1}H NMR (CDCl$_3$, 400 MHz): δ: 0.91 (t, 3H, CH_3, J=6.7 Hz); 1.29-1.34 (m, 6H, 3 CH_2); 1.75-1.78 (m, 2H, CH_2); 2.49 (t, 2H, CH_2, J=7.4 Hz); 4.97 (s, 2H, CH_2); 5.22 (s, 2H, CH_2); 7.27-7.42 (m, 8H, aryl); 7.57 (d, 2H, aryl, J=8.2 Hz); 8.06 (s, 1H, aryl); 8.78 (d, 1H, aryl, J=8.8 Hz); 10.33 (s, 1H, CONH). HR-MS m/z: calcd for C$_{29}$H$_{31}$F$_3$N$_3$O$_5$, [(M+H)$^+$]: 588.2216; found 588.2212.

Benzyl (3-nitro-4-octanamidophenyl)(4-(trifluoromethyl)benzyl)carbamate (42).

Synthesized from **40** and octanoyl chloride following the general procedure B (yield 68%). ^{1}H NMR (CDCl$_3$, 400 MHz): δ: 0.91 (t, 3H, CH_3, J=6.6 Hz); 1.29-1.34 (m, 8H, 4 CH_2); 1.74-1.78 (m, 2H, CH_2); 2.49 (t, 2H, CH_2, J=7.4 Hz); 4.97 (s, 2H, CH_2); 5.22 (s, 2H, CH_2); 7.25-7.36 (m, 8H, aryl); 7.57 (d, 2H, aryl, J=8.1 Hz); 8.08 (s, 1H, aryl); 8.78 (d, 1H, aryl, J=8.7 Hz); 10.33 (s, 1H, CONH). HR-MS m/z: calcd for C$_{30}$H$_{33}$F$_3$N$_3$O$_5$, [(M+H)$^+$]: 572.2372; found 572.2374.

Benzyl (4-decanamido-3-nitrophenyl)(4-(trifluoromethyl)benzyl)carbamate (43).

Synthesized from **40** and decanoyl chloride following the general procedure B (yield 62%). ^{1}H NMR (CDCl$_3$, 400 MHz) δ 0.92 (t, 3H, CH_3, J=6.8 Hz); 1.29-1.38 (m, 12H, 6 CH_2); 1.73-1.78 (m, 2H, CH_2); 2.49 (t, 2H, CH_2, J=7.5 Hz); 4.96 (s, 2H, CH_2); 5.21 (s, 2H, CH_2); 7.27-7.34 (m, 8H, aryl); 7.57 (d, 2H, aryl, J=8.3 Hz); 8.06 (s, 1H, aryl); 8.78 (d, 1H, aryl, J=8.9 Hz); 10.33 (s, 1H, CONH); HR-MS m/z: calcd for C$_{32}$H$_{37}$F$_3$N$_3$O$_5$, [(M+H)$^+$]: 600.2685; found 600.2688.

Benzyl (4-dodecanamido-3-nitrophenyl)(4-(trifluoromethyl)benzyl)carbamate (44).

Synthesized from **40** and dodecanoyl chloride following the general procedure B (yield 55%). ^{1}H NMR (CDCl$_3$, 400 MHz): δ: 0.91 (t, 3H, CH_3, J=6.7 Hz); 1.26-1.37 (m, 16H, 8 CH_2); 1.72-1.78 (m, 2H, CH_2); 2.49 (t, 2H, CH_2, J=7.6 Hz); 4.96 (s, 2H, CH_2); 5.21 (s, 2H, CH_2); 7.26-7.35 (m, 8H, aryl); 7.57 (d, 2H, aryl, J=8.4 Hz); 8.06 (s, 1H, aryl); 8.78 (d, 1H, aryl, J=8.6 Hz); 10.32 (s, 1H, CONH). HR-MS m/z: calcd for C$_{34}$H$_{41}$F$_3$N$_3$O$_5$, [(M+H)$^+$]: 628.2998; found 628.3001.

Benzyl (4-(3,3-dimethylbutanamido)-3-nitrophenyl)(4-(trifluoromethyl)benzyl)carbamate (45).

Synthesized from **40** and 3,3-dimethylbutyryl chloride following the general procedure B (yield 81%). ^{1}H NMR (CDCl$_3$, 400 MHz): δ: 1.13 (s, 9H, 3 CH_3); 2.35 (s, 2H, CH_2); 4.96 (s, 2H, CH_2); 5.21 (s, 2H, CH_2); 7.32-7.45 (m, 8H, aryl); 7.57 (d, 2H, aryl, J=8.3 Hz); 8.06 (s, 1H,

aryl); 8.80 (d, 1H, aryl, J=8.7 Hz); 10.26 (s, 1H, CONH). HR-MS m/z: calcd for $C_{28}H_{29}F_3N_3O_5$, $[(M+H)^+]$: 544.2059; found 544.2057.

Tert-butyl (4-(3,3-dimethylbutanamido)-3-nitrophenyl)(4-(trifluoromethyl)benzyl)carbamate (41').

Synthesized from **40'** and 3,3-dimethylbutyryl chloride following the general procedure B (yield 77%). ^{1}H NMR (CDCl$_3$, 400 MHz): δ: 1.12 (s, 9H, 3 CH_3); 1.46 (s, 9H, 3 CH_3); 2.27 (s, 2H, CH_2); 4.93 (s, 2H, CH_2); 7.36 (d, 2H, aryl, J=8.2 Hz); 7.44 (d, 1H, aryl, J=7.6 Hz); 7.59 (d, 2H, aryl, J=8.2 Hz); 8.08 (s 1H, aryl); 8.75 (d, 1H, aryl, J=8.7 Hz); 10.23 (s, 1H, CONH). HR-MS m/z: calcd for $C_{25}H_{31}F_3N_3O_5$, $[(M+H)^+]$: 510.2216; found 510.2219.

Benzyl (4-(cyclopropanecarboxamido)-3-nitrophenyl)(4-(trifluoromethyl)benzyl)carbamate (46).

Synthesized from **40** and cyclopropanecarbonyl chloride following the general procedure B (yield 77%). ^{1}H NMR (CDCl$_3$, 400 MHz): δ: 0.87-0.91 (m, 2H, CH_2); 0.94-1.00 (m, 2H, CH_2); 1.65-1.68 (t, 1H, CH); 4.96 (s, 2H, CH_2); 5.21 (s, 2H, CH_2); 7.25-7.37 (m, 8H, aryl); 7.57 (d, 2H, aryl, J=8.4 Hz); 8.06 (s, 1H, aryl); 8.75 (d, 1H, aryl, J=8.9 Hz); 10.55 (s, 1H, CONH). HR-MS m/z: calcd for $C_{26}H_{23}F_3N_3O_5$, $[(M+H)^+]$: 514.1590; found 514.1592.

Benzyl (4-(3-cyclohexylpropanamido)-3-nitrophenyl)(4-(trifluoromethyl)benzyl)carbamate (47).

Synthesized from **40** and 3-cyclohexylpropanoyl chloride following the general procedure B (yield 81%). ^{1}H NMR (CDCl$_3$, 400 MHz): δ: 0.92-1.00 (m, 2H, CH_2); 1.18-1.31 (m, 4H, 2 CH_2); 1.60-1.78 (m, 7H, 3 CH_2 and CH); 2.52 (t, 2H, CH_2, J=8.1 Hz); 4.96 (s, 2H, CH_2); 5.21 (s, 2H, CH_2); 7.25-7.36 (m, 8H, aryl); 7.57 (d, 2H, aryl, J=8.2 Hz); 8.06 (s, 1H, aryl); 8.77 (d, 1H, aryl, J=8.7 Hz); 10.32 (s, 1H, CONH). HR-MS m/z: calcd for $C_{31}H_{33}F_3N_3O_5$, $[(M+H)^+]$: 584.2372; found 584.2369.

Benzyl (4-(2-(2-methoxyethoxy)acetamido)-3-nitrophenyl)(4-(trifluoromethyl)benzyl)carbamate (48).

Synthesized from **40** and (2-methoxyethoxy)acetyl chloride following the general procedure B (yield 67%). ^{1}H NMR (CDCl$_3$, 400 MHz): δ: 3.42 (s, 3H, CH_3); 3.68 (t, 2H, CH_2, J=4.7 Hz); 4.40 (t, 2H, CH_2, J=4.7 Hz); 4.50 (s, 2H, CH_2); 5.21 (s, 2H, CH_2); 6.91-7.16 (m, 8H, aryl); 7.35

(d, 2H, aryl, J=8.2 Hz); 7.70 (s, 1H, aryl); 8.37 (d, 1H, aryl, J=8.4 Hz); 9.16 (s, 1H, CON*H*). HR-MS *m/z*: calcd for $C_{27}H_{27}F_3N_3O_7$, $[(M+H)^+]$: 562.1801; found 562.1800.

N-(2-amino-4-((4-(trifluoromethyl)benzyl)amino)phenyl)heptanamide (49).

Synthesized from **41** as an off-white solid in 86% yield using the general procedure E. ^{1}H NMR (CDCl$_3$, 400 MHz): δ: 0.81 (t, 3H, C*H*$_3$, J=6.5 Hz); 1.19-1.25 (m, 6H, 3 C*H*$_2$); 1.55-1.62 (m, 2H, C*H*$_2$); 2.25 (t, 2H, C*H*$_2$, J=7.6 Hz); 4.27 (s, 2H, C*H*$_2$); 5.95-6.00 (m, 2H, aryl); 6.65 (d, 1H, aryl, J=8.4 Hz); 7.42 (d, 2H, aryl, J=8.1 Hz); 7.48 (d, 2H, aryl, J=8.1 Hz). ^{13}C NMR (CD$_3$OD, 100 MHz) δ: 13.0; 22.2; 25.7; 28.7; 31.3; 35.8;100.9; 104.2; 114.1; 124.8; 126.9; 127.3; 128.4; 128.8; 142.9; 145.2; 148.0; 174.1. ^{19}F NMR (CDCl$_3$, 376.3 MHz) δ: -62.43 (3F, C*F*$_3$). HR-MS *m/z*: calcd for $C_{21}H_{27}F_3N_3O$, $[(M+H)^+]$: 394.2106; found 394.2098.

N-(2-amino-4-((4-(trifluoromethyl)benzyl)amino)phenyl)octanamide (50).

Synthesized from **42** as an off-white solid in 82% yield using the general procedure E. ^{1}H NMR (CD$_3$OD, 400 MHz): δ: 0.93 (t, 3H, C*H*$_3$, J=6.9 Hz); 1.34-1.40 (m, 8H, 4 C*H*$_2$); 1.67-1.74 (m, 2H, C*H*$_2$); 2.37 (t, 2H, C*H*$_2$, J=7.6 Hz); 4.40 (s, 2H, C*H*$_2$); 6.08-6.12 (m, 2H, aryl); 6.77 (d, 1H, aryl, J=8.4 Hz); 7.55 (d, 2H, aryl, J=8.3 Hz); 7.60 (d, 2H, aryl, J=8.3 Hz). ^{13}C NMR (CD$_3$OD, 100 MHz) δ: 13.0; 22.3; 25.8; 28.8; 29.0; 31.5; 35.8;100.7; 114.1; 124.8; 126.79; 126.82; 127.3; 128.4; 128.7; 129.2; 142.8; 145.2; 148.0; 174.1. ^{19}F NMR (CD$_3$OD, 376.3 MHz) δ: -63.86 (3F, C*F*$_3$). HR-MS *m/z*: calcd for $C_{22}H_{29}F_3N_3O$, $[(M+H)^+]$: 408.2263; found 408.2271.

N-(2-amino-4-((4-(trifluoromethyl)benzyl)amino)phenyl)decanamide (51).

Synthesized from **43** as an off-white solid in 83% yield using the general procedure E. ^{1}H NMR (CD$_3$OD, 400 MHz): δ: 0.92 (t, 3H, C*H*$_3$, J=7.0 Hz); 1.23-1.42 (m, 12H, 6 C*H*$_2$); 1.67-1.74 (m, 2H, C*H*$_2$); 2.37 (t, 2H, C*H*$_2$, J=7.6 Hz); 4.40 (s, 2H, C*H*$_2$); 6.07-6.12 (m, 2H, aryl); 6.78 (d, 1H, aryl, J=8.4 Hz); 7.55 (d, 2H, aryl, J=8.3 Hz); 7.60 (d, 2H, aryl, J=8.3 Hz). ^{13}C NMR (CD$_3$OD, 100 MHz) δ: 13.0; 22.3; 25.8; 29.0; 29.2; 31.6; 35.8;100.7; 104.2; 114.1; 124.8; 126. 9; 127.3; 142.8; 145.2; 148.0; 174.1. ^{19}F NMR (CDCl$_3$, 376.3 MHz) δ: -62.43 (3F, C*F*$_3$). HR-MS *m/z*: calcd for $C_{24}H_{33}F_3N_3O$, $[(M+H)^+]$: 436.2576; found 436.2582.

N-(2-amino-4-((4-(trifluoromethyl)benzyl)amino)phenyl)dodecanamide (52).

Synthesized from **44** as a white wax in 79% yield using the general procedure E. ^{1}H NMR (CD$_3$OD, 400 MHz): δ: 0.92 (t, 3H, C*H*$_3$, J=7.0 Hz); 1.23-1.38 (m, 16H, 8 C*H*$_2$); 1.67-1.74 (m, 2H, C*H*$_2$); 2.37 (t, 2H, C*H*$_2$, J=7.6 Hz); 4.39 (s, 2H, C*H*$_2$); 6.07-6.12 (m, 2H, aryl); 6.78 (d, 1H,

aryl, J=8.4 Hz); 7.55 (d, 2H, aryl, J=8.3 Hz); 7.60 (d, 2H, aryl, J=8.3 Hz). ^{13}C NMR (CD$_3$OD, 100 MHz) δ: 13.0; 22.3; 25.8; 29.0; 29.3; 31.7; 35.8; 100.7; 104.2; 114.1; 124.8; 126. 9; 127.3; 142.9; 145.2; 148.0; 174.1. ^{19}F NMR (CDCl$_3$, 376.3 MHz) δ: -62.43 (s, 3F, CF_3). HR-MS m/z: calcd for C$_{26}$H$_{37}$F$_3$N$_3$O, [(M+H)$^+$]: 464.2889; found 464.2885.

N-(2-amino-4-((4-(trifluoromethyl)benzyl)amino)phenyl)-3,3-dimethylbutanamide (53).

Synthesized from **45** as a white powder in 86% yield using the general procedure E. ^{1}H NMR (CD$_3$OD, 400 MHz): δ: 1.11 (s, 9H, 3 CH_3); 2.25 (s, 2H, CH_2); 4.40 (s, 2H, CH_2); 6.07-6.12 (m, 2H, aryl); 6.77 (d, 1H, aryl, J=8.4 Hz); 7.55 (d, 2H, aryl, J=8.3 Hz); 7.60 (d, 2H, aryl, J=8.3 Hz). ^{13}C NMR (CD$_3$OD, 100 MHz) δ: 28.9; 30.5; 49.2; 100.7; 104.2; 114.2; 124.79; 124.83; 126. 9; 127.3; 142.9; 145.2; 148.0; 172.4. ^{19}F NMR (CDCl$_3$, 376.3 MHz) δ: -62.43 (3F, CF_3). HR-MS m/z: calcd for C$_{20}$H$_{25}$F$_3$N$_3$O, [(M+H)$^+$]: 380.1950; found 380.1958.

Tert-butyl (3-amino-4-(3,3-dimethylbutanamido)phenyl)(4-(trifluoromethyl)benzyl)carbamate (42').

Synthesized from **41'** as a white powder in 84% yield using the general procedure E.
^{1}H NMR (CDCl$_3$, 400 MHz): δ: 1.11 (s, 9H, 3 CH_3); 1.44 (s, 9H, 3 CH_3); 2.25 (s, 2H, CH_2); 4.80 (s, 2H, CH_2); 6.51 (d, 1H, aryl, J=7.6 Hz); 6.58 (s 1H, aryl); 7.00 (s, 1H, aryl, J=7.5 Hz); 7.36 (d, 2H, aryl, J=8.2 Hz); 7.58 (d, 2H, aryl, J=8.2 Hz). HR-MS m/z: calcd for C$_{25}$H$_{33}$F$_3$N$_3$O$_3$, [(M+H)$^+$]: 480.2474; found 480.2475.

N-(2-amino-4-((4-(trifluoromethyl)benzyl)amino)phenyl)cyclopropanecarboxamide (54).

Synthesized from **46** as a gray powder in 81% yield using the general procedure E.
^{1}H NMR (CD$_3$OD, 400 MHz): δ: 0.84 (d, 2H, CH_2, J=6.9 Hz); 0.93 (s, 2H, CH_2); 1.77 (t, 1H, CH, J=4.0 Hz); 4.39 (s, 2H, CH_2); 6.08-6.12 (m, 2H, aryl); 6.81 (d, 1H, aryl, J=8.0 Hz); 7.55 (d, 2H, aryl, J=7.6 Hz); 7.60 (d, 2H, aryl, J=7.6 Hz). ^{13}C NMR (CD$_3$OD, 100 MHz) δ: 6.3; 13.5; 100.7; 104.2; 114.4; 124.8; 126.8; 127.3; 142.8; 145.3; 148.0; 174.2. ^{19}F NMR (CDCl$_3$, 376.3 MHz) δ: -62.44 (3F, CF_3). HR-MS m/z: calcd for C$_{18}$H$_{19}$F$_3$N$_3$O, [(M+H)$^+$]: 350.1480; found 350.1469.

N-(2-amino-4-((4-(trifluoromethyl)benzyl)amino)phenyl)-3-cyclohexylpropanamide (55).

Synthesized from **47** as an off-white solid in 78% yield using the general procedure E. ^{1}H NMR (CD$_3$OD, 400 MHz): δ: 0.93-1.02 (m, 2H, CH_2); 1.16-1.34 (m, 4H, 2 CH_2); 1.57-1.82 (m, 7H, 3 CH_2 and CH); 2.38 (t, 2H, CH_2, J=8.0 Hz); 4.39 (s, 2H, CH_2); 6.07-6.12 (m, 2H, aryl); 6.77

(d, 1H, aryl, J=8.4 Hz); 7.55 (d, 2H, aryl, J=8.2 Hz); 7.60 (d, 2H, aryl, J=8.2 Hz). ^{13}C NMR (CD$_3$OD, 100 MHz) δ: 26.0; 26.3; 32.85;33.36; 37.41; 100.7; 104.2; 114.1; 124.8; 126.9; 127.3; 142.9; 145.2; 148.0; 174.4. ^{19}F NMR (CDCl$_3$, 376.3 MHz) δ: -62.42 (3F, CF_3); HR-MS m/z: calcd for C$_{23}$H$_{29}$F$_3$N$_3$O, [(M+H)$^+$]: 420.2263; found 420.2271.

N-(2-amino-4-((4-(trifluoromethyl)benzyl)amino)phenyl)-2-(2-methoxyethoxy)acetamide (56).

Synthesized from **48** as a white powder in 71% yield using the general procedure E. ^{1}H NMR (CD$_3$OD, 400 MHz): δ: 3.41 (s, 3H, CH_3); 3.64 (d, 2H, CH_2, J=2.7 Hz); 3.78 (d, 2H, CH_2, J=2.7 Hz); 4.14 (s, 2H, CH_2); 4.40 (s, 2H, CH_2); 6.09-6.12 (m, 2H, aryl); 6.88 (d, 1H, aryl, J=8.3 Hz); 7.55 (d, 2H, aryl, J=7.8 Hz); 7.61 (d, 2H, aryl, J=7.8 Hz). ^{13}C NMR (CD$_3$OD, 100 MHz) δ: 46.7; 57.8; 70.1; 70.6; 71.4; 100.4; 104.0; 112.8; 124.8; 126.9; 127.3; 142.9; 145.2; 148.2; 170.3. ^{19}F NMR (CDCl$_3$, 376.3 MHz) δ: -62.42 (3F, CF_3). HR-MS m/z: calcd for C$_{19}$H$_{23}$F$_3$N$_3$O, [(M+H)$^+$]: 398.1692; found 398.1701.

Tert-butyl (4-(3,3-dimethylbutanamido)-3-(pyrrolidin-1-yl)phenyl)(4-(trifluoromethyl)benzyl)carbamate (57).

Intermediate **57** was synthesized slightly modifying the procedure previously described by Xu and coworkers.[196] Intermediate **17'** (1.0 eq) was dissolved in acetonitrile and added with K$_2$CO$_3$ (2 eq), KI (2 eq) and 1,4-dibromobutane (2.0 eq). The mixture was refluxed under stirring overnight. The organic phase was concentrated in vacuo and diluted with DCM. The DCM was then washed with K$_2$CO$_3$, dried over anhydrous Na$_2$SO$_4$, filtered and concentrated in vacuo. Crude product was purified using a linear gradient of n-hexane/ethyl acetate. ^{1}H NMR (CDCl$_3$, 400 MHz): δ: 1.13 (s, 9H, 3 CH_3); 1.43 (s, 9H, 3 CH_3); 1.59-1.62 (m, 2H, CH_2); 1.70-1.72 (m, 4H, 2 CH_2); 2.26 (s, 2H, CH_2); 2.92 (s, 4H, 2 CH_2); 4.84 (s, 2H, CH_2); 6.84 (d, 1H, aryl, J=8.7 Hz); 7.35 (d, 2H, aryl, J=8.2 Hz); 7.59 (d, 2H, aryl, J=8.2 Hz); 8.09 (s, 1H, aryl); 8.20 (d, 1H, aryl, J=8.4 Hz). HR-MS m/z: calcd for C$_{29}$H$_{39}$F$_3$N$_3$O$_3$, [(M+H)$^+$]: 534.2944; found 534.2947.

Tert-butyl (4-(3,3-dimethylbutanamido)-3-(piperidin-1-yl)phenyl)(4-(trifluoromethyl)benzyl)carbamate (58).

Intermediate **58** was synthesized reacting **42'** with 1,5-dibromopentane under the same experimental conditions described for **57**. ^{1}H NMR (CDCl$_3$, 400 MHz): δ: 1.13 (s, 9H, 3 CH_3); 1.43 (s, 9H, 3 CH_3); 1.92 (s, 4H, 2 CH_2); 2.26 (s, 2H, CH_2); 2.68 (s, 4H, 2 CH_2); 4.84 (s, 2H, CH_2); 6.89 (d, 1H, aryl, J=8.7 Hz); 7.36 (d, 2H, aryl, J=8.2 Hz); 7.57 (d, 2H, aryl, J=8.2 Hz);

8.35 (d, 1H, aryl, J=8.7 Hz); 8.44 (s, 1H, aryl). HR-MS *m/z*: calcd for $C_{29}H_{39}F_3N_3O_3$, [(M+H)$^+$]: 534.2944; found 534.2947.

3,3-dimethyl-N-(2-(pyrrolidin-1-yl)-4-((4-(trifluoromethyl)benzyl)amino)phenyl)butanamide (59).

Synthesized from **57** as a white solid in 92% yield following the general procedure E. ^{1}H NMR (CD$_3$OD, 400 MHz): δ: 1.10 (s, 9H, 3 C*H$_3$*); 1.87-1.90 (m, 4H, 2 C*H$_2$*); 2.22 (s, 2H, C*H$_2$*); 3.13 (t, 4H, 2 C*H$_2$*, J=6.5 Hz); 4.41 (s, 2H, C*H$_2$*); 6.14 (dd, 1H, aryl, J$_1$=6.0 Hz, J$_2$=2.5 Hz); 6.18 (d, 1H, aryl, J=2.4 Hz); 6.96 (d, 1H, aryl, J=8.4 Hz); 7.56 (d, 2H, aryl, J=8.3 Hz); 7.60 (d, 1H, aryl, J=8.4 Hz). ^{13}C NMR (CD$_3$OD, 100 MHz) δ: 24.6; 28.9; 30.7; 49.3; 50.2; 100.7; 104.1; 116.4; 124.79; 124.83; 127.4; 128.4; 145.4; 146.0; 146.1; 147.5; 172.7. ^{19}F NMR (CD$_3$OD, 376.3 MHz) δ: -63.84 (3F, C*F$_3$*); HR-MS *m/z*: calcd for $C_{24}H_{31}F_3N_3O$, [(M+H)$^+$]: 434.2419; found 434.2415.

3,3-dimethyl-N-(2-(piperidin-1-yl)-4-((4-(trifluoromethyl)benzyl)amino)phenyl)butanamide (60).

Synthesized from **58** as a white solid in 89% yield following the general procedure E. ^{1}H NMR (CDCl$_3$, 400 MHz): δ: 1.12 (s, 9H, 3 C*H$_3$*); 1.59 (d, 2H, C*H$_2$*, J=4.01 Hz); 1.70-1.73 (m, 4H, 2 C*H$_2$*); 2.23 (s, 2H, C*H$_2$*); 2.74 (t, 4H, 2 C*H$_2$*, J=4.7 Hz); 4.10 (bs, 1H. NH); 4.39 (s, 2H, C*H$_2$*); 6.39 (d, 1H, aryl, J=8.7 Hz); 6.44 (s, 1H, aryl); 7.49 (d, 2H, aryl, J=7.9 Hz); 7.60 (d, 2H, aryl, J=7.9 Hz); 8.16 (s, 1H, CON*H*), 8.20 (d, 1H, aryl, J=8.7 Hz). ^{13}C NMR (CDCl$_3$, 100 MHz) δ: 24.1; 27.0; 29.9; 48.2; 52.2; 53.7; 105.8; 108.8; 120.6; 122.8; 125.0; 125.50; 125.55; 127.6; 129.3; 129.6; 143.8; 144.1; 169.2. ^{19}F NMR (CDCl$_3$, 376.3 MHz) δ: -62.42 (3F, C*F$_3$*). HR-MS *m/z*: calcd for $C_{25}H_{33}F_3N_3O$, [(M+H)$^+$]: 448.2576; found 448.2577.

N-(2-amino-4-(methyl(4-(trifluoromethyl)benzyl)amino)phenyl)heptanamide (61).

Synthesized following the general procedure G from **49** and formaldehyde as a white powder in 67% yield. ^{1}H NMR (CD$_3$OD, 400 MHz): δ: 0.82 (t, 3H, C*H$_3$*, J=6.5 Hz); 1.19-1.31 (m, 6H, 3 C*H$_2$*); 1.56-1.63 (m, 2H, C*H$_2$*); 2.26 (t, 2H, C*H$_2$*, J=7.4 Hz); 2.89 (s, 3H, C*H$_3$*); 4.47 (s, 2H, C*H$_2$*); 6.08 (dd, 1H, aryl, J$_1$=7.1 Hz, J$_2$=1.5 Hz); 6.16 (s, 1H, aryl); 6.75 (d, 1H, aryl, J=8.6 Hz); 7.29 (d, 2H, aryl, J=7.8 Hz); 7.47 (d, 2H, aryl, J=7.8 Hz). ^{13}C NMR (CD$_3$OD, 100 MHz) δ: 13.0; 22.2; 25.7; 28.7; 31.3; 35.8; 37.85; 55.75; 100.8; 103.5; 114.2; 124.9; 126.9; 127.1; 142.9; 144.1; 149.2; 174.1. ^{19}F NMR (CDCl$_3$, 376.3 MHz) δ: -62.41 (3F, C*F$_3$*). HR-MS *m/z*: calcd for $C_{22}H_{29}F_3N_3O$, [(M+H)$^+$]: 408.2263; found 408.2257.

N-(2-amino-4-(methyl(4-(trifluoromethyl)benzyl)amino)phenyl)-3,3-dimethylbutanamide (62).

Synthesized following the general procedure G from **53** and formaldehyde as a white powder in 63% yield. ^{1}H NMR (CD$_3$OD, 400 MHz): δ: 1.12 (s, 9H, 3 CH_3); 2.26 (s, 2H, CH_2); 3.01 (s, 3H, CH_3); 4.60 (s, 2H, NH_2); 6.20 (dd, 1H, aryl, J$_1$=6.1 Hz, J$_2$=2.6 Hz); 6.28 (d, 1H, aryl, J=2.7 Hz); 6.87 (d, 1H, aryl, J=8.6 Hz); 7.41 (d, 2H, aryl, J=7.8 Hz); 7.59 (d, 2H, aryl, J=7.8 Hz). ^{13}C NMR (CD$_3$OD, 100 MHz) δ: 29.0; 30.5; 37.9; 49.2; 55.7; 100.9; 103.5; 114.3; 124.9; 125.8; 127.1; 128.5; 128.8; 142.9; 144.1; 149.1; 172.4. ^{19}F NMR (CD$_3$OD, 376.3 MHz) δ: -63.76 (3F, CF_3). HR-MS m/z: calcd for C$_{21}$H$_{27}$F$_3$N$_3$O, [(M+H)$^+$]: 394.2106; found 394.2111.

N-(2-amino-4-(propyl(4-(trifluoromethyl)benzyl)amino)phenyl)heptanamide (63).

Synthesized following the general procedure G from **49** and propionaldehyde as a white powder in 71% yield. ^{1}H NMR (CD$_3$OD, 400 MHz): δ: 0.82 (t, 3H, CH_3, J=6.5 Hz); 1.19-1.31 (m, 6H, 3 CH_2); 1.56-1.63 (m, 2H, CH_2); 2.26 (t, 2H, CH_2, J=7.4 Hz); 2.89 (s, 3H, CH_3); 4.47 (s, 2H, CH_2); 6.08 (dd, 1H, aryl, J$_1$=7.1 Hz, J$_2$=1.5 Hz); 6.16 (s, 1H, aryl); 6.75 (d, 1H, aryl, J=8.6 Hz); 7.29 (d, 2H, aryl, J=7.8 Hz); 7.47 (d, 2H, aryl, J=7.8 Hz). ^{13}C NMR (CD$_3$OD, 100 MHz) δ: 13.0; 22.2; 25.7; 28.7; 31.3; 35.8; 37.85; 55.75; 100.8; 103.5; 114.2; 124.9; 126.9; 127.1; 142.9; 144.1; 149.2; 174.1. ^{19}F NMR (CDCl$_3$, 376.3 MHz) δ: -62.41 (3F, CF_3). HR-MS m/z: calcd for C$_{22}$H$_{29}$F$_3$N$_3$O, [(M+H)$^+$]: 408.2263; found 408.2257.

N-(2-amino-4-(N-(4-(trifluoromethyl)benzyl)acetamido)phenyl)heptanamide (64).

Synthesized from **49** and acetyl chloride following the general procedure A as a white powder in 77% yield. ^{1}H NMR (CD$_3$OD, 400 MHz): δ: 0.92-0.98 (m, 6H, 2 CH_3); 1.31-1.45 (m, 6H, 3 CH_2); 1.67-1.74 (m, 4H, 2 CH_2); 2.37 (t, 2H, CH_2, J=7.6 Hz); 3.38 (t, 2H, CH_2, J=7.7 Hz); 4.62 (s, 2H, CH_2); 6.12 (dd, 1H, aryl, J$_1$=8.7 Hz, J$_2$=2.8 Hz); 6.21 (d, 1H, aryl, J=2.7 Hz); 6.82 (d, 1H, aryl, J=8.7 Hz); 7.41 (d, 2H, aryl, J=8.1 Hz); 7.58 (d, 2H, aryl, J=8.1 Hz). ^{13}C NMR (CD$_3$OD, 100 MHz) δ: 10.2; 13.0; 20.2; 22.2; 25.7; 28.7; 31.3; 35.8; 53.2; 53.9; 100.7; 103.5; 113.8; 124.9; 126.9; 142.9; 144.5; 148.0; 174.1. ^{19}F NMR (CD$_3$OD, 376.3 MHz) δ: -63.82 (3F, CF_3). HR-MS m/z: calcd for C$_{24}$H$_{33}$F$_3$N$_3$O, [(M+H)$^+$]: 436.2576; found 436.2583.

2-nitro-4-((4-(trifluoromethyl)benzyl)oxy)aniline (66).

To a solution of 4-amino-3-nitrophenol in DMF were added 4-(trifluoromethyl)benzyl bromide (1.2 eq), K$_2$CO$_3$ (1.2 eq) and a catalytic amount of KI (5% mol). The mixture was refluxed under magnetic stirring for 3 hours. After cooling to room temperature, the crude reaction was

reconstituted with DCM and extracted with an aqueous solution of Na_2CO_3 and brine. The organic phase was dried over Na_2SO_4, filtered and concentrated in vacuo. Intermediate **66** was obtained in 67% yield after flash-chromatographic purification using linear gradients of n-hexane/ethyl acetate as mobile phase. ^{1}H NMR (CDCl$_3$, 400 MHz): δ: 5.11 (s, 2H, C*H*$_2$); 5.94 (bs, 2H, N*H*$_2$); 6.81 (d, 1H, aryl, J=9.1 Hz); 6.16 (dd, 1H, aryl, J$_1$=6.1 Hz, J$_2$=3.0 Hz); 7.57 (d, 2H, aryl, J=8.0 Hz); 7.66-7.69 (m, 4H, aryl). HR-MS *m/z*: calcd for $C_{14}H_{12}F_2N_2O_3$, $[(M+H)^+]$: 313.0800; found 313.0805.

N-(2-nitro-4-((4-(trifluoromethyl)benzyl)oxy)phenyl)heptanamide (67).

Prepared from **66** in 65% yield following the general procedure B. ^{1}H NMR (CDCl$_3$, 400 MHz): δ: 0.81 (t, 3H, C*H*$_3$, J=6.8 Hz); 1.19-1.26 (m, 6H, 3 C*H*$_2$); 1.61-1.71 (m, 2H, C*H*$_2$); 2.39 (t, 2H, C*H*$_2$, J=7.7 Hz); 5.10 (s, 2H, C*H*$_2$); 7.22 (dd, 1H, aryl, J$_1$=6.1 Hz, J$_2$=3.0 Hz); 7.48 (d, 2H, aryl, J=7.9 Hz); 7.60 (d, 2H, aryl, J=7.9 Hz); 7.68 (d, 1H, aryl, J=6.4 Hz); 8.65 (d, 1H, aryl, J=8.7 Hz); 10.05 (s, 1H, CON*H*). HR-MS *m/z*: calcd for $C_{21}H_{24}F_3N_2O_4$, $[(M+H)^+]$: 425.1688; found 425.1691.

N-(2-amino-4-((4-(trifluoromethyl)benzyl)oxy)phenyl)heptanamide (68).

Synthesized according to the general procedure E starting from intermediate **67**. The final compound **68** was isolated in 89% yield as an off-white solid. ^{1}H NMR (CD$_3$OD, 400 MHz): δ: 0.82 (t, 3H, C*H*$_3$, J=6.6 Hz); 1.26-1.33 (m, 6H, 3 C*H*$_2$); 1.59-1.66 (m, 2H, C*H*$_2$); 2.37 (t, 2H, C*H*$_2$, J=7.6 Hz); 5.15 (s, 2H, C*H*$_2$); 6.96 (s, 1H, aryl); 7.04 (d, 1H, aryl, J=9.8 Hz); 7.13 (d, 1H, aryl, J=8.8 Hz); 7.55 (d, 2H, aryl, J=8.1 Hz); 7.60 (d, 2H, aryl, J=8.1 Hz). ^{13}C NMR (CD$_3$OD, 100 MHz) δ: 13.0; 22.2; 25.1; 28.7; 31.3; 35.6; 69.3; 110.2; 115.3; 124.6; 125.1; 126.5; 126.7; 127.5; 129.7; 130.0; 141.1; 157.4; 174.6. ^{19}F NMR (CD$_3$OD, 376.3 MHz) δ: -62.66 (3F, C*F*$_3$). HR-MS *m/z*: calcd for $C_{21}H_{26}F_3N_2O_2$, $[(M+H)^+]$: 395.1946; found 395.1948.

3-nitro-N[1]-(4-(trifluoromethoxy)benzyl)benzene-1,4-diamine (73).

Intermediate **73** was prepared in 56% yield from 2-nitrobenzene-1,4-diamine and 1-(bromomethyl)-4-(trifluoromethoxy)benzene following the general procedure C.

^{1}H NMR (CDCl$_3$, 400 MHz): δ: 4.32 (s, 2H, C*H*$_2$); 5.76 (bs, 2H, N*H*$_2$); 6.73 (d, 1H, aryl, J= 8.8 Hz); 6.87 (dd, 1H, aryl, J$_1$=6.4 Hz, J$_2$=2.7 Hz,); 7.22 (d, 2H, aryl, J=7.9 Hz); 7.33 (s, 1H, aryl,); 7.42 (d, 1H, aryl, J=7.9 Hz). HR-MS *m/z*: calcd for $C_{14}H_{13}F_3N_3O_3$, $[(M+H)^+]$: 328.0909; found 328.0911.

N^1-benzyl-3-nitrobenzene-1,4-diamine (74).

Intermediate **74** was prepared in 59% yield from 2-nitrobenzene-1,4-diamine and (bromomethyl)benzene following the general procedure C. ^{1}H NMR (CDCl$_3$, 400 MHz): δ: 4.32 (s, 2H, CH_2); 5.74 (bs, 2H, NH_2); 6.72 (d, 1H, aryl, J= 8.9 Hz); 6.88 (dd, 1H, aryl, J$_1$=6.6 Hz, J$_2$=2.8 Hz,); 7.22 (d, 2H, aryl, J=7.9 Hz); 7.31-7.39 (m, 6H, aryl,). HR-MS m/z: calcd for C$_{13}$H$_{14}$N$_3$O$_2$, [(M+H)$^+$]: 244.1086; found 244.1089.

4-(4-fluorophenethyl)-2-nitroaniline (75).

Intermediate **75** was prepared in 62% yield from 2-nitrobenzene-1,4-diamine and 1-(bromomethyl)-4-fluorobenzene following the general procedure C. ^{1}H NMR (CDCl$_3$, 400 MHz): δ: 2.92 (t, 2H, J= 6.8 Hz); 3.37 (t, 2H, J= 6.8 Hz); 5.73 (bs, 2H, NH_2); 6.72 (d, 1H, aryl, J=8.9 Hz); 6.81 (dd, 1H, aryl, J$_1$=6.2 Hz, J$_2$=2.7 Hz); 7.03 (t, 2H, aryl, J=8.6 Hz); 7.18-7.22 (m, 2H, aryl); 7.31 (d, 1H, aryl, J= 2.4 Hz). HR-MS m/z: calcd for C$_{14}$H$_{14}$FN$_3$O$_2$, [(M+H)$^+$]: 276.2857; found 276.2860.

N^1-(2,6-difluorobenzyl)-3-nitrobenzene-1,4-diamine (76).

Intermediate **76** was synthesized in 67% yield starting from 2-nitrobenzene-1,4-diamine and 2-(bromomethyl)-1,3-difluorobenzene following the general procedure C. ^{1}H NMR (CDCl$_3$, 400 MHz): δ: 4.32 (s, 2H, CH_2); 5.74 (bs, 2H, NH_2); 6.72 (d, 1H, aryl, J= 8.9 Hz); 6.89-6.93 (m, 3H, aryl); 7.21-7.28 (m, 1H, aryl); 7.46 (d, 1H, aryl, J= 2.8 Hz). HR-MS m/z: calcd for C$_{13}$H$_{14}$N$_3$O$_2$, [(M+H)$^+$]: 244.1086; found 244.1089.

Benzyl (4-amino-3-nitrophenyl)(4-(trifluoromethoxy)benzyl)carbamate (77).

Intermediate **77** was attained by Cbz protection of **73** in 65% yield following the general procedure D. ^{1}H NMR (CDCl$_3$, 400 MHz): δ: 4.84 (s, 2H, CH_2); 5.19 (s, 2H, CH_2); 6.09 (bs, 2H, NH_2); 6.72 (d, 1H, aryl, J= 8.8 Hz); 7.15 (d, 2H, aryl, J=8.0 Hz); 7.28-7.39 (m, 8H, aryl); 7.92 (s, 1H, aryl). HR-MS m/z: calcd for C$_{22}$H$_{19}$F$_3$N$_3$O$_5$, [(M+H)$^+$]: 432.1277; found 462.1279.

Benzyl (4-amino-3-nitrophenyl)(benzyl)carbamate (78).

Intermediate **78** was attained by Cbz protection of **74** in 71% yield following the general procedure D. ^{1}H NMR (CDCl$_3$, 400 MHz): δ: 4.85 (s, 2H, CH_2); 5.20 (s, 2H, CH_2); 6.06 (bs, 2H, NH_2); 6.69 (d, 1H, aryl, J= 8.7 Hz); 7.20 (d, 2H, aryl, J=8.1 Hz); 7.23-7.28 (m, 5H, aryl,); 7.35-7.39 (m, 3H, aryl); 7.92 (s, 1H, aryl). HR-MS m/z: calcd for C$_{21}$H$_{20}$N$_3$O$_4$, [(M+H)$^+$]: 378.1454; found 378.1451.

Benzyl (4-amino-3-nitrophenyl)(4-fluorophenethyl)carbamate (79).

Intermediate **79** was attained by Cbz protection of **75** in 62% yield following the general procedure D. ^{1}H NMR (CDCl$_3$, 400 MHz): δ: 2.87 (t, 2H, CH_2, J=7.0 Hz); 3.87 (t, 2H, CH_2, J=7.0 Hz); 5.15 (s, 2H, CH_2); 6.13 (bs, 2H, NH_2); 6.75 (d, 1H, aryl, J=8.7 Hz); 6.95 (t, 2H, aryl, J=8.4 Hz); 7.02-7.15 (m, 5H, aryl); 7.20-7.40 (m, 3H, aryl); 7.88 (s, 1H, aryl). HR-MS *m/z*: calcd for C$_{22}$H$_{21}$FN$_3$O$_4$, [(M+H)$^+$]: 410.1511; found 410.1515.

Benzyl (4-amino-3-nitrophenyl)(2,6-difluorobenzyl)carbamate (80).

Intermediate **80** was attained by Cbz protection of **76** in 69% yield following the general procedure D. ^{1}H NMR (CD$_3$OD, 400 MHz): δ: 5.09 (s, 2H, CH_2); 5.22 (s, 2H, CH_2); 6.88 (t, 2H, aryl, J=8.1 Hz); 7.26-7.48 (m, 8H, aryl); 7.95 (s, 1H, aryl); 8.22 (d, 1H, aryl, J=9.0 Hz). HR-MS *m/z*: calcd for C$_{21}$H$_{18}$F$_2$N$_3$O$_4$, [(M+H)$^+$]: 414.1216; found 414.1218.

Benzyl (4-heptanamido-3-nitrophenyl)(4-(trifluoromethoxy)benzyl)carbamate (81).

Intermediate **81** was attained from **77** and heptanoyl chloride in 78% yield following the general procedure B. ^{1}H NMR (CDCl$_3$, 400 MHz): δ: 0.91 (t, 3H, CH_3, J=6.7 Hz); 1.23-1.30 (m, 6H, 3 CH_2); 1.72-1.78 (m, 2H, CH_2); 2.49 (t, 2H, CH_2, J=7.6 Hz); 4.90 (s, 2H, CH_2); 5.21 (s, 2H, CH_2); 6.09 (bs, 2H, NH_2); 6.72 (d, 1H, aryl, J= 8.8 Hz); 7.15 (d, 2H, aryl, J=8.0 Hz); 7.28-7.39 (m, 8H, aryl); 7.92 (s, 1H, aryl); 10.32 (s, 1H, CONH). HR-MS *m/z*: calcd for C$_{29}$H$_{31}$F$_3$N$_3$O$_6$, [(M+H)$^+$]: 574.2165; found 574.2169.

Benzyl benzyl(4-heptanamido-3-nitrophenyl)carbamate (82).

Intermediate **82** was attained from **78** and heptanoyl chloride in 75% yield following the general procedure B. ^{1}H NMR (CDCl$_3$, 400 MHz): δ: 0.91 (t, 3H, CH_3, J=6.7 Hz); 1.29-1.41 (m, 6H, 3 CH_2); 1.72-1.79 (m, 2H, CH_2); 2.48 (t, 2H, CH_2, J=7.6 Hz); 4.92 (s, 2H, CH_2); 5.22 (s, 2H, CH_2); 7.20 (dd, 2H, aryl, J$_1$=6.0 Hz, J$_2$=; 1.3 Hz); 7.28-7.42 (m, 9H, aryl); 8.04 (s, 1H, aryl); 8.75 (d, 1H, aryl, J=9.1 Hz); 10.31 (s, 1H, CONH). HR-MS *m/z*: calcd for C$_{28}$H$_{32}$N$_3$O$_5$, [(M+H)$^+$]: 490.2342; found 490.2337.

Benzyl 4-fluorophenethyl(4-heptanamido-3-nitrophenyl)carbamate (83).

Intermediate **83** was attained from **79** and heptanoyl chloride in 72% yield following the general procedure B. ^{1}H NMR (CDCl$_3$, 400 MHz): δ: 0.91 (t, 3H, CH_3, J=6.8 Hz); 1.29-1.42 (m, 6H, 3 CH_2); 1.76-1.80 (m, 2H, CH_2); 2.51 (t, 2H, CH_2, J=7.7 Hz); 2.88 (t, 2H, CH_2, J=7.2 Hz); 3.93 (t, 2H, CH_2, J=7.2 Hz); 5.16 (s, 2H, CH_2); 6.95 (t, 2H, aryl, J=8.6 Hz); 7.05-7.08 (m, 2H, aryl);

7.05-7.38 (m, 6H, aryl); 7.93 (s, 1H, aryl); 8.79 (d, 1H, aryl, J=8.9 Hz); 10.35 (s, 1H CONH). HR-MS m/z: calcd for $C_{29}H_{33}FN_3O_5$, [(M+H)$^+$]: 522.2404; found 522.2410.

Benzyl 2,6-difluorobenzyl(4-(3,3-dimethylbutanamido)-3-nitrophenyl)carbamate (84).

Intermediate **84** was attained from **80** and heptanoyl chloride in 70% yield following the general procedure B. ^{1}H NMR (CDCl$_3$, 400 MHz): δ: 1.13 (s, 9H, 3 CH_3); 2.34 (s, 2H, CH_2); 5.07 (s, 2H, CH_2); 5.20 (s, 2H, CH_2); 6.82 (t, 2H, aryl, J=7.9 Hz); 7.19-7.43 (m, 7H, aryl); 8.04 (s, 1H, aryl); 8.78 (d, 1H, aryl, J=9.1 Hz); 10.30 (s, 1H, CONH). HR-MS m/z: calcd for $C_{27}H_{28}F_2N_3O_5$, [(M+H)$^+$]: 512.1992; found 512.1996.

N-(2-amino-4-((4-(trifluoromethoxy)benzyl)amino)phenyl)heptanamide (85).

Final product **85** was synthesized in 84% yield as a white powder by reduction of intermediate **81** under the conditions described in the general procedure E. ^{1}H NMR (DMSO-d6, 400 MHz): δ: 0.87 (t, 3H, CH_3, J=6.5 Hz); 1.27 (bs, 6H, 3 CH_2); 1.53-1.57 (m, 2H, CH_2); 2.22 (t, 2H, CH_2, J=7.4 Hz); 4.22 (d, 2H, CH_2, J=6.0 Hz); 4.51 (bs, 2H, NH_2); 5.84 (d, 1H, aryl, J=8.4 Hz); 5.95-5.97 (m, 1H, aryl); 6.70 (d, 1H, aryl, J=8.4 Hz); 7.04 (d, 1H, aryl, J=9.8 Hz); 7.30 (d, 1H, aryl, J=8.2 Hz); 7.45 (d, 2H, aryl, J=8.3 Hz); 7.60 (d, 2H, aryl, J=8.3 Hz); 8.80 (s, 1H, CONH). ^{13}C NMR (DMSO-d6, 100 MHz) δ: 14.4; 22.5; 25.8; 28.8; 31.5; 36.1; 46.3; 99.7; 102.2; 114.2; 119.3; 121.9; 127.2; 129.2; 140.8; 143.7; 147.5; 171.6. ^{19}F NMR (CDCl$_3$, 376.3 MHz) δ: -62.66 (3F, CF_3). HR-MS m/z: calcd for $C_{21}H_{27}F_3N_3O_2$, [(M+H)$^+$]: 410.2055; found 410.2059.

N-(2-amino-4-(benzylamino)phenyl)heptanamide (86).

Final product **86** was synthesized in 87% yield as a white powder by reduction of intermediate **82** under the conditions described in the general procedure E. ^{1}H NMR (CD$_3$OD, 400 MHz): δ: 0.82 (t, 3H, CH_3, J=6.4 Hz); 1.19-1.25 (m, 6H, 3 CH_2); 1.55-1.62 (m, 2H, CH_2); 2.25 (t, 2H, CH_2, J=7.6 Hz); 4.17 (s, 2H, CH_2); 5.99 (d, 1H, aryl, J=8.4 Hz); 6.04 (s, 1H, aryl); 6.65 (d, 1H, aryl, J=8.4 Hz); 7.07-7.11 (m, 1H, aryl); 7.17 (t, 1H, aryl, J=7.2 Hz); 7.24 (d, 2H, aryl, J=7.4 Hz). ^{13}C NMR (CD$_3$OD, 100 MHz) δ: 13.0; 22.2; 25.7; 28.7; 31.3; 35.8; 100.9; 104.3; 114.0; 126.3; 126.8; 126.9; 128.0; 140.2; 142.7; 148.4; 174.1. HR-MS m/z: calcd for $C_{20}H_{28}N_3O$, [(M+H)$^+$]: 326.2232; found 326.2230.

N-(2-amino-4-((4-fluorophenethyl)amino)phenyl)heptanamide (87).

Final product **87** was synthesized in 87% yield as an off-white powder by reduction of intermediate **83** under the conditions described in the general procedure E. ^{1}H NMR (CD$_3$OD,

400 MHz): δ: 0.94 (t, 3H, C*H₃*, J=6.8 Hz); 1.35-1.43 (m, 6H, 3 C*H₂*); 1.68-1.76 (m, 2H, C*H₂*); 2.38 (t, 2H, C*H₂*, J=7.6 Hz); 2.86 (t, 2H, C*H₂*, J=7.2 Hz); 3.29 (t, 2H, C*H₂*, J=7.6 Hz); 6.11 (dd, 1H, aryl, J_1=6.0 Hz, J_2=2.4 Hz); 6.19 (d, 1H, aryl, J=2.4 Hz); 6.82 (d, 1H, aryl, J=8.4 Hz); 7.02 (t, 2H, aryl, J=8.8 Hz); 7.23-7.27 (m. 2H, aryl). ¹³C NMR (CD₃OD, 100 MHz) δ: 13.0; 22.2; 25.7; 28.7; 31.3; 34.2; 35.8; 45.3; 100.8; 104.3; 114.2; 114.7; 126.9; 130.1; 135.8; 142.9; 148.2; 160.3; 162.7; 174.1. ¹⁹F NMR (CDCl₃, 376.3 MHz) δ: -62.41 (1F, C*F*). HR-MS *m/z*: calcd for $C_{21}H_{29}FN_3O$, [(M+H)⁺]: 358.2295; found 358.2296.

N-(2-amino-4-((2,6-difluorobenzyl)amino)phenyl)-3,3-dimethylbutanamide (88).

Final product **88** was synthesized in 83% yield as a pink powder by reduction of intermediate **84** under the conditions described in the general procedure E. ¹H NMR (CD₃OD, 400 MHz): δ: 1.11 (s, 9H, 3 C*H₃*); 2.24 (s, 2H, C*H₂*); 4.35 (s, 2H, C*H₂*); 6.18 (d, 1H, aryl, J_1=6.0 Hz, J_2=2.5 Hz); 6.26 (d, 1H, aryl, J=2.5 Hz); 6.79 (d, 1H, aryl, J=8.4 Hz); 6.95 (t, 2H, aryl, J=8.1 Hz); 7.26-7.33 (m, 1H, aryl). ¹³C NMR (CD₃OD, 100 MHz) δ: 29.0; 35.4; 49.2; 101.2; 104.1; 110.8; 111.0; 114.7; 114.9; 115.1; 115.3; 126.9; 129.1; 129.2; 129.3; 142.9; 147.7; 160.5; 160.6, 162.9; 163.0; 172.4. ¹⁹F NMR (CDCl₃, 376.3 MHz) δ: -117.3 (2F, C*F*); HR-MS *m/z*: calcd for $C_{19}H_{24}F_2N_3O$, [(M+H)⁺]: 348.1882; found 348.1889.

3-nitro-N¹-(pyridin-2-ylmethyl)benzene-1,4-diamine (69).

Synthesized in 54% yield from 2-nitrobenzene-1,4-diamine and pyridine 2-carboxaldehyde using the reductive amination conditions described for the general procedure G. ¹H NMR (CDCl₃, 400 MHz): δ: 4.86 (s, 2H, C*H₂*); 5.75 (bs, 2H, N*H₂*); 6.74 (d, 1H, aryl, J=8.8 Hz); 6.98 (dd, 1H, aryl, J_1=6.2 Hz, J_2=2.6 Hz); 7.25-7.39 (m, 3H, aryl); 7.72-7.75 (m, 1H, aryl); 8.61 (d, 1H, aryl, J=3.9 Hz). HR-MS *m/z*: calcd for $C_{12}H_{13}N_4O_2$, [(M+H)⁺]: 245.1039; found 245.1042.

Benzyl (4-amino-3-nitrophenyl)(pyridin-2-ylmethyl)carbamate (70).

Synthesized in 78% yield from **69** using the conditions described for Cbz protection in the general procedure D. ¹H NMR (CDCl₃, 400 MHz): δ: 4.97 (s, 2H, C*H₂*); 5.19 (s, 2H, C*H₂*); 6.10 (bs, 2H, N*H₂*); 6.73 (d, 1H, aryl, J=8.8 Hz); 7.18-7.34 (m, 8H, aryl); 7.64-7.68 (m, 1H, aryl); 8.04 (s, 1H, aryl); 8.55 (d, 1H, aryl, J=3.8 Hz). HR-MS *m/z*: calcd for $C_{20}H_{19}N_4O_4$, [(M+H)⁺]: 379.1406; found 379.1403.

Benzyl (4-heptanamido-3-nitrophenyl)(pyridin-2-ylmethyl)carbamate (71).

Synthesized in 81% yield from **70** and heptanoyl chloride as described in the general procedure B. ^{1}H NMR (CDCl$_3$, 400 MHz): δ: 0.94 (t, 3H, C*H*$_3$, J=6.8 Hz); 1.35-1.43 (m, 6H, 3 C*H*$_2$); 1.68-1.76 (m, 2H, C*H*$_2$); 2.48 (t, 2H, C*H*$_2$, J=7.6 Hz); 5.01 (s, 2H, C*H*$_2$); 5.20 (s, 2H, C*H*$_2$); 7.19-7.32 (m, 7H, aryl); 7.63-7.67 (m, 1H, aryl); 8.26 (s, 1H, aryl); 8.56 (d, 1H, aryl, J=3.7Hz); 8.76 (d, 1H, aryl, J=9.1 Hz); 10.31 (s, 1H, CON*H*). HR-MS *m/z*: calcd for C$_{27}$H$_{31}$N$_4$O$_5$, [(M+H)$^+$]: 491.2294; found 491.2297.

N-(2-amino-4-((pyridin-2-ylmethyl)amino)phenyl)heptanamide (72).

Final product **72** was synthesized as an off-white solid starting from **71** and using the reaction conditions described in the general procedure E. ^{1}H NMR (CD$_3$OD, 400 MHz): δ: 0.94 (t, 3H, C*H*$_3$, J=6.8 Hz); 1.31-1.43 (m, 6H, 3 C*H*$_2$); 1.67-1.74 (m, 2H, C*H*$_2$); 2.37 (t, 2H, C*H*$_2$, J=7.7 Hz); 4.41 (s, 2H, C*H*$_2$); 6.06-6.08 (dd, 1H, aryl, J$_1$=2.3 Hz, J$_2$=8.4 Hz); 6.12 (d, 1H, aryl, J=2.4 Hz); 6.78 (d, 1H, aryl, J=8.0); 7.28 (t, 1H, aryl, J=6.7 Hz); 7.47 (d. 1H, aryl, J=8.0 Hz); 7.74-7.78 (m, 1H, aryl); 8.48 (d, 1H, aryl, J=4.5 Hz). ^{13}C NMR (CD$_3$OD, 100 MHz) δ: 13.0; 22.2; 25.7; 28.7; 31.4; 36.6; 49.1; 100.8; 109.5; 112.9; 115.0; 115.9; 128.0; 128.7; 128.9; 130.2; 133.8; 156.5; 173.3. HR-MS *m/z*: calcd for C$_{19}$H$_{27}$N$_4$O, [(M+H)$^+$]: 327.2185; found 327.2191.

Tert-butyl (4-amino-3-nitrophenyl)carbamate (89).

Synthesized in 67% yield from 2-nitrobenzene-1,4-diamine using the conditions described for Boc protection in the general procedure D. ^{1}H NMR (CDCl$_3$, 400 MHz): δ: 1.53 (s, 9H, 3 C*H*$_3$); 5.95 (bs, 2H, N*H*$_2$); 6.46 (s, 1H, N*H*); 6.77 (d, 1H, aryl, J=9.0 Hz); 7.52 (s, 1H, aryl); 8.06 (s, 1H, aryl). HR-MS *m/z*: calcd for C$_{11}$H$_{16}$N$_3$O$_4$, [(M+H)$^+$]: 254.1141; found 254.1146.

Tert-butyl (4-heptanamido-3-nitrophenyl)carbamate (90).

Intermediate **90** was synthesized in 72% yield by acylation of **89** following the general procedure B. ^{1}H NMR (CDCl$_3$, 400 MHz): δ: 0.91 (t, 3H, C*H*$_3$, J=6.6 Hz); 1.28-1.40 (m, 6H, 3 C*H*$_2$); 1.52 (s, 9H, 3 C*H*$_3$); 1.75-1.78 (m, 2H, C*H*$_2$); 2.48 (t, 2H, C*H*$_2$, J=7.8 Hz); 6.78 (bs, 1H, N*H*); 7.54 (d, 1H, aryl J=7.4 Hz); 8.40 (s, 1H, aryl); 8.71 (d, 1H, aryl, J=9.1 Hz); 10.17 (s, 1H CON*H*). HR-MS *m/z*: calcd for C$_{18}$H$_{28}$N$_3$O$_5$, [(M+H)$^+$]: 366.2029; found 366.2035.

N-(4-amino-2-nitrophenyl)heptanamide (91).

Intermediate **91** was synthesized in 88% yield from **90** following the method for Boc removal described in the general procedure F. ^{1}H NMR (CDCl$_3$, 400 MHz): δ: 0.91 (t, 3H, C*H*$_3$, J=6.6

Hz); 1.27-1.40 (m, 6H, 3 CH_2); 1.73-1.77 (m, 2H, CH_2); 2.45 (t, 2H, CH_2, J=7.8 Hz); 4.51 (bs, 2H, NH_2); 6.98 (d, 1H, aryl J=7.2 Hz); 7.47 (s, 1H, aryl); 8.48 (d, 1H, aryl, J=9.3 Hz); 9.94 (s, 1H CONH). HR-MS *m/z*: calcd for $C_{13}H_{20}N_3O_3$, [(M+H)$^+$]: 266.1505; found 266.1509.

N-(2-amino-4-((pyridin-4-ylmethyl)amino)phenyl)heptanamide (92).

Compound **92** was synthesized slightly modifying the last stages of the general procedure F. In particular, intermediate **91** (1.0 eq) was dissolved in MeOH and added with pyridine 4-carboxaldehyde (1.2 eq) and TFA (1.0 eq). The reaction was refluxed under stirring for 3 hours. Upon cooling the reaction mixture to 0°C, Pd/C 10% (6% mol) was added together with NaBH$_4$ (3.0 eq). In this way, simultaneous reduction of the imine intermediate and of the 2-nitro group was attained. The resulting solution was filtered through Celite 503, concentrated and reconstituted in DCM. Extraction with aqueous K_2CO_3 and brine, separation of the organic phase, drying over anhydrous Na_2SO_4, filtration and concentration in vacuo led to the crude products which was purified by flash chromatography. Final product **53** was isolated as a grey oil in 57% yield. ^{1}H NMR (CD$_3$OD, 400 MHz): δ: 0.94 (t, 3H, CH_3, J=6.7 Hz); 1.34-1.43 (m, 6H, 3 CH_2); 1.67-1.74 (m, 2H, CH_2); 2.37 (t, 2H, CH_2, J=7.6 Hz); 4.38 (s, 2H, CH); 6.04-6.09 (m, 2H, aryl); 6.78 (t, 1H, aryl, J=8.4); 7.43 (d, 2H, aryl, J=6.7 Hz); 8.43 (d, 2H, aryl, J=5.5 Hz). ^{13}C NMR (CD$_3$OD, 100 MHz) δ: 13.0; 22.2; 25.7; 28.7; 31.3; 35.8; 46.0; 100.5; 103.9; 114.2; 122.5; 127.0; 143.0; 147.8; 148.4; 151.8; 174.1. HR-MS *m/z*: calcd for $C_{19}H_{27}N_4O$, [(M+H)$^+$]: 327.2185; found 327.2179.

N-(2-amino-4-((2-fluorobenzyl)amino)phenyl)heptanamide (93).

Compound **93** was synthesized as a white powder in 66% yield starting from **91** and 2-fluoro carboxaldehyde using the same procedure described above for **92**. ^{1}H NMR (CD$_3$OD, 400 MHz): δ: 0.94 (t, 3H, CH_3, J=6.6 Hz); 1.31-1.43 (m, 6H, 3 CH_2); 1.67-1.74 (m, 2H, CH_2); 2.37 (t, 2H, CH_2, J=7.5 Hz); 4.35 (s, 2H, CH_2); 6.11 (d, 1H, aryl, J=8.5 Hz); 6.16 (s, 1H, aryl); 6.78 (d, 1H, aryl, J=8.5 Hz); 7.06-7.11 (m, 2H, aryl); 7.22-7.27 (m, 1H, aryl); 7.40 (t, 1H, aryl, J=7.4 Hz). ^{13}C NMR (CD$_3$OD, 100 MHz) δ: 13.0; 22.2; 25.7; 28.7; 31.3; 35.8; 40.6; 100.7; 104.1; 114.2; 114.4; 114.6; 123.7; 126.9; 128.1; 129.01; 129.06; 142.9; 148.1; 159.7; 162.1; 174.1. ^{19}F NMR (CDCl$_3$, 376.3 MHz) δ: -119.13 (1F, CF). HR-MS *m/z*: calcd for $C_{20}H_{27}FN_3O$, [(M+H)$^+$]: 344.2138; found 344.2141.

Benzyl (4-formylphenyl) carbonate (95).

Intermediate **95** was attained in 72% yield by Cbz protection of the phenol moiety in 4-Hydroxybenzaldehyde as described in the general procedure D. ^{1}H NMR (CDCl$_3$, 400 MHz): δ: 5.32 (s, 2H, CH_2); 7.39-7.46 (m, 7H, aryl); 7.95 (d, 2H, aryl, 7.9 Hz); 10.02 (s, COH). HR-MS m/z: calcd for C$_{15}$H$_{13}$O$_4$, [(M+H)$^+$]: 257.0814; found 257.0821.

Benzyl (4-(hydroxymethyl)phenyl) carbonate (96).

Intermediate **96** was synthesized from **95**. Briefly, **95** (1.0 eq) was dissolved in methanol and the solution cooled in an ice bath before portionwise addition of 3 equivalents of NaBH$_4$. After warming to room temperature, the reaction was stirred for further 15 minutes. The reaction mixture was quenched with aqueous 2N HCl. The aqueous phase was extracted with ethyl acetate and the resulting organic phase washed two times with brine, dried over anhydrous Na$_2$SO$_4$, filtered and evaporated *in vacuo*. After flash chromatographic purification, **96** was obtained in 81% yield. ^{1}H NMR (CDCl$_3$, 400 MHz) δ 4.63 (d, 2H, CH_2, J=3.5 Hz); 5.29 (s, 2H, CH_2); 7.17 (d, 2H, aryl, J= 8.4 Hz); 7.35 (d, 2H, aryl, J= 8.4 Hz); 7.41-7.48 (m, 5H, aryl,). HR-MS m/z: calcd for C$_{15}$H$_{15}$O$_4$, [(M+H)$^+$]: 259.0970; found 259.0973.

Benzyl (4-(iodomethyl)phenyl) carbonate (97).

Synthesized from **96**. Iodine (1.5 eq) and triphenylphosphine (1.5 eq) were solubilized in dry DCM and stirred under a nitrogen stream for 1.5h. Then, 1.5 equivalents of imidazole were added, and the solution was stirred for further 1 hour. Intermediate **96** (1.0 eq) was added to the resulting slurry, that was stirred at room temperature overnight. The resulting suspension was quenched with a saturated aqueous solution of Na$_2$S$_2$O$_3$, the organic layer was separated and further washed with brine. The resulting organic solution was dried over Na$_2$SO$_4$, filtered and concentrated in vacuo. Compound **97** was obtained in 62% yield after purification of the crude product by flash-chromatography using a linear gradient of n-hexane/ethyl acetate as mobile phase. ^{1}H NMR (CDCl$_3$, 400 MHz): δ: 4.47 (s, 2H, CH_2); 5.29 (s, 2H, CH_2); 7.14 (d, 2H, aryl, J= 8.6 Hz); 7.40-7.46 (m, 7H, aryl).

Benzyl (4-(((4-heptanamido-3-nitrophenyl)amino)methyl)phenyl) carbonate (98).

Intermediate **98** was synthesized in 59% yield starting from compounds **91** and **97** and following the method described in the general procedure C. ^{1}H NMR (CDCl$_3$, 400 MHz): δ: 0.90 (t, 3H, CH_3, J=6.6 Hz); 1.32-1.39 (m, 6H, 3 CH_2); 1.73-1.77 (m, 2H, CH_2); 2.45 (t, 2H, CH_2, J=7.6 Hz); 4.61 (s, 2H, CH_2); 4.66 (s, 2H, CH_2); 5.88 (bs, 1H, NH); 6.80-6.83 (m, 2H,

aryl); 7.03-7.10 (m, 3H, aryl,); 7.21-7.24 (m, 2H, aryl); 7.27-7.40 (m, 3H, aryl); 7.49 (d, 1H, aryl, J=2.5 Hz); 8.40 (d, 1H, aryl, J=9.2 Hz); 9.86 (s, 1H, CONH); HR-MS m/z: calcd for $C_{28}H_{32}N_3O_6$, [(M+H)$^+$]: 506.2291; found 506.2298.

N-(2-amino-4-((4-hydroxybenzyl)amino)phenyl)heptanamide (99).

Final product **99** was isolated as a dark gray powder in 82% yield starting from intermediate **98** and following the general procedure E for catalytic hydrogenation.

^{1}H NMR (CD$_3$OD, 400 MHz): δ: 0.94 (t, 3H, CH_3, J=6.5 Hz); 1.31-1.44 (m, 6H, 3 CH_2); 1.67-1.74 (m, 2H, CH_2); 2.37 (t, 2H, CH_2, J=7.6 Hz); 4.17 (s, 2H, CH_2); 6.12 (d, 1H, aryl, J=8.4 Hz); 6.18 (s, 1H, aryl); 6.72-6.79 (m, 3H, aryl); 7.18 (d, 2H, aryl, J=8.2 Hz). ^{13}C NMR (CD$_3$OD, 100 MHz) δ: 13.0; 22.2; 25.7; 28.7; 31.3; 35.8; 101.2; 104.5; 114.1; 114.7; 126.8; 128.3; 130.7; 142.7; 148.5; 156.0; 174.1. HR-MS m/z: calcd for $C_{20}H_{28}NO_2$, [(M+H)$^+$]: 342.2182; found 342.2171.

2-fluoro-N-(4-fluorobenzyl)-4-nitroaniline (101).

Synthesized in 72% yield from 2-fluoro-4-nitroaniline and 1-(bromomethyl)-4-fluorobenzene following the general procedure C. ^{1}H NMR (CDCl$_3$, 400 MHz): δ: 4.47 (d, 2H, CH_2, J=7.2 Hz); 5.05 (bs, 1H, NH); 6.63 (t, 1H, aryl, J= 8.8 Hz); 7.06-7.12 (m, 2H, aryl); 7.33 (dd, 2H, aryl, J$_1$=1.1 Hz, J$_2$=5.3 Hz); 7.91-8.00 (m, 2H, aryl,). HR-MS m/z: calcd for $C_{13}H_{13}$ F$_2$ N$_2$O$_2$, [(M+H)$^+$]: 265.0789; found 265.0791.

2-fluoro-N^1-(4-fluorobenzyl)benzene-1,4-diamine (102).

Obtained in 89% yield by reduction of intermediate **101** under the conditions described in the general procedure E. ^{1}H NMR (CDCl$_3$, 400 MHz): δ: 3.51 (bs, 2H, NH_2); 4.28 (s, 2H, CH_2); 6.36-6.39 (m, 1H, aryl); 6.48 (dd, 1H, aryl, J$_1$=10.2 Hz, J$_2$=2.5 Hz); 6.54 (t, 1H, aryl J=9.2 Hz); 7.04 (t, 2H, aryl J=8.7 Hz); 7.35 (dd, 2H, aryl, J$_1$=2.9 Hz, J$_2$=5.5 Hz). HR-MS m/z: calcd for $C_{13}H_{13}$ F$_2$ N$_2$, [(M+H)$^+$]: 235.1047; found 235.1050.

N-(3-fluoro-4-((4-fluorobenzyl)amino)phenyl)heptanamide (103).

Obtained in 48% yield as an off-white solid by reaction of intermediate **102** with heptanoyl chloride under the conditions described in the general procedure A. ^{1}H NMR (CD$_3$OD, 400 MHz): δ: 0.93 (t, 3H, CH_3, J=6.7 Hz); 1.31-1.39 (m, 6H, 3 CH_2); 1.66-1.73 (m, 2H, CH_2); 2.38 (t, 2H, CH_2, J=7.6 Hz); 4.52 (s, 2H, CH_2); 7.06-7.15 (m, 3H, aryl); 7.25 (d, 1H, aryl, J=8.7 Hz); 7.42 (dd, 2H, aryl, J$_1$=3.1 Hz, J$_2$=5.3 Hz); 7.72 (dd, 1H, aryl, J$_1$=11.4 Hz, J$_2$=1.8 Hz). ^{13}C NMR

(CD$_3$OD, 100 MHz) δ: 13.0; 22.2; 25.3; 28.6; 31.3; 36.5; 51.6; 107.4; 107.7; 115.2; 115.4; 115.8; 131.3; 152.9; 155.3; 161.9; 164.4; 173.4. ^{19}F NMR (CDCl$_3$, 376.3 MHz) δ: -117.01 (1F, C*F*); -120.97 (1F, C*F*). HR-MS *m/z*: calcd for C$_{20}$H$_{25}$F$_2$N$_2$O, [(M+H)$^+$]: 347.1935; found 347.1939.

2-fluoro-4-nitro-N^1-(4-(trifluoromethyl)benzyl)benzene-1,3-diamine (105).

2,3-difluoro-6-nitroaniline (1.0 eq), 4-trifluoromethyl benzylamine (1.2 eq), DIPEA (1.2 eq) and a catalytic amount of I$_2$ were dissolved in DMF. The solution was warmed for 4 hours at 170 °C. The reaction was washed successively with a saturated solution of Na$_2$S$_2$O$_3$, K$_2$CO$_3$ and brine. The organic phase was extracted, dried over anhydrous Na$_2$SO$_4$, filtered and concentrated in vacuo. Crude product was purified using a linear gradient of n-hexane/ethyl acetate giving intermediate **65** in 81% yield. ^{1}H NMR (CD$_3$OD, 400 MHz): δ: 4.49 (s, 2H, C*H*$_2$); 5.95 (dd, 1H, aryl, J$_1$=1.5 Hz, J$_2$=8.1 Hz); 7.42 (d, 2H, aryl, J= 8.0 Hz); 7.53 (d, 2H, aryl, J= 8.0 Hz); 7.64 (dd, 1H, aryl, J$_1$=8.0 Hz, J$_2$=1.7 Hz). HR-MS *m/z*: calcd for C$_{14}$H$_{12}$ F$_4$ N$_3$O$_2$, [(M+H)$^+$]: 330.0866; found 330.0862.

N-(2-amino-3-fluoro-4-((4-(trifluoromethyl)benzyl)amino)phenyl)heptanamide (106).

Synthesized in 59% yield as an off-white powder by reaction of intermediate **105** with heptanoyl chloride under the conditions described in the general procedure H.

^{1}H NMR (DMSO-d6, 400 MHz): δ: 0.87 (t, 3H, C*H*$_3$, J=6.7 Hz); 1.27-1.31 (m, 6H, 3 C*H*$_2$); 1.53-1.57 (m, 2H, C*H*$_2$); 2.24 (t, 2H, C*H*$_2$, J=7.4 Hz); 4.39 (d, 2H, C*H*$_2$, J=6.0 Hz); 4.57 (bs, 2H, N*H*$_2$); 5.78 (t, 1H, N*H*, J=8.8 Hz); 6.02 (t, 1H, aryl, J=5.8 Hz); 6.58 (d, 1H, aryl, J=8.4 Hz); 7.55 (d, 2H, aryl, J=8.0 Hz); 7.66 (d, 2H, aryl, J=8.0 Hz); 8.98 (s, 1H, CONH). ^{13}C NMR (DMSO-d6, 100 MHz) δ: 14.4; 22.5; 25.7; 28.8; 31.5; 36.0; 46.2; 100.1; 115.6; 121.5; 125.5; 127.6; 128.0; 131.4; 131.5; 134.5; 139.6; 141.8; 146.2; 171.9. ^{19}F NMR (CDCl$_3$, 376.3 MHz) δ: -60.72 (3F, C*F*$_3$); -154.89 (1F, C*F*). HR-MS *m/z*: calcd for C$_{21}$H$_{26}$F$_4$N$_3$O, [(M+H)$^+$]: 412.2012; found 412.2018.

N-(2-amino-3-fluoro-4-((4-(trifluoromethyl)benzyl)amino)phenyl)isobutyramide (107).

Synthesized in 62% yield as an off-white powder by reaction of intermediate **105** with isobutyryl chloride under the conditions described in the general procedure H.

^{1}H NMR (DMSO-d6, 400 MHz): δ: 1.06 (d, 6H, 2 C*H*$_3$, J=1.9 Hz); 2.54-2.59 (m, 1H, C*H*); 4.39 (d, 2H, CH$_2$, J=5.6 Hz); 4.54 (s, 2H, C*H*$_2$); 5.79 (t, 1H, aryl, J=8.6 Hz); 6.02 (t, 1H, N*H*, J=5.4 Hz); 6.59 (d, 1H, aryl, J=8.6 Hz); 7.55 (d, 2H, aryl, J=7.5 Hz); 7.66 (d, 2H, aryl, J=7.5 Hz); 8.96 (s, 1H, CON*H*). ^{13}C NMR (DMSO-d6, 100 MHz) δ: 20.1; 34.6; 46.2; 100.2; 115.5; 121.5;

125.6; 128.0; 131.5; 134.4; 134.5; 139.6; 141.9; 146.2; 175.8. ^{19}F NMR (DMSO-d6, 376.3 MHz) δ: -60.74 (3F, CF_3); -154.88 (1F, CF). HR-MS m/z: calcd for $C_{18}H_{20}F_4N_3O$, [(M+H)$^+$]: 37.1543; found 370.1549.

N-(2-amino-3-fluoro-4-((4-(trifluoromethyl)benzyl)amino)phenyl)-3-methylbutanamide (108).

Synthesized in 66% yield as an off-white powder by reaction of intermediate **105** with 3,3-dimethylbutanoyl chloride under the conditions described in the general procedure H. ^{1}H NMR (CD$_3$OD, 400 MHz): δ: 1.03 (d, 6H, 2 CH_3, J=6.6 Hz); 2.12-2.19 (m, 1H); 2.25 (d, 2H, CH_2, J=7.0 Hz); 4.47 (s, 2H, CH_2); 5.98 (t, 1H, aryl, J=8.8 Hz); 6.60 (dd, 1H, aryl, J$_1$=8.6 Hz, J$_2$=1.8 Hz); 7.55 (d, 2H, aryl, J=8.0 Hz); 7.60 (d, 2H, aryl, J=8.0 Hz). ^{13}C NMR (CD$_3$OD, 100 MHz) δ: 21.4; 26.2; 44.9; 46.3; 101.5; 115.2; 121.2; 124.9; 127.2; 135.0; 135.1; 140.1; 142.4; 145.0; 173.5. ^{19}F NMR (CDCl$_3$, 376.3 MHz) δ: -63.84 (3F, CF_3); -157.99 (1F, CF). HR-MS m/z: calcd for $C_{19}H_{22}F_4N_3O$, [(M+H)$^+$]: 384.1699; found 384.1691.

N-(2-amino-3-fluoro-4-((4-(trifluoromethyl)benzyl)amino)phenyl)-3,3-dimethylbutanamide (109).

Synthesized in 66% yield as a white powder by reaction of intermediate **105** with 3,3-dimethylbutanoyl chloride under the conditions described in the general procedure H. ^{1}H NMR (CD$_3$OD, 400 MHz): δ: 1.10 (s, 9H, 3 CH_3); 2.25 (s, 2H, CH_2); 4.47 (s, 2H, CH_2); 5.99 (t, 1H, aryl, J=8.8 Hz); 6.60 (dd, 1H, aryl, J$_1$=6.7 Hz, J$_2$=1.9 Hz); 7.54 (d, 2H, aryl, J=8.2 Hz); 7.60 (d, 2H, aryl, J=8.2 Hz); ^{13}C NMR (CD$_3$OD, 100 MHz) δ: 28.9; 46.3; 49.1; 101.5; 115.2; 121.2; 124.90; 124.93; 127.2; 130.9; 131.0; 135.0; 135.1; 140.2; 142.5; 145.0; 172.5. ^{19}F NMR (CD$_3$OD, 376.3 MHz) δ: -62.48 (3F, CF_3); -158.0 (1F, CF). HR-MS m/z: calcd for $C_{20}H_{24}F_4N_3O$, [(M+H)$^+$]: 398.1856; found 398.1867.

N-(2-amino-3-fluoro-4-((4-(trifluoromethyl)benzyl)amino)phenyl)-3-cyclohexylpropanamide (110).

Synthesized in 66% yield as a white powder by reaction of intermediate **105** with 3-cyclohexylpropanoyl chloride under the conditions described in the general procedure H. ^{1}H NMR (DMSO-d6, 400 MHz): δ: 0.86-0.92 (m, 2H, CH_2); 1.12-1.24 (m, 4H, 2 CH_2); 1.43-1.49 (m, 2H, CH_2); 1.62-1.72 (m, 3H, CH_2 and CH); 2.23-2.27 (m, 2H, CH_2); 4.39 (bs, 2H, NH_2); 4.56-4.57 (m, 2H, CH_2); 5.78 (t, 1H, NH, J=8.3 Hz); 6.00-6.04 (m, 1H, aryl); 6.56-6.58 (m, 1H, aryl); 7.55 (d, 2H, aryl, J=7.6 Hz); 7.67 (d, 2H, aryl, J=7.6 Hz); 8.97 (s, 1H, CONH). ^{13}C NMR

(DMSO-d6, 100 MHz) δ: 26.3; 26.6; 33.1; 33.3; 33.6; 37.3; 46.2; 100.1; 115.6; 121.5; 125.5; 127.6; 127.9; 128.0; 131.4; 134.4; 139.5; 141.8; 146.2; 172.1. ^{19}F NMR (CDCl$_3$, 376.3 MHz) δ: -62.54 (3F, CF_3); -154.87 (1F, CF). HR-MS m/z: calcd for C$_{23}$H$_{28}$F$_4$N$_3$O, [(M+H)$^+$]: 438.2169; found 438.2172.

2-fluoro-N^1-methyl-4-nitro-N^1-(4-(trifluoromethyl)benzyl)benzene-1,3-diamine (111).

To a solution of intermediate **105** (1.0 eq) in DMF, tBuOK (1.2 eq) and CH$_3$I (1.2 eq) were added and the reaction was maintained under microwave irradiation for 1 hour at 140 °C. The resulting slurry was then washed with an aqueous solution of K$_2$CO$_3$ and brine. The organic phase was extracted, dried over anhydrous Na$_2$SO$_4$, filtered and concentrated in vacuo. Crude product was purified using a linear gradient of n-exane/ethyl acetate. Intermediate **71** was isolated in 72% yield. ^{1}H NMR (CDCl$_3$, 400 MHz): δ: 3.06 (s, 3H, CH_3); 4.64 (s, 2H, CH_2); 6.15 (bs, 2H, NH_2); 6.22 (t, 1H, aryl, J= 8.8 Hz); 7.40 (d, 2H, aryl, J=8.0 Hz); 7.64 (d, 2H, aryl, J=8.0 Hz); 7.86-7.90 (m, 1H, aryl). HR-MS m/z: calcd for C$_{15}$H$_{14}$F$_4$N$_3$O$_2$, [(M+H)$^+$]: 344.1022; found 344.1027.

N-(2-amino-3-fluoro-4-(methyl(4-(trifluoromethyl)benzyl)amino)phenyl)-3,3-dimethylbutanamide (112).

Final product **112** was synthesized in 57% yield from **111** and 3,3-dimethylbutanoyl chloride following the general procedure H. ^{1}H NMR (CDCl$_3$, 400 MHz): δ: 1.05 (s, 9H, 3 CH_3); 2.18 (s, 2H, CH_2); 2.65 (s, 3H, CH_3); 4.21 (s, 2H, CH_2); 6.26 (t, 1H, aryl, J=8.9 Hz); 6.70 (dd, 1H, aryl, J$_1$=7.1 Hz, J$_2$=1.6 Hz); 6.97 (s, 1H, CONH); 7.38 (d, 2H, aryl, J=8.0 Hz); 7.50 (d, 2H, aryl, J=8.0 Hz). ^{13}C NMR (CDCl$_3$, 100 MHz) δ: 29.9; 39.4; 50.7; 59.2; 108.4; 119.4; 120.2; 125.2; 125.3; 131.4; 131.6; 138.5; 142.9; 144.1; 146.5; 170.7. ^{19}F NMR (CDCl$_3$, 376.3 MHz) δ: -62.39 (3F, CF_3); -143.21 (1F, CF). HR-MS m/z: calcd for C$_{21}$H$_{26}$F$_4$N$_3$O, [(M+H)$^+$]: 412.2012; found 412.2009.

2,6-difluorobenzene-1,4-diamine (114).

Synthesized in 91% yield by reduction of 2,6-difluoro-4-nitroaniline under the conditions described in the general procedure E. ^{1}H NMR (CDCl$_3$, 400 MHz) δ 3.30 (bs, 2H, NH_2); 3.46 (bs, 2H, NH_2); 6.25 (d, 2H, aryl, J= 9.6 Hz). HR-MS m/z: calcd for C$_6$H$_7$F$_2$N$_2$, [(M+H)$^+$]: 145.0577; found 145.0583.

N-(4-amino-2,6-difluorophenyl)heptanamide (115).

Synthesized in 71% yield from **114** and heptanoyl chloride following the general procedure A. ^{1}H NMR (CDCl$_3$, 400 MHz): δ: 0.82 (t, 3H, CH_3, J=6.6 Hz); 1.18-1.31 (m, 6H, 3 CH_2); 1.59-1.66 (m, 2H, CH_2); 2.24 (t, 2H, CH_2, J=7.5 Hz); 3.42 (bs, 2H, NH_2); 6.99-7.03 (m, 3H, aryl and CONH). HR-MS *m/z*: calcd for C$_{13}$H$_{19}$F$_2$N$_2$O, [(M+H)$^+$]: 257.1465; found 257.1468.

N-(4-amino-2,6-difluorophenyl)-3,3-dimethylbutanamide (116).

Synthesized in 68% yield from **114** and 3,3-dimethylbutanoyl chloride following the general procedure A. ^{1}H NMR (CDCl$_3$, 400 MHz): δ: 1.01 (s, 9H, 3 CH_3); 2.11 (s, 2H, CH_2); 3.30 (bs, 2H, NH_2); 6.93 (s, 1H CONH) 6.99 (d, 2H, aryl, J= 9.8 Hz). HR-MS *m/z*: calcd for C$_{12}$H$_{17}$F$_2$N$_2$O, [(M+H)$^+$]: 243.1309; found 243.1313.

N-(2,6-difluoro-4-((4-(trifluoromethyl)benzyl)amino)phenyl)heptanamide (117).

Final product **117** was obtained as a gray powder in 61% yield from **115** and 1-(bromomethyl)-4-(trifluoromethyl)benzene following the general procedure C. ^{1}H NMR (CD$_3$OD, 400 MHz): δ: 0.84 (t, 3H, CH_3, J=6.5 Hz); 1.22-1.26 (m, 6H, 3 CH_2); 1.55-1.60 (m, 2H, CH_2); 2.23 (t, 2H, CH_2, J=7.6 Hz); 4.39 (s, 2H, CH_2); 7.03 (d, 2H, aryl, J=10.5 Hz); 7.42 (d, 2H, aryl, J=7.9 Hz); 7.50 (d, 2H, aryl, J=7.9 Hz); ^{13}C NMR (CD$_3$OD, 100 MHz) δ: 12.9; 22.2; 25.4; 28.6; 31.3; 36.5; 49.2; 103.3; 103.6; 124.8; 127.6; 130.2; 130.3; 130.5; 145.1; 152.11; 152.21; 154.49; 154.58; 173.12. ^{19}F NMR (CDCl$_3$, 376.3 MHz) δ: -62.49 (3F, CF_3); -126.78 (2F, CF). HR-MS *m/z*: calcd for C$_{21}$H$_{24}$F$_5$N$_2$O, [(M+H)$^+$]: 415.1809; found 415.1810.

N-(2,6-difluoro-4-((4-(trifluoromethyl)benzyl)amino)phenyl)-3,3-dimethylbutanamide (118).

Final product **118** was obtained as a gray powder in 57% yield from **116** and 1-(bromomethyl)-4-(trifluoromethyl)benzene following the general procedure C. ^{1}H NMR (CD$_3$OD, 400 MHz): δ: 0.94 (s, 9H, 3 CH_3); 2.07 (s, 2H, CH_2); 4.36 (s, 2H, CH_2); 6.99 (d, 2H, aryl, J=8.8 Hz); 7.38 (d, 2H, aryl, J=8.1 Hz); 7.46 (d, 2H, aryl, J=8.2 Hz). ^{13}C NMR (CD$_3$OD, 100 MHz) δ: 28.8; 30.7; 49.2; 49.8; 103.4; 103.7; 121.0; 123.0; 124.8; 125.7; 127.6; 128.6; 129.0; 130.1; 145.1; 152.1; 152.2; 154.4; 154.5; 171.6. ^{19}F NMR (CD$_3$OD, 376.3 MHz) δ: -62.51 (3F, CF_3); -127.51 (2F, CF); HR-MS *m/z*: calcd for C$_{20}$H$_{22}$F$_5$N$_2$O, [(M+H)$^+$]: 401.1652; found 401.1655.

(E,Z)-1-nitro-4-(4-(trifluoromethyl)styryl)benzene (120a and 120b).

4-nitrobenzaldheyde (1.0 eq) was dissolved in dichloromethane (DCM, 26.7 mL per gram of aldehyde) and added with 4-trifluoromethylbenzyltriphenylphosphonium bromide, prepared from 4-trifluoromethylbenzy bromide and triphenylphosphine and a catalytic amount of tetrabutylammonium bromide (TBAB, 0.2% mol). To this solution, half volume of aqueous K_2CO_3 (1.0 eq) was added. The resulting mixture was stirred at room temperature for 12h, then the reaction was diluted with DCM and water and the organic phase was extracted, dried over anhydrous Na_2SO_4, filtered and concentrated in vacuo. The crude product was purified by flash chromatography using hexane/ethyl acetate (95:5 v:v) obtaining the mixture of geometric isomers of 1-nitro-4-(4-(trifluoromethyl)styryl)benzene as a yellow solid (65% yield). ^{1}H NMR (CD_3Cl_3, 400 MHz): δ: 6.76 (d, 1H, CH, J=12.3 Hz); 6.84 (d, 1H, CH, J=12.3 Hz); 7.28 (d, 1H, CH, J=9.0 Hz); 7.33 (d, 2H, aryl, J=8.2 Hz); 7.37 (d, 2H, aryl, J=8.6 Hz); 7.53 (d, 2H, aryl, J=8.2 Hz); 7.68 (d, 1H, CH, J=9.0 Hz); 8.11 (d, 2H, aryl, J=8.8 Hz). HR-MS *m/z*: calcd for $C_{15}H_{11}F_3NO_2$, [M+H^{+}]: 294.0742, found: 294.0749.

4-(4-(trifluoromethyl)phenethyl)aniline (121).

Compound **121** was synthesized as an off-white solid starting from the mixture of **120a** and **120b** and following the general procedure E for catalytic hydrogenation (88% yield). ^{1}H NMR ($CDCl_3$, 400 MHz): δ: 2.87 (t, 2H, CH_2, J=5.4 Hz); 2.96 (t, 2H, CH_2, J=5.3 Hz); 3.61 (bs, 2H, NH_2); 6.66-6.68 (m, 2H, aryl); 6.97-7.00 (m, 2H, aryl); 7.27-7.31 (m, 2H, aryl); 7.55-7.57 (m, 2H, aryl). HR-MS *m/z*: calcd for $C_{15}H_{15}F_3N$, [M+H^{+}]: 266.1151, found: 266.1153.

N-(4-(4-(trifluoromethyl)phenethyl)phenyl)heptanamide (122).

Compound **122** was synthesized as a grey solid in 71% yield, starting from **121** and heptanoyl chloride**,** using the general procedure B for N-acylation. ^{1}H NMR ($CDCl_3$, 400 MHz): δ: 0.91 (t, 3H, CH_3, J=7.0 Hz); 1.30-1.39 (m, 6H, 3 CH_2); 1.70-1.78 (m, 2H, CH_2); 2.37 (t, 2H, CH_2, J=7.9 Hz); 2.91 (t, 2H, CH_2, J=6.3 Hz); 2.97 (t, 2H, CH_2, J=6.3 Hz); 7.10 (d, 2H, aryl, J=8.3 Hz); 7.27 (d, 2H, aryl, J=8.0 Hz); 7.46 (d, 2H, aryl, J=8.0 Hz); 7.54 (d, 2H, aryl, J=8.1 Hz). HR-MS *m/z*: calcd for $C_{22}H_{27}F_3NO$, [(M+H)[+]]: 378.2045; found 378.2051.

3,3-dimethyl-N-(4-(4-(trifluoromethyl)phenethyl)phenyl)butanamide (123).

Compound **123** was synthesized as a grey solid in 78% yield, starting from **121** and 3,3-dimethylbutanoyl chloride**,** using the general procedure B for N-acylation. ^{1}H NMR ($CDCl_3$, 400 MHz): δ: 1.12 (s, 9H, 3 CH_3); 2.24 (s, 2H, CH_2); 2.91 (t, 2H, CH_2, J=6.5 Hz); 2.97 (t, 2H,

CH$_2$, J=6.5 Hz); 7.11 (d, 2H, aryl, J=8.4 Hz); 7.27 (d, 2H, aryl, J=7.72 Hz); 7.45 (d, 2H, aryl, J=8.4 Hz); 7.54 (d, 2H, aryl, J=8.0 Hz). HR-MS m/z: calcd for C$_{21}$H$_{25}$F$_3$NO, [(M+H)$^+$]: 364.1888; found 364.1885.

N-(2-nitro-4-(4-(trifluoromethyl)phenethyl)phenyl)heptanamide (124).

Intermediate **122** (1.0 eq) was dissolved in acetic anhydride (40 mL per gram of product) and cooled to 0°C. Then, HNO$_3$ (0.41 mL per mmol of starting product) was added and the reaction was stirred for 30 minutes at the same temperature. After the completation of the reaction, water was added, leading to the precipitation of a yellow solid, which was filtrated. After collection, the precipitate was dried under vacuum and used in the following synthetic step without further purification (83% yield). ^{1}H NMR (CD$_3$OD, 400 MHz): δ: 0.94 (t, 3H, CH$_3$, J=7.0 Hz); 1.35-1.44 (m, 6H, 3 CH$_2$); 1.68-1.76 (m, 2H, CH$_2$); 2.45 (t, 2H, CH$_2$, J=7.6 Hz); 3.06 (s, 4H, 2 CH$_2$); 7.39 (d, 2H, aryl, J=8.0 Hz); 7.50 (dd, 1H, aryl, J$_1$=6.4 Hz, J$_2$=2.0 Hz); 7.57 (d, 2H, aryl, J=8.1 Hz); 7.90 (d, 1H, aryl, J=2.0 Hz); 7.93 (d, 1H, aryl, J=8.4 Hz). HR-MS m/z: calcd for C$_{22}$H$_{26}$F$_3$N$_2$O$_3$, [(M+H)$^+$]: 423.1896; found 423.1901.

3,3-dimethyl-N-(2-nitro-4-(4-(trifluoromethyl)phenethyl)phenyl)butanamide (125).

Intermediate **125** was synthesized according to the procedure described above for **124.** The product was collected as a yellow solid in 79% yield. ^{1}H NMR (CDCl$_3$, 400 MHz): δ: 1.14 (s, 9H, 3 CH$_3$); 2.33 (s, 2H, CH$_2$); 3.01 (s, 4H, 2 CH$_2$); 7.29 (d, 2H, aryl, J=7.9 Hz); 7.45 (dd, 1H, aryl, J$_1$=6.6 Hz, J$_2$=2.1 Hz); 7.57 (d, 2H, aryl, J=7.9 Hz); 8.01 (d, 1H, aryl, J=2.1 Hz); 8.74 (d, 1H, aryl, J=8.6 Hz); 10.24 (s, 1H, NH). HR-MS m/z: calcd for C$_{21}$H$_{24}$F$_3$N$_2$O$_3$, [(M+H)$^+$]: 409.1739; found 409.1743.

N-(2-amino-4-(4-(trifluoromethyl)phenethyl)phenyl)heptanamide (126).

Final product **126** was synthesized in 92% yield as a white solid, starting from compound **124** and using the general procedure E for catalytic hydrogenation. ^{1}H NMR (CD$_3$OD, 400 MHz): δ: 0.94 (t, 3H, CH$_3$, J=6.7 Hz); 1.37-1.45 (m, 6H, 3 CH$_2$); 1.69-1.77 (m, 2H, CH$_2$); 2.42 (t, 2H, CH$_2$, J=7.6 Hz); 2.86 (t, 2H, CH$_2$, J=6.9 Hz); 2.99 (t, 2H, CH$_2$, J=6.9 Hz); 6.58 (dd, 1H, aryl, J$_1$=6.4 Hz, J$_2$=2.1 Hz); 6.72 (d, 1H, aryl, J=1.7 Hz); 6.99 (d, 1H, aryl, J=8.0 Hz); 7.36 (d, 2H, aryl, J=7.8 Hz); 7.54 (d, 2H, aryl, J=7.5 Hz). ^{13}C NMR (CD$_3$OD, 100 MHz) δ: 13.0; 22.2; 25.7; 28.7; 31.3; 35.9; 36.7; 37.1; 117.2; 118.5; 121.9; 124.7; 125.7; 127.6; 127.9; 128.8; 140.3; 141.7; 146.3; 173.8. ^{19}F NMR (CD$_3$OD, 376.3 MHz) δ: -63.81 (3F, CF$_3$). HR-MS m/z: calcd for C$_{23}$H$_{23}$F$_3$N$_2$O, [(M+H)$^+$]: 393.2154; found 3932157.

N-(2-amino-4-(4-(trifluoromethyl)phenethyl)phenyl)-3,3-dimethylbutanamide (127).

Final product **127** was synthesized in 87% yield as a white solid, starting from compound **125** and using the general procedure E for catalytic hydrogenation. ^{1}H NMR (CD$_3$OD, 400 MHz): δ: 1.13 (s, 9H, 3 C*H$_3$*); 2.29 (s, 2H, C*H$_2$*); 2.85 (t, 2H, C*H$_2$*, J=7.1 Hz); 3.00 (t, 2H, C*H$_2$*, J=7.1 Hz); 6.57 (dd, 1H, aryl, J$_1$=6.1 Hz, J$_2$=1.9 Hz); 6.71 (d, 1H, aryl, J=1.8 Hz); 6.97 (d, 1H, aryl, J=8.0 Hz); 7.37 (d, 2H, aryl, J=8.0 Hz); 7.54 (d, 2H, aryl, J=8.1 Hz). ^{13}C NMR (CD$_3$OD, 100 MHz) δ: 28.9; 36.7; 37.1; 49.2; 117.2; 118.4; 122.0, 124.7; 125.7; 127.6; 127.9; 128.8; 140.3; 141.8; 146.3; 172.1. ^{19}F NMR (CD$_3$OD, 376.3 MHz) δ: -63.82 (3F, C*F$_3$*); HR-MS *m/z*: calcd for C$_{21}$H$_{26}$F$_3$N$_2$O, [(M+H)$^+$]: 379.1997; found 379.1992.

3,3-dimethyl-N-(2-(piperidin-1-yl)-4-(4-(trifluoromethyl)phenethyl)phenyl)butanamide (128).

Final product **128** was obtained by reaction of **127** with 1,4-dibromopentane, following the same procedure described for intermediate **58**. ^{1}H NMR (CD$_3$OD, 400 MHz): δ: 1.12 (s, 9H, 3 C*H$_3$*); 1.58-1.60 (m, 2H, C*H$_2$*); 1.70-1.75 (m, 4H, 2 C*H$_2$*); 2.30 (s, 2H, C*H$_2$*); 2.69 (t, 4H, 2 C*H$_2$*, J=5.2 Hz); 2.90 (t, 2H, C*H$_2$*, J=8.7 Hz); 2.97 (t, 2H, C*H$_2$*, J=8.6 Hz); 6.80 (s, 1H, aryl); 6.93 (dd, 1H, aryl, J$_1$=6.5 Hz, J$_2$=1.8 Hz); 7.29 (d, 2H, aryl, J=8.0 Hz); 7.53 (d, 1H, aryl, J=8.0 Hz); 8.00 (d, 1H, aryl, J=8.2 Hz); ^{13}C NMR (CD$_3$OD, 100 MHz) δ: 23.7; 26.4; 28.9; 30.7; 36.8; 37.3; 50.9; 53.5; 120.3; 120.8; 123.2; 124.2; 124.7; 125.9; 127.3; 127.7; 128.0; 128.3; 130.7; 137.2; 146.1; 171.1. ^{19}F NMR (CD$_3$OD, 376.3 MHz) δ: -63.71 (3F, C*F$_3$*). HR-MS *m/z*: calcd for C$_{26}$H$_{34}$F$_3$N$_2$O, [(M+H)$^+$]: 447.2618; found 447.2621.

N-hexyl-2,4-dinitrobenzamide (130).

2,4-dinitrobenzoic acid (1.0 eq) was dissolved in a mixture of DCM/DMF (1:1 v:v) and then added with 1.2 equivalents of benzotriazol-1-yloxytripyrrolidinophosphonium hexafluorophosphate (PyBop) and 2.4 equivalents of DIPEA. The mixture was stirred under reflux for 30 minutes. Then, 1.2 equivalents of hexylamine were added and the mixture was allowed stirring for further 3 hours. Upon completion of the reaction, as witnessed by TLC analysis, the mixture was cooled to room temperature and added with DCM and extracted sequentially (3 times per step) with a HCl (2N) aqueous solution, a saturated solution of NaHCO$_3$ and brine. The organic phase was extracted, dried over anhydrous Na$_2$SO$_4$, filtered and concentrated in vacuo. The crude product was purified by flash chromatography using mixtures of n-hexane/ethyl acetate as solvents. Compound 87 was obtained as a yellowish solid in 77% yield. ^{1}H NMR (CDCl$_3$, 400 MHz): δ: 0.92 (t, 3H, C*H$_3$*, J=6.2 Hz); 1.25-1.34 (m, 6H,

3 CH_2); 1.60-1.65 (m, 2H, CH_2); 3.43 (t, 2H, CH_2, J=9.5 Hz); 6.32 (s, 1H, NH); 6.80 (s, 1H, aryl); 7.71 (dd, 1H, aryl, J$_1$=5.1 Hz, J$_2$=2.3 Hz); 8.49-8.52 (m, 1H, aryl); 8.85 (d, 1H, aryl, J=10.5 Hz). HR-MS *m/z*: calcd for C$_{13}$H$_{18}$N$_3$O$_5$, [(M+H)$^+$]: 296.1241; found 296.1248.

2,4-diamino-N-hexylbenzamide (131).

Compound **131** was prepared starting from intermediate **130** and following the general procedure E for catalytic hydrogenation. The compound was isolated upon flash-chromatography as a dark-grey solid in 89% yield. ^{1}H NMR (CDCl$_3$, 400 MHz): δ: 0.90 (t, 3H, CH_3, J=6.5 Hz); 1.32-1.39 (m, 6H, 3 CH_2); 1.54-1.61 (m, 2H, CH_2); 3.36 (dd, 2H, CH_2, J$_1$=6.9 Hz, J$_2$=6.1 Hz); 4.64 (bs, 4H, 2 NH_2); 5.91-5.99 (m, 3H, aryl and NH); 7.13 (d, 1H, aryl, J=8.4 Hz). HR-MS *m/z*: calcd for C$_{13}$H$_{22}$N$_3$O, [(M+H)$^+$]: 236.1757; found 236.1761

2-amino-N-hexyl-4-((4-(trifluoromethyl)benzyl)amino)benzamide (132).

Final product **132** was obtained by reaction of **131** with 4-trifluoromethylbenzyl bromide, following the general procedure C (yield 69%). ^{1}H NMR (CDCl$_3$, 400 MHz): δ: 0.92 (t, 3H, CH_3, J=6.7 Hz); 1.34-1.41 (m, 6H, 3 CH_2); 1.57-1.63 (m, 2H, CH_2); 3.39 (dd, 2H, CH_2, J$_1$=6.8 Hz, J$_2$=6.1 Hz); 3.82 (bs, 2H, NH_2); 4.44 (s, 2H, CH_2); 5.76 (s, 1H, NH); 5.93-5.96 (m, 2H, aryl); 7.20 (d, 1H, aryl, J=8.4 Hz); 7.49 (d, 2H, aryl, J=7.9 Hz); 7.59 (d, 2H, aryl, J=7.9 Hz); 8.60 (bs, 1H, NH). ^{13}C NMR (CDCl$_3$, 100 MHz) δ: 14.0; 22.6; 22.7; 29.8; 31.6; 39.6; 46.7; 96.6; 102.9; 106.4; 125.5; 127.2; 129.0; 143.7; 150.6; 151.3; 169.7 ^{19}F NMR (CDCl$_3$, 376.3 MHz) δ: -62.38 (3F, CF_3). HR-MS *m/z*: calcd for C$_{21}$H$_{27}$F$_3$N$_3$O, [(M+H)$^+$]: 394.2101; found 394.2098.

6.1.2 Pharmacology
6.1.2.1 Experimental procedures for derivatives of I-III series

Photochemical stability assay

Compounds were dissolved in DMSO and then diluted in buffered aqueous solutions at pH 7.4 to a final concentration of 1 mM, 10 μM, and 1 μM. Quartz cells (1 cm) filled with the abovementioned solutions were irradiated under natural daylight or maintained at 37 °C and irradiated by an UV lamp at 365 and 264 nm wavelength or an artificial daylight D65 lamp (Philips, Amsterdam, Nederland) inside a blackbox UV analyzer. Control samples were maintained at 37 °C and wrapped by aluminum foil to avoid light exposure. At predetermined

intervals, aliquots were withdrawn and analyzed by HPLC (see below) in order to assess the concentration decrease of the starting materials.

In vitro drug metabolism using human liver microsomes

Retigabine, **23a**, and **24a** (2 μL, 1 mM) were incubated with 183 μL of 100 mM phosphate buffer (pH 7.4) and 5 μL of 20 mg/mL pooled human liver S9 fractions (Thermo Fisher Scientific, Bremen, Germany). After preincubation in a water bath for 5 min, the mixture was incubated with 10 μL of the 20 mM NADPH at 37 °C for 60 min in a Thermomixer comfort (Eppendorf, Hamburg, Germany). For the measurement of uridine glucuronide transferases (UGT) activity, before the incubation with NADPH, were added to the reaction mixture 5 mM of the uridine 5′-diphospho-α-D-glucuronic acid, 50 μg of alamethicin/mg of microsomial protein and 1 mM $MgCl_2$. For the measurement of N-acetyl transferases (NAT) activity, before the incubation with NADPH, were added to the reaction mixture 2 mM of dithiothreitol, 60 μg of sulfamethazine/mg of microsomial protein, 4.5 mM of acetyl DL-carnitine, and 0.1 Units/mL of carnitine acetyltransferase. The mixture was incubated at 37 °C for 60 min. The reactions were stopped by the addition of 200 μL of the ice-cold methanol, and then, samples were centrifuged at 10 000 rpm at 25 °C for 5 min (Eppendorf microcentrifuge 5424, Hamburg, Germany). The supernatants were collected and injected in RP-UHPLC-DAD. The control at 0 min was obtained by addition of the organic solvent immediately after incubation with microsomes. As the positive control were used testosterone, 7-hydroxycoumarin, and p-amino benzoic acid, while the negative control was prepared by incubation up to 60 min without NADPH. The extent of metabolism is expressed as a percentage of the parent compound turnover.

Cell culture and transient transfection

Channel subunits were expressed in CHO cells by transient transfection, using plasmids containing cDNAs encoding human $K_{v7.1}$, $K_{v7.2}$, $K_{v7.3}$, and $K_{v7.4}$, all cloned in the pcDNA3.1 vector. According to the experimental protocol, these plasmids were expressed individually or in combination together with a plasmid-expressing enhanced green fluorescent protein (Clontech, Palo Alto, CA) used as a transfection marker. Total cDNA in the transfection mixture was kept at 4 μg. CHO cells were grown in 100 mm plastic Petri dishes in Dulbecco's modified Eagle's medium containing 10% fetal bovine serum, nonessential amino acids (0.1 mM), penicillin (50 U/mL), and streptomycin (50 mg/mL) in a humidified atmosphere at 37 °C with 5% CO_2. At 24 h before transfection, the cells were plated on glass coverslips coated with

poly-L-lysine and were transfected on the next day with the appropriate cDNA using Lipofectamine 2000 (Life Technologies), according to manufacturer's protocol. Electrophysiologic experiments were performed 24 h after transfection.

Whole-cell electrophysiology

Currents from CHO cells were recorded at room temperature (20-22 °C) using the whole-cell configuration of the patch-clamp technique, with glass micropipettes of 3−5 MΩ resistance. During the recording, constant perfusion of extracellular solution was maintained. The extracellular solution contained (in mM) 138 NaCl, 2 $CaCl_2$, 5.4 KCl, 1 $MgCl_2$, 10 glucose, and 10 4-(2-hydroxyethyl)-1-piperazineethanesulfonic acid (HEPES), at pH 7.4, with NaOH. The pipette (intracellular) solution contained (in mM) 140 KCl, 2 MgCl2, 10 EGTA, 10 HEPES, 5 Mg^{2+}-ATP, at pH 7.3-7.4, with KOH. Current was recorded using an Axopatch-200A amplifier, filtered at 5 kHz, and digitized using a DigiData 1440A (Molecular Devices). The pCLAMP software (version 10.2) was used for data acquisition and analysis (Molecular Devices). To evaluate the activity of each compound on $K_{v7.2}$ currents, the cells were clamped at −80 mV, and currents were elicited by 3 s voltage ramps from −80 to +20 mV in the presence and absence of each compound. The ΔV values, calculated as membrane potentials at which currents reached 20 % of their peak value for controls and after drug exposure, were plotted versus log(concentration) of the compound, fitted to a four parameter logistic equation, and EC_{50} values were calculated with SigmaPlot (version 12.3). Indicated EC_{50} values are the mean of at least three independent experiments ± standard deviation (SD).

Statistical analysis

Statistically, significant differences in electrophysiological data were evaluated with the Student t-test, or with ANOVA followed by the Student-Newman-Keuls test when multiple groups were compared, with the threshold set at $p < 0.05$. Data were analyzed using the SigmaPlot 12.3 for Windows (Systat Software Inc, San Jose, CA). Values are expressed as the mean ± SD of at least three cells recorded in at least two independent transfections as the mean ± SD of three independent measurements.

6.1.2.2 Experimental procedures for derivatives of IV series

Instrumentation

UHPLC analyses were performed using a Shimadzu Nexera (Shimadzu, Milan, Italy) UHPLC consisting of two LC 30 AD pumps, a SIL 30AC autosampler, a CTO 20AC column oven, a CBM 20A controller. For UHPLC-MS/MS analysis the above described system was coupled online to a triple quadrupole LCMS 8050 (Shimadzu, Kyoto, Japan) equipped with an Electrospray Ionization (ESI) source.

Sample treatment

Photostability experiments were performed by dissolving compounds in DMSO and then diluting in buffered aqueous solutions at pH 7.4 to a final concentration of 10 µM. 1cm quartz cells, filled with the above mentioned solutions were irradiated by an UV lamp (UV Consulting TQ 150 equipped with duran 50 sleeve and 150W power supply unit, Peschl, Germany) at a fixed distance of 20 cm from the UV source. Control samples were maintained at 37 °C and wrapped by aluminium foils to avoid light exposure. At predetermined intervals aliquots were withdrawn and analyzed by UHPLC in order to assess the concentration decrease of the starting materials and the presence of the dimers usually formed by retigabine. For the assessment of plasmatic concentration, 20 µL of plasma were treated with 100 µL of methanol in a test tube. The tube was vortexed for 30 s. Then, the sample was centrifuged for ten minutes at 14680 rpm, at 4 °C. 90 µL of supernatant were dried under nitrogen, were reconstituted in 150 µL of MeOH and then injected in UHPLC-MS/MS. Brain and liver tissues were lyophilized overnight, then were weighed, carefully homogenized, and treated with methanol in a 10 mg: 0.400 µL tissue: solvent ratio. The samples were vortexed for 30 s, treated in ultrasonic bath for 5 minutes and then centrifuged for ten minutes at 14680 rpm, at 4 °C. The supernatants were dried under nitrogen, were reconstituted in 1 mL of methanol, filtered by 0.45 µM RC-membrane filters and then injected in UHPLC-MS/MS.

UHPLC conditions

Photostability experiments were carried out on a KinetexTM C18 150 × 2.1 mm × 2.6 µm (100 Å) column (Phenomenex, Bologna, Italy). The optimal mobile phase consisted of 0.1% TFA/H₂O v/v (A) and 0.1% TFA/ACN v/v (B). Analysis was performed in gradient elution as follows: 0-13.0 min, 5-65% B; 13-14.0 min, 65-95% B; 14-15.0 min, isocratic to 95% B; 15–15.01 min, 95–5% B; then three minutes for column re-equilibration. Flow rate was 0.5 mL

min^{-1}. Column oven temperature was set to 45 °C. Injection volume was 7 µL of sample. The following PDA parameters were applied: sampling rate, 12.5 Hz; detector time constant, 0.160 s; cell temperature, 40 °C. Data acquisition was set in the range 190–800 nm and chromatograms were monitored at 224 nm to assess the decrease in concentration of the starting material, while a wavelength of 550 nm was used to eventually detect dimerization. UHPLC-MS/MS analyses were performed on a Luna Omega Polar 50 × 2.1 mm, 1.6 µm (Phenomenex ®) employing as mobile phases: A) 0.1% HCOOH in H$_2$O and B) 0.1% HCOOH in ACN, with the following gradient: 0 min, 40% B, 0.01-2.00 min, 40-100% B, isocratic for 1.50 min. Returning to 40% B in 0.10 min. The flow rate was set at 0.5 mL/min. Column oven was set at 45 °C, 5 µL of extract were injected. All additives and mobile phases were LCMS grade and purchased from Merck (Milan, Italy). The ESI was operated in positive mode. MS/MS analysis were conducted in scheduled multiple reaction monitoring (MRM), employing as transitions for Retigabine: 303.9 >109.10 (quantifier ion), 303.9 > 230.10 (qualifier ion); for compound 69: 397.9 > 300.15 (quantifier ion), compound 109: 397.9 & gt; 140.10 (qualifier ion), Dwell time 50 msec. Interface temperature, Desolvation line temperature, Heat Block temperature were set, respectively to 250 °C, 250 °C and 350 °C. Nebulizing gas, drying (N$_2$) and heating gas (air) were set, respectively, to 3, 10 and 10 L/min. Retigabine and compound 109 were selected as external standards for the quantitation. Stock solutions (1 mg/mL) were prepared in DMSO and the calibration curve were obtained in methanol in the concentration range of 1-100 ng/mL (R^2=0.999). Retigabine LOD and LOQ were 0.017 ng/mL and 0.058 ng/mL, respectively. Compound 109 LOD was 0.019 ng/mL while LOQ was 0.063 ng/mL.

FluxOR™ II green potassium ion channel assay

Screening of retigabine derivatives have been performed on stable CHO cell lines co-expressing K$_{v7}$ channel subunits of interest by using a fluorescence based (FluxOR Green Potassium Ion Channel Assay). Briefly, the assay is based on the uses of Thallium (Tl$^+$) as a surrogate for K$^+$ ions and a fluorescent Tl$^+$-sensitive dye called FluxOR™. The dye is loaded into cells as a membrane-permeable aminomethyl (AM) ester, and its permeation is facilitated by the presence of the surfactant PowerLoad™. Once in the cytosol, AM ester dye is cleaved by endogenous esterase to obtain fluorogenic thallium-sensitive form and its cell extrusion is inhibited by the presence of probenecid, a blocker of the organic anion transporter. During the assay, a small amount of thallium is added to the cells with a stimulus to open channels. Thallium then passes into cells through open potassium channels according to a strong inward driving force. Upon binding cytosolic thallium, the de-esterified FluxOR™ dye exhibits a strong increase in

179

fluorescence intensity at its peak emission of 525 nm. CHO cells that stably expressed KCNQ channels were resuspend to 2×10^5 cells/ mL in complete growth medium, and 80 µL/well were plated into a Biocoat Poly-D-Lysine Celleware 96-well plates (Corning,USA) and incubated overnight at 37 °C in a 5% CO_2 incubator. The next day, after manual removal of the medium, 80 µL of 1X Loading Buffer (PowerLoad™ Concentrate 100X 100µL/10ml, FluxOR™ II Reagent 10 µL/ 10ml, deionized water 8.8 mL/10ml, FluxOR™ II Assay Buffer, 10X 1 mL/10ml and probenecid 100µL/10ml) were added into the cell plate, and then incubated in the dark at room temperature for 60 minutes. Subsequently the Loading Buffer was removed and replace with 70 µL/well of Assay Buffer (Deionized water 8.9mL/10mL, FluxOR™ II Assay Buffer 10x1 mL/10mL, Probenecid 100 µL/10mL). Additionally, 10 µl/well of the test compounds were added into the plate. Cell plates were loaded onto an FLUOstar OPTIMA microplate reader (BMG LABTECH). FITC green filters were used (excitation wavelength 485 nm and emission wavelength 520 nm). After 5 seconds of recording, 20 µL/well of stimulus buffer (Chloride-free Stimulus Buffer 2 mL/10mL, thallium Sulfate (Tl_2SO_4) 1 mL/10mL, deionized water 7 mL/10mL) were added and each well was read every second for 50 seconds. The OPTIMA data Analytics software was used for data acquisition.

Whole-cell electrophysiology

Experiments have been performed as procedures describes above.

Animals

Male C57Bl/6 mice (Charles River Laboratories, Italy) had 21 days of age, and they were housed in groups of four per cage under controlled conditions (temperature 21 ± 1 °C, 60 ± 10% relative humidity and 12/12 h light cycle with lights on at 07:00 a.m.). Food and water were available ad libitum. Animals were experimentally naive and were used only once. Sample size (n) is indicated in the figure legends. The experiments were approved by the Italian Ministry of Health (Rome, Italy) and performed in agreement with the ARRIVE (Animals in Research: Reporting In Vivo Experiments) (Kilkenny et al. 2010) guidelines, with the guidelines released by the Italian Ministry of Health (D.L. 26/14) and the European Community Directive 2010/63/EU.

Drugs

Retigabine and compound **109** were dissolved in saline containing 2 % Tween-20 and 2% PEG-400. Retigabine was administered in doses of 3 mg/kg, compound **109** was administered in

doses of 0.1, 0.3 and 1 mg/kg. Thus, each dose was dissolved to allow injection of 0.01 ml/g, i.p. We injected, as a control, only the vehicle solution to a group of mice. Retigabine and compound **109** were administered 30 min prior to induction of seizures based on pharmacokinetics data published in a previous paper of retigabine efficacy against PTZ induced seizures.[197]

Seizure testing

Pentylenetetrazole (P6500-25G, Sigma, USA) (100 mg/kg, s.c.) was dissolved in saline. Animals were removed from their home cage, weighed, numbered, and treated with saline, retigabine, compound **109** 30 min prior to drug administration. Pentetrazol was injected, and animals were placed in clear plexiglass boxes for observation of seizure activity. The severity of convulsions as well as the latency to onset of maximal seizure was recorded. Animals were observed for 30 min following pentetrazol injection.

Seizure scoring

Seizures were scored using an 8-point scoring system modified from Lüttjohann's scale.[198] 0= Wisker trembling, 1= Sudden behavioral arrest, 2= Facial jerking, 3= Neck jerks, 4= Clonic seizures (sitting), 5= Tonic Clonic seizures (lying on belly), 6= Clonic seizures (lying on side), 7= Tonic clonic seizures (lying on side), 8= Wild jumping. The behavioral assessments described above were performed in a blind manner and the observers had to reach a unanimous agreement regarding the scoring of the behavior.

Statistical analysis

Statistically, significant differences in electrophysiological data were evaluated with the Student t-test, or with ANOVA followed by the Student-Newman−Keuls test when multiple groups were compared, with the threshold set at $p < 0.05$. Data were analyzed using the SigmaPlot 12.3 for Windows (Systat Software Inc, San Jose, CA). Values are expressed as the mean ± SD of at least three cells recorded in at least two independent transfections as the mean ± SD of three independent measurements.

6.1.3 Computational details

Structure Preparation

Molecules were sketched using the Maestro GUI and then submitted to the ligprep utility to generate low-energy 3D structures from each input molecule, with various ionization states and tautomers at a pH range of 6−8. For each molecule, the state with the lowest state penalty was retained for the following studies. Compounds were studied for their conformational landscape using MacroModel. The "Mixed torsional/Low mode sampling method" was employed, using the automatic setup of the search variables, with the torsion sampling set to extended; the maximum number of steps was set to 5000 and 200 per molecule and rotatable bond, respectively. Conformers in an energy window of 82 kJ/ mol were saved, discarding the redundant ones (cutoff of maximum atom deviation = 0.5 Å). Minimization of conformers was performed using the Polak-Ribiere conjugate gradient method, using a maximum of 2500 minimization step and a 0.05 J/(Å mol) gradient convergence threshold. OPLS3 was used as force-field. No implicit solvation model was used.

Pharmacophore modeling

Ligand conformations from the above-reported conformational searches were used as input. Hypotheses A, B, and C were developed using the Phase[199] to find the best alignment and common features. Hypothesis were required to match at least half of the active molecules and to have a number of features ranging between 3 and 7, with at least a HBD. For each training set, the best ranked model (by Phase Hypo Score) was retained, finally obtaining models A, B, and C. Model D was built on the basis of the latter three models. Models B and C were both superimposed to model A by the shared features Ar1, Ar2, HY1, HBA, and HBD. The three models were then merged to get the coordinates of features HY2 and HY3 from models B and C, respectively, while features HY1, Ar1, Ar2, HBA, and HBD were inherited from model A.

Homology modeling

The sequence of human $K_{v7.2}$ (Swiss-Prot accession code O43526.2) was downloaded from the NCBI sequence database, and the region of our interest (residues 219-325) was extracted and aligned, using ClustalW,[200] to the CryoEM structure of Xenopus KCNQ1 channel (PDB id: 5VMS-score: 152 bits- expect: 1×10^{-44}-identities: 70/112-positives 88/112-gaps: 5/112). $K_{v7.2(219–325)}$ was modeled, as a homo-tetramer, by homology with the biological assembly 1 of 5VMS, using the energy-based method implemented in Prime. Side chains were optimized, except for those belonging to conserved residues, whose rotamers were retained from the

template structure. Residues not obtained from the templates were minimized. Residue deletions caused by query gaps were closed. No further optimization was carried on.

References

1. Clapham, D.E.; Runnels, L.W.; Strübing, C. The TRP ion channel family. *Nature Reviews Neuroscience*. **2001**, 2 (6), 387-396.

2. Samanta, A.; Hughes, T.E.T.; Moiseenkova-Bell, V.Y. Transient receptor potential (TRP) channels. *Subcellular Biochemistry*. **2018**, 87, 141-165.

3. Pedersen, S.F.; Owsianik, G.; Nilius, B. TRP channels: An overview. *Cell Calcium*. **2005**, 38 (3-4 SPEC. ISS.), 233-252.

4. Katz, B., Minke, B. The Drosophila light-activated TRP and TRPL channels - Targets of the phosphoinositide signaling cascade. *Progress in Retinal and Eye Research*. **2018**, 66, 200-219.

5. Bidaux, G.; Gordienko, D.; Shapovalov, G.; Farfariello, V.; Borowiec, A.S.; Iamshanova, O.; Lemonnier, L.; Gueguinou, M.; Guibon, R.; Fromont, G.; Paillard, M.; Gouriou, Y.; Chouabe, C.; Dewailly, E.; Gkika, D.; López-Alvarado, P.; Carlos Menéndez, J.; Héliot, L.; Slomianny, C.; Prevarskaya, N. 4TM-TRPM8 channels are new gatekeepers of the ER-mitochondria Ca^{2+} transfer. *Biochimica et Biophysica Acta - Molecular Cell Research.* **2018**, 1865 (7), 981-994.

6. Gees, M.; Colsoul, B.; Nilius, B. The role of transient receptor potential cation channels in Ca^{2+} signaling. *Cold Spring Harbor perspectives in biology*. **2010**, *2* (10), a003962.

7. Laing, R.J.; Dhaka, A. ThermoTRPs and Pain. *Neuroscientist*, **2016**, 22 (2), 171-187.

8. Himmel, N.J.; Cox, D.N. Transient receptor potential channels: current perspectives on evolution. *Proceedings of the Royal Society B: Biological Sciences*. **2020**, 287 (1933), 20201309.

9. Koivisto, A.P.; Belvisi, M.G.; Gaudet, R.; Szallasi, A. Advances in TRP channel drug discovery: from target validation to clinical studies. *Nature Reviews Drug Discovery.* **2022**, 21 (1), 41-59.

10. Venkatachalam, K.; Montell, C., TRP channels. *Annual review of biochemistry.* **2007**, *76*, 387-417.

11. Kaneko, Y.; Szallasi, A. Transient receptor potential (TRP) channels: A clinical perspective. *British Journal of Pharmacology*. **2014**, 171 (10), 2474-2507.

12. Huang, S.; Szallasi, A. Transient receptor potential (TRP) channels in drug discovery: Old concepts & new thoughts. *Pharmaceuticals*, **2017**, 10 (3), 64.

13. Belvisi, M.G.; Dubuis, E.; Birrell, M.A. Transient receptor potential A1 channels: Insights into cough and airway inflammatory disease. *Chest*. **2011**, 140 (4), 1040-1047.

14. Voets, T. TRP channels and thermosensation. *Handbook of experimental pharmacology*. **2014**, *223*, 729-41.

15. Caterina, M. J. Transient receptor potential ion channels as participants in thermosensation and thermoregulation. *American Journal of Physiology*. **2007**, *292* (1), R64-R76.

16. Dhaka, A.; Earley, T.J.; Watson, J.; Patapoutian, A. Visualizing cold spots: TRPM8-expressing sensory neurons and their projections. *Journal of Neuroscience*. **2008**, 28 (3), 566-575.

17. Bautista, D.M.; Siemens, J.; Glazer, J.M.; Tsuruda, P.R.; Basbaum, A.I.; Stucky, C.L.; Jordt, S.E.; Julius, D. The menthol receptor TRPM8 is the principal detector of environmental cold. *Nature*. **2007**, 448 (7150), 204-208.

18. McKemy, D.D.; Neuhausser, W.M.; Julius, D. Identification of a cold receptor reveals a general role for TRP channels in thermosensation. *Nature*. **2002**, 416 (6876), 52-58.

19. Bagley, K.C.; Abdelwahab, S.F.; Tuskan, R.G.; Lewis, G.K. Calcium Signaling through Phospholipase C Activates Dendritic Cells to Mature and Is Necessary for the Activation and Maturation of Dendritic Cells Induced by Diverse Agonists. *Clinical and Diagnostic Laboratory Immunology*. **2004**, 11 (1), 77-82.

20. Iftinca, M.; Altier, C. The cool things to know about TRPM8! *Channels*. *2020*, 14 (1), 413-420.

21. Abe, J.; Hosokawa, H.; Sawada, Y.; Matsumura, K.; Kobayashi, S. Ca^{2+}-dependent PKC activation mediates menthol-induced desensitization of transient receptor potential M8. *Neuroscience Letters*. **2006**, 397 (1-2), 140-144.

22. Bavencoffe, A.; Gkika, D.; Kondratskyi, A.; Beck, B.; Borowiec, A.S.; Bidaux, G.; Busserolles, J.; Eschalier, A.; Shuba, Y.; Skryma, R.; Prevarskaya, N. The transient receptor potential channel TRPM8 is inhibited via the α2A adrenoreceptor signaling pathway. *Journal of Biological Chemistry*. **2010**, 285 (13), 9410-9419.

23. Bavencoffe, A.; Kondratskyi, A.; Gkika, D.; Mauroy, B.; Shuba, Y.; Prevarskaya, N.; Skryma, R. Complex regulation of the TRPM8 cold receptor channel: Role of arachidonic acid release following M3 muscarinic receptor stimulation. *Journal of Biological Chemistry*. **2011**, 286 (11), 9849-9855.

24. Zhang, L.; Barritt, G. J. TRPM8 in prostate cancer cells: a potential diagnostic and prognostic marker with a secretory function? *Endocrine-related cancer*. **2006**, 13 (1), 27-38.

25. Pedretti, A.; Marconi, C.; Bettinelli, I.; Vistoli, G. Comparative modeling of the quaternary structure for the human TRPM8 channel and analysis of its binding features. *Bba-Biomembranes*. **2009**, 1788 (5), 973-982.

26. Brauchi, S.; Orta, G.; Salazar, M.; Rosenmann, E.; Latorre, R. A hot-sensing cold receptor: C-terminal domain determines thermosensation in transient receptor potential channels. *Journal of Neuroscience*. **2006**, 26 (18), 4835-4840.

27. Phelps, C. B.; Gaudet, R., The role of the N terminus and transmembrane domain of TRPM8 in channel localization and tetramerization. *Journal of Biological Chemistry*. **2007**, 282 (50), 36474-36480.

28. Rohács, T.; Lopes, C.M.B.; Michailidis, I.; Logothetis, D.E. PI(4,5)P2 regulates the activation and desensitization of TRPM8 channels through the TRP domain. *Nature Neuroscience*. **2005**, 8 (5), 626-634.

29. Hirai, A.; Aung, N.Y.; Ohe, R.; Nishida, A.; Kato, T.; Meng, H.; Ishizawa, K.; Fujii, J.; Yamakawa, M. Expression of TRPM8 in human reactive lymphoid tissues and mature B-cell neoplasms. *Oncology Letters*. **2018**, 16 (5), 5930-5938.

30. Yee, N.S. Roles of TRPM8 ion channels in cancer: Proliferation, survival, and invasion. *Cancers*. **2015**, 7 (4), A13, 2134-2146.

31. Di Donato, M.; Ostacolo, C.; Giovannelli, P.; Di Sarno, V.; Monterrey, I.M.G.; Campiglia, P.; Migliaccio, A.; Bertamino, A.; Castoria, G. Therapeutic potential of TRPM8 antagonists in prostate cancer. *Scientific Reports*. **2021**, 11 (1), 23232.

32. Grolez, G.P.; Gkika, D. TRPM8 puts the chill on prostate cancer. Pharmaceuticals. **2016**, 9 (3).

33. Wang, Y.; Yang, Z.; Meng, Z.; Cao, H.; Zhu, G.; Liu, T.; Wang, X. Knockdown of TRPM8 suppresses cancer malignancy and enhances epirubicin-induced apoptosis in human osteosarcoma cells. *International Journal of Biological Sciences*. **2014**, 10, 90-102.

34. Valero, M.L.I.; Mello de Queiroz, F.; Stuhmer, W.; Viana, F.; Pardo, L.A. TRPM8 ion channels differentially modulate proliferation and cell cycle distribution of normal and cancer prostate cells. *PLoS ONE*. **2012**, 7.

35. Yee, N.S.; Brown, R.D.; Lee, M.S.; Zhou, W.; Jensen, C.; Gerke, H.; Yee, R.K. TRPM8 ion channel is aberrantly expressed and required for preventing replicative senescence in pancreatic adenocarcinoma: Potential role of TRPM8 as a biomarker and target. *Cancer Biology & Therapy*. **2012**, 13, 592-599.

36. Asuthkar, S.; Elustondo, P. A.; Demirkhanyan, L.; Sun, X.; Baskaran, P.; Velpula, K. K.; Thyagarajan, B.; Pavlov, E. V.; Zakharian, E., The TRPM8 Protein Is Testosterone Receptor I. Biochemical evidence for direct TRPM8-testosterone interactions. *Journal of Biological Chemistry*. **2015**, 290 (5), 2659-2669.

37. Caterina, M. J.; Leffler, A.; Malmberg, A. B.; Martin, W. J.; Trafton, J.; Petersen-Zeitz, K. R.; Koltzenburg, M.; Basbaum, A. I.; Julius, D. Impaired nociception and pain sensation in mice lacking the capsaicin receptor. *Science*. **2000**, 288 (5464), 306-313.

38. Pérez De Vega, M.J.; Gómez-Monterrey, I.; Ferrer-Montiel, A.; González-Muñiz, R. Transient Receptor Potential Melastatin 8 Channel (TRPM8) Modulation: Cool Entryway for Treating Pain and Cancer. *Journal of Medicinal Chemistry*. **2016**, 59 (22), 10006-10029.

39. Liu, B.; Fan, L.; Balakrishna, S.; Sui, A.; Morris, J.B.; Jordt, S.E. TRPM8 is the principal mediator of menthol-induced analgesia of acute and inflammatory pain. *Pain*. **2013**, 154 (10), 2169-2177.

40. Knowlton, W.M.; Palkar, R.; Lippoldt, E.K.; McCoy, D.D.; Baluch, F.; Chen, J.; McKemy, D.D. A sensory-labeled line for cold: TRPM8-expressing sensory neurons define the cellular basis for cold, cold pain, and cooling-mediated analgesia. *Journal of Neuroscience*. **2013**, 33 (7), 2837-2848.

41. Gauchan, P.; Andoh, T.; Kato, A.; Kuraishi, Y. Involvement of increased expression of transient receptor potential melastatin 8 in oxaliplatin-induced cold allodynia in mice. *Neuroscience Letters*. **2009**, 458, 93-95.

42. Nam, J.S.; Cheong, Y.S.; Karm, M.H.; Ahn, H.S.; Sim, J.H.; Kim, J.S. Effects of nefopam on streptozotocin-induced diabetic neuropathic pain inrats. *Korean Journal of Pain*. **2014**, 27,326-333.

43. De Caro, C.; Cristiano, C.; Avagliano, C.; Bertamino, A.; Ostacolo, C.; Campiglia, P.; Gomez-Monterrey, I.; La Rana, G.; Gualillo, O.; Calignano, A.; Russo, R. Characterization of New TRPM8 Modulators in Pain Perception. *International Journal of Molecular Sciences*. **2019**, 20 (22).

44. Andersson, D. A.; Chase, H. W. N.; Bevan, S. TRPM8 activation by menthol, icilin, and cold is differentially modulated by intracellular pH. *Journal of Neuroscience*. **2004**, 24 (23), 5364-5369.

45. Xing, H.; Chen, M.; Ling, J.; Tan, W. H.; Gu, J. G. G. TRPM8 mechanism of cold allodynia after chronic nerve injury. *Journal of Neuroscience*. **2007**, 27 (50), 13680-13690.

46. Premkumar, L. S.; Raisinghani, M.; Pingle, S. C.; Long, C.; Pimentel, F. Downregulation of transient receptor potential melastatin 8 by protein kinase C-mediated dephosphorylation. *Journal of Neuroscience.* **2005**, 25 (49), 11322-11329.

47. Stein, R.J.; Santos, S.; Nagatomi, J.; Hayashi, Y.; Minnery, B.S.; Xavier, M.; Patel, A.S.; Nelson, J.B.; Futrell, W.J.; Yoshimura, N.; Chancellor. M.B.; De Miguel, F. Cool (TRPM8) and hot (TRPV1) receptors in the bladder and male genital tract. *Journal of Urology.* **2004**, 172, 1175-1178.

48. Lindstrom, S.; Mazieres, L.; Jiang, C.H. Inhibition of the bladder cooling reflex in the awake state: an experimental study in the cat. *Journal of Urology.* **2004**, 172, 2051-2053.

49. Kanai, A.; Andersson, K. E. Bladder Afferent Signaling: Recent Findings. *Journal of Urology*. **2010**, *183* (4), 1288-1295.

50. Wu, L.; Zhang, J.; Zhou, F.; Zhang, P. Increased Transient Receptor Potential Melastatin 8 Expression in the Development of Bladder Pain in Patients With Interstitial Cystitis/Bladder Pain Syndrome. *Urology.* **2020**, 146, 301.e1-301.e6.

51. Mukerji, G.; Yiangou, Y.; Corcoran, S.L.; Selmer, I.S.; Smith, G.D.; Benham, C.D.; Bountra, C.; Agarwal, S.K.; Anand, P. Cool and menthol receptor TRPM8 in human urinary bladder disorders and clinical correlations. *BMC Urology*. **2006**, 6, 6-11.

52. Lashinger, E.S.R.; Steiginga, M.S.; Hieble, J.P.; Leon, L.A.; Gardner, S.D.; Nigella, R.; Davenport, E.A.; Hoffman, B.E.; Laping, N.J.; Su, X. AMTB, a TRPM8 channel blocker: Evidence in rats for activity in overactive bladder and painful bladder syndrome. *American Journal of Physiology - Renal Physiology*. **2008**, 295 (3), F803-F810.

53. Liu, B. Y.; Qin, F. Functional control of cold- and menthol-sensitive TRPM8 ion channels by phosphatidylinositol 4,5-bisphosphate. *Journal of Neuroscience*. **2005**, 25 (7), 1674-1681.

54. Andersson, D. A. Modulation of the Cold-Activated Channel TRPM8 by Lysophospholipids and Polyunsaturated Fatty Acids. *The Journal of Neuroscience*. **2007**, 27 (12), 3347-3355.

55. González-Muñiz, R.; Bonache, M.A.; Martín-Escura, C.; Gómez-Monterrey, I. Recent progress in TRPM8 modulation: an update. *International Journal of Molecular Sciences*. **2019**, 20 (11), 2618.

56. Clemmensen, C.; Jall, S.; Kleinert, M.; Quarta, C.; Gruber, T.; Sachs, S.; Fischer, K.; Grandl, G.; Loher, D.; Sanchez-Quant, E.; et al. Coordinated targeting of cold and nicotinic receptors synergistically improves obesity and type 2 diabetes. *Nature Communications.* **2018**, 9, 4304.

57. Andersson, D.A.; Chase, H.W.N.; Bevan, S. TRPM8 activation by menthol, icilin, and cold is differentially modulated by intracellular pH. *Journal of Neuroscience*. **2004**, 24 (23), 5364-5369.

58. Janssens, A.; Gees, M.; Toth, B.I.; Ghosh, D.; Mulier, M.; Vennekens, R.; Vriens, J.; Talavera, K.; Voets, T. Definition of two agonist types at the mammalian cold-activated channel TRPM8. *Elife*. **2016**, *5*, e17240/1-e17240/21.

59. DeFalco, J.; Duncton, M.A.; Emerling, D. TRPM8 biology and medicinal chemistry. *Current Topics in Medicinal Chemistry*. **2011**, 11, 2237-2252.

60. Eid, S.R. Therapeutic targeting of TRP channels–the TR(i)P to pain relief. *Current Topics in Medicinal Chemistry*. **2011**, 11, 2118-2130.

61. Premkumar, L.S.; Abooj, M. TRP channels and analgesia. *Life Sciences*. **2013**, 92, 415-424.

62. Docherty, R.J.; Yeats, J.C.; Piper, A.S. Capsazepine block of voltage-activated calcium channels in adult rat dorsal root ganglion neurones in culture. *British Journal of Pharmacology*. **1997**, 121, 1461-1467.

63. Madrid, R.; Donovan-Rodriguez, T.; Meseguer, V.; Acosta, M.C.; Belmonte, C.; Felix, V. Contribution of TRPM8 channels to cold transduction in primary sensory neurons and peripheral nerve terminals. *Journal of Neuroscience*. **2006**, 26, 12512-12525.

64. Gaston, T.E.; Friedman, D. Pharmacology of cannabinoids in the treatment of epilepsy. *Epilepsy & Behavior.* **2017**, 70, 313-318.

65. De Petrocellis, L.; Ligresti, A.; Moriello, A.S.; Allarà, M.; Bisogno, T.; Petrosino, S.; Stott, C.G.; Di Marzo, V. Effects of cannabinoids and cannabinoid-enriched Cannabis extracts on TRP channels and endocannabinoid metabolic enzymes. *British Journal of Pharmacology.* **2011**, 163, 1479-1494.

66. Yin, Y.; Wu, M.; Zubcevic, L.; Borschel, W.F.; Lander, G.C.; Lee, S.Y. Structure of the cold- and menthol-sensing ion channel TRPM8. *Science*. **2018**, 359, 237-241.

67. Descoeur, J.; Pereira, V.; Pizzoccaro, A.; Francois, A.; Ling, B.; Maffre, V.; Couette, B.; Busserolles, J.; Courteix, C.; Noel, J.; Lazdunski, M.; Eschalier, A.; Authier, N.; Bourinet, E. Oxaliplatin-induced cold hypersensitivity is due to remodelling of ion channel expression in nociceptors. *EMBO Molecular Medicine*. **2011**, 3, 266-278.

68. Yamamoto, S.; Egashira, N.; Tsuda, M.; Masuda, S. Riluzole prevents oxaliplatin-induced cold allodynia via inhibition of overexpression of transient receptor potential melastatin 8 in rats. *Journal of Pharmacological Sciences*. **2018**, 138 (3), 214-217.

69. Aierken, A.; Xie, Y.K.; Dong, W.; Apaer, A.; Lin, J.J.; Zhao, Z.; Yang, S.; Xu, Z.Z.; Yang, F. Rational Design of a Modality-Specific Inhibitor of TRPM8 Channel against Oxaliplatin-Induced Cold Allodynia. *Advanced Science.* **2021**, 8 (22), 2101717.

70. Grisold, W.; Cavaletti, G.; Windebank, A.J.; Peripheral neuropathies from chemotherapeutics and targeted agents: Diagnosis, treatment, and prevention. *Neuro-Oncology.* **2012**.

71. Pachman, D.R.; Barton, D.L.; Watson, J.C.; Loprinzi, C.L. Chemotherapy-induced peripheral neuropathy: Prevention and treatment. *Clinical Pharmacology & Therapeutics.* **2011**, 90, 377-387.

72. Weil, A.; Moore, S.E.; Waite, N.J.; Randall, A.; Gunthorpe, M.J. Conservation of functional and pharmacological properties in the distantly related temperature sensors TRVP1 and TRPM8. *Molecular pharmacology.* **2005**, 68 (2), 518-27.

73. De Falco, J.; Steiger, D.; Dourado, M.; Emerling, D.; Duncton, M.A.J. 5-Benzyloxytryptamine as an antagonist of TRPM8. *Bioorganic Medicinal & Chemistry Letters.* **2010**, 20 (23), 7076-7079.

74. Bertamino, A.; Ostacolo, C.; Ambrosino, P.; Musella, S.; Di Sarno, V.; Ciaglia, T.; Soldovieri, M.V.; Iraci, N.; Fernandez Carvajal, A.; De La Torre-Martinez, R.; Ferrer-Montiel, A.; Gonzalez Muniz, R.; Novellino, E.; Taglialatela, M.; Campiglia, P.; Gomez-Monterrey, I. Tryptamine-Based Derivatives as Transient Receptor Potential Melastatin Type 8 (TRPM8) Channel Modulators. *Journal of Medicinal Chemistry.* **2016**, 59 (5), 2179-2191.

75. Meseguer, V.; Karashima, Y.; Talavera, K.; D'Hoedt, D.; Donovan-Rodriguez, T.; Viana, F.; Nilius, B.; Voets, T. Transient receptor potential channels in sensory neurons are targets of the antimycotic agent clotrimazole. *Journal of Neuroscience.* **2008**, 28 (3), 576-86.

76. Journigan, V.B.; Zaveri, N.T. TRPM8 ion channel ligands for new therapeutic applications and as probes to study menthol pharmacology. *Life Sciences.* **2013**, 92 (8-9), 425-437.

77. Premkumar, L. S.; Raisinghani, M.; Pingle, S. C.; Long, C.; Pimentel, F. Downregulation of transient receptor potential melastatin 8 by protein kinase C-mediated dephosphorylation. *Journal of Neuroscience.* **2005**, 25 (49), 11322-9.

78. Zhang, X.; Mak, S.; Li, L.; Parra, A.; Denlinger, B.; Belmonte, C.; McNaughton, P. A. Direct inhibition of the cold-activated TRPM8 ion channel by Galphaq. *Nature cell biology.* **2012**, 14 (8), 851-8.

79. Terada, Y.; Kitajima, M.; Taguchi, F.; Takayama, H.; Horie, S.; Watanabe, T. Identification of Indole Alkaloid Structural Units Important for Stimulus-Selective TRPM8 Inhibition: SAR Study of Naturally Occurring Iboga Derivatives. *Journal of Natural Products*. **2014**, 77 (8), 1831-8.

80. Bertamino, A.; Iraci, N.; Ostacolo, C.; Ambrosino, P.; Musella, S.; Di Sarno, V.; Ciaglia, T.; Pepe, G.; Sala, M.; Soldovieri, M. V.; Mosca, I.; Gonzalez-Rodriguez, S.; Fernandez-Carvajal, A.; Ferrer-Montiel, A.; Novellino, E.; Taglialatela, M.; Campiglia, P.; Gomez-Monterrey, I. Identification of a potent tryptophan-based TRPM8 antagonist with in vivo analgesic activity. *Journal of Medicinal Chemistry*. **2018**, 61 (14), 6140-6152.

81. Bertamino, A.; Ostacolo, C.; Medina, A.; Di Sarno, V.; Lauro, G.; Ciaglia, T.; Vestuto, V.; Pepe, G.; Basilicata, M.G.; Musella, S.; Smaldone, G.; Cristiano, C.; Gonzalez-Rodriguez, S.; Fernandez-Carvajal, A.; Bifulco, G.; Campiglia, P.; Gomez-Monterrey, I.; Russo, R. Exploration of TRPM8 Binding Sites by β-Carboline-Based Antagonists and Their in Vitro Characterization and in Vivo Analgesic Activities. *Journal of Medicinal Chemistry*. **2020**, 63 (17), 9672-9694.

82. Dong, J.; Trieu, T. H.; Shi, X. X.; Zhang, Q.; Xiao, S.; Lu, X. A general strategy for the highly stereoselective synthesis of HR22C16-like mitotic kinesin Eg5 inhibitors from both L- and D-tryptophans. *Tetrahedron: Asymmetry*. **2011**, 22 (20-22), 1865-1873.

83. Lopez-Rodriguez, M. L.; Morcillo, M. J.; Garrido, M.; Benhamu, B.; Perez, V.; de la Campa, J. G. Stereospecificity in the reaction of tetrahydro-.beta.-carboline-3-carboxylic acids with isocyanates and isothiocyanates. kinetic vs thermodynamic control. *Journal of Organic Chemistry*. **1994**, 59 (6), 1583-1585.

84. Mizoguchi, S.; Andoh, T.; Yakura, T.; Kuraishi, Y. Involvement of c-Myc-mediated transient receptor potential melastatin 8 expression in oxaliplatin-induced cold allodynia in mice. *Pharmacological Reports*. **2016**, 68 (3), 645-648.

85. Reker, A. N.; Chen, S.; Etter, K.; Burger, T.; Caudill, M.; Davidson, S. The operant plantar thermal assay: a novel device for assessing thermal pain tolerance in mice. *eNeuro*. **2020**, 7 (2), ENEURO.0210-19.2020.

86. (a) Touska, F.; Winter, Z.; Mueller, A.; Vlachova, V.; Larsen, J.; Zimmermann, K. Comprehensive thermal preference phenotyping in mice using a novel automated circular gradient assay. *Temperature*. **2016**, 3 (1), 77-91. (b) Filliatreau, G.; Attal, N.; Hassig, R.;¨ Guilbaud, G.; Desmeules, J.; Di Giamberardino, L. Time-course of nociceptive disorders induced by chronic loose ligatures of the rat sciatic nerve and changes of the acetylcholinesterase transport along the ligated nerve. *Pain*. **1994**, 59 (3), 405−413. (c)

Wang, Y.; Zhang, X.; Guo, Q. L.; Zou, W. Y.; Huang, C. S.; Yan, J. Q. Cyclooxygenase inhibitors suppress the expression of P2X3 receptors in the DRG and attenuate hyperalgesia following chronic constriction injury in rats. *Neuroscience Letters*. **2010**, 478 (2), 77-81. (d) Wanner, S. P.; Almeida, M. C.; Shimansky, Y. P.; Oliveira, D. L.; Eales, J. R.; Coimbra, C. C.; Romanovsky, A. A. Cold-induced thermogenesis and inflammation associated cold-seeking behavior are represented by different dorsomedial hypothalamic sites: a three-dimensional functional topography study in conscious rats. *Journal of Neuroscience*. **2017**, 37 (29), 6956-6971. (e) Schepers, R. J.; Ringkamp, M. Thermoreceptors and thermosensitive afferents. *Neuroscience & Biobehavioral Reviews*. **2010**, 34, 177-184.

87. Diver, M. M.; Cheng, Y.; Julius, D. Structural insights into TRPM8 inhibition and desensitization. *Science*. **2019**, 365 (6460), 1434-1440.

88. Ungemach, F.; Soerens, D.; Weber, R.; Di Pierro, M.; Campos, O.; Mokry, P.; Cook, J. M.; Silverton, J. V. General method for the assignment of stereochemistry of 1,3-disubstituted 1,2,3,4-tetrahydro-.beta.-carbolines by carbon-13 spectroscopy. *Journal of American Chemical Society*. **1980**, 102 (23), 6976-6984.

89. Cagasova, K.; Ghavami, M.; Yao, Z.-K.; Carlier, P. R.´ Questioning the γ-gauche effect: stereoassignment of 1,3-disubstituted-tetrahydro-β-carbolines using 1H−1H coupling constants. *Organic and Biomolecular Chemistry*. **2019**, 17 (27), 6687-6698.

90. Van Linn, M.L.; Cook, J.M. Mechanistic studies on the cis to trans epimerization of Trisubstituted 1,2,3,4-Tetrahydro-β-carbolines. *Journal of Organic Chemistry*. **2010**, 75 (11), 3587-3599.

91. Bertamino, A.; Lauro, G.; Ostacolo, C.; Di Sarno, V.; Musella, S.; Ciaglia, T.; Campiglia, P.; Bifulco, G.; Gomez-Monterrey, I. M. Ring-fused cyclic aminals from tetrahydro-beta-carboline-based dipeptide compounds. *Journal of Organic Chemistry*. **2017**, 82 (23), 12014-12027.

92. Kuang, Q.; Purhonen, P.; Hebert, H. Structure of potassium channels. *Cellular and Molecular Life Sciences*. **2015**, 72 (19), 3677-3693.

93. Kuo, M.M.; Haynes, W.J.; Loukin, S.H.; Kung, C.; Saimi, Y. Prokaryotic K(+) channels: from crystal structures to diversity. *FEMS Microbiology Review*. **2005**, 29(5), 961-985.

94. Cheng, Q.; Chen, A.; Du, Q.; Liao, Q.; Shuai, Z.; Chen, C.; Yang, X.; Hu, Y.; Zhao, J.; Liu, S.; Wen, G.R.; An, J.; Jing, H.; Tuo, B.; Xie, R.; Xu, J. Novel insights into ion channels in cancer stem cells (Review). *International Journal of Oncology*. **2018**, 53 (4), 1435-1441.

95. Jentsch, T.J. Neuronal KCNQ potassium channels: Physiology and role in disease. *Nature Reviews Neuroscience*. **2000**, 1 (1), 21-30.

96. Buckingham, S.D.; Kidd, J.F.; Law, R.J.; Franks, C.J.; Sattelle, D.B. Structure and function of two-pore-domain K^+ channels: contributions from genetic model organisms. *Trends in Pharmacological Sciences.* **2005**, 26(7), 361-367.

97. Ficker, E.; Taglialatela, M.; Wible, B.A.; Henley, C.M.; Brown, A.M. Spermine and spermidine as gating molecules for inward rectifier K^+ channels. *Science*. **1994**, 266 1068-1072.

98. Kurata, H.T.; Rapedius, M.; Kleinman, M.J.; Baukrowitz, T.; Nichols, C.G. Voltage-dependent gating in a "voltage sensor-less" ion channel. *PLoS Biology*. **2010**, 8 (2), e100031.

99. Kim, D. Physiology and pharmacology of two-pore domain potassium channels. *Current Pharmaceutical Design*. **2005**, 11 (21), 2717-2736.

100. González, C.; Baez-Nieto, D.; Valencia, I.; Oyarzún, I.; Rojas, P.; Naranjo, D.; Latorre, R. K^+ channels: Function-structural overview. *Comprehensive Physiology*. **2012**, 2 (3), 2087-2149.

101. MacKinnon, R. Potassium channels. *FEBS Letters.* **2003**, 555 (1), 62-65.

102. Doyle, D.A.; Morais, Cabral. J.; Pfuetzner, R.A.; Kuo, A.; Gulbis, J.M.; Cohen, S.L.; Chait, B.T.; MacKinnon, R. The structure of the potassium channel: molecular basis of K^+ conduction and selectivity. *Science.* **1998**, 280 (5360), 69-77.

103. Valiyaveetil, F.I.; Leonetti, M.; Muir, T.W.; Mackinnon, R. Ion selectivity in a semisynthetic K^+ channel locked in the conductive conformation. *Science.* **2006**, 314 (5801), 1004-1007.

104. Thompson, A.N.; Kim, I.; Panosian, T.D.; Iverson, T.M.; Allen, T.W.; Nimigean, C.M. Mechanism of potassium-channel selectivity revealed by Na(+) and Li(+) binding sites within the KcsA pore. *Nature Structural & Molecular Biology.* **2009**, 16 (12), 1317-1324.

105. Jepps, T.A.; Barrese, V.; Miceli, F. Editorial: Kv7 Channels: Structure, Physiology, and Pharmacology. *Frontiers in Physiology*. **2021**, 12, 679317.

106. O'Grady, S.M.; So, Y.L. Molecular diversity and function of voltage-gated (Kv) potassium channels in epithelial cells. International Journal of Biochemistry and Cell Biology. **2005**, 37 (8), 1578-1594.

107. Sanguinetti, M.C.; Curran, M.E.; Zou, A.; Shen, J.; Spector, P.S.; Atkinson, D.L.; Keating, M.T. Coassembly of K(V)LQT1 and minK (IsK) proteins to form cardiac I(Ks) potassium channel. *Nature*. **1996**, 384 (6604), 80-83.

108. Herbert, E.; Trusz-Gluza, M.; Moric, E.; Śmiłowska-Dzielicka, E.; Mazurek, U.; Wilczok, T. KCNQ1 gene mutations and the respective genotype-phenotype correlations in the long QT syndrome. *Medical Science Monitor*. **2002**, 8 (10), RA240-RA248.

109. Neyroud, N.; Tesson, F.; Denjoy, I.; Leibovici, M.; Donger, C.; Barhanin, J.; Fauré, S.; Gary, F.; Coumel, P.; Petit, C.; Schwartz, K.; Guicheney, P. A novel mutation in the potassium channel gene KVLQT1 causes the Jervell and Lange-Nielsen cardioauditory syndrome. *Nature Genetics*. **1997**, 15 (2), 186-189.

110. Roepke, T.K.; Anantharam, A.; Kirchhoff, P.; Busque, S.M.; Young, J.B.; Geibel, J.P.; Lerner, D.J.; Abbott, G.W. The KCNE2 potassium channel ancillary subunit is essential for gastric acid secretion. *Journal of Biological Chemistry*. **2006**, 281 (33), 23740-23747.

111. Brown, D.A.; Passmore, G.M. Neural KCNQ (Kv7) channels. *British Journal of Pharmacology*. **2009**, 156 (8), 1185-1195.

112. Schroeder, B.C.; Kubisch, C.; Stein, V.; Jentsch, T.J. Moderate loss of function of cyclic-AMP-modulated KCNQ2/KCNQ3 K+ channels causes epilepsy. Nature. **1998**, 396 (6712), 687-690.

113. Bordas, C.; Kovacs, A.; Pal, B. The M-current contributes to high threshold membrane potential oscillations in a cell type-specific way in the pedunculopontine nucleus of mice. *Frontiers in Cellular Neuroscience*. **2015**, 9 (APR), 121.

114. Singh, N.A.; Westenskow, P.; Charlier, C.; Pappas, C.; Leslie, J.; Dillon, J.; Anderson, V.E.; Sanguinetti, M.C.; Leppert, M.F. KCNQ2 and KCNQ3 potassium channel genes in benign familial neonatal convulsions: Expansion of the functional and mutation spectrum. *Brain*. **2003**, 126 (12), 2726-2737.

115. Dirkx, N.; Miceli, F.; Taglialatela, M.; Weckhuysen, S. The Role of Kv7.2 in Neurodevelopment: Insights and Gaps in Our Understanding. *Frontiers in Physiology*. **2020**. 11, 570588.

116. Miceli, F.; Soldovieri, M.V.; Ambrosino, P.; De Maria, M.; Migliore, M.; Migliore, R.; Taglialatela, M. Early-onset epileptic encephalopathy caused by gain-of-function mutations in the voltage sensor of Kv7.2 and Kv7.3 potassium channel subunits. *Journal of Neuroscience*. **2015**, 35 (9), 3782-3793.

117. Søgaard, R.; Ljungstrøm, T.; Pedersen, K.A.; Olesen, S.P.; Skaaning Jensen, B.O. KCNQ4 channels expressed in mammalian cells: Functional characteristics and pharmacology. *American Journal of Physiology - Cell Physiology*. **2001**, 280 (4 49-4), C859-C866.

118. Kimitsuki, T.; Komune, N.; Noda, T.; Takaiwa, K.; Ohashi, M.; Komune, S. Property of IK,n in inner hair cells isolated from guinea-pig cochlea. *Hearing Research*. **2010**, 261 (1-2), 57-62.

119. Kubisch, C.; Schroeder, B.C.; Friedrich, T.; Lütjohann, B.; El-Amraoui, A.; Marlin, S.; Petit, C.; Jentsch, T.J. KCNQ4, a novel potassium channel expressed in sensory outer hair cells, is mutated in dominant deafness. *Cell*. **1999**, 96 (3), 437-446

120. Jepps, T.A.; Chadha, P.S.; Davis, A.J.; Harhun, M.I.; Cockerill, G.W.; Olesen, S.P.; Hansen, R.S.; Greenwood, I.A. Downregulation of Kv7.4 channel activity in primary and secondary hypertension. *Circulation*. **2011**, 124 (5), 602-611.

121. Lerche, C.; Scherer, C.R.; Seebohm, G.; Derst, C.; Wei, A.D.; Busch, A.E.; Steinmeyer, K. Molecular cloning and functional expression of KCNQ5, a potassium channel subunit that may contribute to neuronal M-current diversity. *Journal of Biological Chemistry*. **2000**, 275 (29), 22395-22400.

122. Lehman, A.; Thouta, S.; Mancini, G.M.S.; Naidu, S.; van Slegtenhorst, M.; McWalter, K.; Person, R.; Mwenifumbo, J.; Salvarinova, R.; Adam, S.; du Souich, C.; Elliott, A.M.; Nelson, T.N.; van Karnebeek, C.; Friedman, J.M.; Boelman, C.; Bolbocean, C.; Buerki, S.E.; Candido, T.; Eydoux, P.; Evans, D.M.; Gibson, W.; Horvath, G.; Huh, L.; Sinclair, G.; Tarling, T.; Toyota, E.B.; Townsend, K.N.; Van Allen, M.I.; Vercauteren, S.; Guella, I.; McKenzie, M.B.; Datta, A.; Connolly, M.B.; Kalkhoran, S.M.; Poburko, D.; Farrer, M.J.; Demos, M.; Desai, S.; Claydon, T. Loss-of-Function and Gain-of-Function Mutations in KCNQ5 Cause Intellectual Disability or Epileptic Encephalopathy. *American Journal of Human Genetics*. **2017**, 101 (1), 65-74.

123. Schroeder, B.C.; Hechenberger, M.; Weinreich, F.; Kubisch, C.; Jentsch, T.J. KCNQ5, a Novel Potassium Channel Broadly Expressed in Brain, Mediates M-type Currents. *Journal of Biological Chemistry*. **2000**, 275 (31), 24089-24095.

124. Caminos, E.; Vaquero, C.F.; Martinez-Galan, J.R. Relationship between rat retinal degeneration and potassium channel KCNQ5 expression. *Experimental Eye Research*. **2015**, 131, 1-11.

125. Doyle, D.A.; Cabral, J.M.; Pfuetzner, R.A.; Kuo, A.; Gulbis, J.M.; Cohen, S.L.; Chait, B.T.; MacKinnon, R. The structure of the potassium channel: Molecular basis of K+ conduction and selectivity. Science. **1998**, 280 (5360), 69-77.

126. Kuo, A.; Gulbis, J.M.; Antcliff, J.F.; Rahman, T.; Lowe, E.D.; Zimmer, J.; Cuthbertson, J.; Ashcroft, F.M.; Ezaki, T.; Doyle, D.A. Crystal structure of the potassium channel KirBac1.1 in the closed state. *Science*. **2003**, 300 (5627), 1922-1926.

127. Grizel, A.V.; Glukhov, G.S.; Sokolova, O.S. Mechanisms of activation of voltage-gated potassium channels. *Acta Naturae.* **2014**, 6 (23), 10-26.

128. Kim, D.M.; Nimigean, C.M. Voltage-gated potassium channels: A structural examination of selectivity and gating. *Cold Spring Harbor Perspectives in Biology*. **2016**, 8 (5), 19.

129. Sokolova, O. Structure of cation channels, revealed by single particle electron microscopy. *FEBS Letters*. **2004**, 564 (3), 251-256.

130. Abbott, G.W. KCNQs: Ligand- and Voltage-Gated Potassium Channels. *Frontiers in Physiology*. **2020**, 11, 583.

131. Long, S.B.; Tao, X.; Campbell, E.B.; Mackinnon, R. Atomic structure of a voltage-dependent K+ channel in a lipid membrane-like environment. *Nature*. **2007**, 450, 376-382.

132. Barros, F.; Domínguez, P.; de la Peña, P. Cytoplasmic domains and voltage-dependent potassium channel gating. *Frontiers in Pharmacology*. **2012**, 3 MAR, 49.

133. Zaydman M.A.; Silva, J.R.; Delaloye, K.; Li, Y.; Liang, H.; Larsson, H.P.; Shi, J.; Cui, J. Kv7.1 ion channels require a lipid to couple voltage sensing to pore opening. *Proceedings of the National Academy of Sciences*. **2013**, USA 110, 13180-13185.

134. Li, Y.; Gamper, N.; Hilgemann, D.W.; Shapiro, M.S. Regulation of Kv7 (KCNQ) K+ channel open probability by phosphatidylinositol 4,5-bisphosphate. *Journal of Neuroscience*. **2005**, 25, 9825-9835.

135. Zhang, Q.; Zhou, P.; Chen, Z.; Li, M.; Jiang, H.; Gao, Z.; Yang, H. Dynamic PIP2 interactions with voltage sensor elements contribute to KCNQ2 channel gating. *PNAS*. **2013**, 110, 20093-20098.

136. Sun, J.; MacKinnon, R. Cryo-EM Structure of a KCNQ1/CaM Complex Reveals Insights into Congenital Long QT Syndrome. *Cell*. **2017**, 169, 1042-1050.

137. Alaimo, A.; Villarroel, A. Calmodulin: A multitasking protein in Kv7.2 potassium channel functions. *Biomolecules*. **2018**, 8 (3), 57.

138. Kang, S.; Xu, M.; Cooper, E.C.; Hoshi, N. Channel-anchored protein kinase CK2 and protein phosphatase 1 reciprocally regulate KCNQ2-containing M-channels via phosphorylation of calmodulin. *Journal of Biological Chemistry*. **2014**, 289 (16), 11536-11544.

139. Pan, Z.; Kao, T.; Horvath, Z.; Lemos, J.; Sul, J.Y.; Cranstoun, S.D.; Bennett, V.; Scherer, S.S.; Cooper, E.C. A common ankyrin-G-based mechanism retains KCNQ and NaV channels at electrically active domains at the axon. *Journal of Neuroscience*. **2006**, 26, 2599-2613.

140. Kole, M.H.P.; Cooper, E.C. Axonal Kv7.2/7.3 channels. *Channels*. **2014**, 8 (4), 288-289.

141. Chow, L.W.C.; Leung, Y.M. The versatile Kv channels in the nervous system: actions beyond action potentials. *Cellular and Molecular Life Sciences*. **2020**, 77 (13), 2473-2482.

142. Lauritano, A.; Moutton, S.; Longobardi, E.; Tran Mau-Them, F.; Laudati, G.; Nappi, P.; Soldovieri, M.V.; Ambrosino, P.; Cataldi, M.; Jouan, T.; Lehalle, D.; Maurey, H.; Philippe, C.; Miceli, F.; Vitobello, A.; Taglialatela, M. A novel homozygous KCNQ3 loss-of-function variant causes non-syndromic intellectual disability and neonatal-onset pharmacodependent epilepsy. *Epilepsia Open*. **2019**, 4 (3), 464-475.

143. Weckhuysen, S.; Mandelstam, S.; Suls, A.; Audenaert, D.; Deconinck, T.; Claes, L.R.F.; Deprez, L.; Smets, K.; Hristova, D.; Yordanova, I.; Jordanova, A.; Ceulemans, B.; Jansen, A.; Hasaerts, D.; Roelens, F.; Lagae, L.; Yendle, S.; Stanley, T.; Heron, S.E.; Mulley, J.C.; Berkovic, S.F.; Scheffer, I.E.; De Jonghe, P. KCNQ2 encephalopathy: Emerging phenotype of a neonatal epileptic encephalopathy. *Annals of Neurology*. **2012**, 71 (1), 15-25.

144. Ronen, G.M.; Rosales, T.O.; Connolly, M.; Anderson, V.E.; Leppert, M. Seizure characteristics in chromosome 20 benign familial neonatal convulsions. *Neurology*. **1993**, 43, 1355-60.

145. Zhou, X.; Ma, A.; Liu, X.; Huang, C.; Zhang, Y.; Shi, R.; Mao, S.; Geng, T.; Li, S. Infantile seizures and other epileptic phenotypes in a Chinese family with a missense mutation of KCNQ2. *European Journal of Pediatry*. **2006**, 165,691-695.

146. Zara, F.; Specchio, N.; Striano, P.; Robbiano, A.; Gennaro, E.; Paravidino, R.; Vanni, N.; Beccaria, F.; Capovilla, G.; Bianchi, A.; Caffi, L.; Cardilli, V.; Darra, F.; Bernardina, B.D.; Fusco, L.; Gaggero, R.; Giordano, L.; Guerrini, R.; Incorpora, G.; Mastrangelo, M.; Spaccini, L.; Laverda, A.M.; Vecchi, M.; Vanadia, F.; Veggiotti, P.; Viri, M.; Occhi, G.; Budetta, M.; Taglialatela, M.; Coviello, D.A.; Vigevano, F.; Minetti, C. Genetic testing in benign familial epilepsies of the first year of life: clinical and diagnostic significance. *Epilepsia*. **2013**, 54, 425,43.

147. Singh, N.A.; Westenskow, P.; Charlier, C.; Pappas, C.; Leslie, J.; Dillon, J.; Anderson, V.E.; Sanguinetti, M.C.; Leppert, M.F KCNQ2 and KCNQ3 potassium channel genes in benign familial neonatal convulsions: expansion of the functional and mutation spectrum. *Brain*. **2003**, 126, 2726-2737.

148. Bosch, D.G.; Boonstra, F.N.; de Leeuw, N.; Pfundt, R.; Nillesen, W.M.; de Ligt, J. Gilissen, C.; Jhangiani, S.; Lupski, J.R.; Cremers, F.P.; de Vries, B.B. Novel genetic

causes for cerebral visual impairment. *European Journal of Human Genetics*. **2016**, 24, 660-665.

149. Sands, T.T.; Miceli, F.; Lesca, G.; Beck, A.E.; Sadleir, L.G.; Arrington, D.K.; Schönewolf-Greulich, B.; Moutton, S.; Lauritano, A.; Nappi, P.; Soldovieri, M.V.; Scheffer, I.E.; Mefford, H.C.; Stong, N.; Heinzen, E.L.; Goldstein, D.B.; Perez, A.G.; Kossoff, E.H.; Stocco, A.; Sullivan, J.A.; Shashi, V.; Gerard, B.; Francannet, C.; Bisgaard, A.M.; Tümer, Z.; Willems, M.; Rivier, F.; Vitobello. A.; Thakkar, K.; Rajan, D.S.; Barkovich, A.J.; Weckhuysen, S.; Cooper, E.C.; Taglialatela, M.; Cilio, M.R. Autism and developmental disability caused by KCNQ3 gain-of-function variants. *Annals of Neurology*. **2019**, 86, 181-192.

150. Schroeder, B.C.; Kubisch, C.; Stein, V.; Jentsch, T.J. Moderate loss of function of cyclic-AMP-modulated KCNQ2/KCNQ3 K+ channels causes epilepsy. *Nature*. **1998**, 396, 687-690.

151. Dedek, K.; Kunath, B.; Kananura, C.; Reuner, U.; Jentsch, T.J.; Steinlein, O.K. Myokymia and neonatal epilepsy caused by a mutation in the voltage sensor of the KCNQ2 K+ channel. *PNAS*, **2001**, 98, 12272-12277.

152. Singh, N.A.; Westenskow, P.; Charlier, C.; Pappas, C.; Leslie, J.; Dillon, J.; Anderson, V.E.; Sanguinetti, M.C.; Leppert, M.F. KCNQ2 and KCNQ3 potassium channel genes in benign familial neonatal convulsions: expansion of the functional and mutation spectrum. *Brain*. **2003**, 126, 2726-2737.

153. Miceli, F.; Soldovieri, M.V.; Lugli, L.; Bellini, G.; Ambrosino, P.; Migliore, M.; del Giudice, E.M.; Ferrari, F.; Pascotto, A.; Taglialatela, M. Neutralization of a unique, negatively-charged residue in the voltage sensor of K V 7.2 subunits in a sporadic case of benign familial neonatal seizures. *Neurobiology of Disease*. **2009**, 34, 501-510.

154. Miceli, F.; Soldovieri, M.V.; Ambrosino, P.; De Maria, M.; Migliore, M.; Migliore, R.; Taglialatela, M. Early-onset epileptic encephalopathy caused by gain-of-function mutations in the voltage sensor of Kv7.2 and Kv7.3 potassium channel subunits. *Journal of Neuroscience*. **2015**, 35: 3782-3793.

155. Millichap, J.J.; Miceli, F.; De Maria, M.; Keator, C.; Joshi, N.; Tran, B.; Soldovieri, M.V.; Ambrosino, P.; Shashi, V.; Mikati, M.A.; Cooper E.C.; Taglialatela, M. Infantile spasms and encephalopathy without preceding neonatal seizures caused by KCNQ2 R198Q, a gain-of-function variant. *Epilepsia*. **2017**, 58, e10-e15.

156. Nappi, P.; Miceli, F.; Soldovieri, M.V.; Ambrosino, P.; Barrese, V.; Taglialatela, M. Epileptic channelopathies caused by neuronal Kv7 (KCNQ) channel dysfunction. *Pflugers Archiv European Journal of Physiology*. **2020**, 472 (7), 881-898.

157. Martire, M.; Castaldo, P.; D'Amico, M.; Preziosi, P.; Annunziato, L.; Taglialatela, M. M channels containing KCNQ2 subunits modulate norepinephrine, aspartate, and GABA release from hippocampal nerve terminals. *Journal of Neuroscience*. **2004**, 24, 592-7.

158. Seaman, C.A.; Sheridan, P.H.; Engel, J.; Molliere, M.; Narang, P.K.; Nice, F.J.; Meldrum, B.S.; Porter, R.J. Flupirtine. In *New anticonvulsant drugs* Eds.; Libbey: London, UK, **1986**. 135-146.

159. Rostock, A.; Tober, C.; Rundfeldt, C.; Bartsch, R.; Engel, J.; Polymeropoulos, E.E.; Kutscher, B.; Loscher, W.; Honack, D.; White, H.S.; Wolf, H.H. D-23129: A new anticonvulsant with a broad spectrum activity in animal models of epileptic seizures. *Epilepsy Research*. **1996**, *23*, 211-223.

160. Ihara, Y.; Tomonoh, Y.; Deshimaru, M.; Zhang, B.; Uchida, T.; Ishii, A.; Hirose, S. Retigabine, a Kv7.2/Kv7.3-channel opener, attenuates drug-induced seizures in knock-in mice harboring KCNQ2 mutations. *PloS One*. **2016**, 11(2), e0150095.

161. Rundfeldt, C. The new anticonvulsant retigabine (d-23129) acts as an opener of K$^+$ channels in neuronal cells. *European Journal of Pharmacology*. **1997**, *336*, 243-249.

162. Main, M.J.; Cryan, J.E.; Dupere, J.R.; Cox, B.; Clare, J.J. Burbidge, S.A. Modulation of KCNQ2/3 potassium channels by the novel anticonvulsant retigabine. *Molecular pharmacology*. **2000**, 58, 253-262.

163. Tatulian, L.; Delmas, P.; Abogadie, F.C. Brown, D.A. Activation of expressed KCNQ potassium currents and native neuronal M-type potassium currents by the anti-convulsant drug retigabine. *The Journal of Neuroscience*. **2001**, 21, 5535-5545.

164. Dupuis, D.S.; Schroder, R.L.; Jespersen, T.; Christensen, J.K.; Christophersen, P.; Jensen, B.S. Olesen, S.P. Activation of KCNQ5 channels stably expressed in HEK293 cells by BMS-204352. *European Journal of Pharmacology*. **2002**, 437, 129-137.

165. Tatulian, L.; Brown, D.A. Effect of the KCNQ potassium channel opener retigabine on single KCNQ2/3 channels expressed in CHO cells. *The Journal of Physiology*. **2003**, 549, 57-63.

166. Schenzer, A.; Friedrich, T.; Pusch, M.; Saftig, P.; Jentsch, T.J.; Grotzinger, J. Schwake, M. Molecular determinants of KCNQ (Kv7) K+ channel sensitivity to the anticonvulsant retigabine. *Journal of Neuroscience*. **2005**, 25, 5051-5060.

167. Lange, W.; Geissendörfer, J.; Schenzer, A.; Grotzinger, J.; Seebohm, G.; Friedrich, T.; Schwake, M. Refinement of the binding site and mode of action of the anticonvulsant retigabine on KCNQ K+ channels. Molecular Pharmacology. **2009**, 75, 272-280.

168. Kim, R.Y.; Yau, M.C.; Galpin, J.D.; Seebohm ,G.; Ahern, C.A.; Pless, S.A.; Kurata, H.T. Atomic basis for therapeutic activation of neuronal potassium channels. *Nature Communications*. **2015**, 6, 8116.

169. Li, T.; Wu, K.; Yue, Z.; Wang, Y.; Zhang, F.; Shen, H. Structural Basis for the Modulation of Human KCNQ4 by Small-Molecule Drugs. *Molecular Cell*. **2021**, 81, 25-37.

170. Li, X.; Zhang, Q.; Guo, P.; Fu, J.; Mei, L.; Lv, D.; Wang, J.; Lai, D.; Ye, S.; Yang, H.; Guo, J. Molecular basis for ligand activation of the human KCNQ2 channel. *Cell Research*. **2021**, 31, 52-61.

171. Barrese, V.; Miceli, F.; Soldovieri, M. V.; Ambrosino, P.; Iannotti, F. A.; Cilio, M. R.; Taglialatela, M. Neuronal potassium channel openers in the management of epilepsy: role and potential of retigabine. *Clinical Pharmacology.* **2010**, 2, 225-236.

172. Zhou, P.; Zhang, Y.; Xu, H.; Chen, F.; Chen, X.; Li, X.; Pi, X.; Wang, L.; Zhan, L.; Nan, F.; Gao, Z. P-Retigabine: An N-Propargyled Retigabine with Improved Brain Distribution and Enhanced Antiepileptic Activity. *Molecular Pharmacology*. **2015**, 87, 31-38.

173. Jankovic, S.; Ilickovic, I. The preclinical discovery and development of ezogabine for the treatment of epilepsy. *Expert Opinion in Drug Discovery*. **2013**, 8, 1429-1437.

174. Kumar, M.; Reed, N.; Liu, R.; Aizenman, E.; Wipf, P.; Tzounopoulos, T. Synthesis and evaluation of potent KCNQ2/3- specific channel activators. *Molecular Pharmacology*. **2016**, 89, 667-677.

175. Groseclose, M.R., Castellino, S. An Investigation into Retigabine (Ezogabine) Associated Dyspigmentation in Rat Eyes by MALDI Imaging Mass Spectrometry. *Chemical Research in Toxicology*. **2019**, 32 (2), 294-303.

176. Kalappa, B.I.; Soh, H.; Duignan, K.M.; Furuya, T.; Edwards, S.; Tzingounis, A.V. Tzounopoulos, T. Potent KCNQ2/3-specific channel activator suppresses in vivo epileptic activity and prevents the development of tinnitus. *Journal of Neuroscience*. **2015**, 35, 8829-8842.

177. Kumar, M.; Reed, N.; Liu, R.; Aizenman, E.; Wipf, P.; Tzounopoulos, T.; Synthesis and Evaluation of Potent KCNQ2/3-Specific Channel Activators. *Molecular Pharmacology*. **2016**, 89, 667-677.

178. Zhou, P.; Zhang, Y.; Xu, H.; Chen, F.; Chen, X.; Li, X.; Pi, X.; Wang, L.; Zhan, L.; Nan, F.; Gao, Z. P-retigabine: an N-propargyled retigabine with improved brain distribution and enhanced antiepileptic activity. *Molecular pharmacology*. **2015**, 87, 31-38.

179. Wu, Y.J.; He, H.; Sun, L.Q.; L'Heureux, A.; Chen, J.; Dextraze, P.; Starrett, J.E.; Boissard, C.G.; Gribkoff, V.K.; Natale, J.; Dworetzky, S.I. Synthesis and structure-activity relationship of acrylamides as KCNQ2 potassium channel openers. *Journal of Medicinal Chemistry*. **2004**, 47, 2887-2896.

180. Peretz, A.; Degani, N.; Nachman, R.; Uziyel, Y.; Gibor, G.; Shabat, D.; Attali, B. Meclofenamic acid and diclofenac, novel templates of KCNQ2/Q3 potassium channel openers, depress cortical neuron activity and exhibit anticonvulsant properties. *Molecular Pharmacology*. **2005**, 67, 1053-1066.

181. Boehlen, A.; Schwake, M.; Dost, R.; Kunert, A.; Fidzinski, P.; Heinemann, U.; Gebhardt, C. The new KCNQ2 activator 4-Chlor-N-(6-chlor-pyridin-3-yl)-benzamid displays anticonvulsant potential. *British Journal of Pharmacology*. **2013**, 168, 1182-1200.

182. Fang, Z.; Song, Y.; Zhan, P.; Zhang, Q.; Liu, X. Conformational restriction: an effective tactic in "follow-on"-based drug discovery. *Future Medicinal Chemistry*. **2014**, 6, 885-901.

183. Ulmschneider, S.; Müller-Vieira, U.; Klein, C. D.; Antes, I.; Lengauer, T.; Hartmann, R. W. Synthesis and evaluation of (pyridylmethylene)tetrahydronaphthalenes/-indanes and structurally modified derivatives: potent and selective inhibitors of aldosterone synthase. *Journal of Medicinal Chemistry*. **2005**, 48, 1563-1575.

184. Tatulian, L.; Delmas, P.; Abogadie, F. C.; Brown, D. A. Activation of expressed KCNQ potassium currents and native neuronal M-type potassium currents by the anti-convulsant drug retigabine. *Journal of Neuroscience*. **2001**, 21, 5535-5545.

185. Wickenden, A. D.; Yu, W.; Zou, A.; Jegla, T.; Wagoner, P. K. Retigabine, a novel anti-convulsant, enhances activation of KCNQ2/Q3 potassium channels. *Molecular Pharmacology*. **2000**, 58, 591-600.

186. Dousa, M.; Srbek, J.; Radl, S.; Cerny, J.; Klecan, O.; Havlicek, J.; Tkadlecova, M.; Pekarek, T.; Gibala, P.; Novakova, L. Identification, characterization, synthesis and HPLC quantification of new processrelated impurities and degradation products in retigabine. *Journal of Pharmaceutical and Biomedical Analysis*. **2014**, 94, 71-76.

187. Lai, J.; Chang, L.; Yuan, G. I2/TBHP Mediated C−N and C−H bond cleavage of tertiary amines toward selective synthesis of sulfonamides and β-arylsulfonyl enamines: the solvent effect on reaction. *Organic Letters*. **2016**, 18, 3194-3197.

188. Groseclose, M. R.; Castellino, S. An investigation into retigabine (ezogabine) associated dyspigmentation in rat eyes by MALDI imaging mass spectrometry. *Chemical Research in Toxicology*. **2019**, 32, 294-303.

189. Li, X., Zhang, Q., Guo, P., Fu, J., Mei, L., Lv, D., Wang, J., Lai, D., Ye, S., Yang, H., Guo, J. Molecular basis for ligand activation of the human KCNQ2 channel. Cell Research. **2021**, 31 (1), 52-61.

190. Heravi, M.M., Kheilkordi, Z., Zadsirjan, V., Heydari, M., Malmir, M. Buchwald-Hartwig reaction: An overview. Journal of Organometallic Chemistry. **2018**, 861, 17-104.

191. Quast, H.; Ross, K.-H.; Philipp, G.; Hagedorn, M.; Hahn, H.; Banert, K. Syntheses and 15N NMR spectra of iminodiaziridines ring-expansions of 1-aryl-3-iminodiaziridines to 1H- and 3aHbenzimidazoles, 2H-indazoles, and 5H-dibenzo[d,f][1,3]diazepines. *European Journal of Organic Chemistry*. **2009**, 3940-3952.

192. Plsikova, J.; Janovec, L.; Koval, J.; Ungvarsky, J.; Mikes, J.; Jendzelovsky, R.; Fedorocko, P.; Imrich, J.; Kristian, P.; Kasparkova, J.; Brabec, V.; Kozurkova, M. 3,6-Bis(3-alkylguanidino)acridines as DNAintercalating antitumor agents. *European Journal of Medicinal Chemistry*. **2012**, 57, 283-295.

193. Thuo, M. M.; Reus, W. F.; Nijhuis, C. A.; Barber, J. R.; Kim, C.; Schulz, M. D.; Whitesides, G. M. Odd−Even Effects in Charge Transport across Self-Assembled Monolayers. *Journal of American Chemical Society*. **2011**, 133, 2962-2975.

194. Madabhushi, S.; Jillella, R.; Sriramoju, V.; Singh, R. Oxyhalogenation of thiols and disulfides into sulfonyl chlorides/bromides using oxone-KX (X = Cl or Br) in water. *Green Chemistry*. **2014**, 16, 3125-3131.

195. Ulmschneider, S.; Müller-Vieira, U.; Klein, C. D.; Antes, I.; Lengauer, T.; Hartmann, R. W. Synthesis and evaluation of (pyridylmethylene)tetrahydronaphthalenes/-indanes and structurally modified derivatives: potent and selective inhibitors of aldosterone synthase. *Journal of Medicinal Chemistry*. **2005**, 48, 1563-1575.

196. Xu, B.; Li, M.-L.; Zuo, X.-D.; Zhu, S.-F.; Zhou, Q.-L. Catalytic Asymmetric Arylation of α-Aryl-α-diazoacetates with Aniline Derivatives. *Journal of the American Chemical Society*. **2015**, 137 (27), 8700-8703.

197. Forcelli, P.A.; Janssen, M.J.; Vicini, S.; Gale, K. Neonatal exposure to antiepileptic drugs disrupts striatal synaptic development. *Annals of Neurology*. **2012**, 72 (3), 363-372.

198. Lüttjohann, A.; Fabene, P.F.; van Luijtelaar, G. A revised Racine's scale for PTZ-induced seizures in rats. *Physiology and Behavior*. **2009**, 98 (5), 579-586.

199. Dixon, S. L.; Smondyrev, A. M.; Knoll, E. H.; Rao, S. N.; Shaw, D. E.; Friesner, R. A. PHASE: a new engine for pharmacophore perception, 3D QSAR model development, and 3D database screening: 1. Methodology and preliminary results. *Journal of Computer-Aided Molecular Design*. **2006**, 20, 647-671.

200. Thompson, J. D.; Higgins, D. G.; Gibson, T. J. CLUSTAL W: improving the sensitivity of progressive multiple sequence alignment through sequence weighting, position-specific gap penalties and weight matrix choice. *Nucleic Acids Research*. **1994**, 22, 4673-4680.